APAE No. 92

AEC Research and
Development Report
UC-81, Reactors-Power
(Special Distribution)

STARTUP TESTING OF THE PM-2A NUCLEAR POWER PLANT

Experiments and Analysis by:

W.J. McCool
R.M. Ryan
W.M.S. Richards
P.L. Bradley
L.D. Stephenson
J.F. Cox
E.W. Schrader

Compiled by:

W.J. McCool, Head, Reactor Experiments

Approved by:

M.H. Dixon, Project Engineer

Issued: March 31, 1962

Contract No. AT(30-1)-2639
with U.S. Atomic Energy Commission
New York Operations Office

ALCO PRODUCTS, INC.
Nuclear Power Engineering Department
Post Office Box 414
Schenectady 1, N.Y.

ABSTRACT

A detailed description of the PM-2A reactor, primary system and instrumentation is presented. A general description of the secondary system and plant arrangement at Camp Century, Greenland is included. The results of the startup physics, shielding, thermal and hydraulics and radiochemistry test are presented. The analysis performed on the shielding and thermal and hydraulic tests is included. The shielding problem at startup and the shielding modification made to the piant are described along with the radiation measurements made in these areas.

ACKNOWLEDGMENTS

Appreciation is extended for the full cooperation of the U.S. Army crews associated with the PM-2A while the startup and associated tests were conducted. The effort of the many Alco personnel involved with this report is also acknowledged.

TABLE OF CONTENTS

TABLE OF CONTENTS (CONT'D)

TABLE OF CONTENTS (CONT'D)

TABLE OF CONTENTS (CONT'D)

TABLE OF CONTENTS (CONT'D)

TABLE OF CONTENTS (CONT'D)

TABLE OF CONTENTS (CONT'D)

TABLE OF CONTENTS (CONT'D)

TABLE OF CONTENTS (CONT'D)

TABLE OF CONTENTS (CONT'D)

LIST OF FIGURES

LIST OF FIGURES (CONT'D)

LIST OF FIGURES (CONT'D)

LIST OF FIGURES (CONT'D)

LIST OF FIGURES (CONT'D)

LIST OF FIGURES (CONT'D)

LIST OF FIGURES (CONT'D)

LIST OF FIGURES (CONT'D)

LIST OF TABLES

LIST OF TABLES (CONT'D)

LIST OF TABLES (CONT'D)

LIST OF TABLES (CONT'D)

LIST OF TABLES (CONT'D)

LIST OF TABLES (CONT'D)

SUMMARY

This report describes the PM-2A nuclear power plant's installation and initial startup tests at Camp Century, Greenland. The PM-2A was designed, constructed, and operated through the 400-hr test by Alco Products, Inc., under a fixed price contract,* DA-30-347-ENG-284, with no direct development effort assigned. The characteristics specific to this small, air transportable, reactor which employs fewer fuel elements and control rod assemblies and operates at higher temperature and pressure than previous ALCO designed cores are included in this report.

The PM-2A attained criticality on Oct. 2, 1960. Several weeks of plant testing which are described in this report followed. This testing included that associated directly with the design contract, plus additional tests supported by the Pressurized Water Reactor Support & Development Contract **AT(30-1)-2639. The physics testing established the optimum operating characteristics of the nuclear instrumentation, the adequacy of the spent fuel rack, the differential and integral worths of the control rods, the core reactivity effects of pressure, temperature and xenon concentration and provided an evaluation of the neutron source. This testing confirmed the analytical design and the zero power tests conducted at the Alco Products, Inc. Criticality Facility.

The PM-2A was designed for minimum weight, minimum size, ease of construction, simplicity of design and installation in a snow environment. At startup during radiation surveys, it was learned that the shielding did not meet certain design objectives such as spent fuel handling at full power operation could not be met. The report includes the radiation measurements made prior to and subsequent to a shielding modification made to this plant. A description of the shielding is also included, as is an evaluation of the modified PM-2A shielding.

Thermal and hydraulic tests were conducted to measure the steady state and transient behavior of the PM-2A primary system during (1) plant heatup, (2) steady-state operation, (3) load transients, and (4) loss of primary coolant flow.

Also included are radiochemistry measurements which develop methods for predicting, controlling, and ultimately reducing primary system activity and radiation levels.

The PM-2A was accepted by the U. S. Army on March 8, 1961 after completion of a 400-hour test.

---

* With U.S. Army Corps of Engineers, Eastern Ocean District.
** With U.S. Atomic Energy Commission, N. Y. Operations Office.

The main conclusions and recommendations from the work reported are as follows:

Physics Tests

1. Results of startup channel calibrations indicate satisfactory operation.

2. Spent fuel rack tests indicated that the rack is adequate to store the spent PM-2A Core I without any criticality hazard.

3. The initial loading was satisfactory with the count rates and bank positions agreeing with those predicted by the ZPE results.

4. The use of a moveable startup chamber was demonstrated to be an advantage over the stationary chambers used at the SM-1. Chamber calibrations can be performed when the chamber is in the withdrawn position and the life expectancy is improved by removing the BF_3 chamber from near the core during full power operations.

5. Measured PM-2A control rod worths are greater than those measured at the SM-1. The measured integral worth of the central rod at $50^{o}F$ was \$11.40 and the measured integral worth of an eccentric rod at $60^{o}F$ was \$6.85.

6. Temperature coefficient measurements revealed a higher temperature defect for PM-2A than for SM-1. The PM-2A temperature coefficient at operating conditions is 5.5 to 6.0 $¢/^{o}F$ and the hot-to-cold temperature defect is approximately \$11.00.

Shielding Measurements and Analysis

1. Radiation levels measured show that an individual can work the required 84 hour week in the PM-2A plant in areas requiring access. The values measured indicate that the reactor operating crew would normally be subjected to an exposure of 20 to 30 mr/wk.

2. Radiation levels in the working areas above the spent fuel tank are between 100 and 200 mr/hr during full power reactor operation, i.e., 10 Mwt. These values will permit limited access to the upper spent fuel tank platform.

3. Dose rate measurements made within the vapor container indicate the radiation level is from 4 to 60 mr/hr, 8 hr after shutdown following full power reactor operation, i.e., 10 Mwt. This will permit safe access to the vapor container for operating and maintenance duties.

4. A need for additional experimentation exists in the areas of radiation on the primary shield tank surface, on and in the snow walls, and on the upper platform of the reactor building. The results of experimentation would provide data to evaluate effectiveness of the boral cladding in the primary shield, improve estimates of dose rates on the upper platform contributed by gamma scattering and neutron capture in the snow and evaluate snow attenuation data to verify the behavior of snow as water having a reduced density.

Thermal and Hydraulic Tests and Analysis

1. No difficulties were encountered in bringing the primary system up to operating pressure and temperature.

2. Test values of temperature and volume changes during the load transient tests were in favorable agreement with analog simulation results.

3. Test pressure changes during increase in load transients were of the same order of magnitude as the analog simulation, while loss of load values were conservative by a factor of 2.

4. Comparisons of the decay heat removal test results showed good agreement with analog results.

5. Measurement of primary loop flow rate was 7% higher than anticipated. This provides for possible reduction in operating pressure.

Radiochemical Tests

1. Gross fission product iodine activity levels in the primary coolant are not a radiation hazard.

2. Long-lived radiation levels are comparable to long-lived radiation levels on SM-1 primary components after an equivalent period of operation.

3. No significant defects exist in PM-2A Core I elements.

1.0 INTRODUCTION

The PM-2A reactor was designed and constructed under a fixed price contract (DA-30-347 ENG-284) between Alco Products, Inc., and the Eastern Ocean District of The Corps of Engineers of the U.S. Army. There was no prior development associated with this fixed price contract. The reactor and its component parts had to be designed for minimum weight, minimum size, ease of construction, and simplicity of design.

Certain tests were required under the original contract, and other tests were conducted under the Pressurized Water Reactor Support and Development Contract, AT(30-1)-2639 with the U.S. Atomic Energy Commission. This report, prepared under Item 2.6, 2.10, and 4.4 of the Program Plan for Engineering Support and Development of Army Pressurized Water Reactor Power Plants,* combines all of the test results involved in the startup and initial operation of the PM-2A.

1.1 GENERAL DESCRIPTION OF THE REACTOR SITE

Camp Century is located on the Greenland ice cap, approximately 150 trail miles east of the Thule Air Force Base. The camp latitude and longitude are: 77° 10' N and 61° 08' W, respectively. (Fig. 1.1) The Greenland ice cap is a massive land bound glacier covering an area of approximately 800,000 sq mi and is approximately 10,000 ft thick near the center. The Camp Century site is 6,000 to 7,000 ft above sea level. Seismic soundings at the camp indicate that the ice cap is 5,000 to 6,000 ft thick at that site.

Meteorological data collected hourly between May 11, 1960 and January 31, 1961, indicated a prevailing ESE wind and an average wind speed of 12 mph. The maximum recorded hourly averaged wind speed during this period was 40 mph, and the lowest and highest recorded temperatures were: -63.5°F and + 48°F. respectively. During the above period, there was 35.4 inches of snowfall.

Camp Century is operated by the Polar Research and Development Command of the U.S. Army's Corps of Engineers. The camp and its nuclear power plant has a multipurpose mission: First, the camp is to provide a base of operations for conducting basic research in Meteorology, Geology, and

---

* AP Note 286, Addendum 1 Revision 1, May 1, 1961.

Glacier Formation and Deformation. Second, it acts as an actual environmental testing laboratory for applied research, from which an evaluation of materials, equipment, and personnel can be obtained under the most severe artic conditions. Third, the construction, operation, and maintenance of the camp itself is to permit the development of arctic construction methods, which minimize the effects of plastic flow of foundations, and which also minimizes logistic support, erection time, and fuel requirements, that make maximum use of local building materials, and that provide maximum protection from the local environment. Fourth, in addition to supplying electric power and steam heat to Camp Century the PM-2A power plant is intended to develop the engineering know-how required for transport, erection, and operation of nuclear plants by a minimum size military crew operating in a remote arctic environment.

Camp Century covers an area of approximately 35 acres. It is composed of a network of 21 interconnected tunnels, four of which contain the various nuclear power plant components (See Figure 1.2.) The tunnels are of the cut and cover variety in which a trench of the appropriate width and depth is cut into the surface of the ice cap, an arched corrugated steel roof is erected over the trench, and the roof is then back-filled with snow, which upon compacting, forms a semi-rigid roof. Inside melting and plastic flow of the tunnel walls are minimized by a series of air wells. These wells draw air through the relatively porous snow walls, expel it into the tunnels and thus maintain a relatively low tunnel temperature of -40 to +15^{o} F. Billet, mess, recreation, and some shop areas inside the tunnels are enclosed in T-5 prefabricated buildings.

Personnel transportation to and from camp is provided by ski-equipped aircraft operating from Camp Tuto, which is located at the edge of the ice cap, and from Thule Air Base, which is located on the south shore of Wolstenholme Fjord. Personnel and freight surface transportation is provided year around by caterpillar drawn and ski-equipped trains, known locally as "Heavy Swings." Surface transportation for personnel is sometimes provided by means of lighter and faster track-equipped vehicles, known locally as "Pole Cats."

Communication with Camp Century is by means of normal military two-way radio and by military mail service.

1.2 GENERAL DESCRIPTION OF THE PM-2A REACTOR CONCEPT

1.2.1 BASIC DESIGN CONCEPT

The PM-2A (Portable Medium Power Reactor 2A) employs a modular design concept which permits:

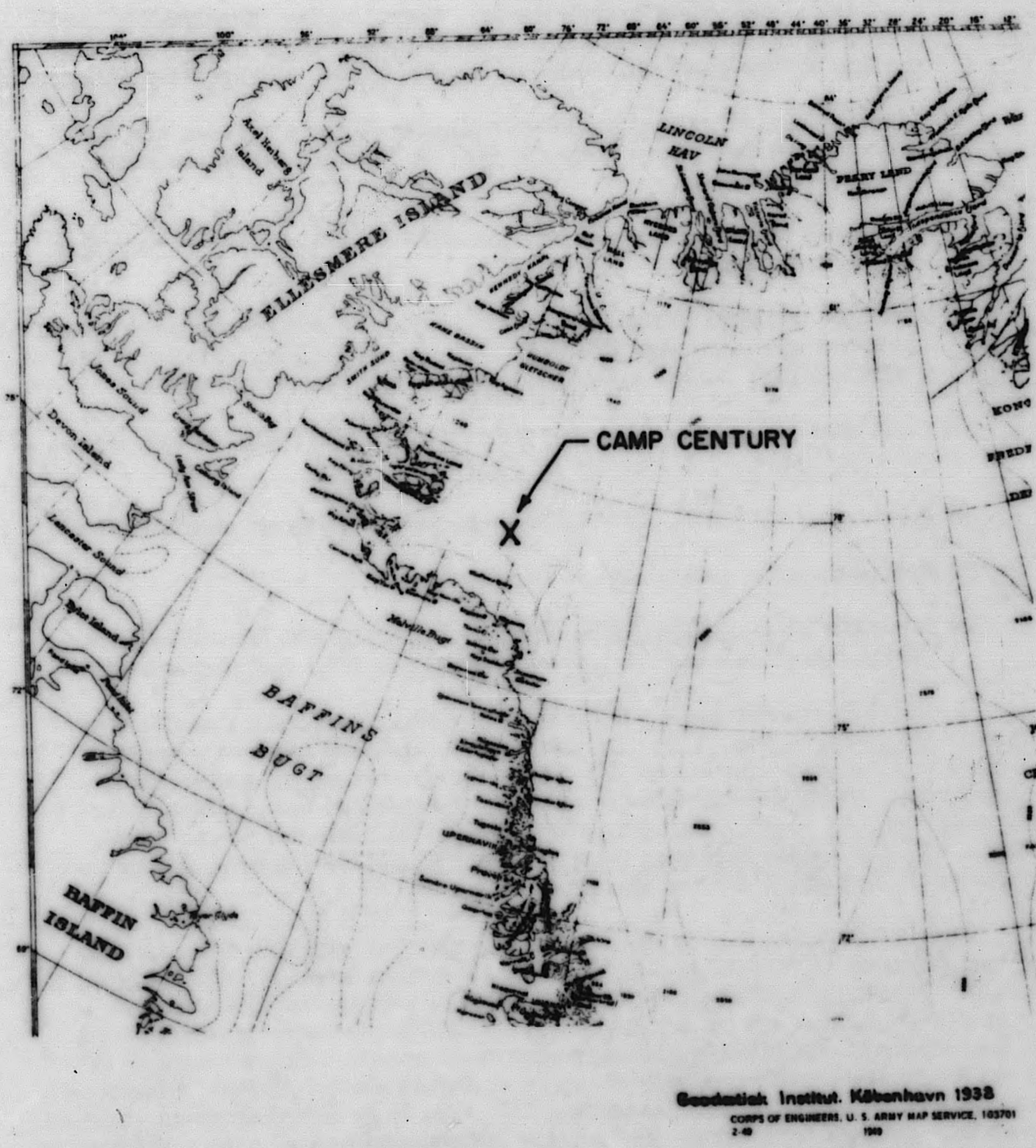

Figure 1.1. Northwest Greenland Showing the Location of Camp Century

1) Complete power plant prefabrication, fitup, testing, dismantling, and packaging for shipment in the U.S. at domestic labor rates, thus minimizing on site construction labor, skills, costs, and erection schedules.

2) Dismantling and relocation of the complete power plant to a remote military site using only basic military skills and a minimum size military crew.

3) Air transport of each power plant module and miscellaneous packages by C-130 aircraft.

4) A simple and safe design, that permits the use of standard power plant hardware wherever possible to increase reliability and minimize replacement part costs, inventories, and procurement schedules.

5) Core operation for at least one year at 80% of the design rating without refueling.

6) Interchangeability of core components with other Army reactor plants.

7) Semi-automatic power level control.

8) Minimum plant capital and fuel costs in keeping with the above plant design objectives and the current status of reactor fuel technology.

A cutaway artist's concept of the PM-2A plant configuration at Camp Century is shown in Fig. 1.3. The design objective was to allow complete access to all plant areas except the reactor tunnel during full power plant operations. A shadow shield is provided for the reactor core, which makes entrance into the vapor container permissible 8 hrs after full power operations. Bulk radiation shielding for all normal work areas is provided by the snow walls separating each of the tunnels.

The PM-2A plant is a pressurized water reactor with a 10 mw thermal rating (2000 kw electrical gross), or a net electrical output of 1560 kw plus 1×10^6 Btu/hr for heating purposes. Stationary fuel assemblies are composed of 18 parallel plates brazed to inert stainless steel side plates to form a fuel element. Each fuel plate contains a fully enriched UO_2 dispersion in a stainless steel matrix, and is clad with stainless steel. Reactor control is maintained by means of withdrawal and insertion of absorber sections equipped with fuel element followers. The control rod absorbers are of the open box construction. They are composed of a Eu_2O_3 dispersion in a stainless steel matrix, and clad with stainless steel.

The plant employs the basic engineering concepts previously established in the SM-1 prototype (APPR-1) now operating at Ft. Belvoir, Virginia.

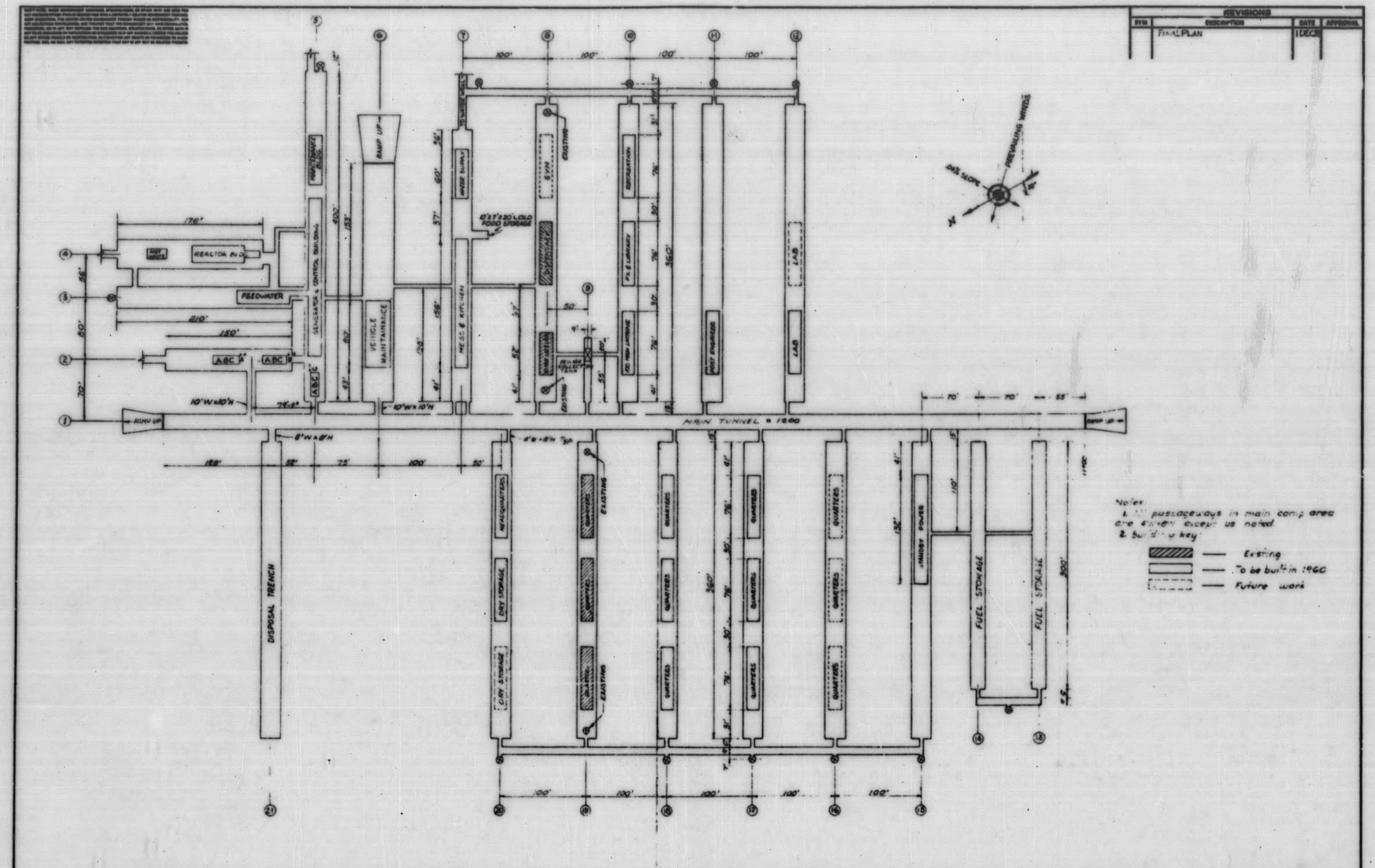

Figure 1. 2. Plot Plan of Camp Century Greenland

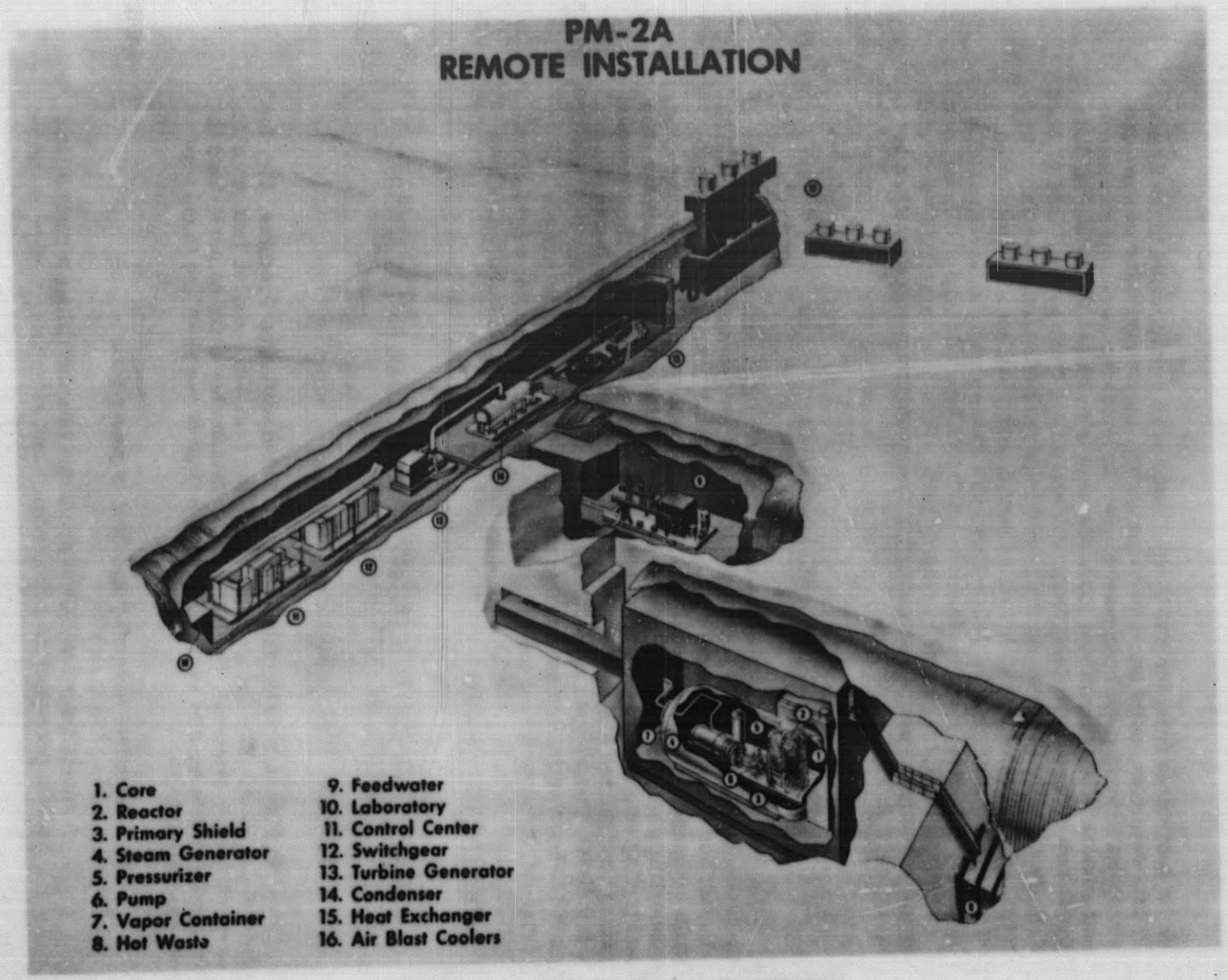

Figure 1.3. PM-2A Remote Installation

Major departures from the SM-1 experience were incorporated in the areas of: heat rejection, solid state instrumentation, steam generator design, and transportability of plant components. Due to the arctic environment, latent heat removal from the turbine exhaust steam is by means of an intermediate glycol loop between a surface condenser and an air blast cooler. Use of solid state components has reduced the power required by the instrumentation and permitted the use of a single isolated power supply for all instrumentation, thus providing complete isolation from plant voltage transients. The steam generator design is of the horizontal evaporator type to comply with shipping dimensional limitations on the primary skid. Plant transportability and total weight reduction is achieved by utilizing the modular concept described in paragraph 1.2.2.

1.2.2 PM-2A MODULES AND PACKAGES

The complete PM-2A plant is composed of 8 functional modules. Five of these modules are further subdivided to permit air transportability by C-130 aircraft and to render 13 basic modular packages. In addition to the basic plant components, 27 additional packages are required for transporting interconnecting piping, auxiliary equipment, spare parts, and miscellaneous shop and testing equipment essential to plant assembly and startup. The maximum package weight and dimension for the C-130 aircraft is 30,000 lb and 9 ft x 9 ft x 30 ft. The weight of the 13 basic modular packages for the PM-2A plant has been estimated as approximately 288 tons, which is roughly 10% of the estimated weight of the prototype SM-1 plant. The total weight of the PM-2A plant including the 27 additional packages described above has been estimated as approximately 413 tons.

1.2.3 SCHEDULE FOR DELIVERY, ERECTION AND STARTUP TESTING OF THE PM-2A PLANT

1.2.3.1 Prefabrication and Stateside Testing

In February 1959, the Army contracted with Aico Products, Inc. for the PM-2A plant. The design concept and the contract required that prior to preparation for shipment, the following stateside shop tests be performed to insure minimum on-site erection time and fitup of the plant and to enhance on-site reliability.

1. A complete assembly and fitup of power plant.
2. A non-nuclear test of the primary system utilizing a conventional steam generator as a heat source and simulating design operating pressure and temperature.

3. A complete secondary system test at full load.

4. Low power nuclear testing of the reactor core to insure that the core met design, fuel, and poison loading specifications.

The first three of these tests were performed at Alco's Dunkirk plant during April 1960, and it was satisfactorily demonstrated to Corps of Engineers' inspectors that the system was abie to produce a full electrical output of 2000 kw and to operate satisfactorily in parallel with emergency diesel generator units.

Nuclear testing of the PM-2A reactor core was performed at Alco's Critical Facility during July 1960. The purpose of the test was to verify the fuel and burnable poison loading in each element, the reactivity available in the core, the critical bank position at room temperature, and the stuck rod positions. During the test, a loading procedure was developed which made possible complete core loading of the pretested core on site without the benefit of the traditional and time-consuming inverse multiplication approach to criticality.

1.2.3.2 Transport to Camp Century

Subsequent to the completion of the Dunkirk shop test, the PM-2A plant was disassembled and packaged for shipment according to a prearranged plan that allowed rapid and sequential access to the equipment as needed on site. The packaging of the entire plant required 8 weeks to complete. The plant was loaded on 18 railway flat cars and shipped to Buffalo, N.Y. for loading onto the USNS Marine Fiddler. Four days were required for loading plus two additional days for blocking and tying down the packages in the hold of the ship. The ship left port on the night of June 27, 1960, destination Thule, Greenland, by way of the Welland Canal and the St Lawrence Seaway.

At Thule, the entire PM-2A plant was unloaded by the U.S. Army Transportation Corps from the ship, loaded on trucks, and transported 15 miles inland to Camp Tuto and thence to Camp Century by means of heavy swing. The first heavy swing transporting the PM-2A left Camp Tuto on July 13 and arrived at Camp Century on July 17. A heavy swing consists of several trains of 10- and/or 20-ton capacity ski-equipped flat beds towed by modified D-8 caterpiller tractors for freight shipment, plus a radio-equipped command train with billet and mess facilities for the crew and passengers. Delivery of all major components of the PM-2A plant to Camp Century was completed by the end of July 1960.

The Corps of Engineers did not consider air shipment of the plant necessary at that time because of the high cost of air transport; however, the con-

cept of air transportability was satisfactorily proven when an air blast cooler was air transported from Dover AFB to Thule, Greenland, on May 27, 1960, having been selected chiefly because it met the maximum size and weight limitations. The PM-2A fuel elements and control rod absorbers were air shipped from Dover AFB to Thule, Greenland, in August 1960. The fuel-shipping containers consisted of twelve 55-gal drums filled with rubberized filaments and slotted to allow the insertion of four fuel element sections into each barrel.

1.2.3.3 On Site Erection of the PM-2A Plant

The first heavy swing arrived at Camp Century on July 17, 1960, with 18 modules and packages, and construction was started the same day. Polar Research and Development Command (PRDC) construction forces on site were responsible for handling and moving the major components onto their respective foundations. The military operating crew of the nuclear power plant were responsible for the erection of all interconnecting piping, wiring, checking, testing, and operation of the power plant. The construction and erection personnel for the PM-2A was made up of 19 military crewmen who had received formal reactor operations training at the Army's SM-1 plant at Ft. Belvoir and had also taken part in the shop assembly, testing, disassembly, and packaging of the PM-2A at Alco's Dunkirk, N.Y. plant. This crew was supplemented by 12 military construction men from the PRDC forces at Camp Century. The supervision consisted of three officers and six Alco Engineers to handle around-the-clock construction operations.

The on-site construction proceeded approximately as scheduled for about three weeks. In this period, all major components had been pulled into position inside the tunnels, leveled, and secured to the foundations. After three weeks, it became evident, however, that the six weeks construction schedule would not be met due to delays in other non-nuclear power plant areas, such as late deliveries of some of the power plant buildings, heating and ventilating equipment, and the glycol pipe enclosures - all of which delayed facilities construction, and consequently systems testing, because certain buildings were incomplete and without heat.

1.2.3.4 Initial Fueling and Startup Testing of the PM-2A Plant

Late in September, these utility construction problems had been solved to the extent that would allow the core to be loaded and low-power nuclear testing to commence. The core was fueled in the previously tested sequence and geometry, and the reactor attained criticality at 06:52, October 2, 1960.

Following initial criticality, low-power nuclear tests were performed in parallel with the completion of the remaining camp buildings and utilities.

These measurements were directed to neutron source evaluation, stuck rod measurements, control rod calibrations, temperature and pressure coefficients, cold and hot critical control rod bank positions and shielding survey measurements.

In November, the PM-2A was put on the line for power runs of 2, 3, and 10 hr duration, respectively and assumed the full camp electrical load, which was approximately 600-800 kw at that time. It has also operated satisfactorily in parallel with the stand-by diesel power units. During these early power runs, it was determined that excessively high radiation levels existed on the upper level of the reactor building and around the primary shield. Several plant survey and radiation mapping experiments were performed in order to locate the source and intensity of these radiations and to provide data upon which a shielding modification could be based. The plant was not operated for power generating purposes during the months of December 1960 and January 1961, in order to prevent activation of plant components and to allow a shielding modification to be made.

On February 9, 1961, the plant was placed in service; and it satisfactorily completed the acceptance testing power run on February 26, 1961. The plant was formally accepted by the Army on March 8, 1961.

2.0 PM-2A SYSTEM DESCRIPTION

2.1 PM-2A CORE DESCRIPTION AND COMPOSITION

The major design objectives for the PM-2A Core I was to obtain a core with a thermal rating of 10 Mw and a core life expectancy of one year at an 80% load factor. The core is composed of 32 stationary- and 5 control-rod fuel assemblies arranged in a 7 x 7 array with three assemblies missing from each corner, (1) Fig. 2.1. The core is water moderated, cooled, and reflected. Core control is maintained by withdrawal or insertion of five control rod assemblies, each of which contains an absorber and a fuel element follower. Upon withdrawal of the control rod absorbers, the fuel element follower is simultaneously inserted from the bottom of the core. The PM-2A Core I contains 19.49 kg of fully enriched U-235 in the form of UO_2 and 17.0 gm of B-10 in the form of B_4C. Calculations[2] based upon zero power experiments[3] and the tests obtained at the start of core life (ref. chapter 3) indicate that the excess core reactivity was 14.3%ρ at a core temperature of 68° F. At a power level of 10 Mwt and with equilibrium xenon concentration in the core and a core temperature of 510° F., the excess core reactivity was calculated as 5.34%ρ . Based upon these measurements and calculations, the life expectancy of the PM-2A Core I is estimated as 10.7 MWYRS.

2.2 PM-2A FUEL AND CONTROL ROD ASSEMBLIES

A stationary fuel assembly[4] is illustrated in Fig. 2.2. These fuel assemblies consist of 18 parallel fuel plates brazed to inert stainless steel side plates. Each of the individual fuel plates is fueled with 25 w/o UO_2 dispersed in a stainless steel matrix. The fuel matrix is then clad with stainless steel to prevent fuel and fission product contamination of the primary coolant. The fuel matrix is 0.020 in. thick and has 0.005 in. cladding on each side. End boxes provide structural support and alignment for stationary fuel elements. Each stationary element contains 542.34 gm U-235 and an average of 0.473 gm B-10 as determined by chemical analysis.

PM-2A control rod assemblies consist of a control rod fuel element[5], Fig. 2.3, and a control rod absorber, Fig. 2.4, contained in a control rod basket, Fig. 2.5. The manufacturing and composition of control rod and stationary fuel elements are similar; however, the control rod elements contain only 16 fuel plates, have smaller dimensions than the stationary fuel elements, and are not provided with end boxes. An integral flux suppressor composed of Eu_2O_3 dispersed in stainless steel forms the top 7/8 in. of each control rod fuel matrix. The fuel and poison loading for control rod fuel elements are 427.2 gm U-235 and 0.373 gm B-10, respectively.

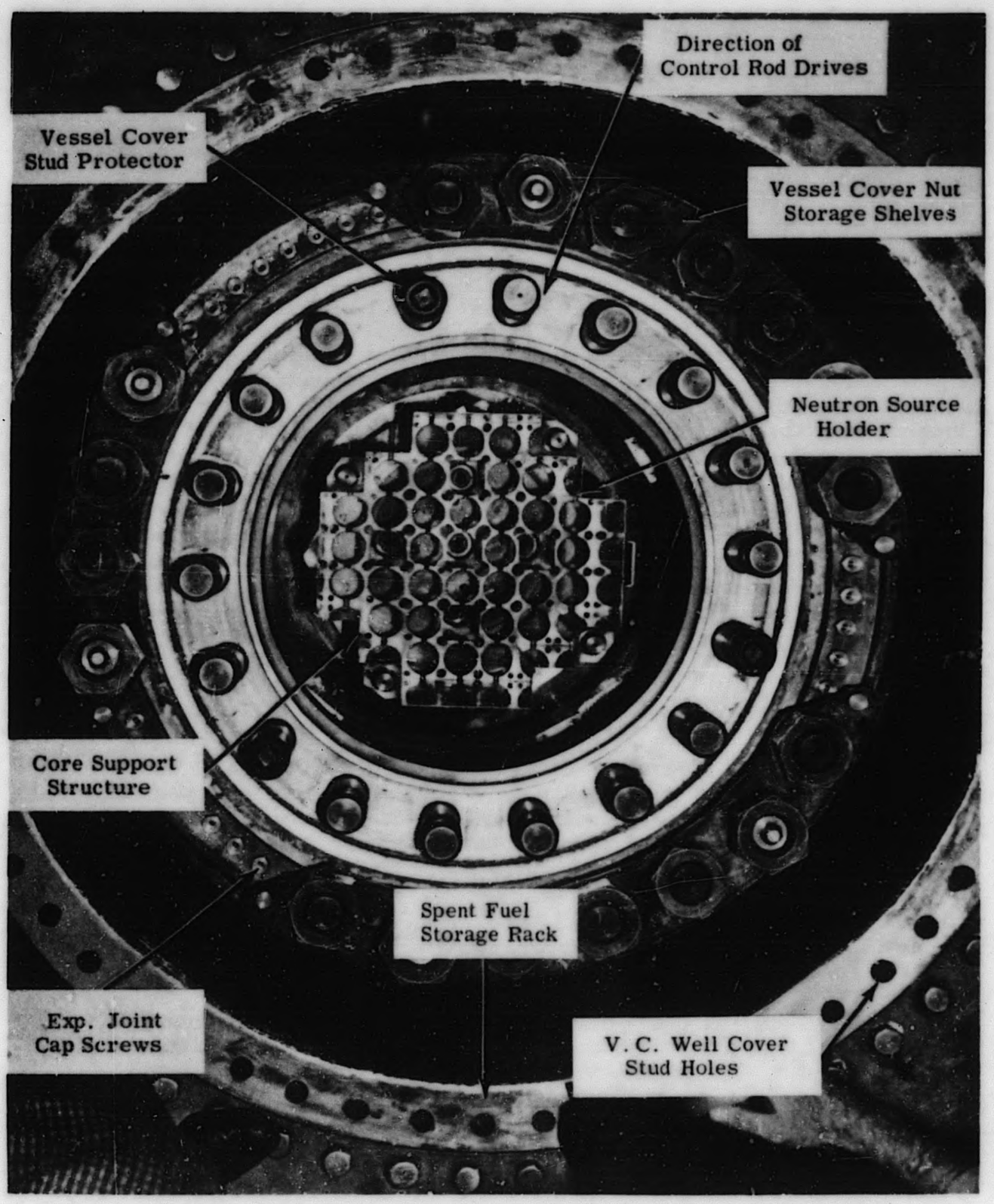

Figure 2.1. Plan View of PM-2A Core and Vessel with Pressure Vessel Cover Removed

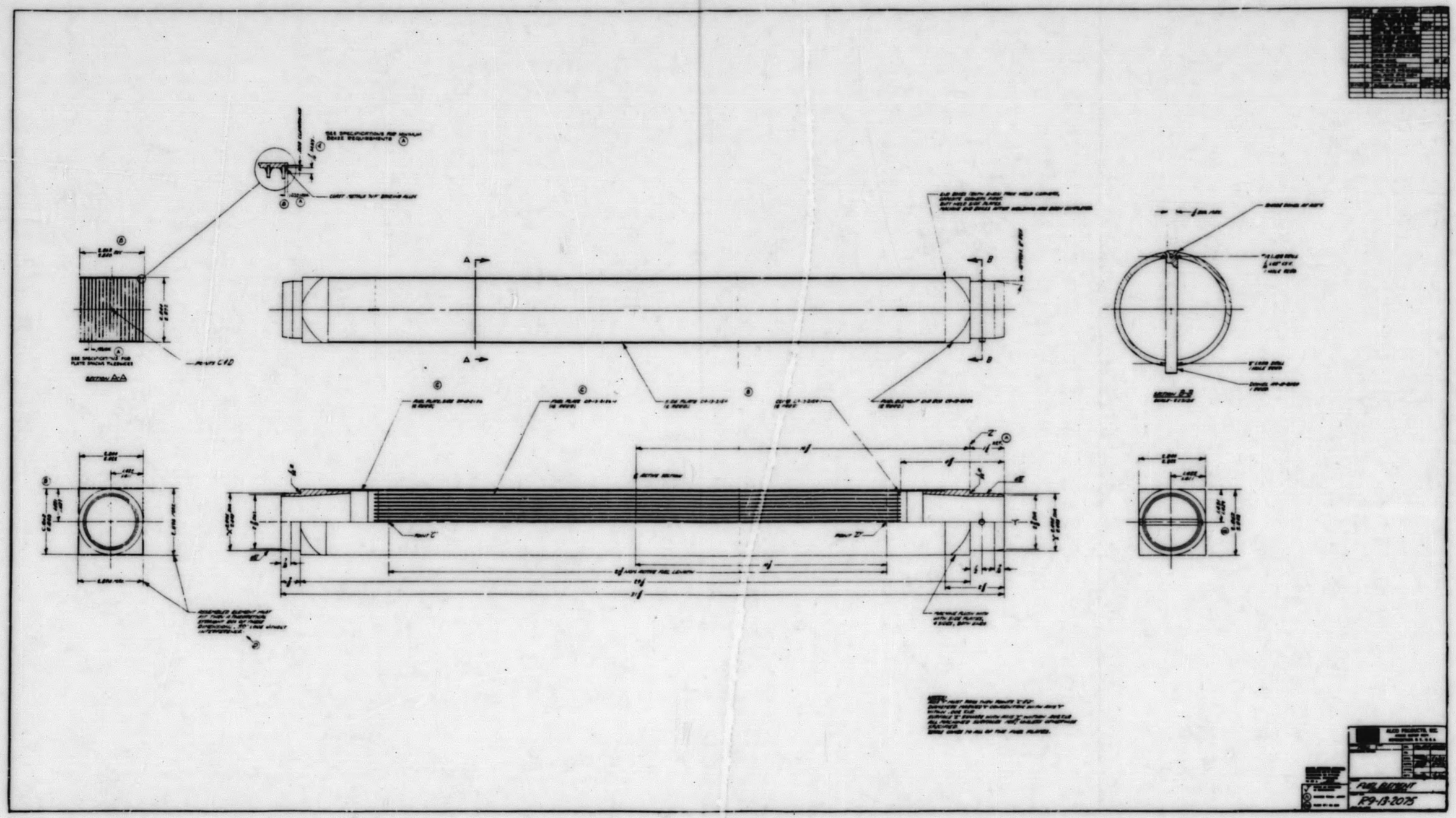

Figure 2.2. PM-2A Stationary Fuel Element

The control rod absorber section,[6] Fig. 2.4, consists of an open box formed by welding four absorber plates together along the edges. The absorber plates are fabricated in a manner similar to that utilized for fuel plates. The absorber plates are composed of europium oxide dispersed in a stainless steel matrix and clad with stainless steel. Each absorber plate is 0.156 in. thick.

The complete control rod assembly, Fig. 2.5, consists of a fuel element, absorber section, cap and a tube, and a piston and rack assembly. The fuel element and absorber section are housed in the square tube and held in place by means of the control rod cap. The configurations of the fuel element, the absorber, and the cap are such that the control rod cannot be improperly assembled; i.e., the element must be properly oriented and installed first and the absorber must follow the fuel element into the control tube for the cap to engage the tube properly. Furthermore, the cap is so designed that the handling tool cannot be disengaged from the cap until the cap is properly installed in a control tube.

The rack assembly is bolted and keyed to the piston. Locomotion is provided for the control rod assembly by means of a pinion and the control rod drive mechanism. Upon reactor scram the control rod assembly falls under the force of gravity until the piston on the control rod assembly (Fig. 2.5) enters a dashpot on the carrier pinion bearing support (Fig. 2.6) thus providing deceleration over the lower end of travel.

2.3 CORE SUPPORT STRUCTURE

The core support structure,[7] Fig. 2.2 and 2.6, locates and supports the stationary fuel elements and guides the control rods. The structure is shop fabricated and is lowered as a complete unit into the reactor pressure vessel. The components of the structure consist of the orifice plate, the top plate, the upper skirt, the bottom plate, the lower skirt, the support plate, the baffle plate, the pinion-bearing support carrier, the pinion-bearing supports, and the necessary latches, tie rods, and fasteners.

The five pinion bearing supports, which include the control rod dashpots and the control rod rack rollers, are supported by the pinion bearing support carrier which in turn is spaced and supported from the support plate. The baffle, which distributes the inlet flow, is retained by the carrier at the bottom and by the support plate at the top.

The bottom plate is supported by and spaced from the support plate. The lower skirt, which straightens the flow up-stream of the bottom plate, is retained by the support plate at the bottom and by the bottom plate at the top. The bottom plate locates and orients the lower end of the stationary fuel ele-

ments in large pilot holes. Square holes permit passage of the control rods through the bottom plate. A clearance of approximately 1/8 in. is provided between the control rod assembly and the bottom plate. The pilot holes provide an entrance passage for coolant flow from the lower plenum into the stationary fuel elements. In addition, smaller holes in the plate provide entrance passage for coolant around the stationary fuel elements and the control rod tubes or through the lattice.

The top plate is supported by and spaced from the bottom plate, and is held in place by four latches. The orifice plate is fixed to the top plate and becomes an integral part of the top plate. The upper skirt, which confines the total coolant flow within the active core area and regulates the flow velocity, is retained by the top and bottom plates. The orifice plate is designed to distribute the flow and regulate pressure drop through the core. Square holes permit passage of the control rods through the top plate and provide lateral support to the top of the control rod assembly. A total nominal clearance of 0.028 in. is provided between the top plate and the control rod.

2.4 REACTOR VESSEL

The reactor core, including control rod assemblies, is enclosed within a pressure vessel[7], Fig. 2.7. The pressure vessel, which is 124-9/16 in. long (including insulation and drain nozzle), consists of a cylindrical shell, 37-1/2 in. I.D., a 39-1/2 in. hemispherical head to close the bottom of the vessel, and a flanged elliptical head for the top closure. The top closure is sealed by an octagonal gasket and is attached by means of 18 studs, 2-3/4 in. diameter, threaded into the upper flange of the pressure vessel.

The vessel is designed and fabricated in accordance with applicable sections of the ASME Boiler and Pressure Vessel Code, Section VIII, "Unfired Pressure Vessels," 1956, and Code Case 1234. The octagonal gasket is made from 304 stainless steel, and all internal surfaces of the pressure vessel are clad with 3/16 in. thick 304 stainless steel.

The pressure vessel shell and fixed head are penetrated at five points; i.e., two, 10-in., integrally reinforced, primary coolant nozzles, one 1-1/4 in. nozzle for the decay heat system, one 1-1/4 in. nozzle in the bottom head for the decay heat system and draining, and one multiple-opening penetration for the five tubular members which house the control rod drive shafts. The latter tubes extend outward in a cluster a distance of 54 in. from the centerline of the pressure vessel.

Four vessel supports 90° apart and 84 in. below the vessel flange locate and position the pressure vessel in the shield tank on the primary skid. Four

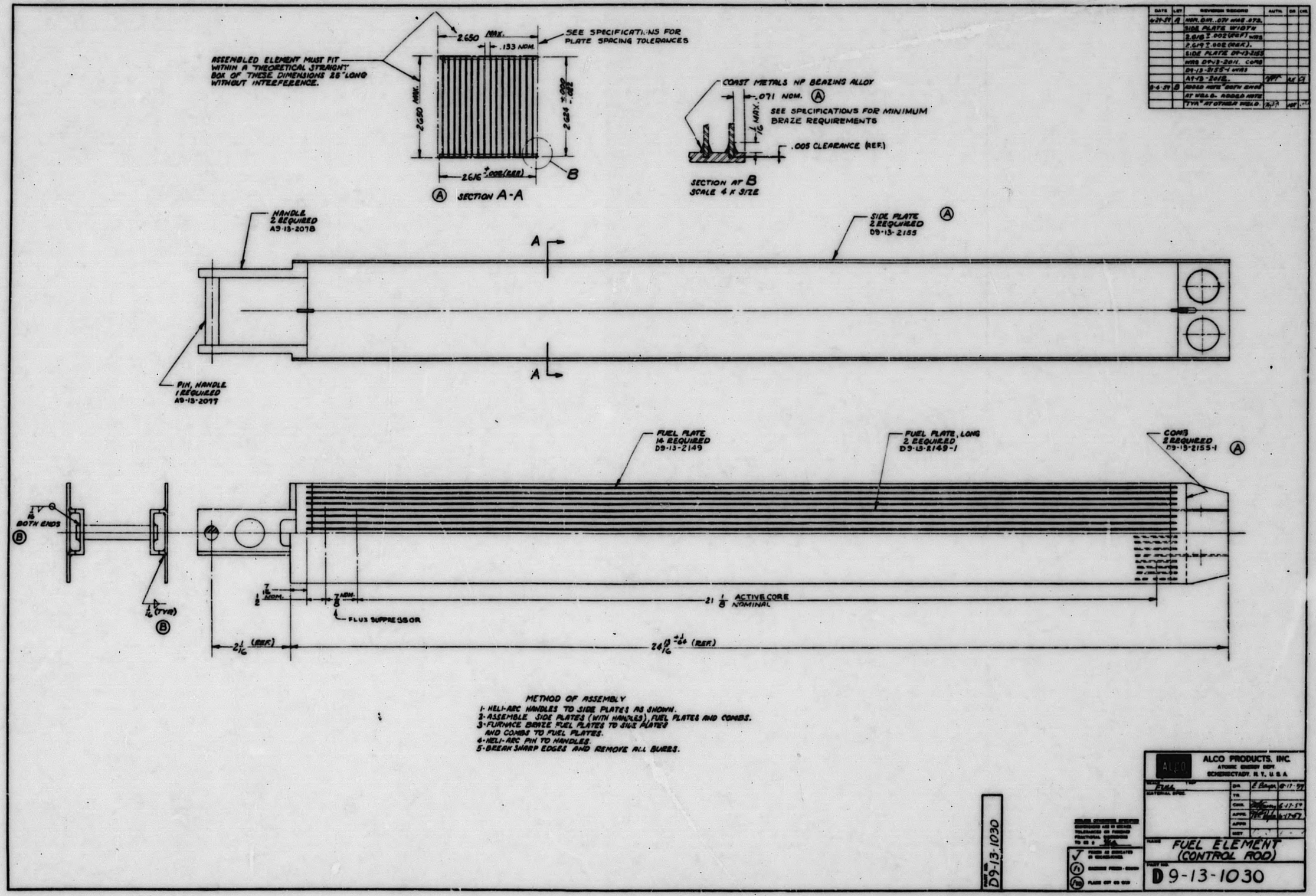

DATE	LET	REVISION RECORD	AUTH.	DR	CHK.
4-29-59	A	MIN. DIM. .071 WAS .072.			
		SIDE PLATE WIDTH			
		2.616 ±.002 (REF.) WAS			
		2.619 ±.002 (MAX.).			
		SIDE PLATE D9-13-2155			
		WAS D9-13-2011, COMB			
		D9-13-2155-1 WAS			
		A9-13-2018.	[illegible]	[illegible]	[illegible]
8-6-59	B	ADDED NOTE "BOTH ENDS"			
		AT WELD. ADDED NOTE			
		"TYP." AT OTHER WELD.	[illegible]	[illegible]	[illegible]

METHOD OF ASSEMBLY
1. HELI-ARC HANDLES TO SIDE PLATES AS SHOWN.
2. ASSEMBLE SIDE PLATES (WITH HANDLES), FUEL PLATES AND COMBS.
3. FURNACE BRAZE FUEL PLATES TO SIDE PLATES AND COMBS TO FUEL PLATES.
4. HELI-ARC PIN TO HANDLES.
5. BREAK SHARP EDGES AND REMOVE ALL BURRS.

ALCO PRODUCTS, INC.
ATOMIC ENERGY DEPT.
SCHENECTADY, N. Y., U. S. A.

DR.	E. Sharpe	6-17-59
TR.		
CHK.		6-17-59
APPR.		6/17/59
APPR.		
SHT.		

FUEL ELEMENT (CONTROL ROD)

D9-13-1030

D9-13-1030

Figure 2.3. PM-2A Control Rod Fuel Element

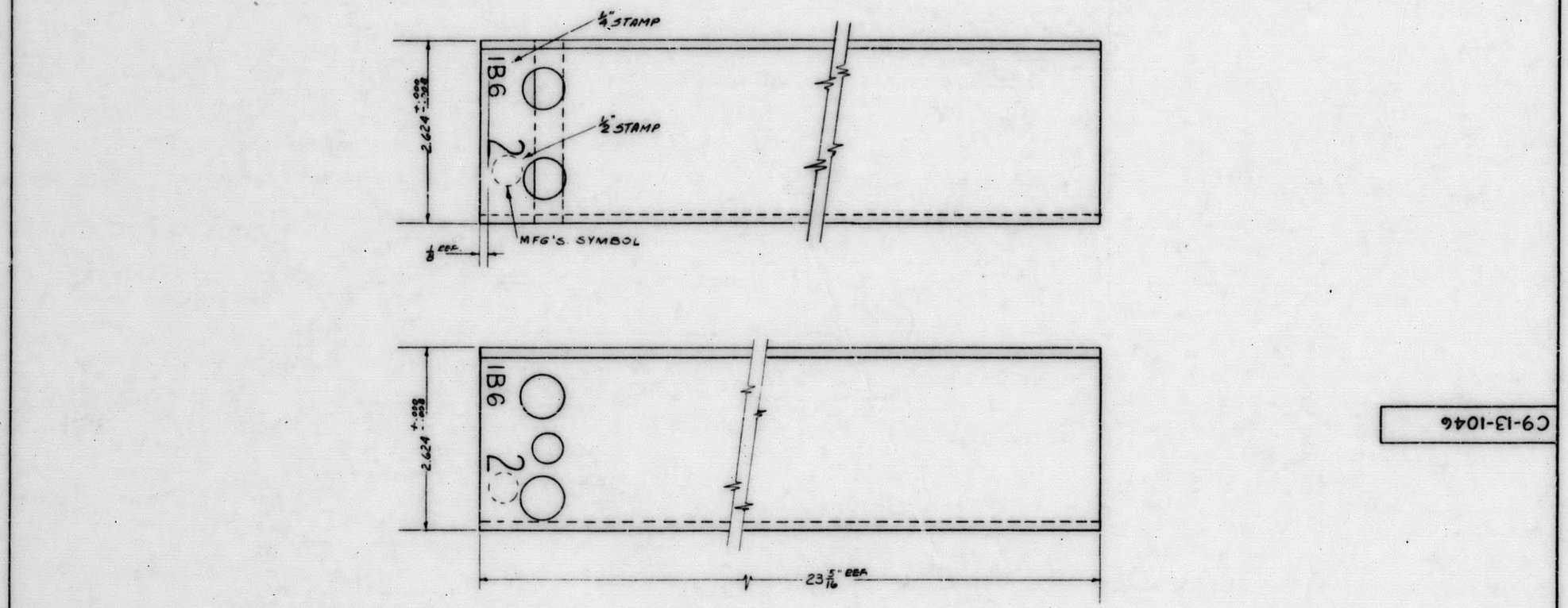

C9-13-1046

ALCO PRODUCTS INC.
NUCLEAR POWER ENGINEERING DEPT.
SCHENECTADY N.Y. U.S.A.

SCALE: FULL	DRP	DR.	C.L.	7-21-60
MATERIAL SPEC.		TR.		
		CHK.		
		APPR.		
		APPR.		
		MET		

NAME
ASSEMBLY ABSORBER SECT.
PM 2A

PART NO.
C9-13-1046

Figure 2.4. PM-2A Control Rod Absorber Section

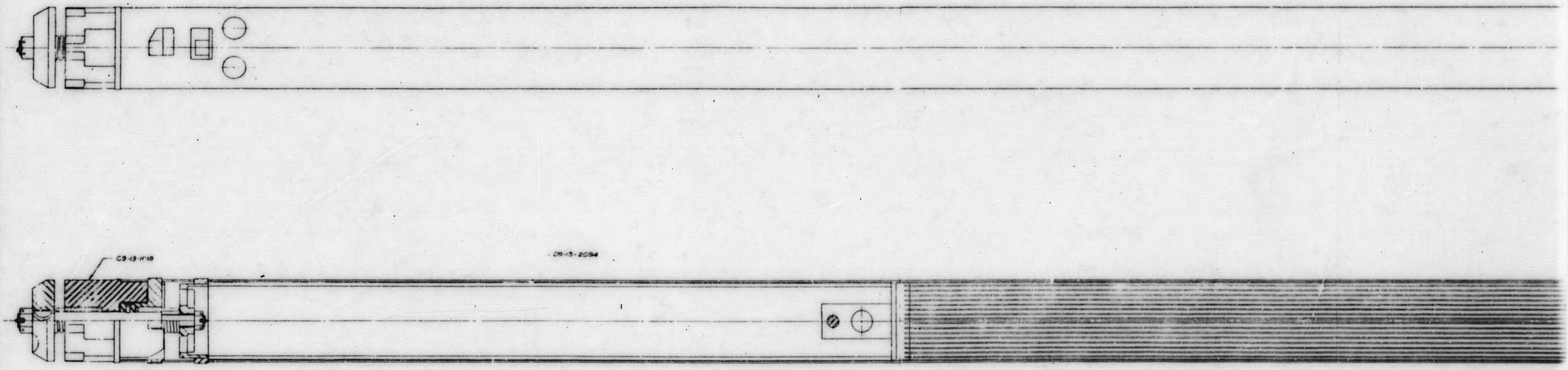
C9-13-1119
D9-13-2094

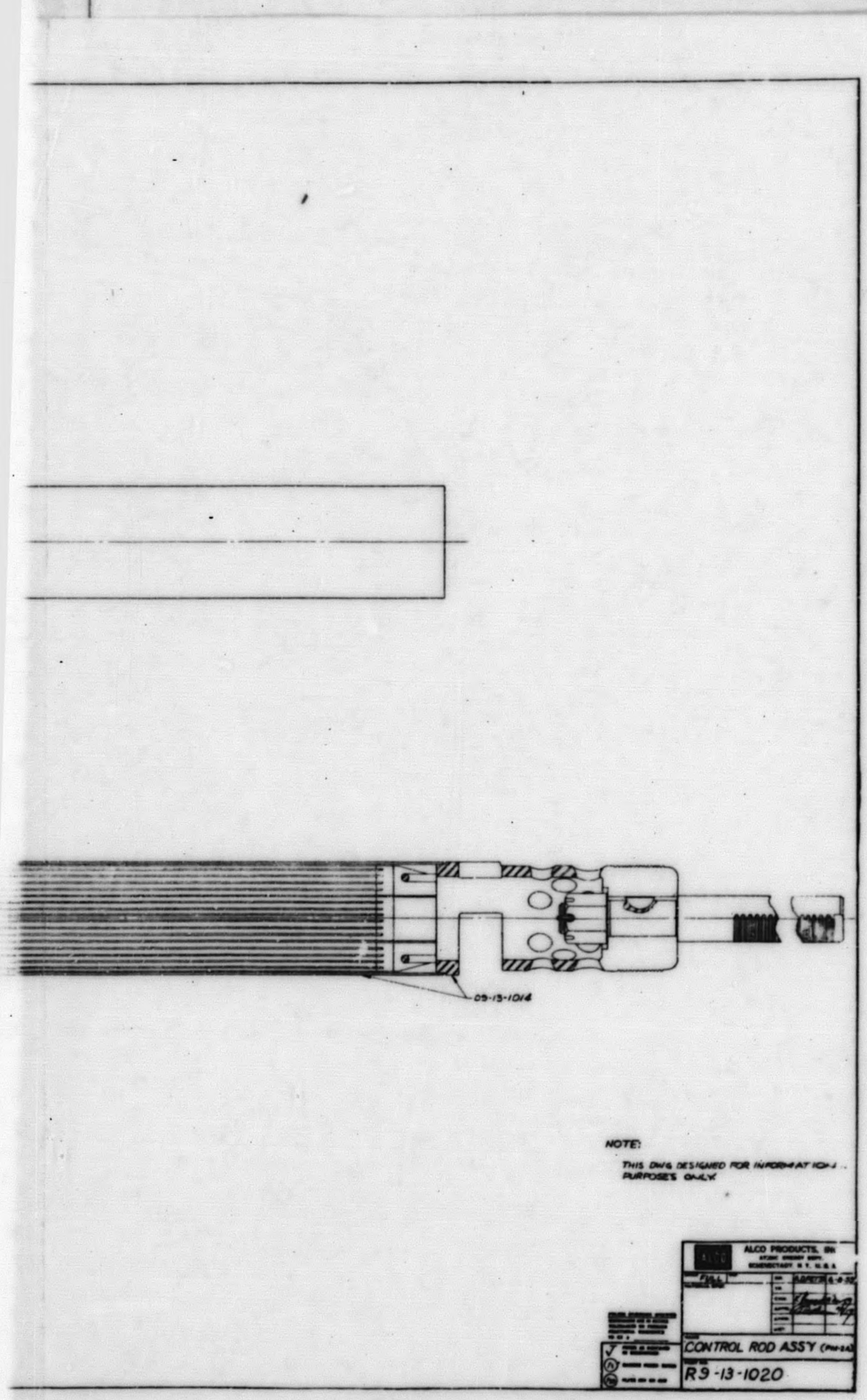

Figure 2.5. PM-2A Control Rod Assembly

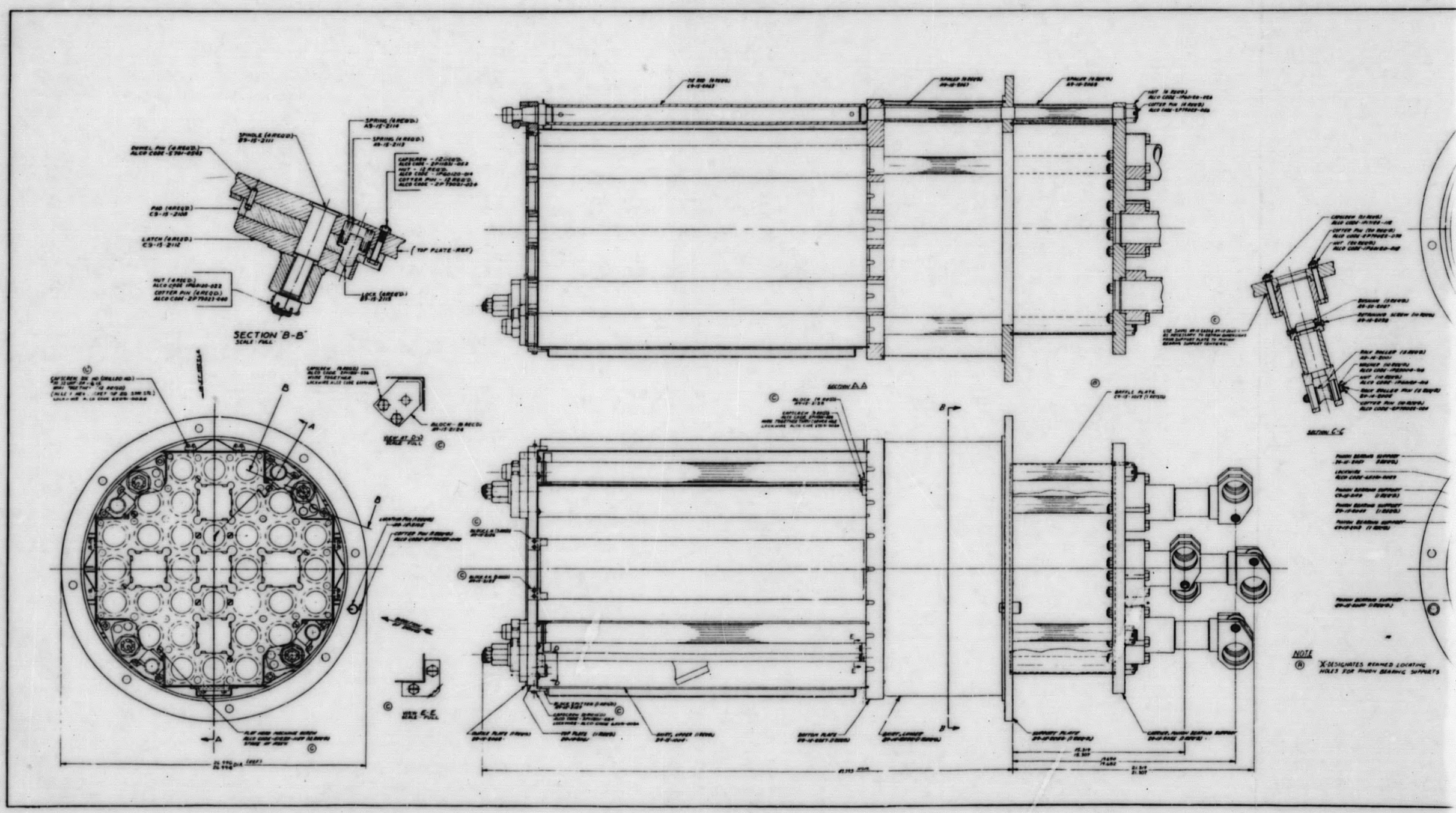
SECTION "B-B"
SCALE - FULL
SECTION A-A
SECTION C-C
NOTE
Ⓐ X-DESIGNATES REAMED LOCATING HOLES FOR PINION BEARING SUPPORTS

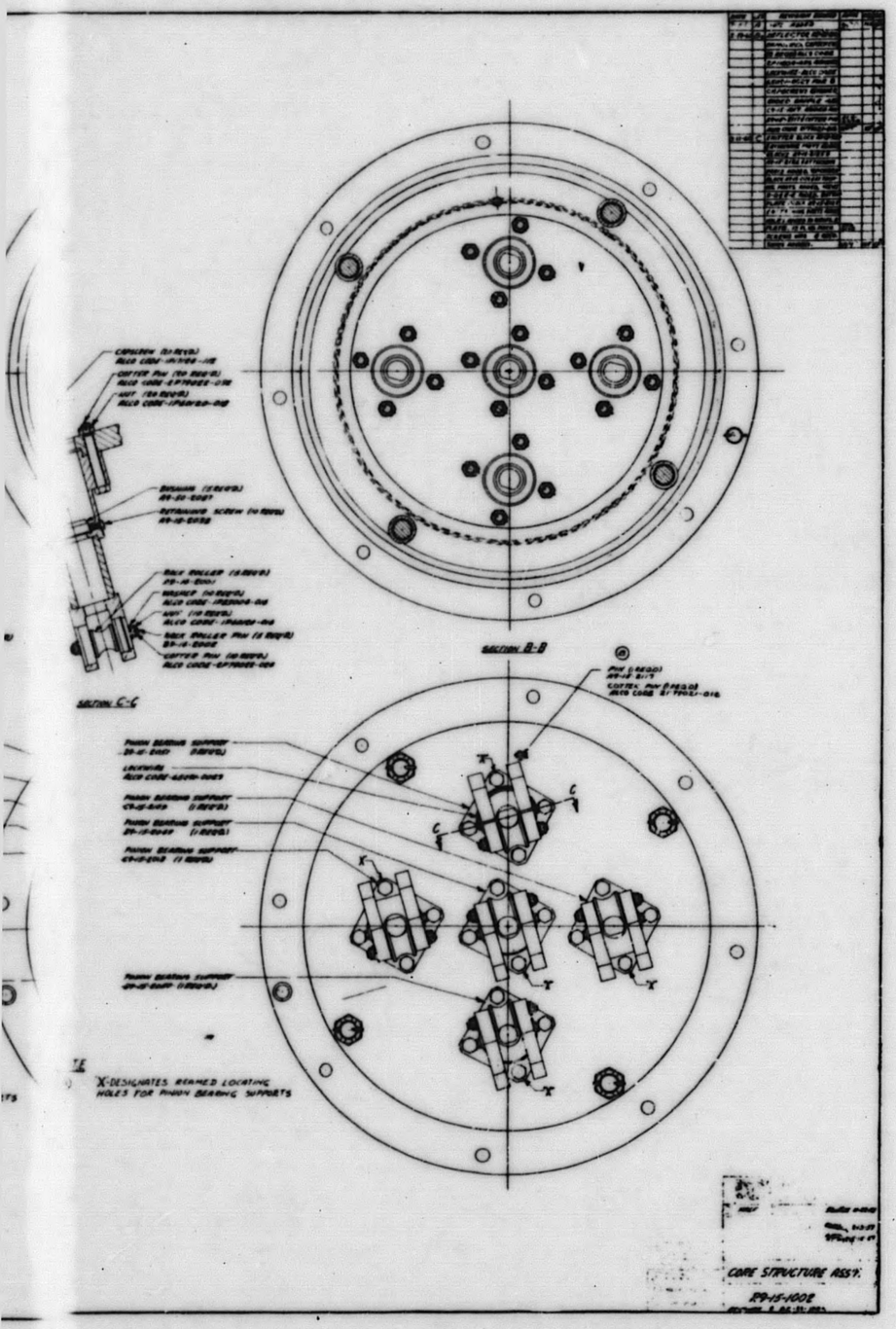

Figure 2.6. PM-2A Core Structure

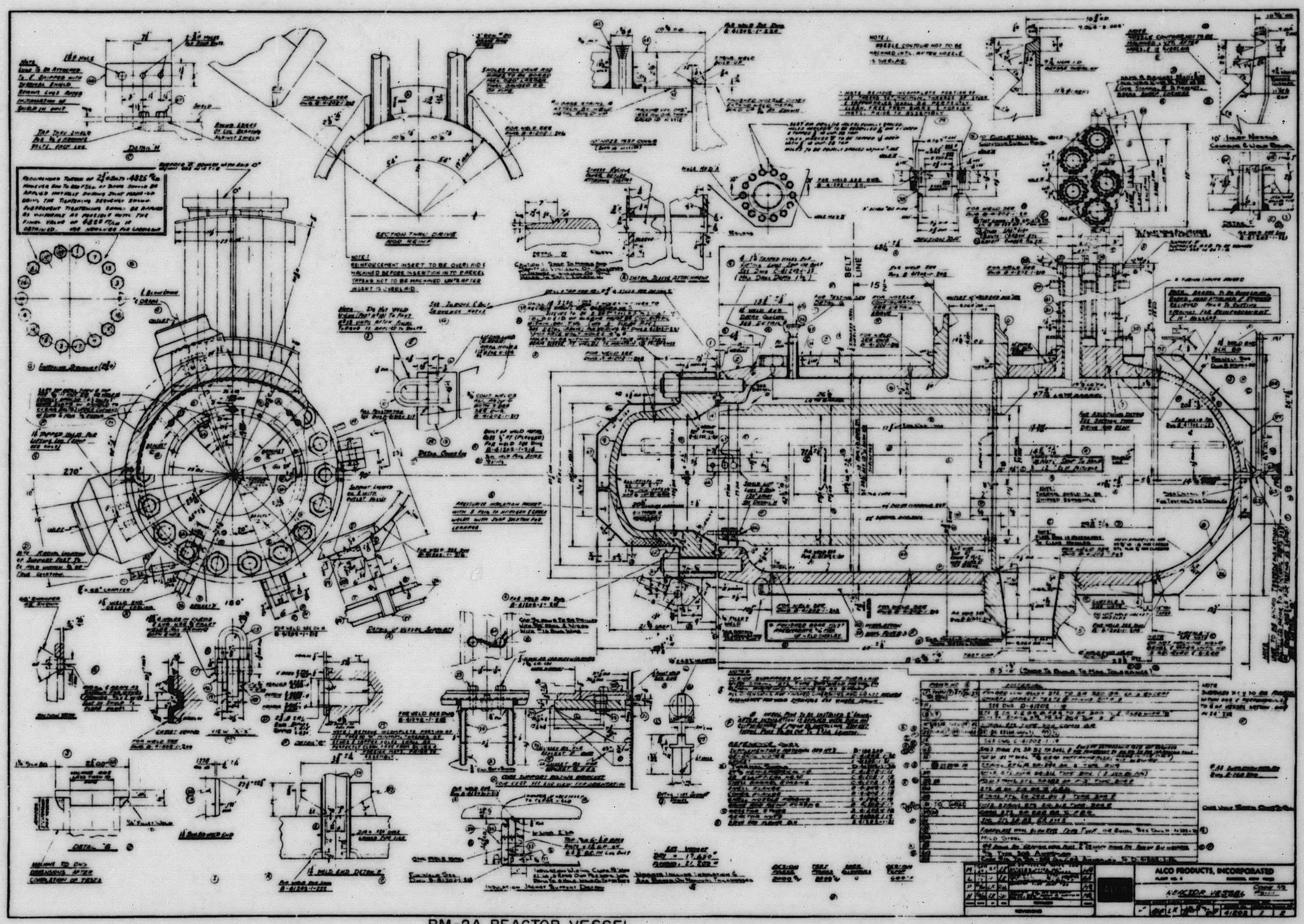

Figure 2.7. PM-2A Pressure Vessel

core support bolting brackets are located internally 90° apart at a level midway between the inlet and outlet primary coolant nozzles. The latter brackets locate and secure the support ring which in turn locates and secures the core support structure, helical baffle, and thermal shield.

The thermal shield is a two-in. thick cylinder, 23-1/2 in. I.D., made of cast SA-351 Gr. CF8 stainless steel. A thermal shield surrounds the active core inside the pressure vessel and reduces thermal stresses in the vessel wall caused by gamma heating. The 360° helical baffle is located between the thermal shield and the pressure vessel wall to provide positive circulation of primary coolant.

The pressure vessel shell and the removable head are surrounded by 2 in. of thermal insulation which is jacketed with 1/8 in. thick 304 stainless steel around the vessel and 3/16 in. thick 304 stainless steel over the cover.

2.5 PM-2A PRIMARY SYSTEM COMPONENTS AND AUXILIARIES

The primary system is composed of the reactor, which has been covered previously, the primary pump, steam generator, pressurizer interconnecting piping, and auxiliaries. Descriptions of these items follow. Figure 2.8 shows the primary system skid arrangement, and Fig. 2.9 is a flow diagram of the PM-2A primary system.

2.5.1 PRIMARY CIRCULATING PUMP

The primary pump[8] is a vertical-shaft, single-stage, single-suction, centrifugal pump having vertical inlet and horizontal discharge, and a "canned rotor" induction-type drive motor. The pump is hermetically sealed and designed for double thrust; i.e., both up and down. The pump circulates the primary coolant through the reactor and steam generator. The pump case is welded into the primary piping. The motor and impeller assembly is flanged into the pump case and removable from it. Provision is made for seal welding, but will be used only in the event of damage to the gasket or flange faces. Zero leakage is a specific requirement. The pump output is 4890 gpm at 49 ft head and 500° F. The major components of this assembly are constructed of Type 304 stainless steel.

The unit is designed for a minimum of 18,000 hr of maintenance-free operation at rated operating conditions and has a normal life expectancy of 20 yr. The unit has no mechanical seals or stuffing boxes between motor and pump. Sealing is maintained by having motor cavity and pump at the same pressure. This is accomplished by flooding the motor cavity with the fluid being pumped. A "canned motor" means that the rotor and stator of the motor

are canned in liners of highly corrosion resistant material to eliminate access of fluid pumped to the rotor or stator. Because the fluid pumped is at high temperature, the motor is encased by a cooling coil to remove the electrical and mechanical heat generated. Heat is dissipated to the auxiliary cooling water system.

2.5.2 STEAM GENERATOR

The steam generator[7], a horizontally mounted tube-in-shell, two-pass unit with "U" bend tubes, is fabricated in accordance with Section VIII of the "ASME Unfired Pressure Vessel Code." It supplies 37,700 lb of dry, saturated steam per hr. at 480 psia and 462.8° F. It is basically a carbon steel vessel, but all materials in contact with the primary fluid are stainless steel Type 304, either solid or integrally clad on carbon steel.

The unit, which is approximately 144 in. in over-all length, consists of a cylinder, 48 in. ID by 47 in. long that has a 2:1 elliptical head on one end and a transition piece necking the other end down to the integral closing flange and tube sheet. The closure consists of a flat head with two penetrations to which standard 10 in., 1500 weld neck flanges are welded. These flanges are the primary coolant water inlet and outlet piping connections. The flat head is 10-3/4 in. thick and is sealed by an octagonal stainless steel gasket and attached by means of 22 alloy steel studs, 2-3/4 in. in diameter, threaded into the integral closing flange and tube sheet. All nozzle penetrations are suitably reinforced.

The steam generator is covered by 4 in. of insulation and secured to the skid, allowing movement horizontally along its long axis for expansion.

2.5.3 PRESSURIZER

The primary loop pressurizer[7] performs the basic function of maintaining the primary loop system at the operating pressure. This is accomplished by keeping its contained water, which is essentially static, at saturation temperature corresponding to the desired pressure. The upper portion of the pressurizer volume is occupied by steam in thermal equilibrium with the water, and exerts system pressure on the primary loop. A secondary function of the pressurizer is to suppress the pressure excursions resulting from changes in plant load and their associated temperature transients in the primary coolant system.

The pressurizer is a cylindrical pressure vessel 25-1/2 in. ID with hemispherical heads. The wall thickness of the cylindrical section is 2-1/16

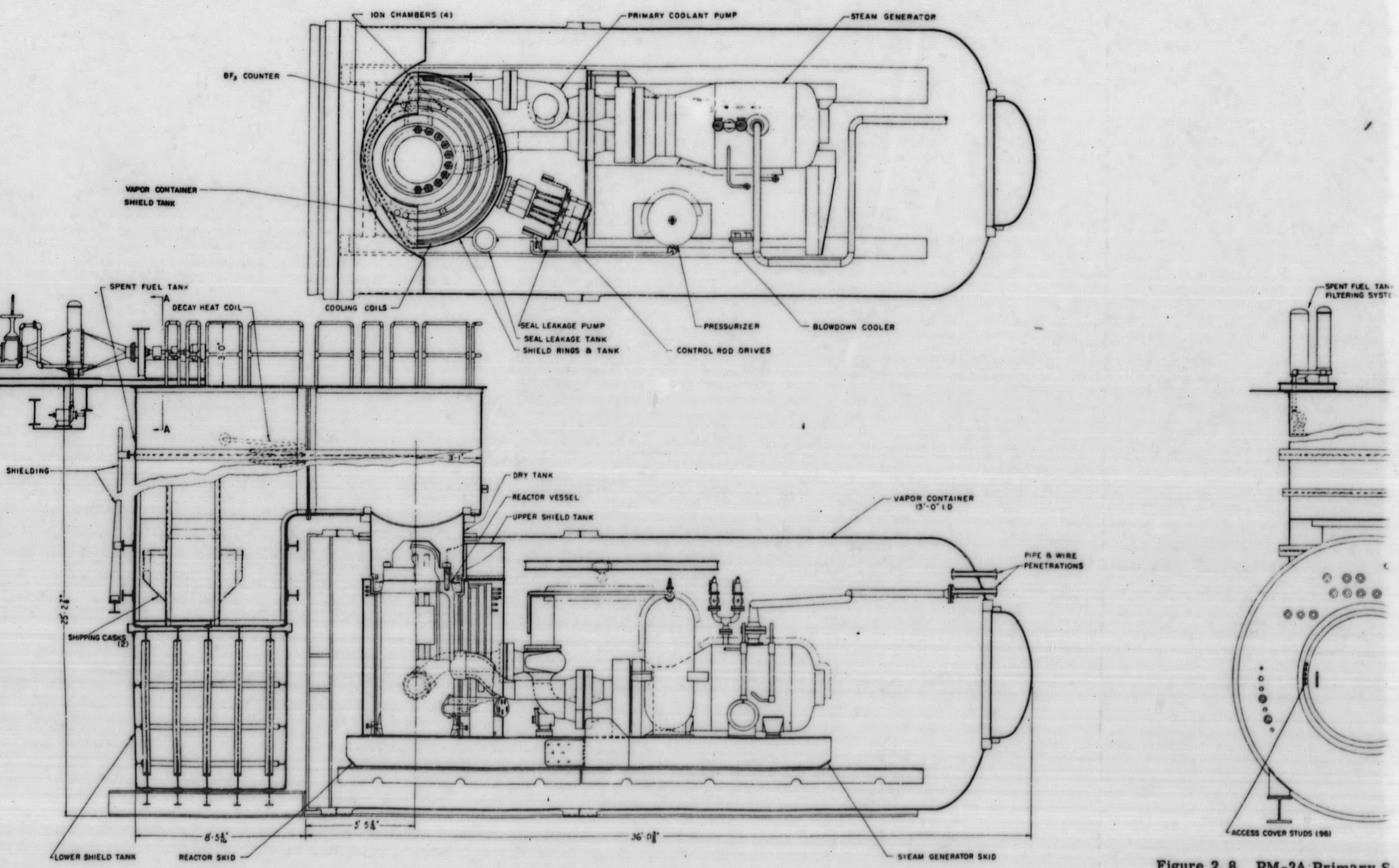

Figure 2.8. PM-2A Primary S

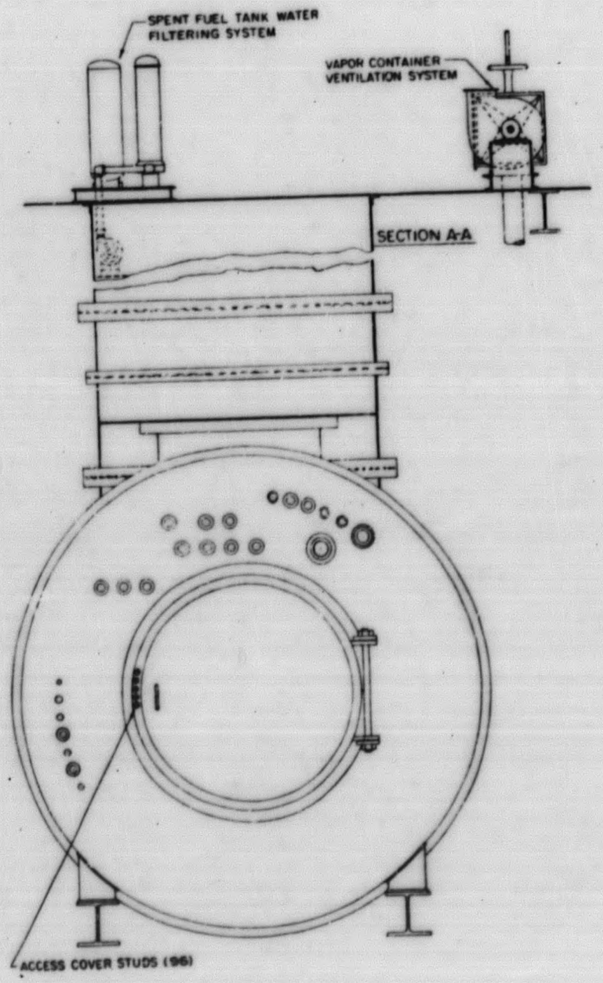

e 2.8. PM-2A Primary System Skid Arrangement

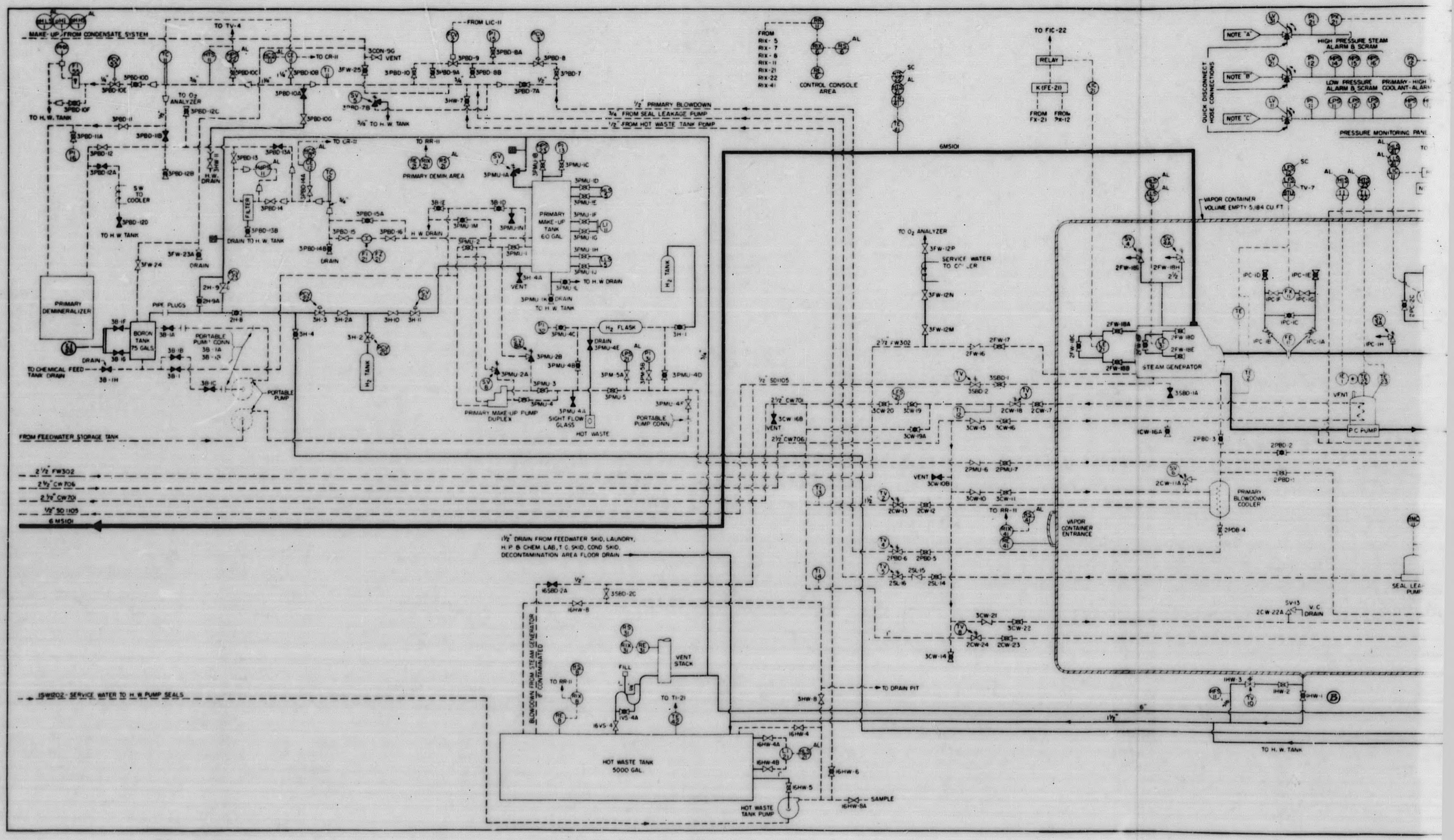
MAKE-UP FROM CONDENSATE SYSTEM
TO TV-4
FROM LIC-11
3CON-9G VENT
TO CR-11
TO O2 ANALYZER
TO H.W. TANK
3PBD-11
3PBD-12
3PBD-12A
SW TO COOLER
3PBD-12D
TO H.W. TANK
3PBD-12B
3PBD-12C
3PBD-10A
3PBD-10G
3/4" TO H.W. TANK
3PBD-7B
3HW-7
3PBD-9
3PBD-8A
3PBD-8
3PBD-7
3PBD-10
3PBD-9A
3PBD-8B
3PBD-7A
1/2" PRIMARY BLOWDOWN
3/4" FROM SEAL LEAKAGE PUMP
1/2" FROM HOT WASTE TANK PUMP
FROM RIX-5 RIX-7 RIX-8 RIX-11 RIX-21 RIX-22 RIX-41
CONTROL CONSOLE AREA
TO FIC-22
RELAY
K(FE-21)
FROM FX-21
FROM FX-12
QUICK DISCONNECT HOSE CONNECTIONS
NOTE "A"
NOTE "B"
NOTE "C"
HIGH PRESSURE STEAM ALARM & SCRAM
LOW PRESSURE ALARM & SCRAM
PRIMARY - HIGH COOLANT - ALARM
PRESSURE MONITORING PANEL
6MS101
TO RR-11
PRIMARY DEMIN. AREA
3PMU-1A
3PMU-1B
3PMU-1C
3PMU-1D
3PMU-1E
3PMU-1F
3PMU-1G
3PMU-1H
3PMU-1J
3PMU-1L
PRIMARY MAKE-UP TANK 60 GAL
3PBD-13
3PBD-13A
3PBD-14A
3PBD-14
3PBD-15
3PBD-15A
3PBD-16
3PBD-14B
FILTER
H.W. DRAIN
DRAIN TO H.W. TANK
DRAIN
3B-1E
3B-1D
3PMU-1M
3PMU-1N
3PMU-2
3PMU-3
3H-4A
VENT
3PMU-1K DRAIN TO H.W. TANK
TO H.W. DRAIN
3FW-23A
3FW-24
DRAIN
2H-9
2H-9A
PIPE PLUGS
2H-8
PRIMARY DEMINERALIZER
BORON TANK 75 GALS
3B-1F
3B-1A
3B-1B
3B-1G
3B-1H
3B-1I
3B-1C
PORTABLE PUMP CONN
DRAIN
TO CHEMICAL FEED TANK DRAIN
PORTABLE PUMP
FROM FEEDWATER STORAGE TANK
3H-3
3H-2A
3H-10
3H-11
3H-4
3H-2
3H-1
H2 TANK
H2 FLASK
3PMU-4C
3PMU-4E
DRAIN
3PMU-2B
3PMU-4B
3PMU-2A
3PMU-5A
3PMU-4D
3PMU-3
3PMU-4
3PMU-4A
SIGHT FLOW GLASS
3PMU-5
3PMU-4F
PORTABLE PUMP CONN
PRIMARY MAKE-UP PUMP DUPLEX
HOT WASTE
1/2" SD1105
2 1/2" CW701
3CW-16B
VENT
2 1/2" CW706
3SBD-1
3SBD-2
3SBD-1A
3CW-20
3CW-19
3CW-19A
3CW-15
3CW-16
2CW-18
2CW-7
1CW-16A
2PBD-3
2PBD-2
P.C. PUMP
2 1/2" FW302
2 1/2" CW 706
2 1/2" CW 701
1/2" SD 1105
6 MS101
2PMU-6
2PMU-7
VENT
3CW-10B
3CW-10
3CW-11
2CW-13
2CW-12
2CW-11A
2PBD-1
PRIMARY BLOWDOWN COOLER
TO RR-11
VAPOR CONTAINER ENTRANCE
2PBD-4
2PBD-6
2PBD-5
2SL-15
2SL-16
2SL-14
3CW-21
3CW-22
2CW-24
2CW-23
3CW-14
SEAL LEA PUMP
SV-13
2CW-22A
V.C. DRAIN
1 1/2" DRAIN FROM FEEDWATER SKID, LAUNDRY, H.P. & CHEM. LAB, T.G. SKID, COND SKID, DECONTAMINATION AREA FLOOR DRAIN
1SW1202 - SERVICE WATER TO H.W. PUMP SEALS
1/2"
16SBD-2A
3SBD-2C
16HW-8
BLOWDOWN FROM STEAM GENERATOR IF CONTAMINATED
VENT STACK
FILL
TO RR-11
TO TI-21
16VS-4A
16VS-4
HOT WASTE TANK 5000 GAL
3HW-8
TO DRAIN PIT
16HW-4
16HW-4A
16HW-4B
16HW-6
16HW-5
HOT WASTE TANK PUMP
16HW-5A
SAMPLE
1HW-3
1HW-2
1HW-1
TO H.W. TANK
6"
1 1/2"
VAPOR CONTAINER VOLUME EMPTY 5,184 CU.FT
TO O2 ANALYZER
3FW-12P
SERVICE WATER TO COOLER
3FW-12N
3FW-12M
2 1/2" FW302
2FW-17
2FW-16
2FW-15
2FW-18H
2 1/2"
2FW-18A
2FW-18C
2FW-18D
2FW-18E
2FW-18B
STEAM GENERATOR
IPC-1D
IPC-1E
IPC-1F
IPC-1G
IPC-1C
IPC-1B
IPC-1A
IPC-1H
2PC-2C
TE
TE 23
VENT

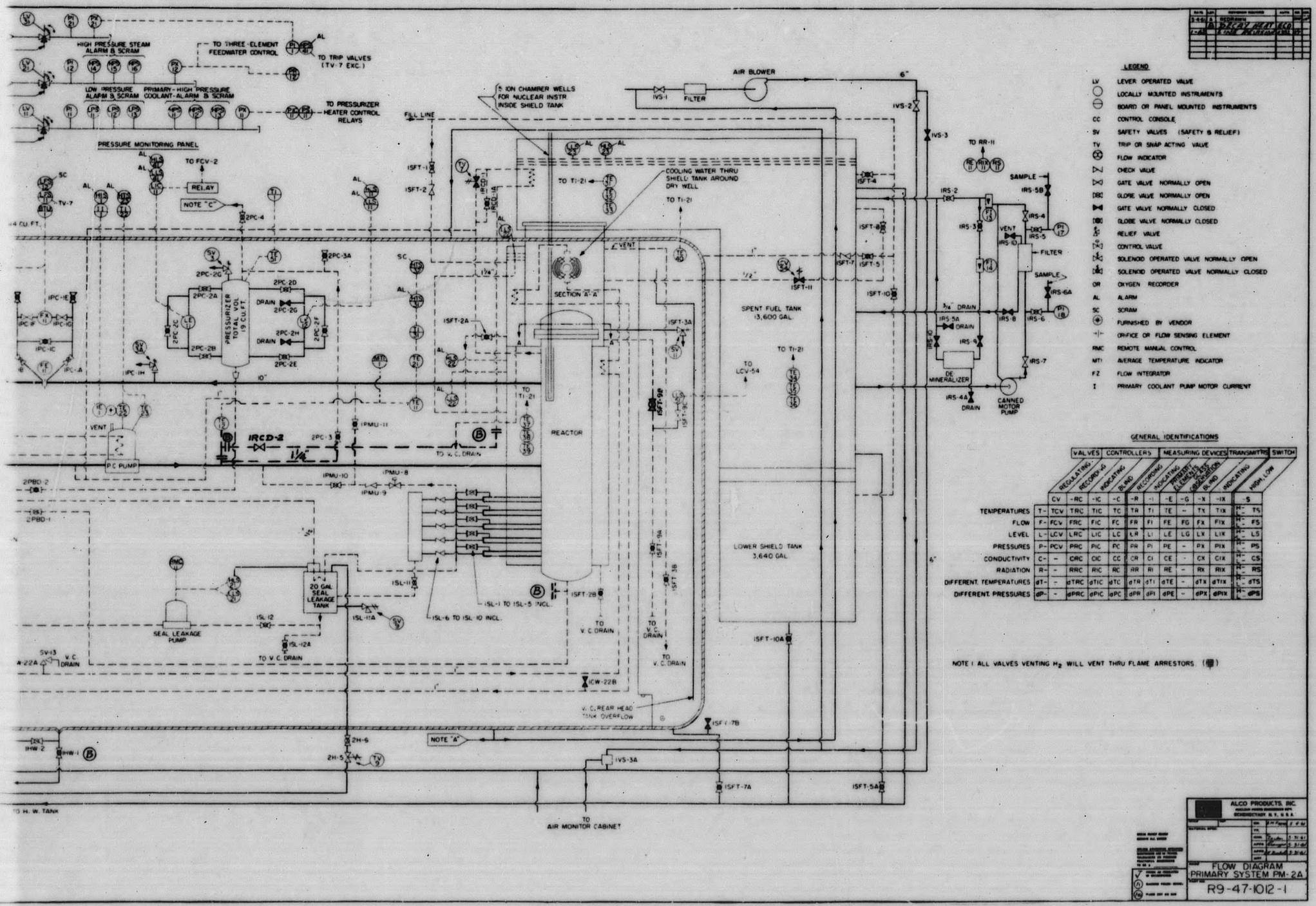

Figure 2.9. PM-2A Primary System Flow Diagram

in. The over-all length is approximately 83-3/4 in. It contains 20 commercial type electric heaters which provide 20 kw for steam generation. Each heater is inserted in a heater well. The heater wells, located in the lower section of the pressurizer, are sealed against primary system water. The heater can be replaced without interference with the primary circuit.

The pressurizer vessel is designed and constructed in accordance with Section VIII of the ASME Unfired Pressure Vessel Code and is so stamped. Operating conditions are 1750 psia and 617° F. The normal water volume is 5.1 cu ft and normal vapor volume is 13.8 cu ft. These volumes limit maximum over-pressure to approximately 200 psi on loss of load. The pressurizer is fabricated of stainless steel type 304. Its insulation is similar to that of the steam generator previously described.

2.5.4 PRIMARY PIPING

The primary coolant piping[7] completes the circuit of pressurized and demineralized water used to transfer heat from the reactor core to the steam generator under forced circulation. It consists of two legs of 10 in. Schedule 120 pipe (0.843 in. wall). The hot leg is the leg from the reactor outlet nozzle to the steam generator, and the cold leg is the leg from the reactor inlet nozzle to the primary circulating pump. Both legs are welded to their respective reactor nozzles and run through the lower shield tank, terminating with standard 1500 lb flanges. The hot leg is bolted to the steam generator; and the cold leg, to the primary circulating pump. The primary pump is also bolted to the steam generator. All bolted connections in the main primary piping are sealed by octagonal stainless steel gaskets.

All primary piping is constructed of stainless steel Type 304 except for a short straight length of carbon steel pipe with a stainless steel clad overlay on the inside. This carbon steel piece is in the cold leg to compensate for the expansion differential caused by the difference in length and temperature between the hot and cold legs.

A fiberglas blanket insulates the primary piping where it is inside the lower shield tank. Thermoasbestos insulation is used on all the remainder of the primary piping, which is external to the shield tanks.

2.5.5 PRIMARY PURIFICATION SYSTEM

The purification system[7] was designed to perform the following basic functions:

1. Continuously remove the impurities from the primary coolant, thereby minimizing radioactivity buildup.

2. Scavenge the dissolved oxygen and minimize corrosion.

3. Control of pH.

4. Protect moving parts and small orifices from clogging or sticking.

A small portion of the primary coolant is continuously withdrawn from the bottom of the reactor vessel, treated, and returned to the system through a 1/2 in. connection in the 10 in. primary piping. The purification loop consists of the following basic components: primary blowdown cooler, pressure reducing and flow control station, disposable demineralizer filter, makeup tank and positive displacement pump. In addition, the system contains all the necessary piping, valves, instrumentation and controls. Primary water enters the purification system at 510° F. and 1750 psi at the rate of 1 to 1.7 gpm. In order to protect the demineralizer resin from thermal damage and to prevent water flashing into steam while flowing across pressure reducing stations, the temperature is reduced to about 110° F. in the blowdown cooler, which is located on the primary skid. The pressure reducing and flow control stations located on the feedwater skid reduce the pressure to less than 100 psi, before the water is processed through the demineralizer.

Demineralizer influent includes a small amount of control rod seal leakage from the seal leakage tank, and makeup water from the condensate system to compensate for sampling and other losses. The demineralizer is a non-regenerative, disposable unit, with design pressure of 50 psig, and functions as both a filter and an exchanger. A replaceable stainless mesh cartridge type filter downstream of the demineralizer picks up any entrained demineralizer resin. A signal from the pressure differential switch across the filter indicates when the filter is due for cartridge replacement.

After passing through flow indicator, the purified water is collected and stored in the primary make-up tank on the feedwater skid, where a positive hydrogen pressure is maintained over the water in the tank to prevent air (oxygen) in-leakage and minimize corrosion.

The primary make-up pump is of a duplex, horizontal, plunger type with manual stroke adjustment, (during pump shutdown) and capacity up to 1.7 gpm. On the pump discharge side, provisions have been made for hydrogen addition. Hydrogen is supplied from the H_2 cylinders connected to H_2 flasks, valved into primary make-up piping. The primary make-up pump with suction from the primary make-up tank, delivers the purified coolant to the control rod seals and to the primary system, thus completing the closed cycle.

2.5.6 SEAL LEAKAGE[7]

Each seal has an individual line from the primary make-up line to the seal coolant inlet tap. Since the primary make-up water is at a slightly higher pressure than primary system, some of the seal coolant water bleeds through the seal into the primary system. The remainder of the coolant travels through the breakdown seals and is collected in a 20-gal seal leakage tank. Thus, the seal coolant water reduces the seal operating temperature, and thereby reduces the seal leakage rates. The seal coolant water also reduces the radioactivity of the seal leakage water by minimizing primary coolant water leaking past the seals.

A hydrogen blanket is established in the seal leakage tank.

A canned rotor, centrifugal seal leakage pump empties seal leakage tank as required and delivers the seal leakage to the demineralizer which is located near the feedwater skid. Should the seal leakage become contaminated for any reason, it can be manually diverted to the hot waste tank instead of the demineralizer by action from the control room.

2.5.7 DECAY HEAT REMOVAL LOOP

The purpose of the decay heat removal loop,[1],[7] Fig. 2.8, 2.9 and 5.20, is to remove fission product decay heat from the reactor vessel when the primary circulating pump is inoperative. The decay heat removal loop performs this function by opening a normally closed solenoid-operated valve upon loss of primary coolant flow. The decay heat removal loop operates by natural convection, and a coolant thermal driving head is maintained during normal plant operations by continually circulating the primary coolant water through that part of the loop between the reactor vessel and the normally closed solenoid valve.

2.5.8 PM-2A VAPOR CONTAINMENT

2.5.8.1 Physical Description of the Vapor Container

The PM-2A vapor container,[7] illustrated in Fig. 2.8, is a horizontal cylindrical pressure vessel designed to 150 psi at 400° F. in accordance with the ASME Unfired Pressure Vessel Code. It consists of a shell 156 in. ID with an ASME 2:1 elliptical head at one end and a reinforced flat head at the other end, for an over-all length of approximately 36 ft. The container is supported by 14 uniformly spaced support pads. Access is provided by a hatchway, 6 ft. ID, centered in the elliptical head, and by a port, 54-7/8 in. ID, in the top of the container approximately 66 in. from the flat-

head end. To permit shipping, the shell is flanged at the flat head and approximately 13 ft. 8 in. from the flat head. Internal support brackets positioned over the external support pads locate the tracks which receive and align the primary skid.

The shell and heads of the container are fabricated from carbon steel SA-212, Grade B. F.B.Q., 11/16 in. thick minimum, and the flanges are SA-106, Grade II. Type 304 stainless steel is used in the fabrication of those components of the access port which may contact primary coolant.

The heat losses from the primary system equipment to the interior of the vapor container are balanced by the heat transfer through the vapor container walls to the interior of the reactor building. The reactor building is thermostatically regulated between 60 and 70° F., by cold air intake or electric space heating, as required. No insulation is used on the vapor container wall; hence, the vapor container heat loss replaces the heat loss from the building to the reactor tunnel. This equilibrium condition provides a satisfactory vapor container ambient temperature without the need for a space cooler in the vapor container.

2.5.8.2 Vapor Container Penetrations

To insure the integrity of the vapor container all outlet fluid penetrations are equipped with electrically operated, fail safe trip valves located directly outside the vapor container.[7], [9] These valves close automatically if the pressure in the vapor container rises 10-15 psi. The pressure sensing device controlling these trip valves is a pressure switch located on the pressure monitoring panel on the feedwater skid. This pressure switch is connected to the vapor container by means of 1/2 in. tubing attached to the 6 in. vapor container bypass vent line. The pressure switch is wired in series in the 28 volt d-c power circuit to the trip valves. The switch is normally closed; and with a 10-15 psi vapor container pressure increase, the switch opens and all trip valves close. All inlet fluid penetrations are equipped with check valves to prevent leakage of primary coolant, liquid or vapor, from the vapor container. The check valves are backed by manually operated globe valves.

All electrical penetrations are provided with leak-tight seals that will contain 200 psi internal pressure. The access port and hatchway are of leak-tight gasketed and bolted construction, designed to contain the 150 psi design pressure.

2.6 PM-2A SECONDARY SYSTEM COMPOSITION AND ARRANGEMENT

The secondary system is comprised of: (1) a turbine generator unit, (2) a surface condenser, (3) an ethylene glycol cooling system consisting of three airblast coolers, auxiliary heat exchanger, expansion tanks, and circulating pumps, (4) a condensate and boiler feedwater system consisting of condensate and boiler feedwater pumps and high- and low-pressure feedwater heaters, (5) a primary and secondary water makeup system with evaporator, demineralizers, pumps, and tanks, (6) electrical system with electrical switchgear, controls, and other auxiliaries, (7) water treatment system consisting of sulphite and morpholine injection units with pumps and tanks, (8) an auxiliary cooling water system with pumps and expansion tanks, (9) a spent fuel tank recirculation system with pumps and cooling coils and (10) controls and auxiliaries.

Units of the secondary system equipment are mounted on individual skids of approximately 9 ft x 9 ft x 30 ft and are installed in the snow tunnels, as illustrated in Fig. 1.3. The skids for the turbine generator, condenser, heat exchangers, unit substation, control center unit, and laboratory unit are installed in a building within the main plant tunnel. The feedwater package is installed in a building within a tunnel off the main plant tunnel. This building is connected to the enclosure in the main plant tunnel by a corridor. One airblast cooler skid is located in the main plant tunnel outside the building. The other two airblast cooler skids are located in a separate tunnel off the main tunnel.

2.6.1 STEAM SYSTEM[7]

Dry and saturated steam at 480 psia is produced by a horizontal kettle-type steam generator located in the vapor container, Fig. 2.8 and 2.9. The steam is supplied to the turbine-generator through a 6-in. pipe, Fig. 2.10. Twin safety valves located in the steam line inside the vapor container serve to protect the system. A trip valve in the main steam line isolates the steam generator in the vapor container in case of a high pressure scram.

An in-line moisture separator is located upstream of the turbine inlet to protect the turbine against possible damage from entrained moisture. The pressure drop characteristic of the steam generator causes steam to condense on the walls of the steam pipe during decreasing load transients when the pressure and temperature of the steam increase. The wall temperature stays at a lower level due to the time required to store heat in the pipe wall. The main steam line also supplies steam to the evaporator and condenser air-ejector. The evaporator produces low pressure steam for snow melting and other auxiliary purposes. The drains from the evaporator are discharged into the low pressure feedwater heater.

2.6.2 TURBINE

The turbine is designed to operate with varying inlet pressures and temperatures as developed by the steam generator over the load range. The turbine is protected against overspeed by an emergency governor which trips the oil pressure dump valve and closes the trip and throttle valve upon overspeed. A low oil pressure alarm warns the operator if the bearing oil pressure falls below a minimum of 4 lb. If the back pressure at the turbine goes above 5 psig, the back pressure trip causes an oil dump and shuts down the unit by closing the throttle valve.

The geared turbine-generator unit (6) is rated at 2500 kva at unity power factor when operating at 8 in. back pressure and 440 psia dry and saturated steam at the inlet of the turbine. The 1200-rpm generator is geared to the 7450 rpm turbine. Two extraction points on the turbine provide steam to the high and low pressure feedwater heaters. The exhaust steam of the turbine is condensed in the condenser under 8 in. of Hg abs pressure.

The generator is air-cooled by forcing ventilating air through the machine by fan blades attached to the rotor of the generator. An air-to-ethylene glycol cooler rejects the heat from the generator in the air-blast cooler.

2.6.3 CONDENSATE AND BOILER FEED SYSTEM(7)

A surface condenser condenses the exhaust steam from the turbine. The condensate is collected in the hot well. De-aeration of the condenser is accomplished by air-ejectors, and the heat of condensation is rejected to the atmosphere via the circulating ethylene glycol cooling system. The level of radioactivity in the hot well is measured and recorded, and an alarm is activated upon high radioactivity level.

Condensate pumps remove the condensate from the hot well and pump it through the air-ejector after-condenser and the low pressure feedwater heater to the suction of the boiler feed pumps. The boiler feed pumps pump the condensate through the high pressure feedwater heater to the steam generator in the vapor container. The drains from the feedwater heaters are cascaded to the condenser. A three-element feedwater controller controls the feedwater flow into the steam generator. Steam flow and feedwater flow are sensed, and the error signal is used to set the control valve. The control action is biased by a signal from the liquid level in the steam generator.

Morpholine and sulfite are injected into the condensate line upstream of the low pressure feedwater heaters by positive displacement pumps.

The low pressure feedwater heater receives the drains from the evaporator.

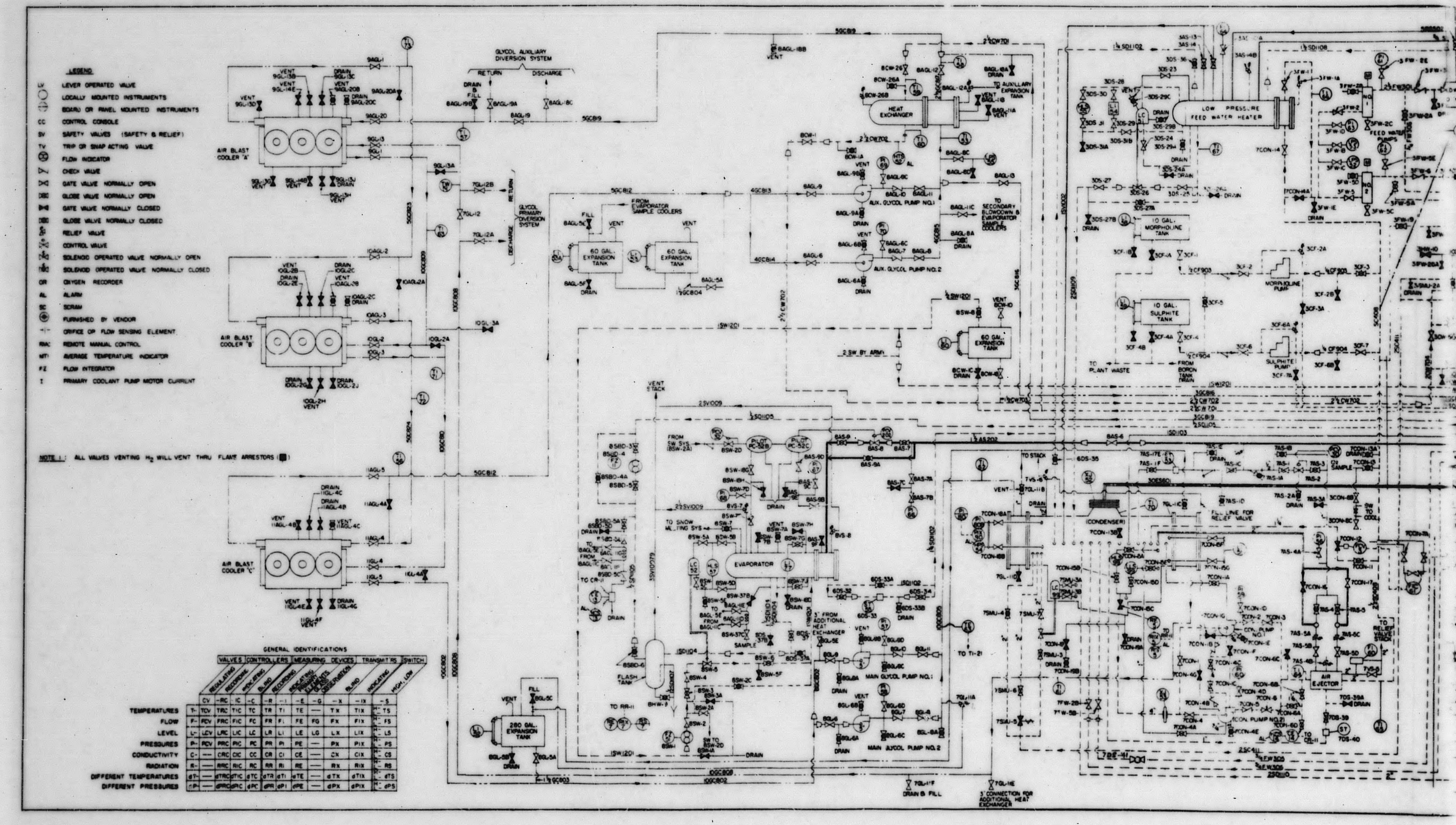
LEGEND
LV LEVER OPERATED VALVE
LOCALLY MOUNTED INSTRUMENTS
BOARD OR PANEL MOUNTED INSTRUMENTS
CC CONTROL CONSOLE
SV SAFETY VALVES (SAFETY & RELIEF)
TV TRIP OR SNAP ACTING VALVE
FLOW INDICATOR
CHECK VALVE
GATE VALVE NORMALLY OPEN
GLOBE VALVE NORMALLY OPEN
GATE VALVE NORMALLY CLOSED
GLOBE VALVE NORMALLY CLOSED
RELIEF VALVE
CONTROL VALVE
SOLENOID OPERATED VALVE NORMALLY OPEN
SOLENOID OPERATED VALVE NORMALLY CLOSED
OR OXYGEN RECORDER
AL ALARM
SC SCRAM
FURNISHED BY VENDOR
ORIFICE OR FLOW SENSING ELEMENT
RMC REMOTE MANUAL CONTROL
MTI AVERAGE TEMPERATURE INDICATOR
FZ FLOW INTEGRATOR
I PRIMARY COOLANT PUMP MOTOR CURRENT
NOTE 1: ALL VALVES VENTING H_2 WILL VENT THRU FLAME ARRESTORS
GENERAL IDENTIFICATIONS
VALVES CONTROLLERS MEASURING DEVICES TRANSMITTERS SWITCH
REGULATING RECORDING INDICATING BLIND RECORDING INDICATING RECORDING OR INTEGRATING OBSERVATION BLIND INDICATING HIGH, LOW
TEMPERATURES T- TCV TRC TIC TC TR TI TE — TX TIX - TS
FLOW F- FCV FRC FIC FC FR FI FE FG FX FIX - FS
LEVEL L- LCV LRC LIC LC LR LI LE LG LX LIX - LS
PRESSURES P- PCV PRC PIC PC PR PI PE — PX PIX - PS
CONDUCTIVITY C- — CRC CIC CC CR CI CE — CX CIX - CS
RADIATION R- — RRC RIC RC RR RI RE — RX RIX - RS
DIFFERENT TEMPERATURES dT- — dTRC dTIC dTC dTR dTI dTE — dTX dTIX - dTS
DIFFERENT PRESSURES dP- — dPRC dPIC dPC dPR dPI dPE — dPX dPIX - dPS
GLYCOL AUXILIARY DIVERSION SYSTEM
RETURN
DISCHARGE
AIR BLAST COOLER 'A'
AIR BLAST COOLER 'B'
AIR BLAST COOLER 'C'
GLYCOL PRIMARY DIVERSION SYSTEM
60 GAL. EXPANSION TANK
280 GAL. EXPANSION TANK
FROM EVAPORATOR SAMPLE COOLERS
AUX. GLYCOL PUMP NO.1
AUX. GLYCOL PUMP NO.2
MAIN GLYCOL PUMP NO.1
MAIN GLYCOL PUMP NO.2
TO SECONDARY BLOWDOWN & EVAPORATOR SAMPLE COOLERS
HEAT EXCHANGER
TO AUXILIARY EXPANSION TANK
EVAPORATOR
FLASH TANK
LOW PRESSURE FEED WATER HEATER
FEED WATER PUMPS
10 GAL. MORPHOLINE TANK
10 GAL. SULPHITE TANK
MORPHOLINE PUMP
SULPHITE PUMP
TO PLANT WASTE
FROM BORON TANK TRAIN
(CONDENSER)
FILL LINE FOR RELIEF VALVE
AIR EJECTOR
CON. PUMP NO.1
CON. PUMP NO.2
TO RELIEF VALVE STACK
TO STACK
VENT STACK
FROM SW SYS (BSW-2A)
TO SNOW MELTING SYS
3" FROM ADDITIONAL HEAT EXCHANGER
3" CONNECTION FOR ADDITIONAL HEAT EXCHANGER
TO TI-21
TO RR-11
TO CR-11
DRAIN & FILL
SW TO BSW-2D
SAMPLE

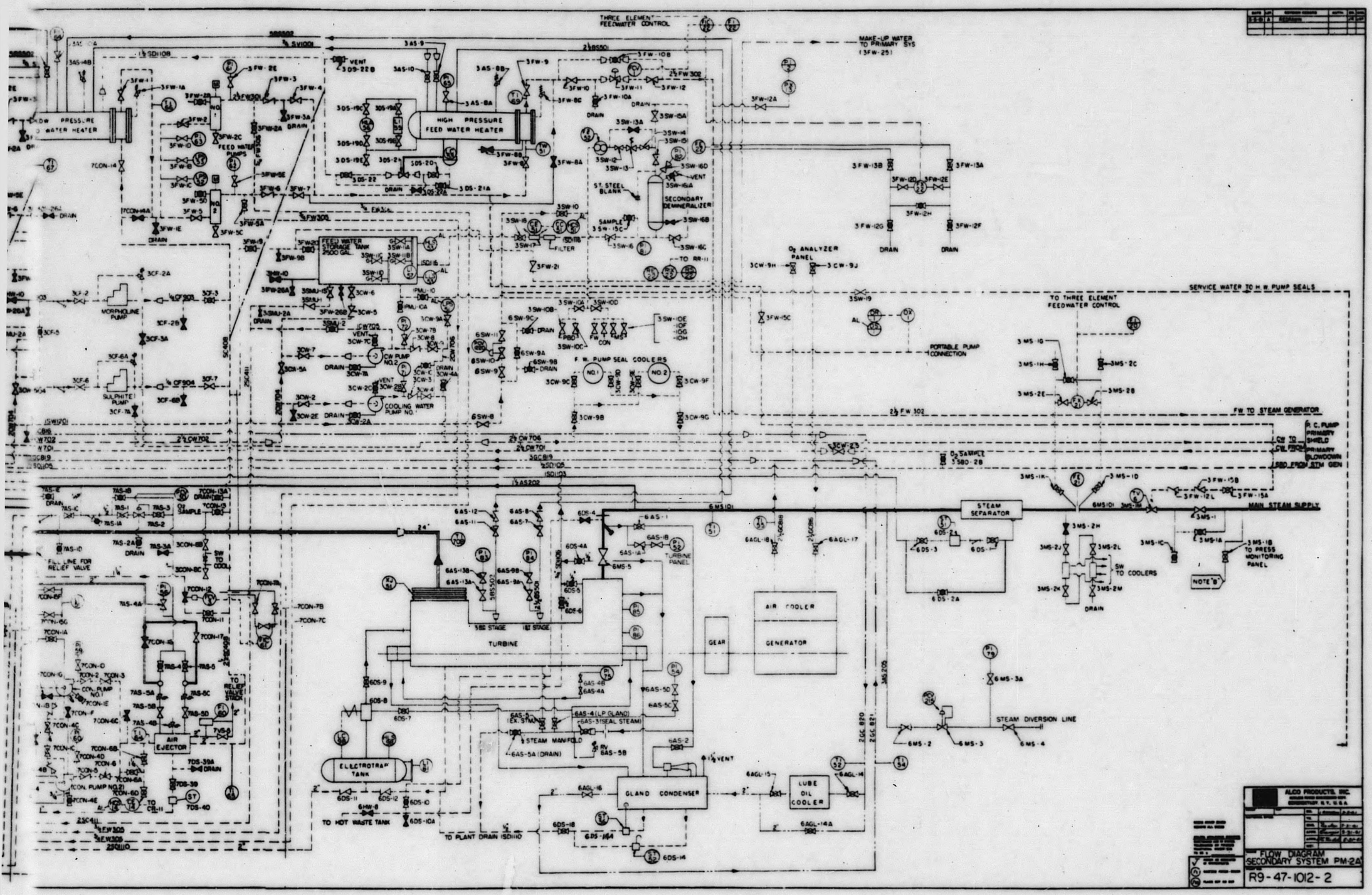

Figure 2.10. PM-2A Secondary System Flow Diagram

2.6.4 CIRCULATING ETHYLENE-GLYCOL, AUXILIARY ETHYLENE-GLYCOL, AND AUXILIARY WATER COOLANT SYSTEMS[7]

The condenser coolant is a 60% ethylene glycol solution circulated by two centrifugal pumps. Three airblast coolers reject the heat to the atmosphere. In the airblast coolers, motor driven fans blow air from the snow tunnel through a fin tube core and ductwork to the atmosphere. This results in a negative pressure in the tunnel of approximately one inch of water relative to atmospheric.

An auxiliary glycol cooling system rejects heat from the generator cooler, turbine lube oil cooler, and from the auxiliary heat exchanger, which couples the auxiliary system to the primary system. The auxiliary glycol cooling system has its own circulating pumps and expansion tank. The glycol-to-air fin tube type cores for the final heat rejection to the atmosphere are an integral part of the airblast coolers, which serve the condenser coolant system described above.

The auxiliary cooling-water system provides cooling for plant components located within the vapor container and for the boiler feed pump seal coolers. The plant components within the vapor container are the shield tank cooling coil, the primary pump cooling coil, and the primary blowdown cooler. The auxiliary cooling water system has its individual pumps, which circulate water through the coolers and through the intermediate cooling water heat exchanger where the heat is given off to the auxiliary glycol cooling system.

2.6.5 PRIMARY AND SECONDARY MAKE-UP SYSTEM[7]

Water losses in the primary and secondary system are made up by individual make-up systems consisting of storage tank, pump, demineralizers, filters, etc.

Make-up for the primary system is provided from the condensate system described above. The primary make-up water enters via the primary blowdown line to the primary demineralizer to the primary make-up tank and then to the primary make-up pump.

For the secondary system, snow is melted by steam from the evaporator. The snow water is demineralized and pumped into the feedwater storage tank and from there is supplied to the condenser hotwell as required. Secondary steam is not used directly for snow melting purposes but indirectly through the evaporator, since snow water is used for purposes other than make-up.

2.6.6 SPENT FUEL TANK RECIRCULATION SYSTEM[7]

The spent fuel recirculating system consists of a canned rotor centrifugal pump, replaceable cartridge filter, demineralizer, and two rotometers. The recirculating pump draws water from the lowest portion of the spent fuel tank and pumps it through the filter and back into the tank near the top. The pump is back-flushed by water taken downstream of the filter. The pump is capable of providing a flow rate of 40 gpm and has a built-in restricting orifice to prevent flows in excess of 40 gpm, in order to prevent pump cavitation when the filter is clean. The filter contains nine removable filter elements in 3 tiers. Normally 5-micron filter cartridges are used. However, if the condition of the water is such that excessive amounts of large particles are present, 25-micron filters may be used for initial filtering. The demineralizer is a duplicate of the primary system purification demineralizer. Flow rates through the demineralizer are limited to a maximum of 10 gpm to avoid excessive flow loading.

The spent fuel recirculating system is used primarily before and during core changes, when the spent fuel tank water will be allowed to intermix with primary water or at any time the spent fuel tank water becomes turbid. The demineralizer is used only when the filter is unable to reduce the activity level of the water to a safe level or when the conductivity of the water becomes excessively high (resistivity of below 100,000 ohm-cm).

2.7 ELECTRICAL POWER GENERATION AND DISTRIBUTION SYSTEM[7]

2.7.1 GENERAL

The power distribution system consists of two major sub-systems; the unit station 4160-volt bus and the motor control center 480-volt bus. The main generator feeds 4160 volts to the high-voltage substation for distribution to two 1200 amp capacity site-feeder lines and to plant service distribution. A standby diesel generator tie-in line connects to the substation bus. A station service transformer reduces the 4160 volts to 480 volts for distribution through the motor control center to the plant components mounted on the skids.

The high voltage substation is mounted on one skid and includes standard switchgear, the station service transformer and equipment for control of the turbine-generator. The 480-volt motor control center together with auxiliary power supplies, lighting distribution equipment, and the main control console are mounted on a second skid.

The auxiliary power supply systems consist of a 115-volt a-c instrument power, non-regulated power, preferred power, lighting system, and a 28-volt d-c power supply.

2.7.2 GENERATOR(7), (10)

The generator is a 2000-kw, 6-pole, 3-phase, wye-connected, revolving-field, synchronous a-c machine of enclosed dripproof construction.

The magnetic amplifier voltage regulator equipment serves as an exciter for the generator as well as an automatic generator voltage controller (4160 volts). Generator excitation can be controlled manually at the console by a rheostat. Two sources of excitation energy are used; the 346 to 31.4-amp current transformers, and the 3-phase, 60-cycle, 480-volt supply through a 3-phase power magnetic amplifier whose output is rectified and applied to the generator field. Generator terminal voltage is controlled within ± 1% of rated voltage over the entire load range.

2.7.3 UNIT SUBSTATION(7)

Ten units of metal-clad high-voltage switchgear containing air circuit breakers, busses, current transformers, potential transformers, protective relays, and secondary control devices accomplish control of the 4160 volt circuits. High-tension compartments enclosing the current transformers and bus connections require the removal of bolted-on covers for entry.

Circuits are provided for incoming lines from the turbine generator, a station service line and transformer, two outgoing site feeder lines and one incoming line from stand-by power.

The 500-kva station service transformer of nonexplosive, fire-resistant, air insulated dry type construction is cooled by natural air circulation through the windings. The enclosure can be entered only after the bolted-on doors have been removed. This transformer supplies station power.

The 225-kva utilities transformer is liquid-insulated self-cooled by a fireproof, nonexplosive liquid. Its construction is such that all live parts and conductors are completely shielded and can be entered only after removal of bolted covers. This transformer supplies power to a distribution panel that feeds the tunnel heating and ventilation system and a portion of the lighting system.

2.7.4 CONTROL CENTER[7]

The motor control center, located on the control center skid, houses the 480-volt power distribution equipment, motor starters, and ausiliary power supplies. The motor starters are electrically operated across the line type, equipped with thermal overload relays, auxiliary interlocks, manual reset and short-circuit protection.

All PM-2A process instrumentation is located in the main control console.

2.7.5 AUXILIARY POWER SUPPLY SYSTEMS[7]

A 430-volt, 30-amp, main circuit breaker, a 480-120 volt power transformer, and a six-circuit distribution panel are provided for 115-volt, a-c instrument power. A 480-volt 15-amp main circuit breaker, a 480-120 volt transformer and a six-circuit distribution panel are provided for 115-volt a-c non-regulated power. 115-volt a-c preferred power is produced for certain instruments, which must remain in operation at all times. The 28-volt d-c system supplies power to tripping circuits of the 4160-volt circuit breakers, certain instruments, and controls. The system is powered by a rectifier charger and a 20-cell, nickel-cadmium, 24-volt battery for emergency use when a-c power fails. The electronic rectifier charger converts 115-volt a-c to d-c power at constant voltage.

2.7.6 STANDBY DIESEL GENERATORS

Three 300-kw diesel generators supply standby and emergency power for Camp Century. One unit is required for a cold startup of the PM-2A. If the turbine generator unit trips off the line, the diesel units are started manually. Battery powered, automatically operated lighting units are installed for emergency lighting in the event of a PM-2A power failure.

2.8 PM-2A INSTRUMENTATION AND CONTROL SYSTEM[7],[11]

2.8.1 GENERAL CONTROL FEATURES

The instrumentation and control system for the PM-2A plant is entirely electrical. Figures 2.11 through 2.17 illustrate the instrument and control center for the PM-2A plant. The legends for these figures are listed in Tables 2.1 through 2.6 and identify the indicator or control, explain the function, and list the expected reading or position for normal full power operation. For "off" normal plant operating conditions, the readings or positions may be other than listed. The control console, Fig. 2.11, is a U-shaped unit with three sections. It is located at one end of the control center skid. The details of these control panels are shown in Fig. 2.12, 2.13 and 2.14. Figure 2.15 shows the radiation monitoring panel and Fig. 2.16 the nuclear instrumentation panel.

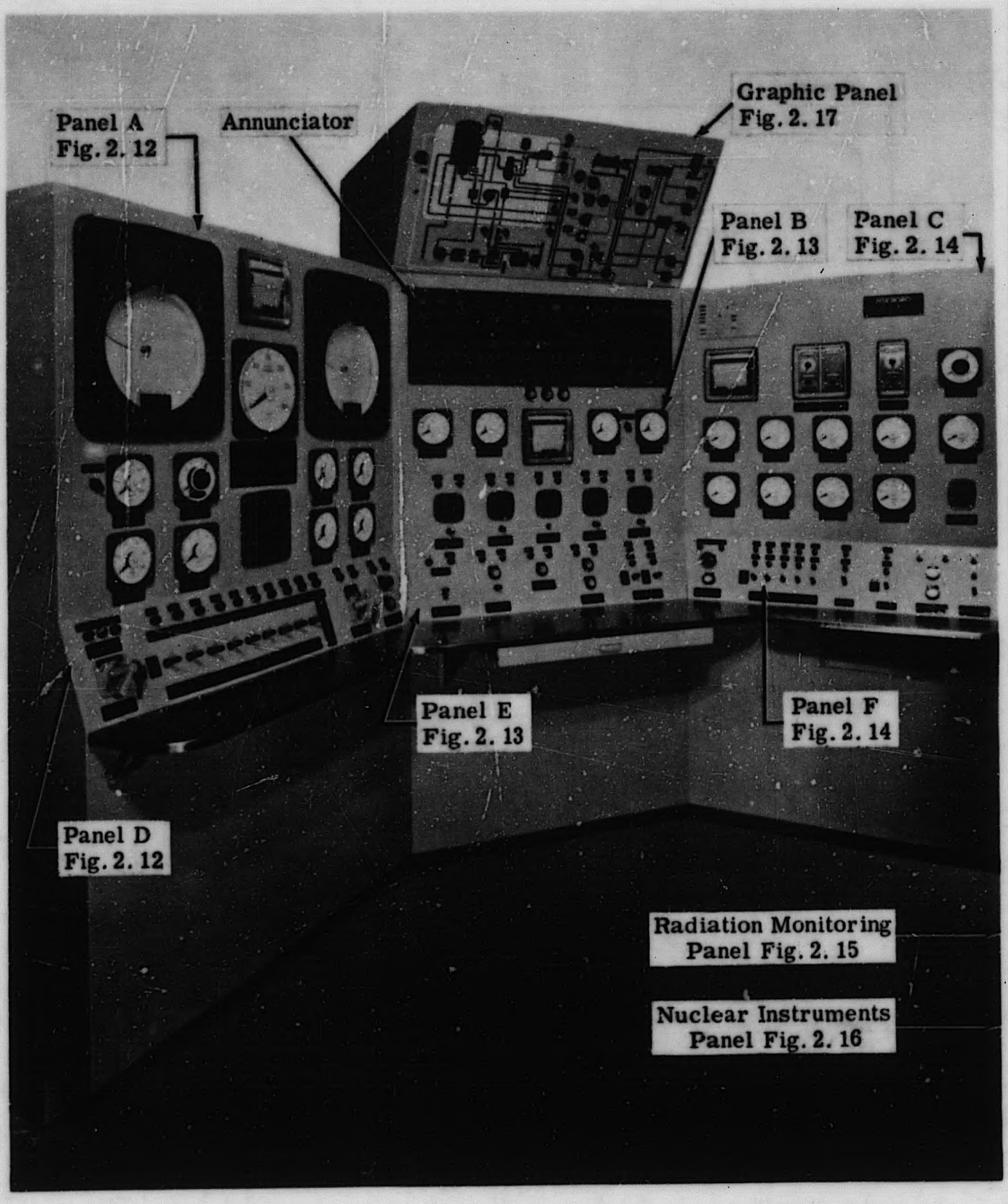

Figure 2. 11. PM-2A Control Console

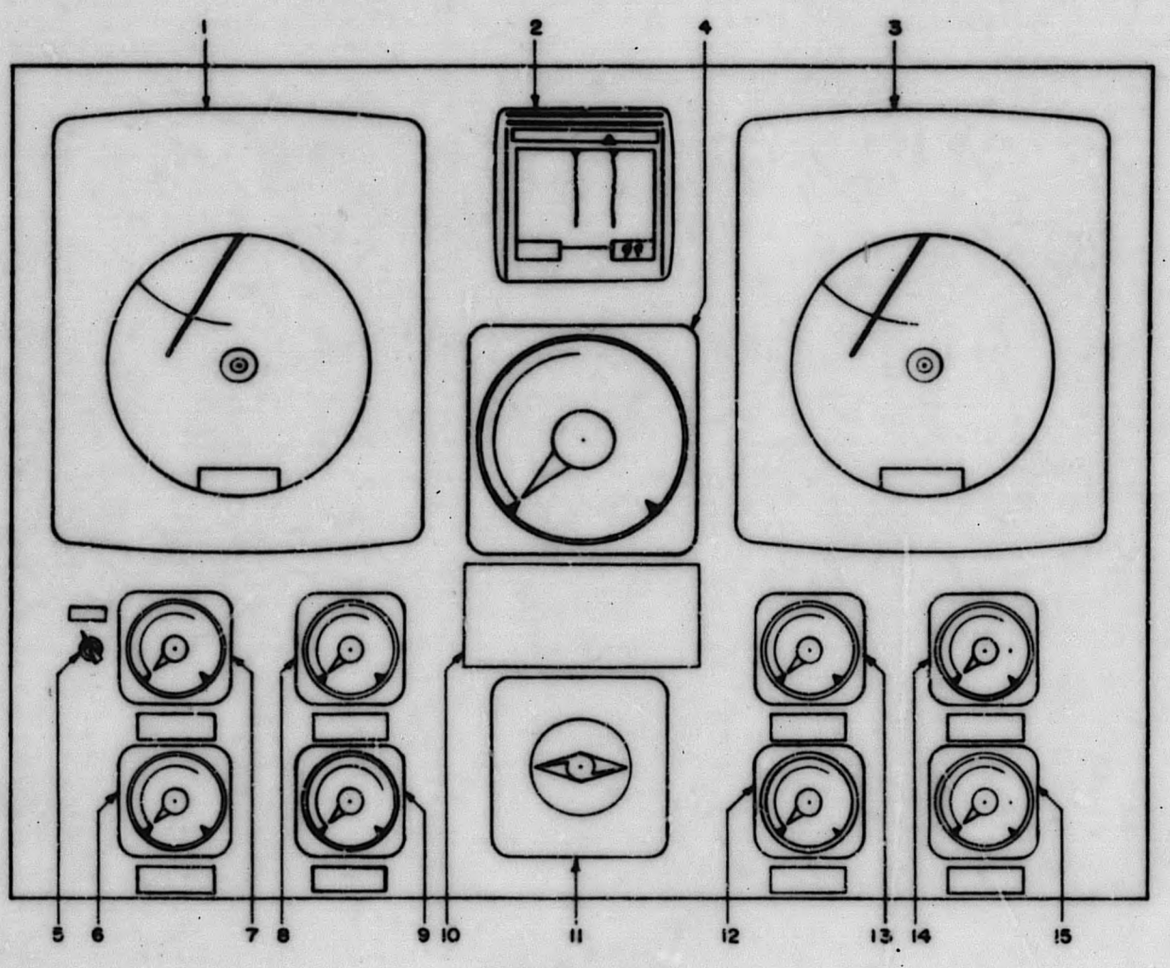

PANEL - A -

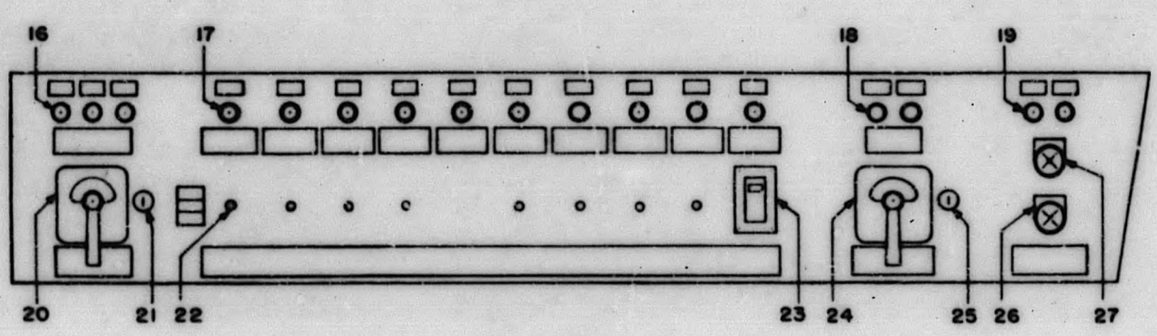

PANEL - D -

Figure 2. 12. PM-2A Control Console Panels A and D

TABLE 2.1
IDENTIFICATION, FUNCTION AND NORMAL OPERATIONAL READING FOR PM-2A INSTRUMENTATION LOCATED ON CONTROL CONSOLE PANELS A AND D

Ref. No.	Control or Indicator	Color Code	Function	Reading or Position
1	4 Channel Conductivity Recorder (CR-11)	Red	CE-11 Upstream Primary Demineralizer	.5 meg ohm
		Blue	CE-12 Downstream Primary Demineralizer	1 meg ohm
		Black	CE-13 Secondary Blowdown	50K - 800K ohm-cm
		Green	CE-14 Condenser Hot Well	200K - 500K ohm-cm
2	3 Channel Dissolved Oxygen Recorder (OR-1)	Red	1. Main Steam or Secondary Blowdown Sample	.03 PPM
		Red	2. Condensate Sample	.03 PPM
		Red	3. Primary Blowdown Sample	.03 PPM
			4. Marking Trace	
3	Temperature Indicator (TI-21)		1. Outer Shield Tank TE-31	135°F
			2. Outer Shield Tank TE-32	135°F
			3. Outer Shield Tank TE-33	59°F
			4. Spent Fuel Tank TE-34	51°F
			5. Spent Fuel Tank TE-35	49°F
			6. Spent Fuel Tank TE-36	44°F
			7. Inner Shield Tank TE-37	90°F
			8. Inner Shield Tank TE-38	82°F
			9. Inner Shield Tank TE-39	81°F
			10. Vapor Container TE-40	142°F
			11. Hot Waste Tank TE-42	58°F
			12. Glycol Inlet-Cond. TE-63	52°F
			13. ----------	-
			14. ----------	-
			15. ----------	-
4	8 Channel Radiation Recorder (RR-11)	Red	1. RE8 - Hot Waste Tank Monitor	10^{-3} Micro C/ml
		Blue	2. RE11 - Vapor Container Air Monitor (Not Connected)	10^{-10} Micro C/ml
		Black	3. RE22 - Feedwater Skid Monitor	0 mr/hr
		Green	4. RE6 - Control Console Monitor	0 mr/hr
		Purple	5. RE7 - Heat Exchanger Skid Monitor	0 mr/hr
		Orange	6. RE5 - Condenser Hotwell Monitor	0 mr/hr
		Red	1. RE41 - Vapor Container Monitor	5 mr/hr
		Blue	2. RE21 - Primary Demineralizer Monitor	3 mr/hr
5	Selector Switch		4 positions. See No. 9	Position as required
6	Dry Cap Level Transfer Switch		Maintains Dry Cap Water Level (Manual and Automatic Positions)	Automatic
7	Dry Cap Fill Valve		Manual Control of Dry Cap Level (Open and Close Positions)	-
8	Pressure Indicator (PI-1)		Vapor Container Pressure	0 psig
9	Temperature Indicator (TI-22)		Primary Coolant Pump and Dry Cap	
			Pos. 1 - Top Bearing	90°F
			Pos. 2 - Bottom Bearing	100°F
			Pos. 3 - ------	-
			Pos. 4 - Dry Cap Water	180°F
10	pH Indicator (pHI-1)		Feed to Primary Demineralizer	6.5 - 6.0 pH
11	Vacuum Indicator (PI-80)		Condenser	22 in. hg.
12	Nameplate		See No. 2	-
13	Selector Switch - 15 Positions		See No. 3	Position as required
14	Level Indicator (LI-21)		Hot Waste Tank	24 in.
15	Power Level Indicator (NUI-11)		Safety Channel #1	100%
16	Power Level Indicator (NUI-12)		Safety Channel #2	100%
17	Power Level Indicator (NUI-16)		Safety Channel #3	100%
18	Indicating Lights - Operation Mode Switch		Green - Routine; Amber - Off; Green - Zero Power	Routine
19	Indicating Lights - Trip Valves		Yellow - Open (TV-7 Closed)	Open
20	Indicating Lights - Reactor Control Power		Green - On; Red - Off	On
21	Indicating Lights - Evacuation Warning		Yellow - On; Green - Off	Off
22	Operation Model Switch		Routine; Off; Zero Power	Routine
23	Locking Key		Permits turning of Operation Mode Switch	-
24	Selector Switches - Trip Valves		Manual; Auto; Test	Auto
25	Master Trip Switch		Turn on Trip Valve Power	On
26	Reactor Control Switch		On; Off	On
27	Locking Key		Permits Turning of Reactor Control Switch	-
28	Pushbutton		Evacuation Warning; On	As Required
29	Pushbutton		Evacuation Warning; Off	Off

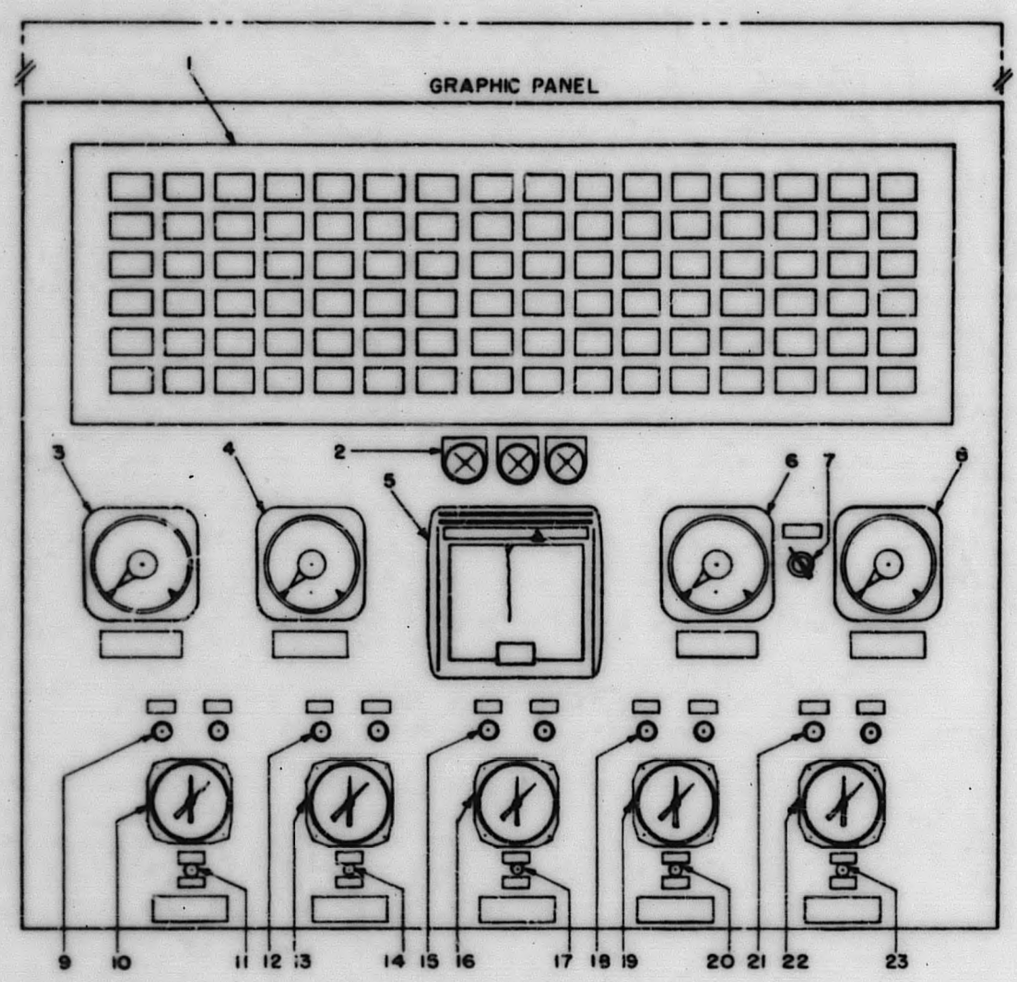

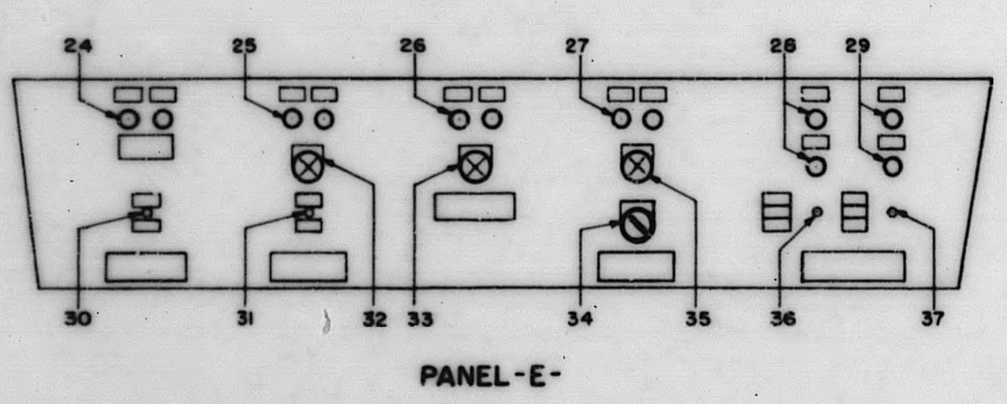

Figure 2.13. PM-2A Control Console Panels B and E

TABLE 2.2
IDENTIFICATION, FUNCTION AND NORMAL OPERATIONAL READING FOR PM-2A INSTRUMENTATION LOCATED ON CONTROL CONSOLE PANELS B AND E

Ref. No.	Control or Indicator	Function	Reading or Position
1	96 Point Annunciator	Announces alarm condition	Ref. paragraph 2.9 (PM-2A Oper. Manual Part I-Chap. 2)
2	Annunciator Pushbuttons	Test; Acknowledge; Reset	-
3	Low Range Period (NUI-14)	Indicates reactor period from -30 to +3 seconds	Used only for startup
4	Log Count Rate (BF_3) (NUI-15)	Indicates neutron flux level from 1 to 10^6 cps	Used only for startup
5	Log N Recorder (NUR-13)	Records reactor output from 0 to 100% rated power	100%
6	Temperature Indicator (MTI-1)	Primary Coolant Average Temperature	510°F
7	Range Selector Switch 1. 0-400°F 2. 400-600°F	See No. 6	400 - 600°F
8	High Level Period (NUI-17)	Indicates reactor period from -30 to +3 secs.	Infinity
9	Shim Rod #1 Position Limit Indicating Lights	Red - Up Limit; Green - Low Limit	-
10	Shim Rod #1 Position Indicator	Inner Scale - 22 in.; Outer Scale - 3 in.	Varies
11	Shim Rod #1 Control Switch	Out; Off; In	Off
12	Shim Rod #2 Position Limit Indicating Lights	Red - Up Limit; Green - Low Limit	-
13	Shim Rod #2 Position Indicator	Inner Scale - 22 in.; Outer Scale - 3 in.	Varies
14	Shim Rod #2 Control Switch	Out; Off; In	Off
15	Shim Rod #3 Position Limit Indicating Lights	Red - Up Limit; Green - Low Limit	-
16	Shim Rod #3 Position Indicator	Inner Scale - 22 in.; Outer Scale - 3 in.	Varies
17	Shim Rod #3 Control Switch	Out; Off; In	Off
18	Shim Rod #4 Position Limit Indicating Lights	Red - Up Limit; Green - Low Limit	-
19	Shim Rod #4 Position Indicator	Inner Scale - 22 in.; Outer Scale - 3 in.	Varies
20	Shim Rod #4 Control Switch	Out; Off; In	Off
21	Shim Rod #5 Position Limit Indicating Lights	Red - Up Limit; Green - Low Limit	-
22	Shim Rod #5 Position Indicator	Inner Scale - 22 in.; Outer Scale - 3 in.	Varies
23	Shim Rod #5 Control Switch	Out; Off; In	Off
24	Rod Withdrawal Permissive Indicator Lights	Amber - No; Green - Yes	Yes
25	Low Pressure Scram Bypass Indicator Lights	Red - Bypass; Green - Normal	Normal
26	Low Range Period Bypass Indicator Lights	Red - Bypass; Green - Normal	Normal
27	Intermediate Range Bypass Indicator Lights	Red - Bypass; Green - Normal	Bypass
28	Pressurizer Heater Control Indicator Lights	Amber - Emergency; Amber - Auto	Auto
29	Pressurizer Heater Control Indicator Lights	Amber - Manual; Amber - Auto	Auto
30	5 Rod Gang Switch	Out; Off; In	Off
31	Low Pressure Scram Bypass Control Switch	Bypass; Normal	Normal
32	Low Pressure Scram Bypass Acknowledge Pushbutton	Acknowledge Bypass	-
33	Low Range Period Bypass Acknowledge Pushbutton	Acknowledge Bypass	-
34	Intermediate Range Bypass Control Switch	Normal; Bypass	Bypass
35	Intermediate Range Bypass Acknowledge Pushbutton	Acknowledge Bypass	-
36	Pressurizer Heater Control Switch	Auto; Off; Emergency	Auto
37	Pressurizer Heater Control Switch	Auto; Off; Manual	Auto

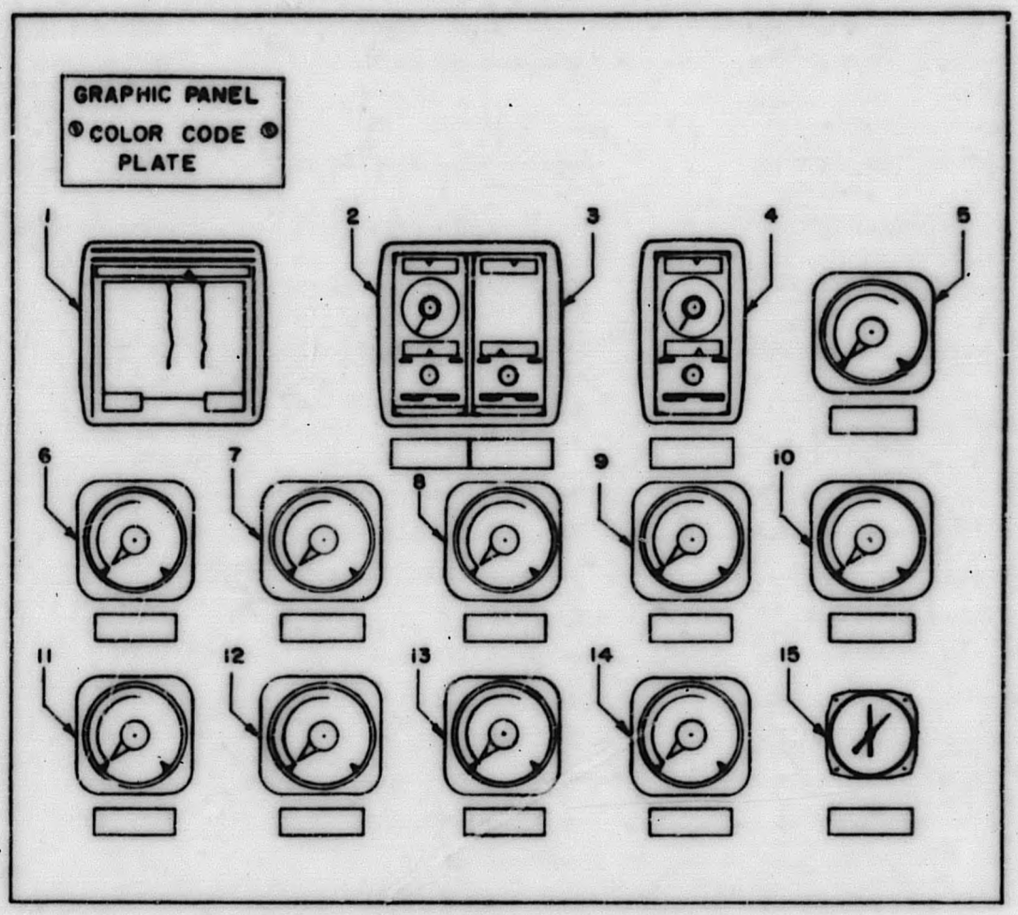

PANEL - C -

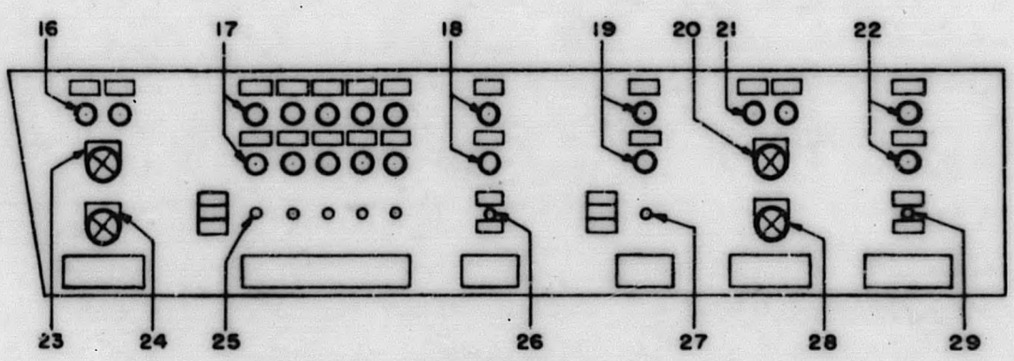

PANEL - F -

Figure 2. 14. PM-2A Control Console Panels C and F

TABLE 2.3
IDENTIFICATION, FUNCTION AND NORMAL OPERATIONAL READING FOR PM-2A INSTRUMENTATION LOCATED ON CONTROL CONSOLE PANELS C AND F

Ref. No.	Control or Indicator	Function	Reading or Position
1	Main Steam Recorder (TR-41, PR-12)	Red - Temperature Green - Pressure	465°F 440 psig
2	Water Level Controller (LIC-21)	Steam Generator	14 in.
3	Flow Controller (LIC-11)	Feedwater	37, 000 lbs/hr
4	Level Controller (LIC-11)	Pressurizer	17 in.
5	Ammeter (II-1)	Primary Coolant Pump Running Current	+100 amps
6	Flow Indicator (FI-20)	Main Steam	36, 665 lbs/hr
7	Level Indicator (LIC-21)	Steam Generator	14 in.
8	Flow Indicator (FI-22)	Feedwater	37, 000 lbs/hr
9	Level Indicator (LIC-11)	Pressurizer	17 in.
10	BTU Indicator (BTU-1)	Primary Coolant	Varies
11	Pressure Indicator (PIC-11)	Primary Coolant	1750 psig
12	Temperature Indicator (TI-31)	Primary Coolant	520°F
13	Pressure Indicator (PI-2)	Feedwater	550 psig
14	Temperature Indicator (TI-1)	Pressurizer	618°F
15	Position Indicator	BF_3 Lifting Mechanism	6 ft
16	Indicating Lights - Manual Scram	Red - Scram; Green - Reset	Reset
17	Indicating Lights - Pressurizer Heaters	Green - On; Amber - Off	On as required
18	Indicating Lights - Primary Makeup Pump	Green - On; Red - Off	On
19	Indicating Lights - Seal Leakage Pump	Green - On; Amber - Off	On as required
20	Pushbutton - Primary Coolant Pump	Turn On	On
21	Indicating Lights - Primary Coolant Pump	Green - On; Red - Off	On
22	Indicating Lights - BF_3 Lifting Mechanism	Purple - Up Limit; Amber - Low Limit	Up
23	Pushbutton - Manual Scram	On	
24	Pushbutton - Manual Scram	Reset	Reset
25	Control Switches - Pressurizer Heaters	Auto; Off; Manual	Auto
26	Control Switch - Primary Makeup Pump	On; Off	On
27	Control Switch - Seal Leakage Pump	Manual; Off; Auto	Auto
28	Pushbutton - Primary Coolant Pump	Turn Off	
29	Control Switch - BF_3 Lifting Mechanism	Up; Off; Down	Off

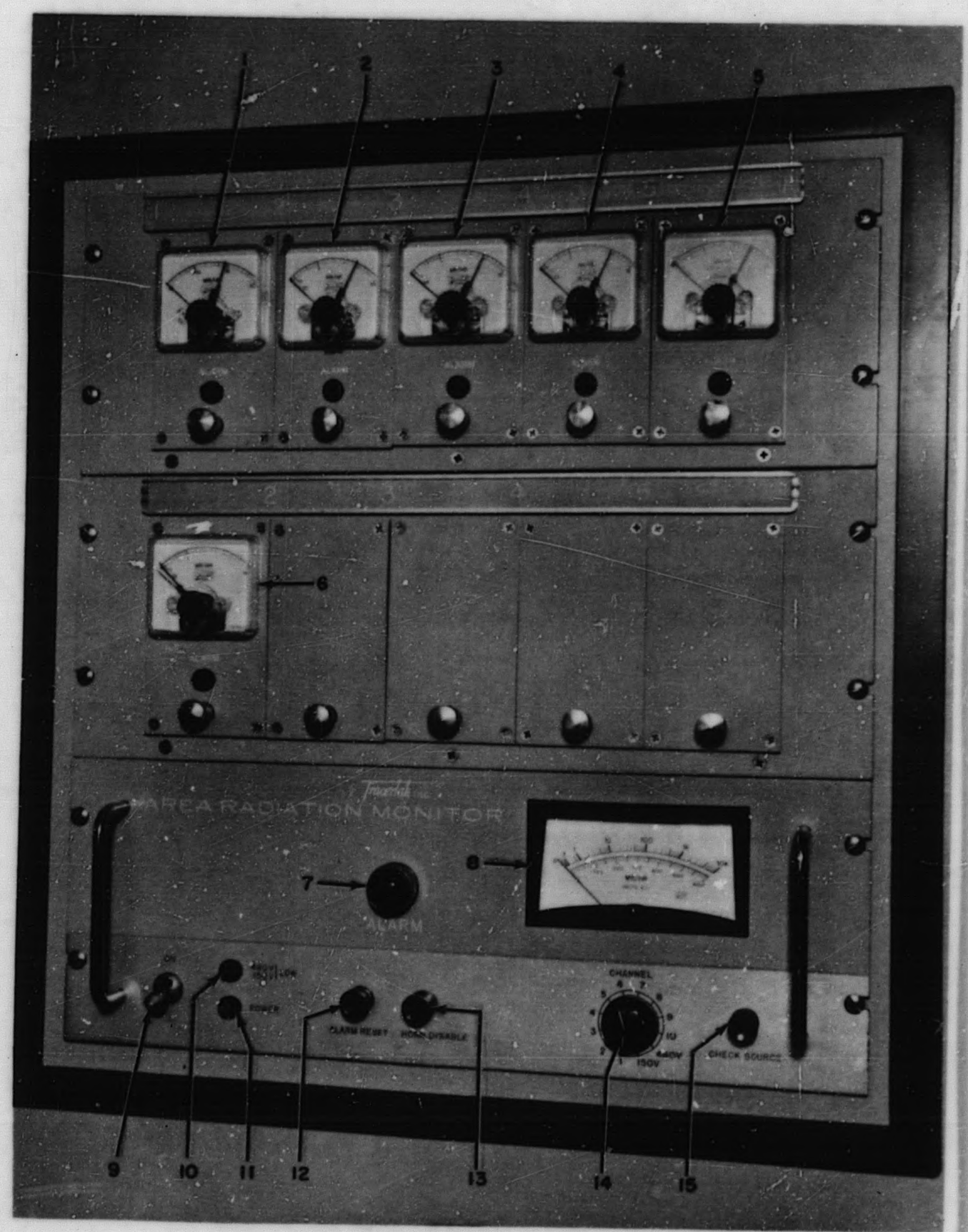

Figure 2. 15. PM-2A Radiation Monitoring Panel

TABLE 2.4
IDENTIFICATION, FUNCTION AND NORMAL OPERATIONAL READING FOR PM-2A INSTRUMENTATION LOCATED ON CONSOLE RADIATION MONITORING PANEL

Ref. No.	Control or Indicator	Function	Reading or Position
1	Indicating Meter and Alarm Unit	Vapor Container	1 r/hr Alarm
2	Indicating Meter and Alarm Unit	Primary Demineralizer	50 mr/hr Alarm
3	Indicating Meter and Alarm Unit	Feedwater Skid	5 mr/hr Alarm
4	Indicating Meter and Alarm Unit	Control Skid	5 mr/hr Alarm
5	Indicating Meter and Alarm Unit	Heat Exchanger Skid	5 mr/hr Alarm
6	Indicating Meter and Alarm Unit	Condenser Hot Well	5 mr/hr Alarm
7	Indicating Light	Red - Alarm	Off
8	Master Meter	Read out for channels and voltages (see 14)	As Selected
9	Power Control Switch	On - Locks in "On" position Off - Turns system off	On
10	Indicating Light +480V +150V Low	Red - Failure of either power supply	-
11	Indicating Light	Clear - Power on	On
12	Pushbutton Alarm Reset	Reset alarm lights on indicating meters	-
13	Pushbutton Horn Disable	Reset alarm horn	-
14	Selector Switch	Select any one of 10 channels or either power supply voltage for display on master meter (see 8)	As selected
15	Pushbutton	Energizes check source at probe selected	As required

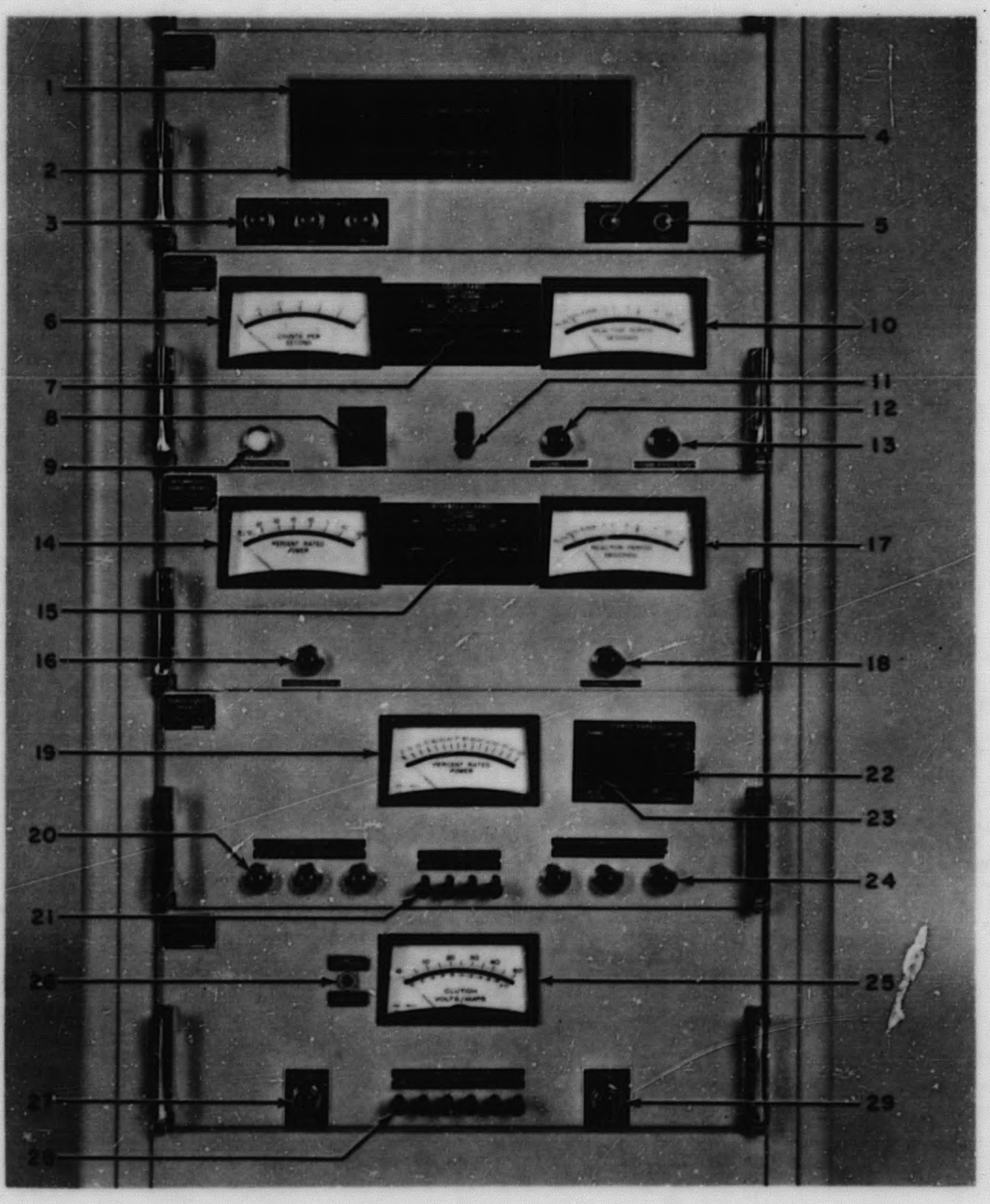

Figure 2. 16. PM-2A Nuclear Instrumentation Panel

TABLE 2.5
IDENTIFICATION, FUNCTION AND LOCATION FOR PM-2A NUCLEAR INSTRUMENTATION PANEL

Ref. No.	Control or Indicator	Function	Location (Drawer)
1	Indicating Lights - Bistable Condition	White light when bistable is tripped, dark when bistable is untripped. (3,4,5, off when tripped).	Self Testing and Display
2	Indicating Lights	White light when corresponding bistable is being tested; stays lighted to indicate a failure.	Self Testing and Display
3	Indicating Lights - Scram Logic Power Failure	Red indicates a failure or discrepancy for each type of scram logic power supply.	Self Testing and Display
4	Manual Test Pushbutton	Permits manual advance of bistable test sequence after a failure is indicated.	Self Testing and Display
5	Lamp Test Pushbutton	Checks condition of bistable indicator lamps.	Self Testing and Display
6	Counts per Second Meter	Indicates neutron flux level in counts/second from 1 to 10^6.	Source Range
7	Source Range Test Signal Switch	Provides test signals for checking calibration of source range circuitry.	Source Range
8	Audible Scaler Switch	Selects mode of operation of audible scaler.	Source Range
9	Indicating Light - Audible Scaler Active	White indicates that audible scaler is providing signals to audible amplifier.	Source Range
10	Reactor Period Meter	Indicates reactor period from - 30 seconds through infinity to +3 seconds.	Source Range
11	BF_3 High Voltage Switch	Supplies high voltage to BF_3 chamber.	Source Range
12	Indicating Light - Channel Test	Red indicates when source range test switch is in any test signal position.	Source Range
13	Indicating Light - Period Bypass Active	Blue indicates when intermediate range is bypassing source range.	Source Range
14	Percent Rated Power Meter	Indicates reactor output from 0 to 100% rated power.	Intermediate Range
15	Intermediate Range Test Signals Switch	Provides test signals for checking calibration of intermediate range circuitry.	Intermediate Range
16	Indicating Light - Period Bypass Active	Blue indicates when intermediate range period function is bypassed by power range in conjunction with the manual permissive switch.	Intermediate Range
17	Reactor Period Seconds Meter	Indicates reactor period from -30 seconds through infinity to +3 seconds.	Intermediate Range
18	Indicating Lights - Channel Test	Red indicates when intermediate range test switch is in any test signal position.	Intermediate Range
19	Percent Rated Power Meter	Indicates reactor output from 0 to 150%.	Power Range
20	Indicating Lights - Channel Failure	Yellow indicates discrepancy between any two power range channels.	Power Range
21	Channel Push to Test	Selects channel to be tested.	Power Range
22	Power Range Test Signals Switch	Provides test signals for checking calibration of power range circuitry.	Power Range
23	Power Range Meter Selector Switch	Selects channel to be monitored by percent rated power meter.	Power Range
24	Indicating Lights - Channel Test	Red indicates channel currently under test.	Power Range
25	Clutch Volts-Amps Meter	Indicates scram bus voltage or indicates current to solenoid selected by Meter Selector (28).	Scram Logic
26	Scram Reset Switch	Resets power to clutches.	Scram Logic
27	Indicating Light SSR Failure	Red indicates failure of left hand solid state relay	Scram Logic
28	Scram Logic Meter Selector	Selects scram solenoid for current measurement.	Scram Logic
29	Indicating Light SSR Failure	Red indicates failure of right hand solid state relay.	Scram Logic

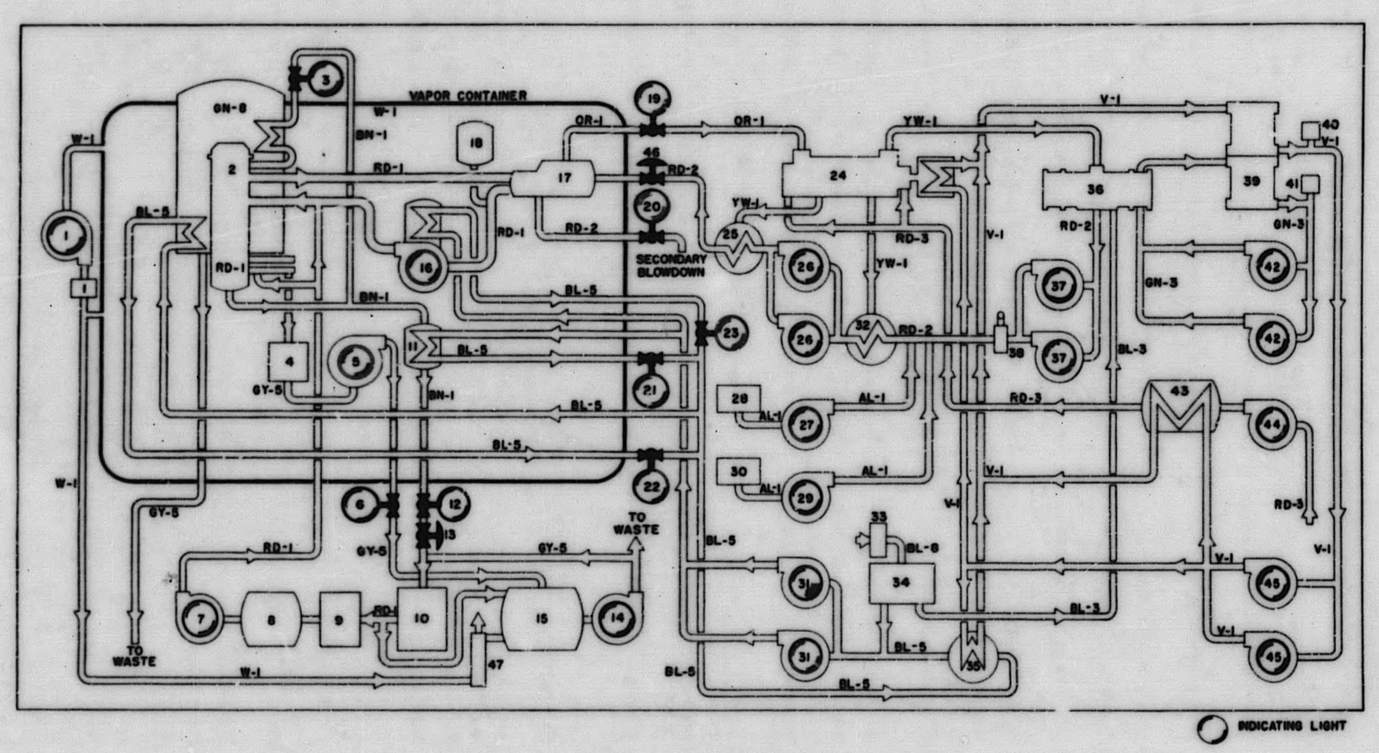

Figure 2. 17. PM-2A Console Graphic Panel

TABLE 2.6
IDENTIFICATION OF COMPONENTS PRESENTED ON THE PM-2A GRAPHIC PANEL

1. Vapor Container Ventilation Blower and Filter
2. Reactor
3. TV-7
4. Seal Leakage Tank
5. Seal Leakage Pump
6. TV-5
7. Primary Makeup Pump
8. Primary Makeup Tank
9. Primary Makeup Filter
10. Primary Demineralizer
11. Primary Blowdown Cooler
12. TV-4
13. Blowdown Flow Control Valve
14. Hot Waste Tank Pump
15. Hot Waste Tank
16. Primary Coolant Pump
17. Steam Generator
18. Pressurizer
19. TV-6
20. TV-1
21. TV-2
22. TV-8
23. TV-3
24. Turbine-Generator
25. High Pressure Feedwater Heater
26. Feedwater Pumps
27. Morpholine Pump
28. Morpholine Tank
29. Sulphite Pump
30. Sulphite Tank
31. Cooling Water Pumps
32. Low Pressure Feedwater
33. Secondary Demineralizer
34. Feedwater Storage Tank
35. Heat Exchanger
36. Condenser
37. Condensate Pumps
38. Air Ejector
39. Air Blast Cooler
40. Auxiliary Glycol Expansion Tank
41. Main Glycol Expansion Tank
42. Main Glycol Pumps
43. Turbine Lube Oil Cooler
44. Turbine Lube Oil Pump
45. Auxiliary Glycol Pumps
46. Feedwater Flow Control Valve
47. Vent Stack

Color Symbol	Color Description	System
BL-5	Blue	Cooling Water
RD-2	Pink Red	Condensate and Feedwater
OR-1	Orange	High Pressure Steam
RD-1	Cherry Red	Reactor, Primary Loop and Primary Makeup
RD-3	Purple Red	Turbine Lube Oil
YW-1	Yellow	Low Pressure Steam
GY-5	Dark Gray	Seal Leakage
BN-1	Brown	Primary Blowdown
W-1	White	Vapor Container and Blower to Stack
BL-3	Medium Blue	Secondary Makeup
V-1	Violet	Auxiliary Glycol
AL-1	Aluminum	Chemical Feed
GN-3	Green	Main Glycol
BL-8	Light Blue	Service Water

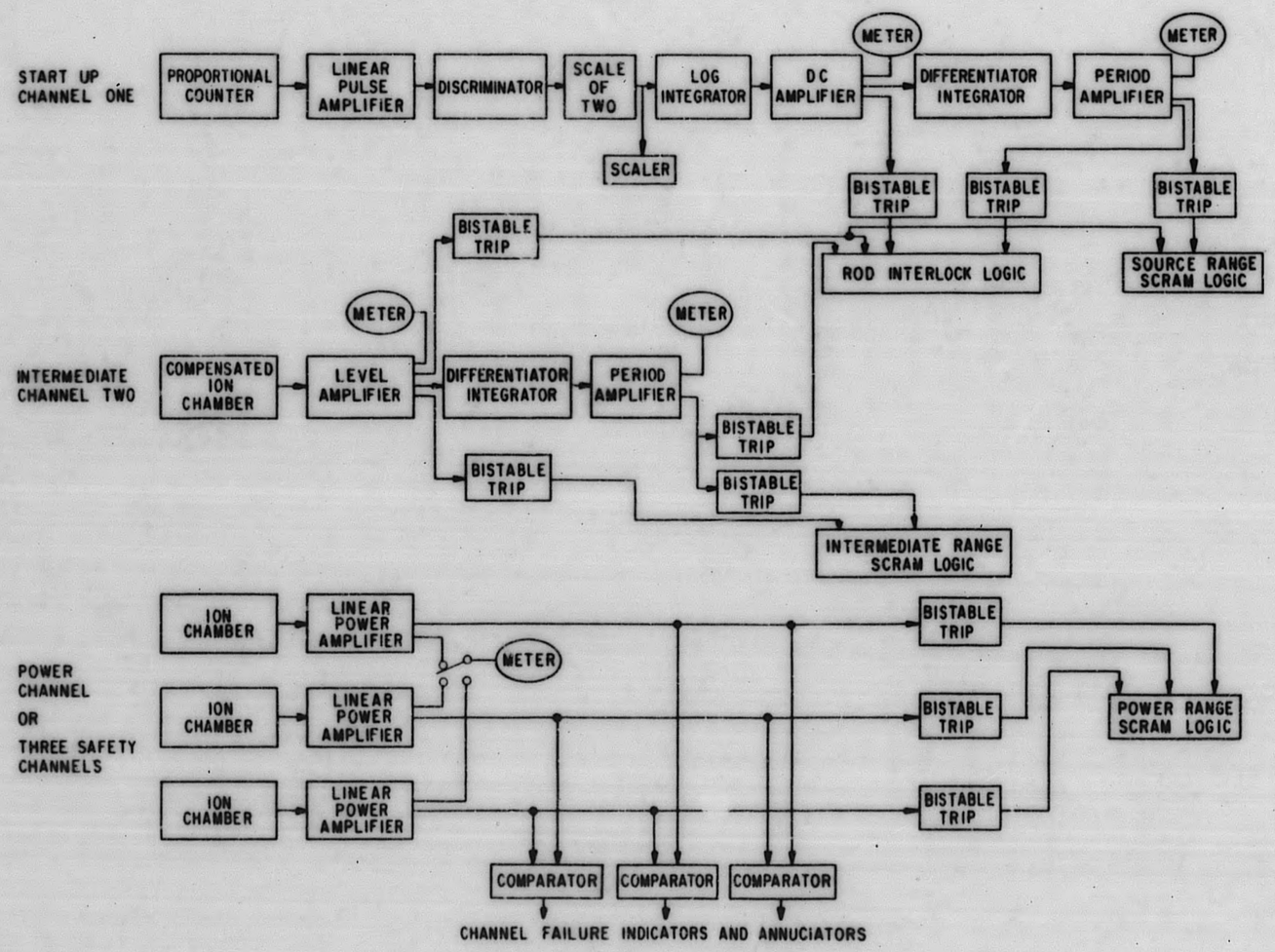

Figure 2.18. PM-2A Nuclear Instrumentation

2.8.2 PM-2A NUCLEAR INSTRUMENTATION[11]

The nuclear instrumentation and control shown in the block diagram in Fig. 2.17, uses military standard silicon transistors exclusively for maximum reliability. All the circuits are wired, plug-in modules, so that downtime for required maintenance is reduced. If there is trouble in a given nuclear channel, it is remedied by replacing a module. This particular module is then repaired in the instrument laboratory or returned to the manufacturer.

The nuclear instrumentation shown in block diagram in Fig. 2.18, is used to indicate the nuclear behavior and to maintain safe limits of operation. It accomplishes this by monitoring the neutron flux level and providing automatic rod interlock and reactor scram control in three overlapping ranges. Nuclear instrumentation and control is comprised of:

1. The Source Range or Startup Channel.
2. The Intermediate Range Channel.
3. Three Power Range or Safety Channels.
4. Scram Logic Circuitry.
5. Self-testing Circuitry.

All ionization chambers and the BF_3 counter are equipped with ceramic connectors, and insulators to insure that the instrumentation circuitry is receiving a reliable signal with minimum influence of electrical interference. A lifting mechanism is provided for the startup channel which permits the operator to withdraw the BF_3 chamber from the region of high neutron flux during high power operation. This decreases the chance of malfunction due to radiation damage of the BF_3 chamber and increases its useful life.

A neutron check source is used to check startup channel performance. This consists of a neutron source which is attached to the outside of the instrument well penetration and rests on the bottom of the spent fuel tank. Before startup, the BF_3 chamber is lifted to a point opposite the neutron source, and the chamber output is monitored at the console for indication of count rate. After establishing satisfactory chamber response, the chamber is lowered into the operating position for reactor startup.

2.8.2.1 Source Range or Startup Channel[11]

The source range instrumentation or startup channel (Fig. 2.13, 2.16 and 2.18; Tables 2.2 and 2.5) utilizes a BF_3 proportional counter as the sensing element and monitors a range of power from shutdown to approximately 10^{-2} percent of full power when located in the normal startup position. This channel provides the following safety signals:

1. A rod interlock signal to prevent rod withdrawal when the count rate is less than 3 cps.

2. A rod interlock signal to prevent rod withdrawal when the reactor period is less than 10 sec.

3. A scram signal when the period is within trip region of the period duration curve of Fig. 2.12.

2.8.2.2 Intermediate Range Channel[11]

The intermediate range instrumentation[8] (Figures 2.13, 2.16 and 2.18; Tables 2.2 and 2.5) or Log N channel monitors a power range of approximately 10^{-4} percent to 100%. A compensated ion chamber is used as the sensing element. Two decades of overlap between this channel and the startup channel are present to insure reliability and safe switchover between channels. This channel provides the following safety signals:

1. A rod interlock which prevents rod withdrawal when the reactor period is less than 10 sec.

2. A scram signal when the period is within the trip region of the period duration curve of Fig. 8.4.

2.8.2.3 Power Range or Safety Channels[11]

The three power range channels[9] (Figures 2.12, 2.16 and 2.18; Tables 2.1 and 2.5) monitor reactor power from 7 to 150 percent of full power. The power range instrumentation employs three uncompensated ion chambers as sensing elements.

The power channels provide a scram signal when the power level exceeds 120 percent full power. Two-out-of three coincidence is used to initiate a high level power scram. This insures safety and reliability in the range most used in plant operation. To further increase safety and reliability, the

outputs of each power range channel are compared and a variation of ± 5 percent is annunciated, so that corrective action may be taken.

2.8.2.4 Scram Logic Circuitry[11]

The scram logic circuitry (Figures 2.16 and 2.18; Table 2.5) performs the proper logic operation required to determine scram functions and prevention of rod withdrawal upon receipt of certain nuclear and process instrumentation signals. Logic circuitry is provided to permit testing one of the instrumentation channels without causing false scrams. This circuitry also allows the removal of one process channel to permit maintenance and repairs.

The scram logic circuitry utilizes two solid state relays which supply a half-wave rectified voltage to the control rod solenoids and automatic drive-down relays during normal operation. The solid state relays become non-conducting on a scram signal, thus releasing the scram solenoids. Either solid state relay is capable of supplying current to the scram solenoids and auto drive-down relays. Two are used for reliability.

A manual reset button is provided and requires a manual resetting by the operator of the scram circuitry to permit rod withdrawal after a scram. Upon initiation of a reactor scram, the scram logic circuitry locks itself out to prevent re-energizing the clutches before the rods have dropped all the way down. To override this lockout and reactivate the reactor, it is necessary for the operator to push the manual reset button.

2.8.2.5 Self-Testing Circuitry[11]

The self-testing circuitry (Figure 2.16 and Table 2.5) provides continuous comparison and self-testing of the critical circuits and functions of the nuclear instrumentation system. Normal circuit operation is not affected by the testing, and any failure or abnormal condition is indicated and annunciated. Five separate testing sub-systems are provided and include the following:

1. A bistable trip test sub-system which indicates the operating condition of each bistable and also indicates and annunciates the failure of any bistable trip.

2. A test alarm sub-system which actuates an annunciator when any two channels are removed for test at the same time.

3. A power range channel comparison sub-system which indicates and annunciates any failure or discrepancy between the safety channels.

4. A power supply test sub-system, which monitors the pairs of power supplies in the scram logic circuitry and indicates and annunciates any failure or discrepancy between the two.

5. A solid-state relay test sub-system, which indicates and annunciates failure of any solid state relay in the scram logic drawer.

2.8.2.6 Period Duration

Figure 2.19 is a curve of period duration vs period. The period scram circuitry will scram the reactor when the period duration falls within the trip region of the curve shown in Fig. 2.19. Requiring that a period must be sensed for some definite length of time eliminates false scrams caused by short duration or spurious period signals.

2.8.2.7 Process Instrumentation Scram Signals[11]

There are six non-nuclear inputs to the scram logic circuitry. These include:

1. Primary Coolant Low Flow

2. Primary Coolant Low Pressure

3. Primary Coolant High Pressure

4. Primary Coolant High Temperature

5. Steam High Temperature

6. Steam High Pressure

Items 2, 3, and 6 depend upon pressure signals. The pressure sensing elements are made up of three pressure switches each. These pressure switches are connected in two-out-of-three coincidence. Alarms are also provided through separate contacts on each pressure switch. The same pressure switch is used for both alarm and scram to insure that both functions will be correctly sequenced. Items 4 and 5 utilize platinum resistance bulbs for the sensing devices.

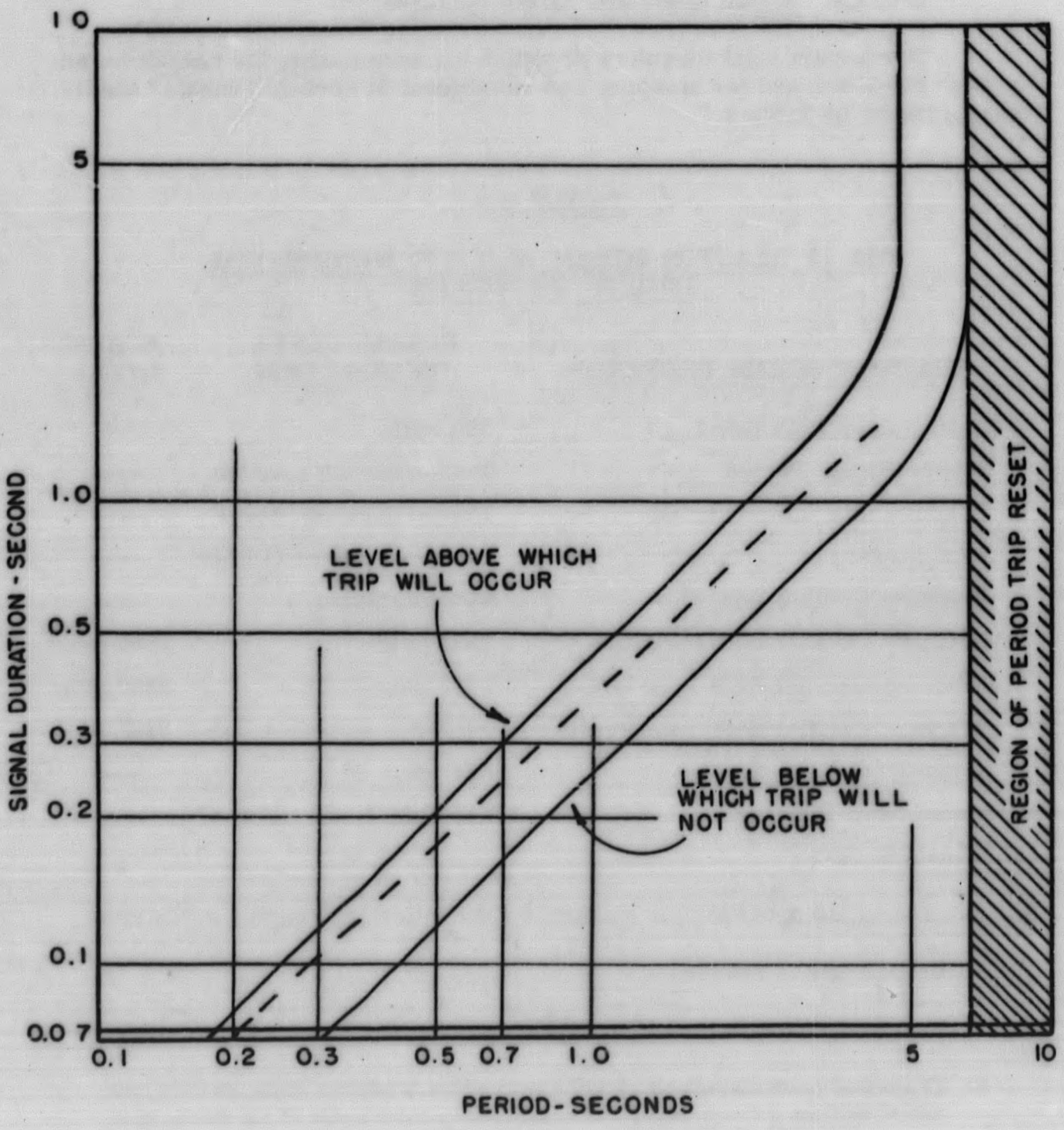

Figure 2.19. Reactor Period Trip Limits for the PM-2A

2.8.2.8 Scram Logic and Safety Features[11]

The scram logic circuitry provides for scramming the reactor in an "unsafe" condition and for stopping rod withdrawal in certain "unsafe" conditions as listed in Table 2.7.

TABLE 2.7

PM-2A REACTOR SCRAM AND ROD WITHDRAWAL INHIBIT PROVISIONS

REACTOR SCRAM PROVISION	SCRAM LEVEL OR DURATION	ALARM LEVEL
1. Zero Power High Level	500 watts	----
2. Source Range Period	Period duration curve	----
3. Intermediate Range Period	Period duration curve	----
4. High Power	120% full power (12 Mw)	----
5. Primary Coolant Low Flow	90% full flow	----
6. Primary Coolant Low Pressure	1575 psig	1635 psig
7. Primary Coolant High Pressure	1925 psig	1880 psig
8. Primary Coolant High Temperature	545° F	535° F
9. Steam High Temperature	523° F	----
10. Steam High Pressure	815 psig	----
11. Manual Scram	----	----

Rod withdrawal is prevented or stopped by the following reactor conditions:

1. Until 2 cps is reached.
2. Reactor period is less than 10 sec.
3. Transfer lock switch is at OFF, or when transfer lock switch is at ROUTINE and the primary coolant pump interlock is de-energized.

During the initial critical loading and during subsequent reactor loadings, it is necessary to operate the control rods when the primary coolant pump is in the OFF position. An operation mode switch on the console has the three positions: ZERO POWER, OFF, and ROUTINE.

In the ZERO POWER position, the primary coolant low-flow and low-pressure scrams protection are bypassed, and the ZERO POWER scram protection is activated. The rods can be withdrawn but the primary coolant pump cannot be started.

When the switch is in the ROUTINE position, an interlock prevents rod withdrawal until 90 percent full flow exists.

The OFF position initiates a scram. A scram is also initiated if the switch is thrown from ZERO POWER to ROUTINE or vice versa, because both operations must encounter the OFF position when switching.

The period protection circuitry may be bypassed by the operator at his discretion when a 40 percent power level is reached and the plant is operating at steady state. The activation of this bypass is visibly indicated. The period protection is automatically reactivated when the power level drops below 40 percent.

To decrease the probability of an inadvertent and continuous five-rod-bank withdrawal, a rod drive interlock is normally in the system to prohibit rod withdrawal if a period as short as 10 sec is reached.

In summary, during normal operation, an interlock prohibits rod withdrawal on periods of 10 sec or less. This is backed up by the period scram and power scram functions. An analog study has shown that a power scram is initiated prior to the period scram because of the negative temperature coefficient when the reactor is operating near design power. On this basis, the period scram will be the prime safety interlock only after failure of the power scram and the 10-sec rod drive preventative interlock. The three functions are continuously monitored to alarm any malfunction.

As an integral part of the control rod drive mechanism, there is a traverse nut with cams riding on a worm screw which follows rod "in and out" motion. When the rod is withdrawn to the upper limit of travel, the appropriate cam actuates the upper limit microswitch. This switch de-energizes contacts of the reversible motor starter. Hence, the operator has set limits within which he can move the control rods by means of the rod drive motor. For initial operation, the upper limit switch was set to stop rod withdrawal at 15.5 in. As the core ages, this setting will be increased. The purpose of the lower limit switch is to interrupt the motor power near the lower limit of

control rod travel to prevent the rod from bottoming against the core structure and generating unnecessary stresses in the control rod drive mechanism.

These circuits are independent of the scram circuit and a malfunction of these switches will not prevent a reactor scram.

2.9 REFERENCES FOR CHAPTER 2

1. "Design Analysis for a Prepackaged Nuclear Power Plant for an Ice Cap Location", APAE No. 39, Alco Products, Inc., January 15, 1959.

2. Paluszkiewicz, S., Byrne, B.F., "Analysis of Zero Power Experiments on the PM-2A Core I', APAE Memo No. 277, January 17, 1961.

3. Raby, T.M., "PM-2A Core I Zero Power Experiment", APAE No. 75, October 21, 1960.

4. "Specifications and Fabrication Procedures for PM-2A Stationary Fuel Elements", APAE Memo No. 201, Alco Products, Inc., June 11, 1959.

5. "Specifications and Fabrication Procedures for PM-2A Control Rod Fuel Elements", APAE Memo No. 202, Alco Products, Inc., June 11, 1959.

6. "Specifications and Fabrication Procedures for PM-2A Neutron Absorber Sections", APAE Memo No. 203, Alco Products, Inc., June 11, 1959.

7. "Technical Manual PM-2A Army Nuclear Power Plant", Vol. 1, Part 1 Operations, Alco Products, Inc., August 1961.

8. "Technical Manual PM-2A Army Nuclear Power Plant", Vol. 1, Part 1 "Operations" and Vol. 6, "Pumps", Alco Products, Inc., August 1961.

9. "Technical Manual PM-2A Army Nuclear Power Plant", Vol. 8, "Valves", Alco Products, Inc., August 1961.

10. "Technical Manual PM-2A Army Nuclear Power Plant", Vol. 7, "Turbine-Generator", Alco Products, Inc., August 1961.

11. "Technical Manual PM-2A Army Nuclear Power Plant", Vols. 10 and 11, "Process Instrumentation", Vols. 12, 13, and 14, "Nuclear Instrumentation System", Alco Products, Inc., August 1961.

3.0 PM-2A CORE I STARTUP PHYSICS TESTING

Startup nuclear testing was performed on the PM-2A Core I to establish the optimum operating characteristics of the nuclear instrumentation, the adequacy of the spent fuel rack, the differential and integral worth of the control rods, the core reactivity effects of pressure, temperature and xenon concentration and to provide an evaluation of the neutron source. These tests employed methods previously established at the SM-1 and other power reactors, and were justified by the untested close-packed spent fuel rack, the new solid state nuclear instrumentation, the new control rod and core geometry, the higher operating temperature and pressure, and the larger photo neutron source. Each of these features in the PM-2A design is different from the SM-1 prototype design.

3.1 NUCLEAR INSTRUMENTATION CALIBRATION

3.1.1 STARTUP CHANNEL CALIBRATION

The startup channel block diagram is given in Fig. 2.18 and the location of the chamber relative to the core is shown in Fig. 3.1 and 3.2.

The startup chamber for the PM-2A is an Anton Type 305 Neutron Counter Tube filled to a pressure of 55 cm mercury with boron trifluoride enriched to 96% B-10. The chamber is 12 in. long and 1 in. in diameter, has a recommended operating voltage of 2400 volts and a 200 volt minimum plateau. The counter tube is designed for use in a neutron flux range of 2.5×10^{-1} to 2.5×10^{4} neutron/cm^2 second and the specified thermal neutron sensitivity is 4.5 counts/ neutron/cm^2. High voltage is supplied to the BF_3 tube through a rectifier in the Source Range Drawer.

The pulse output from the BF_3 tube is fed through a preamplifier to the pulse amplifier and discriminator. The discriminator circuit feeds a binary scalar which in turn supplies a readout through a log integrator to the count rate meter (1).

The modules in each drawer are preset at the time of manufacture. The pulse height discriminator in the pulse amplifier is set internally at a level where the amplifier noise and the ratio of gamma-to-neutron response is negligible in the operating range of the BF_3 tube. The gain adjustment, a single turn potentiometer on the pulse amplifier, can be used to vary the effective level of the discriminator. The Hi-voltage range is also preset so that it spans only slightly more than the operating range of the BF_3 tube. Hence both voltage and gain curves obtained for the PM-2A startup channel were confined by the limits of their respective adjustment controls.

Figure 3.1 illustrates the locations of the detecting chambers with respect to the shield rings and core. Figure 3.2 is a vertical cross section through AA of Fig. 3.1. Since all the chambers are the same radial distance from the core centerline, the section through the BF_3 is typical of a section through any other chamber. Figure 3.2 will be referred to again in Section 3.4 to explain various responses of the BF_3 as a function of its position in the well.

The BF_3 chamber is installed with a lifting mechanism attached so that it can be removed from its position near the reactor core when not in use. An indicator on the control console shows the position of the chamber. At the lower limit of travel, the chamber is located approximately 8 inches below the core centerline; at the upper limit of travel, the chamber is above the base of the upper shield tank, 64 in. above the core centerline. The chamber is located at its lower limit during reactor startups. The chamber is removed from the core to its upper limit after the reactor has reached full power, thus keeping it in a lower neutron flux and gamma ray field.

Figure 3.2 shows the various positions of the BF_3 relative to the core centerline and also the location of the check source.

A Po-Be neutron check source was provided for use in calibrating and checking the operation of the BF_3 chamber. The check source had a strength of 18.45 curies and a yield of 4.71×10^7 neuts/sec on August 18, 1960. The source was initially located adjacent to the startup channel tube penetration between the vapor container and the bottom of the upper shield tank. Subsequent to the shield modification (see Section 4), the check source was relocated to the inside of the upper shield tank and was placed on the bottom of the upper shield tank resting against the BF_3 housing penetration. These are identified as positions A and B respectively in Fig. 3.2. The check source [2] is mounted in a stainless steel housing 3-1/4 in. high and 7-1/4 in. in diameter, with a 3-1/8 in. annulus of paraffin between the source and the outer housing wall. The housing wall is 1/8 in. thick.

The Po-Be neutron startup source located adjacent to the PM-2A reactor coil (Fig. 3.2) had a strength of 31.69 curies and a yield of 8.09×10^7 neutrons/sec on August 17, 1960.

3.1.2 BF_3 VOLTAGE CALIBRATION

Figure 3.3 illustrates the BF_3 response to the Po-Be check source neutrons as a function of voltage. Curve 1 was obtained prior to reactor operations in the absence of any gamma field. In order to obtain the neutron response curve of the BF_3, the chamber was moved from its normal position and placed next to the check source at position A outside the vapor container. The normal range

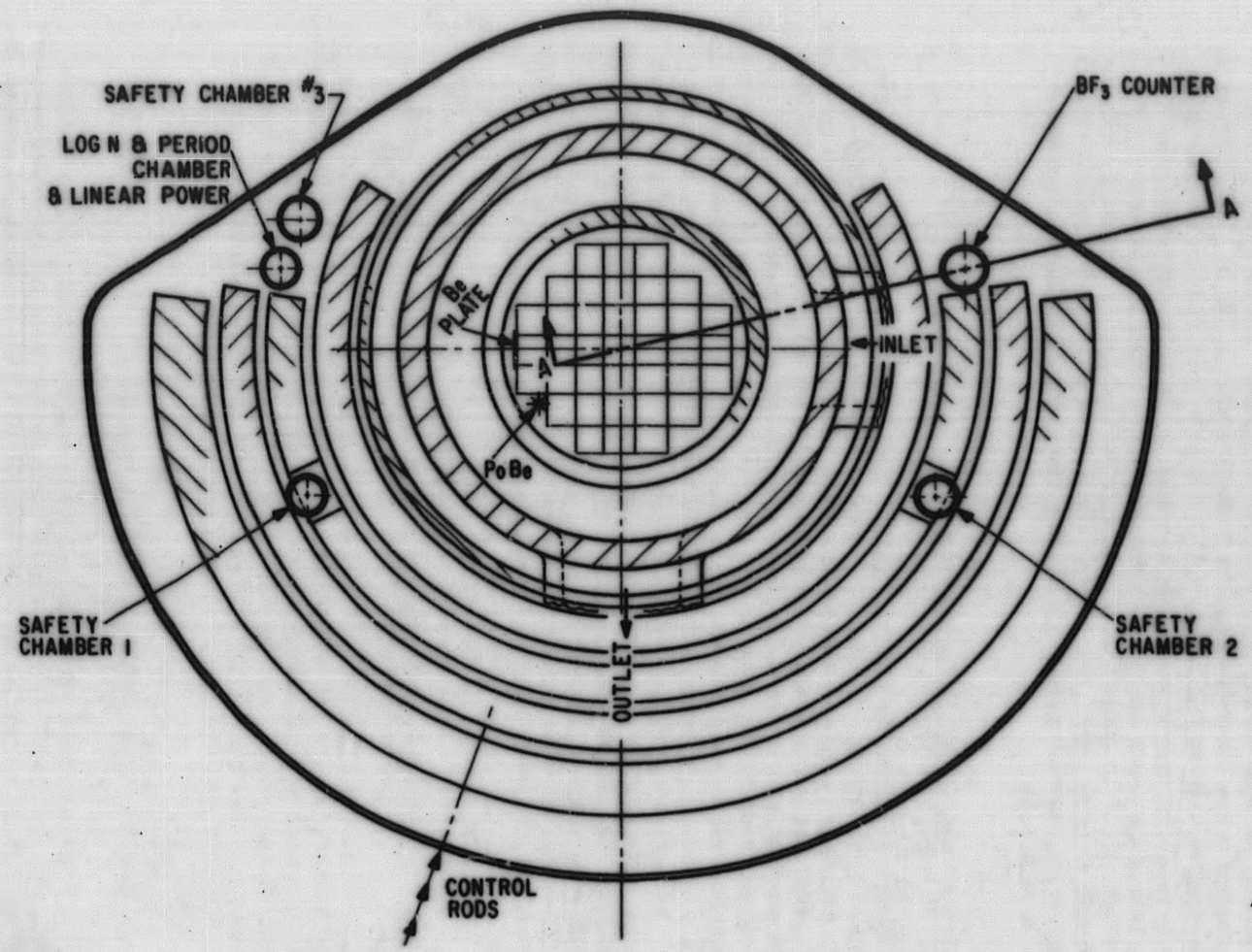

Figure 3.1. Plan View of PM-2A Core, Vessel and Primary Shielding Arrangement

of the BF_3 high voltage power supply was extended for these measurements by shunting the appropriate power supply resistors. Curve 2 of Figure 3.3 is a voltage curve taken two days after shutdown from 387 hr. operation at an average electrical load of 725 kw. Curve 2 was obtained over the allowable voltage range by removing the BF_3 chamber to its fully withdrawn position alongside of the check source at position B in the upper shield tank 5-1/2 ft above the core. An inspection of the two curves shows the operating voltage remaining at 2450 volts. The shift in the plateau of curve 2 is due to a small change in the over-all gain of the startup detector and amplifying system (Ref. Sec. 3.1.4).

3.1.3 BF_3 GAIN CALIBRATION

Figure 3.4 gives the startup channel response as a function of the pulse amplifier gain setting. Curves 1, 2 and 3 were obtained with the BF_3 near the check source at position A outside the vapor container prior to power operation of the plant and curve 4 was obtained by raising the BF_3 tube to its fully withdrawn position next to the check source at position B in the upper shield tank subsequent to the 387 hr plant endurance test. The abscissa of the gain curves is identified as degrees rotation of the single turn gain potentiometer where 90^o is the minimum gain position and 360^o is the position of maximum amplifier gain. As in the case of the voltage curves, the range of gain settings covers only that portion of the complete gain curve which is pertinent to the operation of the BF_3. By plotting the gain curve in reverse (360^o to 90^o) a reasonable reproduction of the pulse height distribution curve in the operating range of the equipment should be obtained. The pulse amplifier module was changed after Curve 1 was obtained, due to the abnormal "saddle" shape of this response curve.

3.1.4 DISCUSSION OF THE STARTUP CHANNEL TESTING DATA

In the following treatment differences in absolute counting rates are not considered of prime importance. Since the calibration data collected prior to plant operations and following the 387 hr acceptance run were obtained in different environments, and with different chamber and neutron check source geometries at positions A and B, it was expected that the absolute counting rates would not be identical.

3.1.4.1 Shift in Voltage and Gain Curves

The shift to the right and left of the startup channel voltage and gain curves, Fig. 3.3 and 3.4, respectively, are elemental to proportional counter operation. Pulse amplification is obtained from a BF_3 proportional counter by

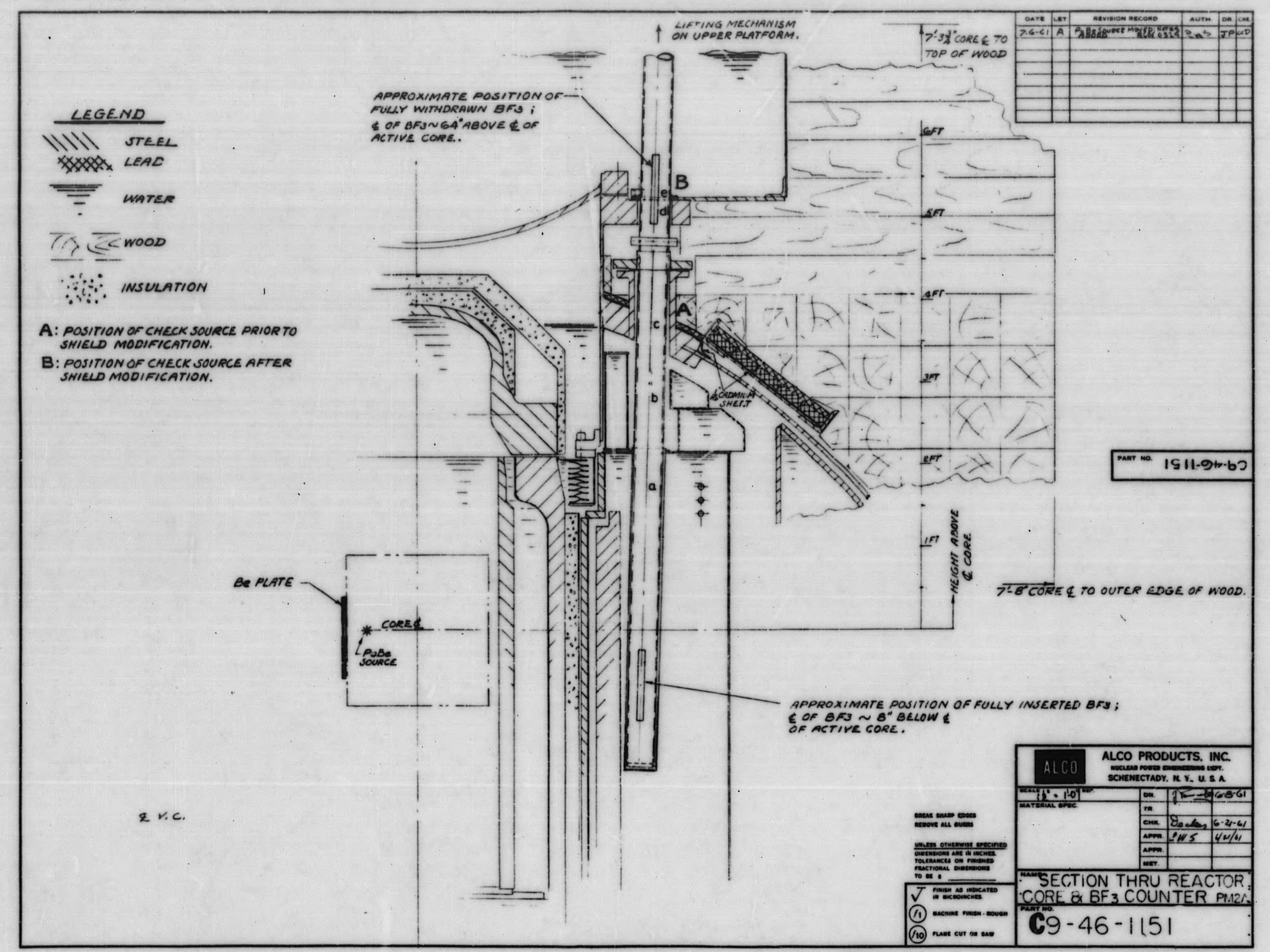

Figure 3.2. Vertical Section Thru PM-2A Reactor

two methods: first, by gas amplification in the chamber; and second, by electronic pulse amplification in the amplifier. The gas amplification is controlled by the voltage applied across the chamber electrodes and the electronic amplification is controlled by the gain adjustment on the electronic amplifier.

The PM-2A startup channel pulse amplifier employs a fixed discriminator and a variable gain control through a single turn potentiometer. Thus, the "effective" discriminator level varies inversely with the amplifier gain, and exact reproducibility of pulse height distribution is not expected due to the rather coarse gain control. As a consequence of the small change in over-all system gain, as illustrated by the slight shift to the left in Curve 4, Figure 3.4, there is a corresponding change in effective discriminator level. A slightly higher applied chamber voltage is therefore required to provide sufficient gas amplification of pulses to pass the higher effective discriminator level, as illustrated by the shift to the right from voltage Curve 1 to 2, Fig. 3.3. These voltage and amplifier gain phenomena are normal to proportional counter operation, and one is a natural consequence of the other where the amplifier discriminator level is fixed.

3.1.4.2 Curve Shape for Voltage and Gain Data

The voltage curves shown in Fig. 3.3 exhibit the shape normally expected from BF_3 proportional counters when exposed to neutron radiations. The short voltage span of Curve 2 is a consequence of the narrow range over which the voltage may be selected. However, the curve does indicate satisfactory chamber response.

The gain curves of Fig. 3.4 are similar in shape; however, Curve 4 is shifted to the left as a consequence of the small change in over-all system gain. From these data, it is not possible to identify the cause for the change in gain. A possible reason is the replacement of the pulse amplifier module with a modified version in the interim period between Curves 1 and 4. Other contributing factors could be aging effects in amplifier components, radiation effects on the BF_3 chamber, and higher operating temperature of the BF_3 chamber, when Curve 4 data was collected following the acceptance test run.

3.1.4.3 Conclusions and Recommendations

1. The voltage calibration curves indicate that the power supply will provide the minimum voltage required for the BF_3 chamber; however, it appears advisable to extend the range of the high voltage power supply to include 2200 to 2600 volts in order to provide adequate coverage for changes in instrument response due to radi-

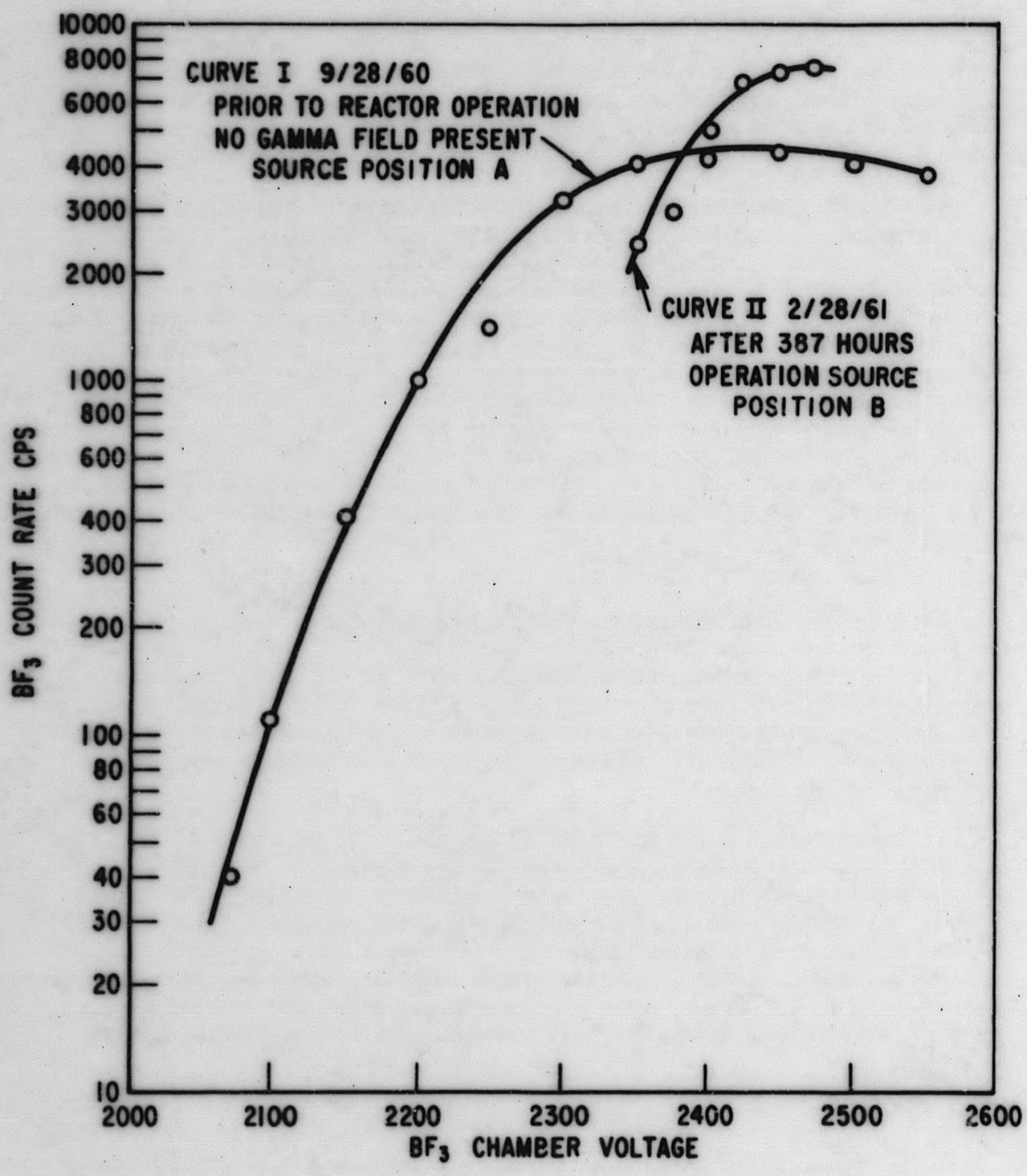

Figure 3.3. BF_3 Count Rate Vs BF_3 Chamber Voltage for the PM-2A Startup Channel (Core I)

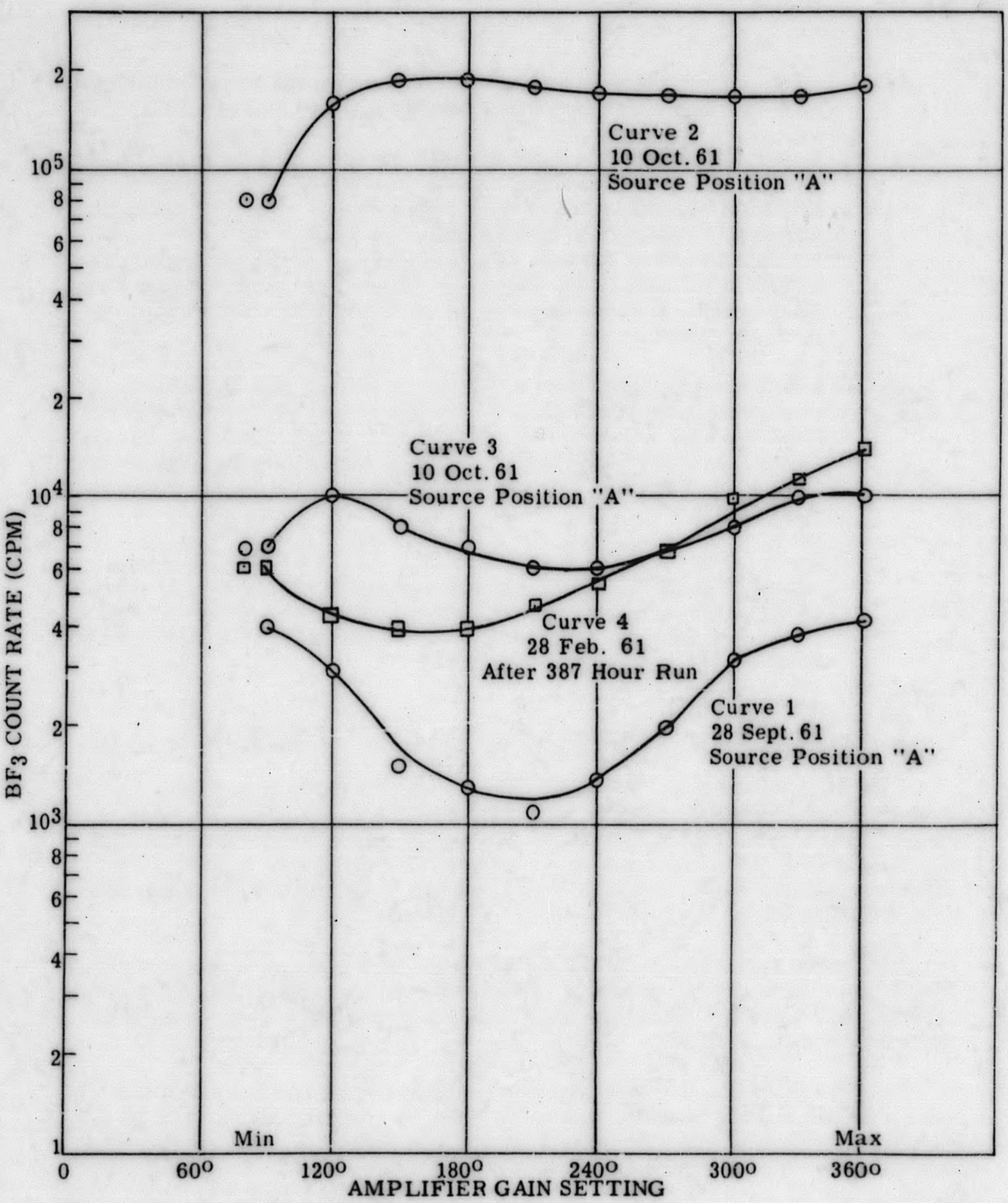

Figure 3.4. BF_3 Count Rate Vs Gain Setting

ation, temperature and aging effects, and permit adequate adjustment to compensate for changes in the gain of pulse amplifier.

2. Inspection of Fig. 3.4 indicates that the over-all gain in the startup system is probably high and results in some overloading of the amplifier as evidenced by the peaking of the curves with decreasing amplifier gain. The peak in system response rates at the lower gain settings may also indicate some tendency of the pulse amplifier to behave as an oscillator. However, these tendencies are small and should not be considered a hazard to safe startup channel and reactor operation.

3. Further quantitative analysis of the PM-2A startup channel characteristics requiring additional environmental testing is recommended, and should include oscillographs as well as hand recorded data under varying conditions of chamber voltage, amplifier gain, temperature, gamma ray and neutron radiation intensity, and integral radiation dose effects.

4. On the basis of the results shown in Fig. 3.3 and 3.4, optimum settings chosen for initial startup were 2450 volts and 210° rotation on the gain potentiometer. Optimum settings chosen for startup in a high gamma field (after 400 hr at 725 kw) were 2450 volts and 90° rotation on the gain potentiometer.

3.1.5 INTERMEDIATE RANGE CHANNEL

The intermediate range chamber is an Anton 807 ionization chamber with a boron lining 96% enriched in B-10. The chamber has a sensitive length of 14 in. The recommended operating voltage is 300 to 800 volts and provision is available for -10 to -80 volts compensation. The chamber is designed to operate in a flux of 2.5×10^2 to 2.5×10^{10} neuts/cm^2-sec and has a thermal neutron sensitivity of 4×10^{-14} amp/n/cm^2-sec.

The output signal to the intermediate range drawer supplies percent rated power and reactor period readouts. The intermediate range drawer is also supplied with bistable trips which indicate unsafe conditions if the reactor period exceeds a preset value.(1)

The intermediate range channel is normally operated with gamma compensating voltage applied in order to provide a signal response which is in direct proportion to the neutron flux and consequently the reactor power level. The intermediate channel response is adjusted to render a direct readout in percent rated power by adjusting the chamber location inside the instrument penetration. Once the intermediate range chamber voltage and location has been selected it remains undisturbed during power operations.

3.1.6 POWER RANGE CHANNEL

The power range (or safety) chambers are Anton 807 ionization chambers identical to those of the intermediate range chamber. The power range chamber is operated uncompensated because the gamma-to-neutron ratio at full power is quite small.

The output signal from the safety chambers goes to a local reactor power meter located on the nuclear instrumentation panel. By means of a three-way selector switch (Item 23, Fig. 2.16) the power level at any chamber can be read on the meter. The three chambers feed bistable trips; exceeding a preset level on one chamber indicates an unsafe condition and an unsafe condition on two chambers simultaneously causes a reactor scram (1). In addition to the single power channel monitoring on the nuclear instrumentation panel, all three power channels are monitored simultaneously on the reactor console panel.

Figure 3.5 illustrates the PM-2A nuclear instrumentation range characteristics. The intermediate and power ranges are fixed, however, the range of the BF_3 proportional counter can be extended (as shown in note B of Fig. 3.5) by simply withdrawing the BF_3 50 in. from the core. It must be noted that the BF_3 chamber should not be withdrawn during startup operations until the count rate is approximately 10^5 cps where a significant overlap has been established with the intermediate range Log N instrumentation.

3.2 SPENT FUEL RACK TESTING

3.2.1 DESCRIPTION

The spent fuel rack was fabricated from 1% boron steel (3) (1/4 in. thick grid 28 in. high) and was designed to be subcritical when submerged in the spent fuel pit, and loaded with a full core of fresh PM-2A fuel elements. In order to be assured of the adequacy of the spent fuel storage rack, a criticality test was performed on site since the rack had not been tested previously. For the purposes of the test, it was assumed that the rack might attain criticality with 7.8 kg U^{235} in it. This is the minimum critical mass as measured during the ZPE. (4)

The BF_3 startup chamber and the 30 curie neutron startup source were waterproofed and mounted on opposite sides of, and directly adjacent to, the spent fuel rack, as indicated in the diagram of Fig. 3.6. The fuel elements were loaded with the plates perpendicular to the source - BF_3 axis, thus maintaining the PM-2A core orientation. Fuel elements were added individually and all fuel additions were made with the five control rod absorbers fully in-

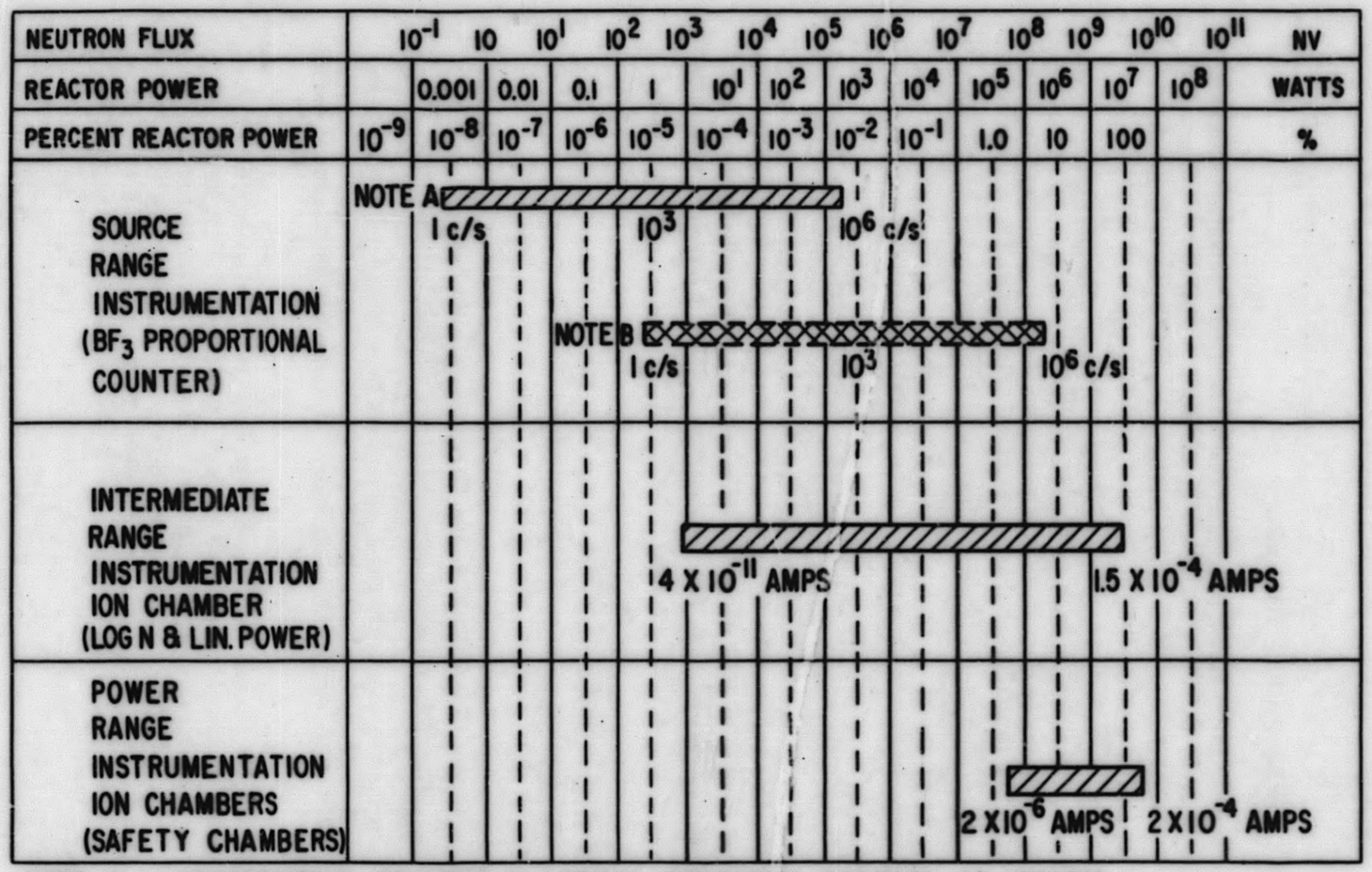

NOTE A - PROPORTIONAL COUNTER IN NORMAL OPERATING POSITION (0 INCHES)
NOTE B - PROPORTIONAL COUNTER WITHDRAWN 50 INCHES

Figure 3.5. PM-2A Nuclear Instrumentation Range Characteristics

serted into the fuel rack. The BF_3 count rates were continually monitored at the control console during this test and constant communication maintained between the control skid and the loading team on the upper platform.

3.2.2 SPENT FUEL RACK LOADING

Figure 3.6 illustrates the spent fuel rack, neutron source, and detector geometry; the fuel loading sequence and the location of each fuel element loaded into the spent fuel rack. In general the loading procedure followed a sequence in which all fuel additions were made with the control rod absorbers in their equivalent core lattice positions. The absorbers were then withdrawn one at a time from the spent fuel rack. As a safety precaution, the center control rod absorber was held just above the spent fuel rack during the absorber removal operation and while obtaining multiplication data on the BF_3. After the loading of the 32 stationary elements plus the 4 spare stationary fuel elements the absorbers were removed one at a time and replaced by the appropriate control rod fuel element sections. A "cocked absorber" was maintained during the control rod fuel element loading operation in a manner similar to that described above.

Table 3.1 is a tabulation of the sequential fuel movements and location, the total fuel inventory in the spent fuel rack up to the respective loading steps, the BF_3 count rate and the inverse multiplication. Figure 3.7 is the inverse multiplication plot obtained from this test and extrapolates to a critical mass of approximately 24 kg. A total of 36 stationary elements and 6 control rod elements were loaded, corresponding to a total of 22.06 kg U-235.

The extrapolated critical mass of 24 kg U-235 is probably conservative since the final fuel additions were made to the center of the spent fuel rack in the control rod fuel element position where the fuel worth is relatively high. Any additional fuel would necessarily be added to lattice positions along the outer boundaries of the assembly where they would have a lower relative worth and consequently the inverse multiplication curve would tend to extrapolate to some higher value for a minimum critical mass when fuel is added along the outer boundaries.

3.2.3 CONCLUSIONS AND RECOMMENDATIONS

1. The spent fuel rack test adequately demonstrates the sub-criticality of the PM-2A spent fuel rack when fully loaded with PM-2A Core I plus 5 spares.

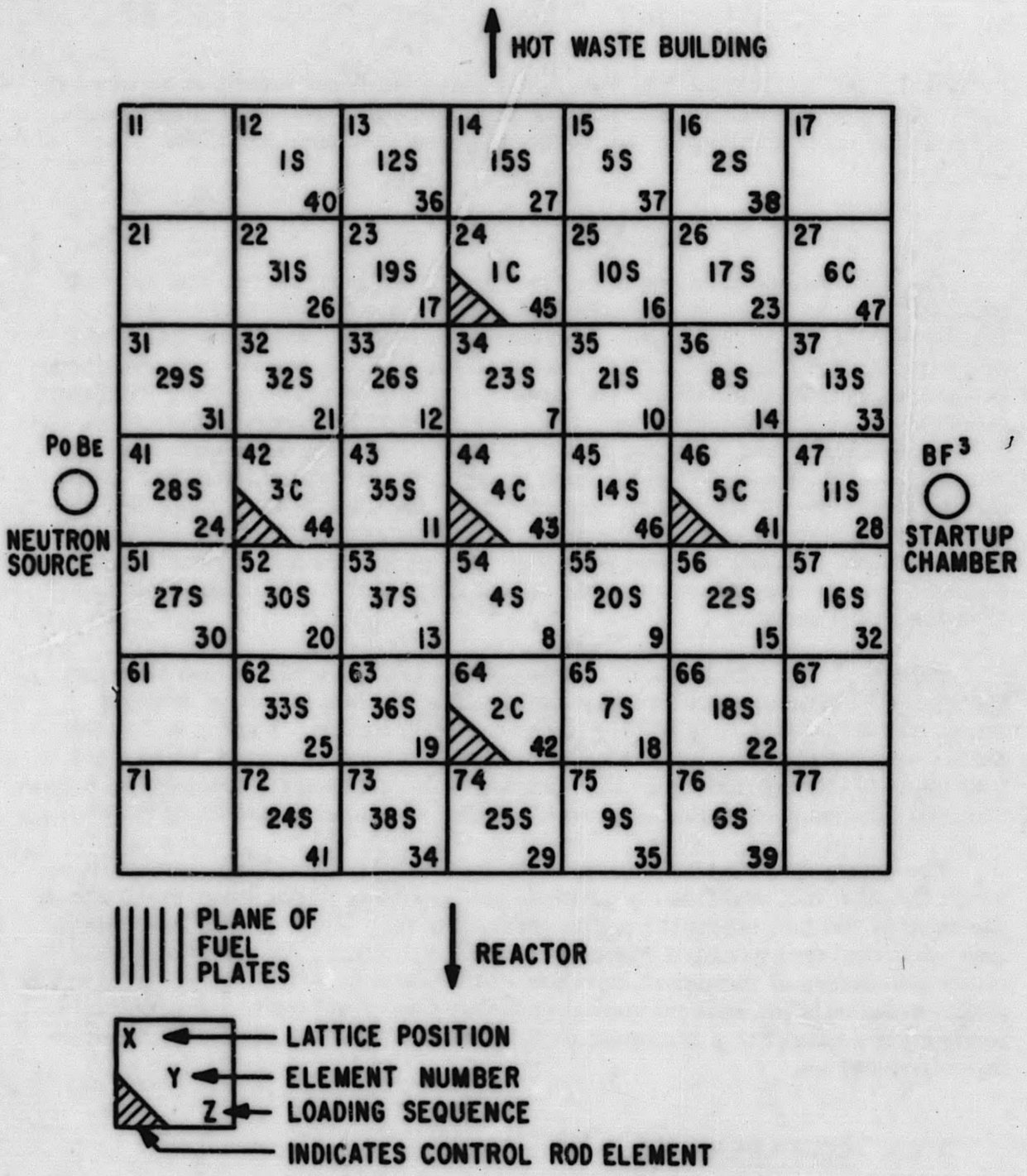

Figure 3.6. Fuel Element Loading Chart for the PM-2A Spent Fuel Rack Criticality Test

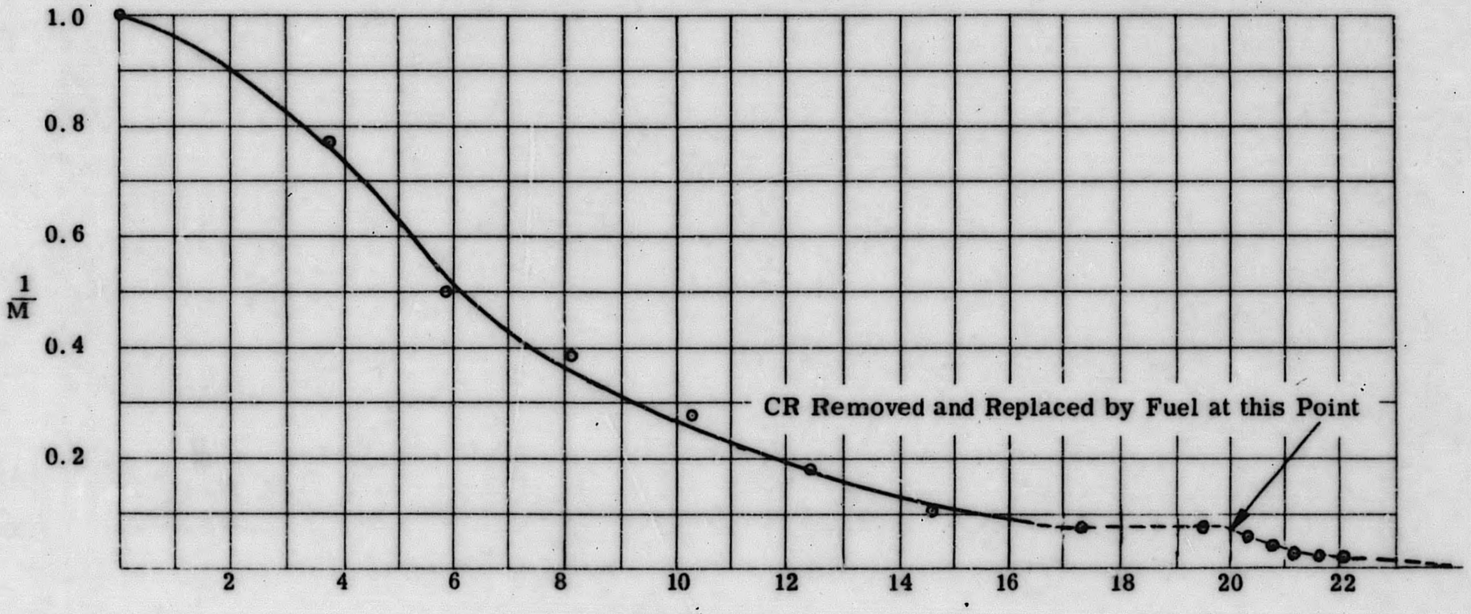

Figure 3.7. PM-2A Spent Fuel Rack Test M^{-1} Curve

TABLE 3.1

LOADING TABLE FOR THE PM-2A CORE I SPENT FUEL RACK TEST

Element Loaded	SFR Lattice Position	Total Fuel Loaded, Kg	BF_3, Cps	M^{-1}	Extrapolated Critical Mass, Kg
0	0	0	5.0	1	
4A	44	0	4.5-5.0		
3A	42	0	5.0-6.0		
1A	24	0	4.5		
5A	46	0	5.0		
2A	64	0	4.5-5.0		
14S	45		5.0		
23S	34				
4S	54				
20S	55				
21S	35				
35S	43				
26S	33	3.79	6.07	0.77	12.5
37S	53				
8S	36		8.0		
22S	56		9.0		
10S	25	5.96	10.0	0.50	11.3
19S	23				
7S	65		11.0		
36S	63		11.0		
30S	52	8.12	13.0	0.385	16.1
32S	32				
18S	66				
17S	26				
28S	41	10.3	18.0	0.278	16.1
33S	62				
31S	22				
15S	14				
11S	47	12.45	28.0	0.179	16.1
25S	74				
27S	51				
29S	31				
16S	57	14.62	43	0.116	18.2
13S	37		55		
38S	73				
9S	75				
12S	13				
5S	15	17.35	70	0.0715	22.0
2S	16				
6S	76				
1S	12				
24S	72	19.52	70	0.0715	22
* 2C	64				
4C	44	20.37	95	0.0527	
3C	42	20.80	125	0.0398	
1C	24	21.22	175	0.0286	
5C	46	21.64	225	0.0222	
6C	27	22.06	250	0.0200	23-24

* Throughout the stationary element loadings, absorbers were in positions 64, 44, 42, 24, and 46. The remaining additions consisted of replacing each of those absorbers with control rod fuel elements.

2. The spent fuel rack must be the subject of additional testing and/or modification if the PM-2A is ever refueled with cores of greater excess reactivities than that of Core I.

3. Inspection of Fig. 3.7 reveals a distinct change in the slope of the 1/M curve when elements were added in control rod positions. The loading up to 20 kg would lead one to suspect an infinite critical mass if the five control rod positions were left vacant.

4. It is recommended that several positions be plugged with dummies or otherwise to insure a larger margin of negative reactivity in the fully loaded rack. The control rod elements would be placed around the outer edge of the rack in the vacant stationary element positions.

3.3 INITIAL CORE LOADING

During the PM-2A Zero Power Experiment[4], an extensive core assembly test was performed. For this test, the core, startup channel, and shielding material between them, was mocked up to approximate the actual plant configuration. On the basis of the mockup, a loading procedure was established which provided shutdown margins, startup channel count rates and critical bank positions for each successive stage of the on site core fueling operation. Following these loading procedures, the core was loaded with five control rod fuel elements and absorbers initially and a BF_3 count rate obtained. Each succeeding fuel addition consisted of the sequential loading of three or four stationary elements and intermediate timed checks of the predicted startup channel counting rates were made until the core was fully loaded. Shutdown BF_3 count rates with the control rods fully inserted were obtained which accurately reproduced those predicted by the ZPE.

The initial core loading followed the sequence of Table 3.2. The critical five rod bank position for the fully loaded clean cold core on site was 6.25 in. withdrawn. The analytical bank position predicted by the ZPE was 6.40 inches. However to correct this to the on-site reading, 0.20 in. must be subtracted to account for differences in the core support structures. Making this correction, the ZPE prediction is 6.20 in., which is in good agreement with the site measurements. In addition, the ZPE was performed without benefit of the actual PM-2A control rod absorbers or the core skirt; hence, the predicted analytical critical bank position was the result of applying corrections to the position measured in the ZPE.

Figure 3.8 shows the PM-2A Core I orientation, lattice numbers and element locations with respect to the control rod drives and the coolant inlet and outlet pipes.

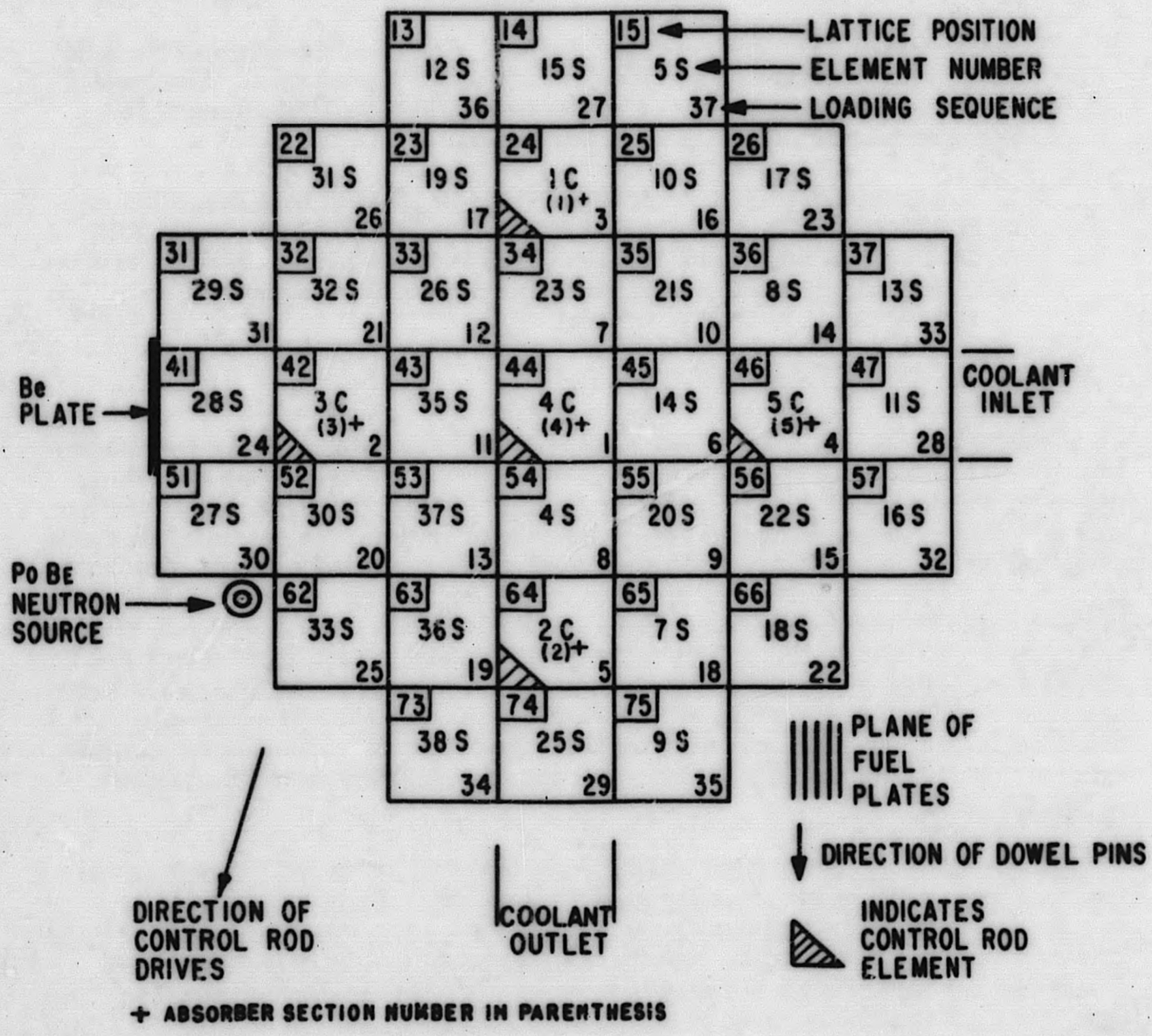

Figure 3.8. PM-2A Core I Loading Chart

TABLE 3.2

PM-2A CORE I LOADING TABLE

Loading Sequence	Element Number	Lattice Position	Loaded U-235 Mass, Kg	BF_3 Count Rates*, Cps	Predicted Count Rates From ZPE
1	4C (4)+	44			
2	3C (3)	42			
3	1C (1)	24			
4	5C (5)	46			
5	2C (2)	64	2.14		
6	14S	45			
7	23S	34			
8	4S	54	3.76		
9	20S	55			
10	21S	35			
11	35S	43	5.39		
12	26S	33			
13	37S	53	6.47		
14	8S	36	7.02		
15	22S	56	7.56		
16	10S	25	8.10	0.27	0.35
17	19S	23			
18	7S	65			
19	36S	63			
20	30S	52	10.27	0.50	0.63
21	32S	32			
22	18S	66			
23	17S	26			
24	28S	41	12.44	0.76	0.95
25	33S	62			
26	31S	22			
27	15S	14			
28	11S	47	14.61	1.5-2.0	1.8
29	25S	74			
30	27S	51			
31	29S	31			
32	16S	57	16.78	2.5	3.1
33	13S	37			
34	38S	73			
35	9S	75	18.41	5.1	6.5
36	12S	13			
37	5S	15	19.49	4.5	7.0

* Five rod bank fully inserted

\+ Absorber section numbers in parenthesis

3.4 BF_3 STARTUP CHAMBER RESPONSE VERSUS LOCATION

3.4.1 DESCRIPTION

The BF_3 chamber well is located approximately 32 in. from the core centerline and extends upward through the upper shield tank to the refueling platform. A lifting mechanism on the upper platform is attached to the BF_3 chamber in order to insert or remove the chamber from the core. (See Fig. 3.2.) Removing the chamber from the core not only protects the chamber from high neutron and gamma ray fields during full power operation but also extends the useful operating range of the BF_3 itself.

3.4.2 MEASUREMENTS MADE PRIOR TO THE PM-2A SHIELD MODIFICATION

In order to determine the adequacy of the startup channel, and to establish the relative magnitude of the various neutron sources contributing to the total BF_3 response rate, the BF_3 response was obtained as a function of position for various core conditions. The data listed in Table 3.3 were obtained prior to the shield modifications.

The chamber was operated at 2450 volts and a gain setting of 210° rotation (Ref. Sec. 3.1.1). The neutron check source was attached to the BF_3 penetration housing between the vapor container and the bottom of the upper shield tank and was located approximately 4 ft above the core centerline for runs 2 and 3, (Position A).

3.4.3 MEASUREMENTS MADE SUBSEQUENT TO THE SHIELD MODIFICATION

The data listed in Table 3.4 was obtained after the shield modification, and prior to the acceptance test run. The operating voltage was 2450 volts and the gain potentiometer setting was 210° rotation. The source was placed at position B inside the upper shield tank above the vapor container resting on the floor of the upper shield tank against the BF_3 well approximately 65 in. above the core centerline, Fig. 3.2.

The data in Table 3.5 was taken after the 387 hr endurance run. The high voltage was 2450 and the gain was set at 90° rotation.

TABLE 3.3

PM-2A CORE I BF_3 RESPONSE AS A FUNCTION OF POSITION (10/6/60) PRIOR TO SHIELD MODIFICATION

RUN #1: Reactor Critical - Five Rod Bank Position 6.25 in. withdrawn - Check source not in position. Data normalized to log N power level of 6.0×10^{-5}

RUN #2: Reactor Shutdown - Five Rod Bank Fully Inserted - Check source positioned outside vapor container at base of upper shield (Fig. 3.2).

RUN #3: Reactor Critical - Five Rod Bank Position 6.93 in. withdrawn - Check source positioned as in Run 2. Data normalized to Log N power level of 6.0×10^{-5}. Temperature 250°F. Pressure 1700 psi.

BF_3 Location, Inches	Run #1 Response, Cps	Run #2 Response, Cps	Run #3 Response, Cps
0	39000	3	28600
2	38000	4	31000
4	38400	4	31300
6	37600	4.5	29900
8	36900	5	27000
10	35300	6.5	25000
12	31900	8	21400
14	26100	10	18700
16	23100	15	15000
18	18500	21	13400
20	14900	33	9600
22	11400	52	7500
24	9600	95	5800
27		140	4500
30	3380	140	2900
33		100	1600
36	774	60	710
39		55	492
42	381	55	394
45		75	370
48	150	160	370
51		280	410
54	34	280	380
57		230	305
60	19	150	250
63		140	220
66	19	180	280
69	29	320	600
72	38	400	850

TABLE 3.4

PM-2A CORE I BF_3 RESPONSE AS A FUNCTION OF POSITION (2/7/61) AFTER SHIELD MODIFICATION

RUN #1: Reactor Shutdown - Five Rod Bank Fully Inserted. Check Source not in position.

RUN #2: Reactor Shutdown - Five Rod Bank Fully Inserted - Check source located inside upper shield tank against BF_3 penetration housing.

RUN #3: Reactor Critical - Five Rod bank position 6.81 in. withdrawn - Check source located same as Run #2. Data normalized to log N power level of 6.0×10^{-5}.

RUN #4: Reactor Critical - Five Rod Bank Position 6.81 in. withdrawn - Check source not in position. Data normalized to log N power level of 6.0×10^{-5}.

BF_3 Location, Inches	Run #1 Response, Cps	Run #2 Response, Cps	Run #3 Response, Cps	Run #4 Response, Cps
0	2.5	2.2	80000	80000
2	2.5	2.0	85000	88000
4	2.5	2.2	89000	90000
6	2.8	2.6	89000	86000
8	3.0	2.5	82000	80900
10	2.6	2.6	75000	73500
12	2.6	2.4	65000	64100
14		2.4	55000	54400
16	2.2	2.6	46900	44400
18	2.2	2.2	37800	35300
20	1.9	2.2	27800	26300
22	1.8	2.8	21800	20600
24	1.8	3.5	15800	14300
28	1.5	4.5	11800	7280
32	1.3	11	3340	2900
38	0.15	23	1170	938
42		35	606	536
44		45	439	337
46		32	292	228
48		35	214	131
50	0.02	48	165	76
52		70	126	42
54		130	160	31
56	190	190	190	21
58		280	380	18
60	0.07	420	380	17
62		500	450	16
64		650	590	14
66		1000	980	12
70		3500	3400	9.6
72	0.15	4500	5200	8.6

TABLE 3.5

PM-2A CORE I BF_3 RESPONSE AS A FUNCTION OF POSITION (FOLLOWING 387 HR OPERATION AT 725 KW)

Reactor shutdown - Five Rod bank fully inserted. Check source in position inside upper shield tank near BF penetration housing. Log N reading 0 Measurement taken 62 hours after shutdown.

BF_3 Location, Inches	Response Cps	BF_3 Location, Inches	Response CPS
0	9.34	38	30
2	10.0	40	42
4	11.3	42	52
6	10.3	44	58
8	12.2	46	50
10	9.75	48	45
12	9.67	50	50
14	9.00	52	75
18	7.34	54	100
20	6.50	56	160
22	6.00	58	240
24	6.66	62	440
28	8.66	64	620
32	15.65	66	1200
		68	2800
		70	4500
		72	6000

3.4.4 COMPARATIVE RESULTS

Figure 3.9 presents a comparison of the measurements obtained during shutdown operations: Curve I was obtained prior to the shield modification with the check source located at (Position A, Fig. 3.2), outside the vapor container; Curve II was obtained after the shield modification and before any power operations, the check source positioned at (Position B, Fig. 3.2), inside the upper shield tank; and Curve III was obtained 62 hr after the completion of the 387 hr acceptance test, the check source again positioned at (Position B, Fig. 3.2), inside the upper shield tank. The response of Curve II is almost a factor of 10 higher than that of Curve I in the check source region. The check source strength had decayed 47% between the time of the two measurements,

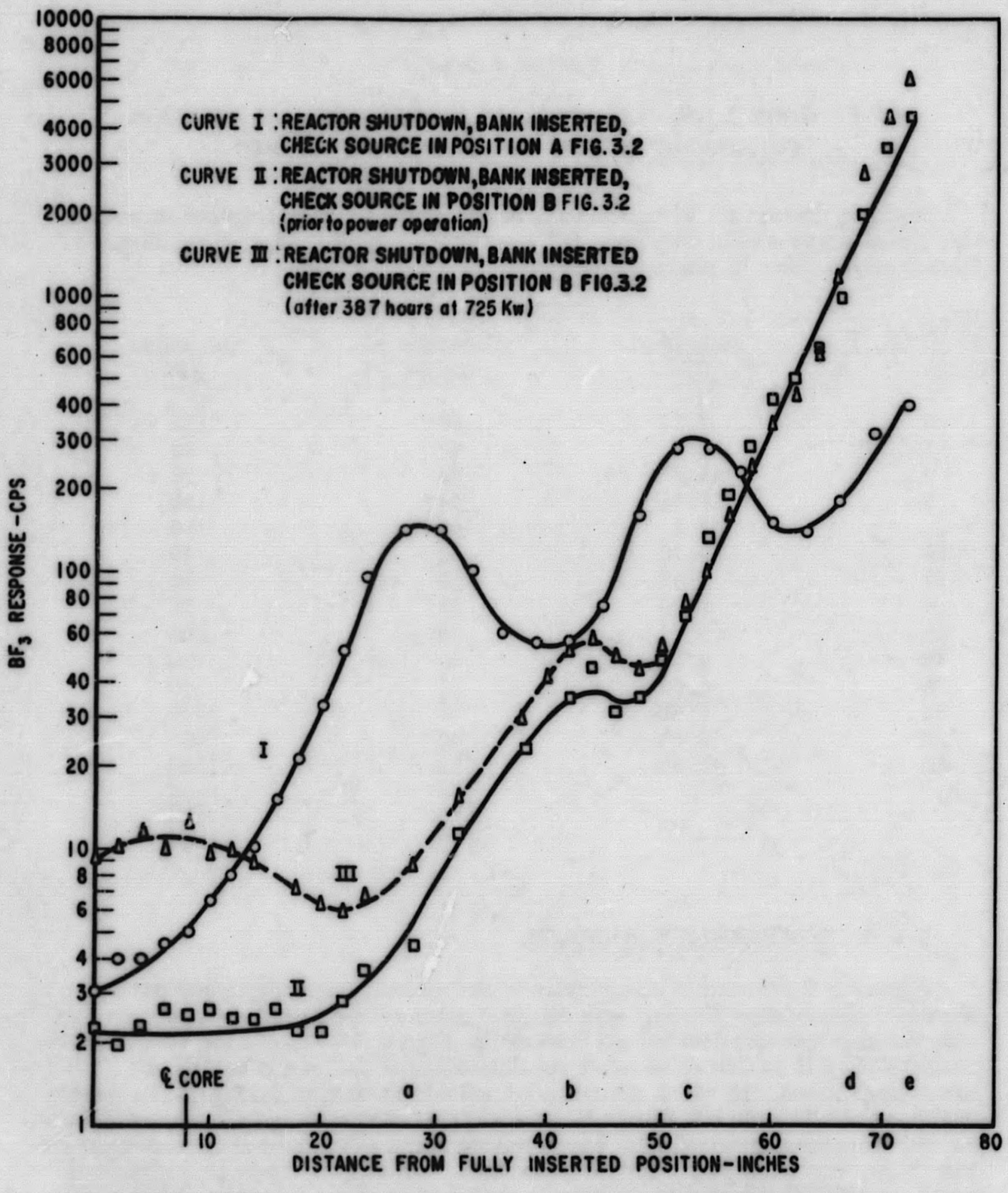

Figure 3.9. BF_3 Chamber Count Rate Vs Chamber Location

Curve I data having been obtained in October 1960 and Curve II data in February 1961. In addition the relatively flat region of Curve II near the core centerline indicates that relocation of the check source has minimized the amount of neutron streaming down the instrument penetration tubes from the neutron check source as illustrated in Curve I.

Best estimates indicate that the fully inserted position of the startup chamber centerline is located approximately 8 in. below the core centerline. Therefore, in order to correlate the chamber positions as shown in Fig. 3.2. with that of Fig. 3.9 relative to the core centerline, the two figures have been marked so that locations a, b, c, d and e on Fig. 3.9 correspond to locations a, b, c, d and e in the BF_3 well in Fig. 3.2.

As the BF_3 chamber is withdrawn from full in to full out, it passes the dry cap region (location "a"), the original check source position (location "c"), and into the upper shield tank (location "d"). At its fully withdrawn position it is adjacent to the new check source position (location "e"). The peak at point "a" on Curve I is probably due to scattering and thermalizing of fast neutrons at the water-air interface; the minimum at point "b" on Curve I is a result of the gap in that region prior to the shield modifications. The peak at "c" is due to neutrons thermalized in the paraffin around the source, the minimum between points "c" and "d" are again due to the air gap in that region. The increase in the region near the fully withdrawn position results from neutron thermalization in the bottom of the shield tank. The minimum near point "b" in Curves II and III is a result of adding the cadmium shielding material to that region as part of the shield modifications.

Figure 3.10 illustrates the relative effect of the source during reactor operation. Curve I was obtained with the reactor critical and the check source inside the upper shield tank. Curve II was obtained with the reactor critical and without a check source present.

3.4.5 CONCLUSIONS

1. Comparison of Curves I and II in Fig. 3.9 shows that the shield modification and relocation of the check source has greatly improved the effectiveness of the neutron check source. This is attributed to the increased amount of thermalizing media surrounding the check source in its relocated position (B in Fig. 3.2).

2. The initial count of 4.5 cps has been reduced to 2.2 cps as a result of relocating the check source from A to B; neutron streaming down the instrument penetration was reduced, and the check source contribution to the BF_3 response in the core region was negligible.

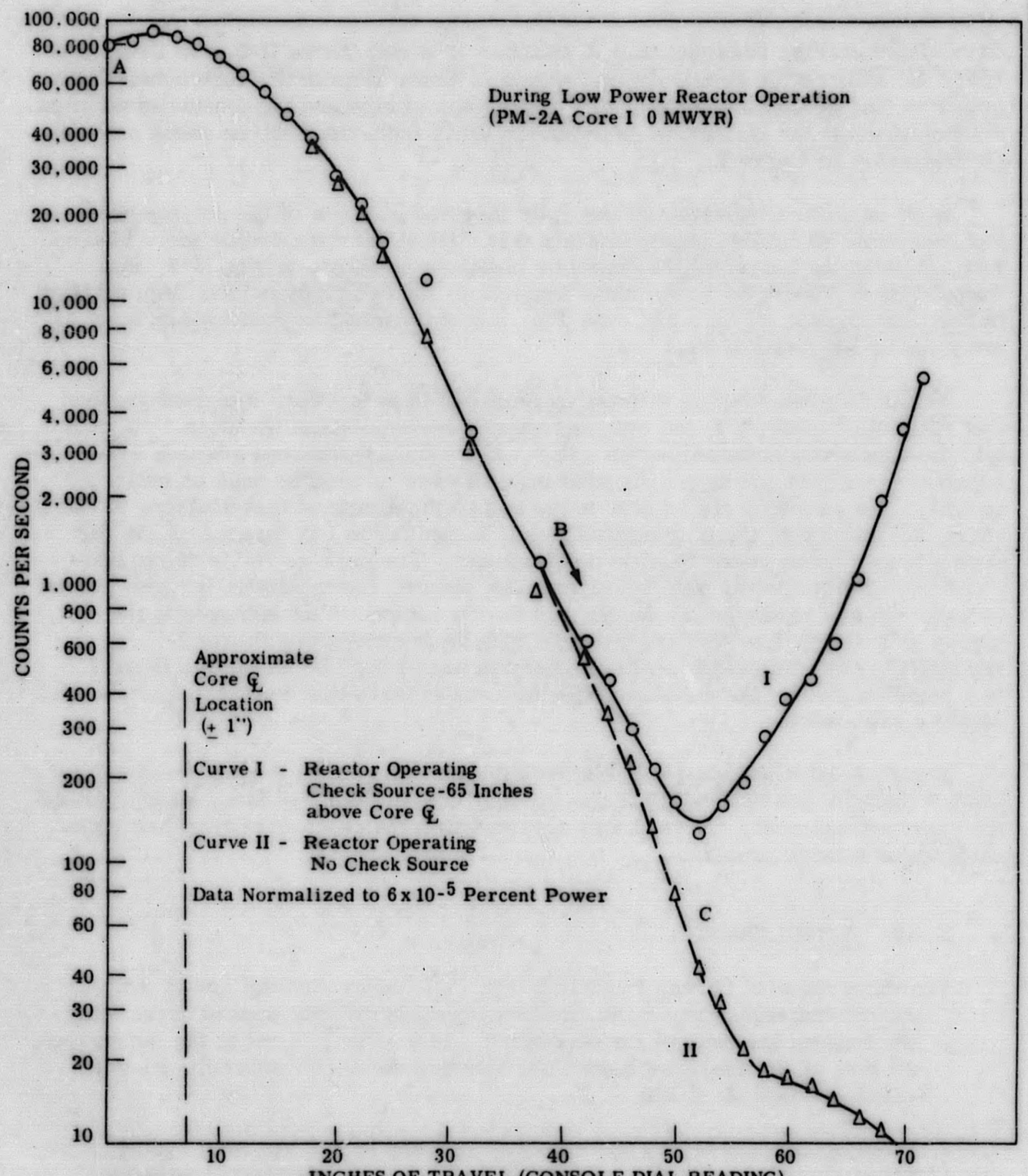

Figure 3. 10. BF_3 Startup Channel Response Vs Location

3. The BF_3 response is approximately five times higher in the core region after 387 hr of operation than in the cold, clean core (refer to Curves II and III, Fig. 3.9). This effect is due to photoneutron emission (γ, n reaction) from the beryllium block following the 400 hr acceptance test (see Section 3.11).

3.5 CONTROL ROD CALIBRATIONS

Control rods were calibrated for various core conditions (as a function of the movement of the remaining four rods as a bank) using the positive period technique and the in-hour equation.

The calibrated rods were then used for obtaining temperature, pressure, and xenon coefficients of reactivity, four rod bank worths and core reactivity. For the purpose of uniformity and comparison with future calibrations, the curves were plotted using a 4th degree polynomial least squares machine fit of the data points.

3.5.1 ROD 4 CALIBRATIONS (CENTER CONTROL ROD)

Rod 4 (Position 44) was calibrated at 60° F, 250° F, and 510° F. It was also calibrated as a function of temperature and position for temperature coefficient measurements which will be discussed in Section 3.7. Figure 3.11 shows the Rod 4 calibrations obtained for the two lower temperatures at O MWYR. The data obtained at 60° F and 250° F appear to coincide - within estimated ±10% statistical limits of the experiment - hence, one curve is drawn through the experimental points obtained at both temperatures to indicate the rod worth over the lower temperature ranges. It can be seen, nevertheless, that a definite shift in calibration is obtained in going from the 250°F curve of Fig. 3.11 to the 510° F curve shown in Fig. 3.12. This shift is attributed to the change in the four rod bank position between the two calibrations which resulted from increased temperatures rather than to the change in the temperature itself. The Rod 4 calibration as a function of temperature and at a constant bank position, Fig. 3.13, peaks in approximately the same location as the 60° F and 250° F calibration curves. Comparison of the four rod bank movements for the various curves justifies the foregoing conclusions. This is also consistent with the SM-1 Core I results.(6)

3.5.2 ECCENTRIC ROD CALIBRATIONS

Figure 3.14 presents calibration data obtained for Control Rod 5 (Position 46) at 60° F and 250° F and for Control Rod 1 (Position 24) at 60° F. Inspec-

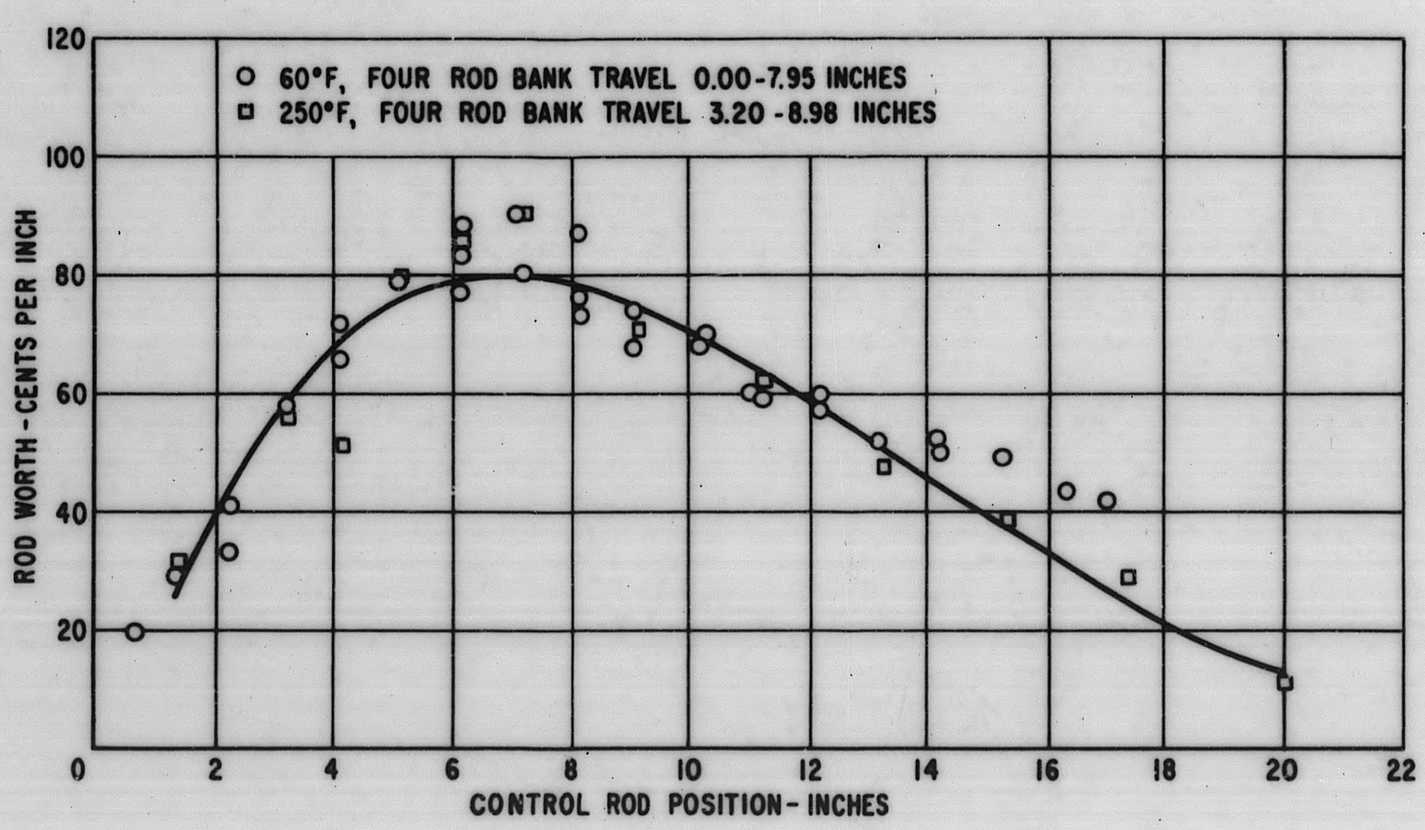

Figure 3.11. PM-2A Control Rod 4 Worth Vs Control Rod Position (at 60°F and 250°F)

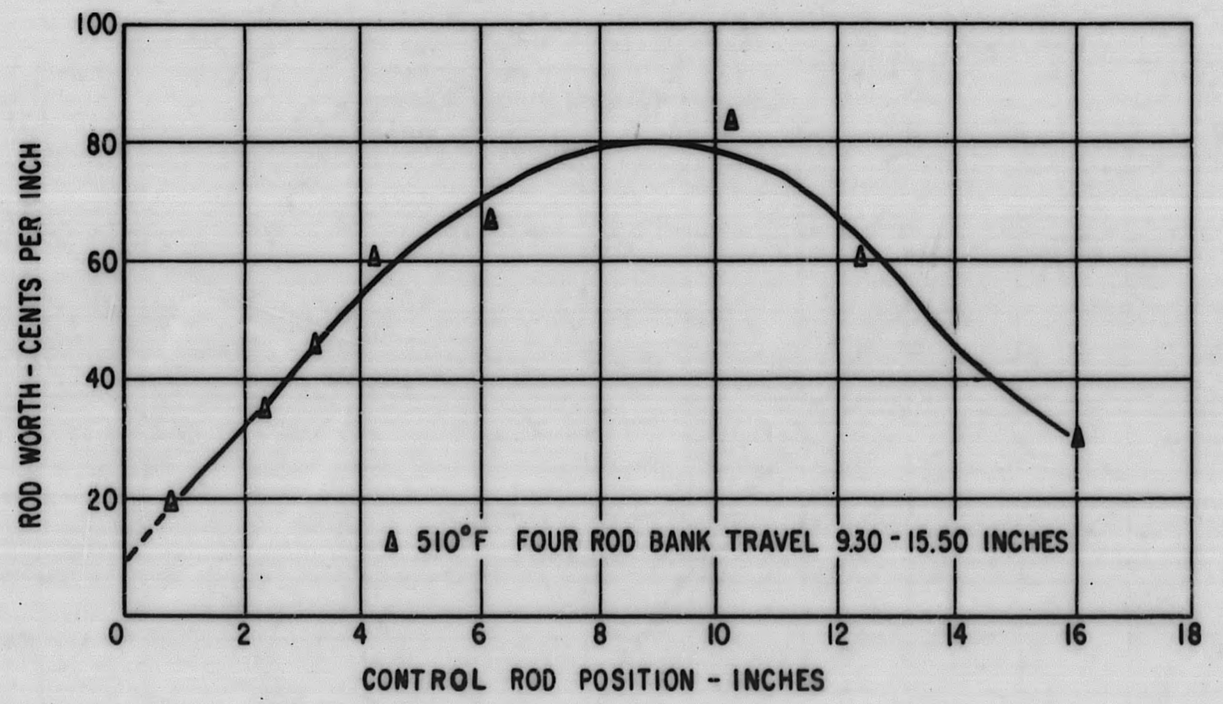

Figure 3.12. PM-2A Control Rod 4 Worth Vs Control Rod Position (at 510°F)

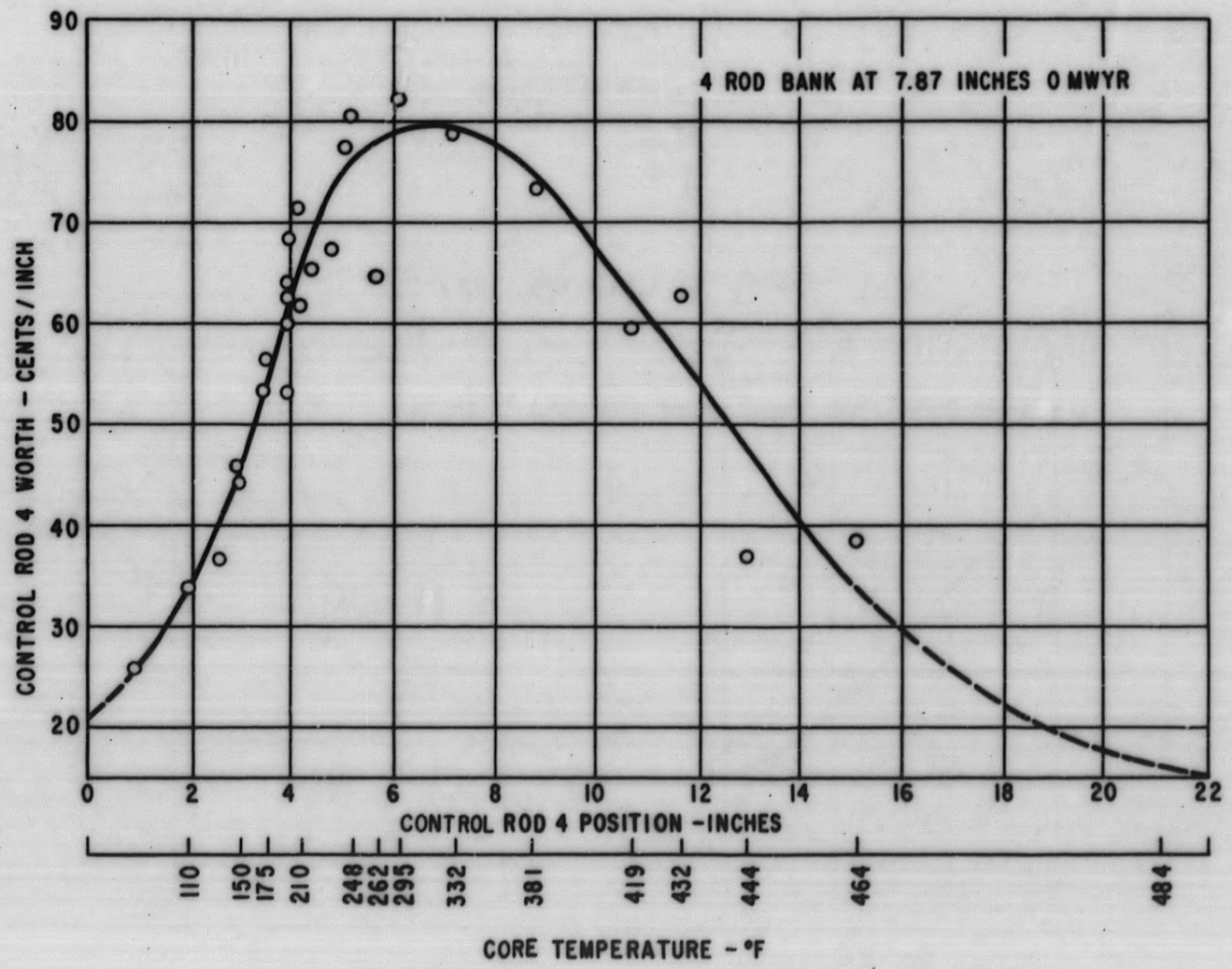

Figure 3.13. PM-2A Control Rod 4 Worth Vs Control Rod Position with Varying Core Temperature

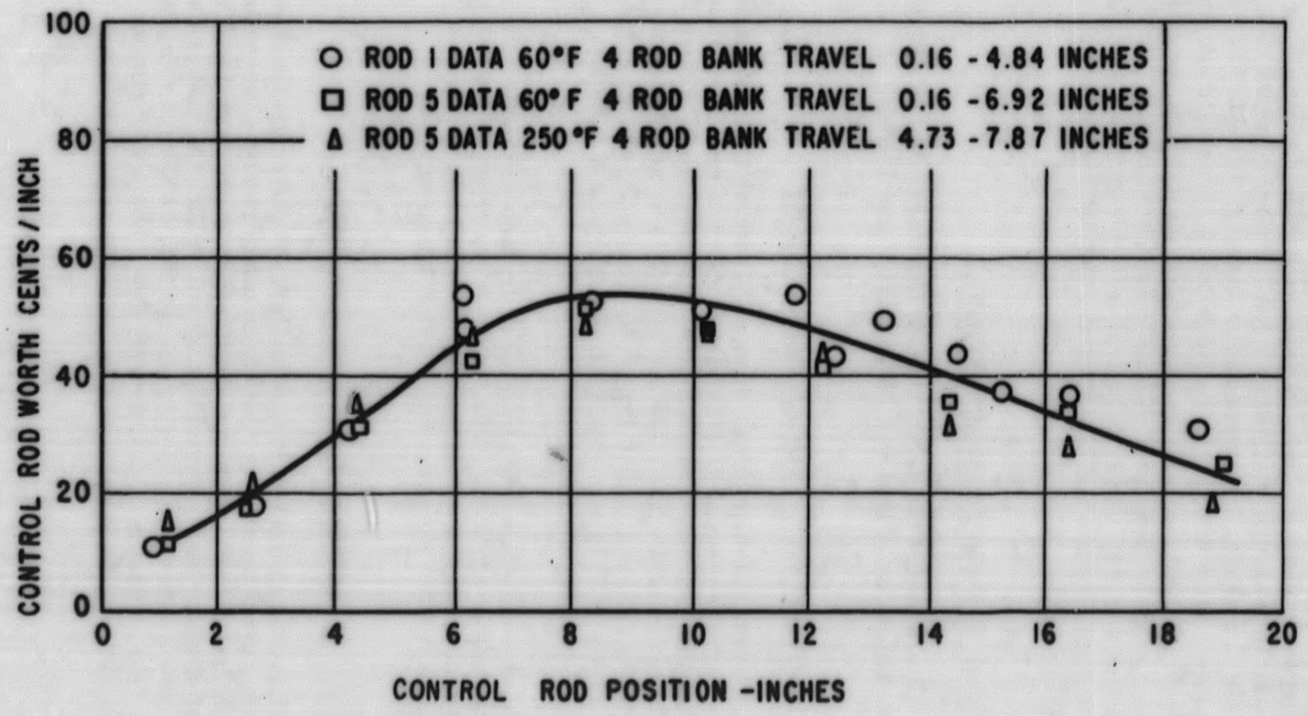

Figure 3.14. PM-2A Eccentric Control Rod Worth Vs Control Rod Location

tion of Fig. 3.14 reveals very strong similarity between the three calibrations. This is to be expected since the rods are symmetrically located in the coil. Hence, one curve is presented to illustrate the differential worth of any eccentric PM-2A control rod over the temperature range of 60° F to 250° F. This curve is a 4th order least square fit of data from all three calibrations. The range of travel of the four rod bank is similar for all three calibrations. However, it is appropriate to assume a shift in the peak calibration (similar to that illustrated for Rod 4 in Fig. 3.12) will result as the rod bank moves out, and that the shift in peak location and control rod worth will be identical for all four eccentric control rods.

3.5.3 FOUR ROD BANK CALIBRATION

Figure 3.15 illustrates the calibration of Control Rods 1, 2, 3, and 5 as a bank using the calibration of Rod 4 at 60° F, 250°, and 510° F.

3.5.4 CALCULATED INTEGRAL ROD WORTHS

In order to determine quickly the reactivity control available in the various rods, integral worths were calculated using Simpson's rule for Rods 4 and 5, and the four rod bank. These are illustrated in Fig. 3.16, 3.17 and 3.18 respectively. Using the assumption that the integral rod worths are additive, and adding numerically the integrals of Fig. 3.16, Curve B, and Fig. 3.18 over the interval from 11.61 to 22 in., a total core reactivity of $11.40 was obtained (operating temperature and pressure).

A decrease in the total worth of Rod 4 at the higher temperature (Fig. 3.16) amounts to approximately $1.40. This is not in agreement with SM-1 data; however, increased neutron leakage resulting from the increased operating temperature and decreased core size may explain this disagreement.

3.5.5 AXIAL THERMAL FLUX DISTRIBUTION

The relative axial thermal neutron flux through the core centerline was approximated by taking the square root of the worth of Rod 4 (normalized to an average of 1.00) at 510° F. This flux distribution is illustrated in Fig. 3.19. Since no power mapping has been performed on the PM-2A, this is the only experimental data available to approximate the PM-2A Core I relative power distribution. This compares favorably with SM-1 data under similar conditions where the max/ave is 1.63 at the 6 to 7 in. position.

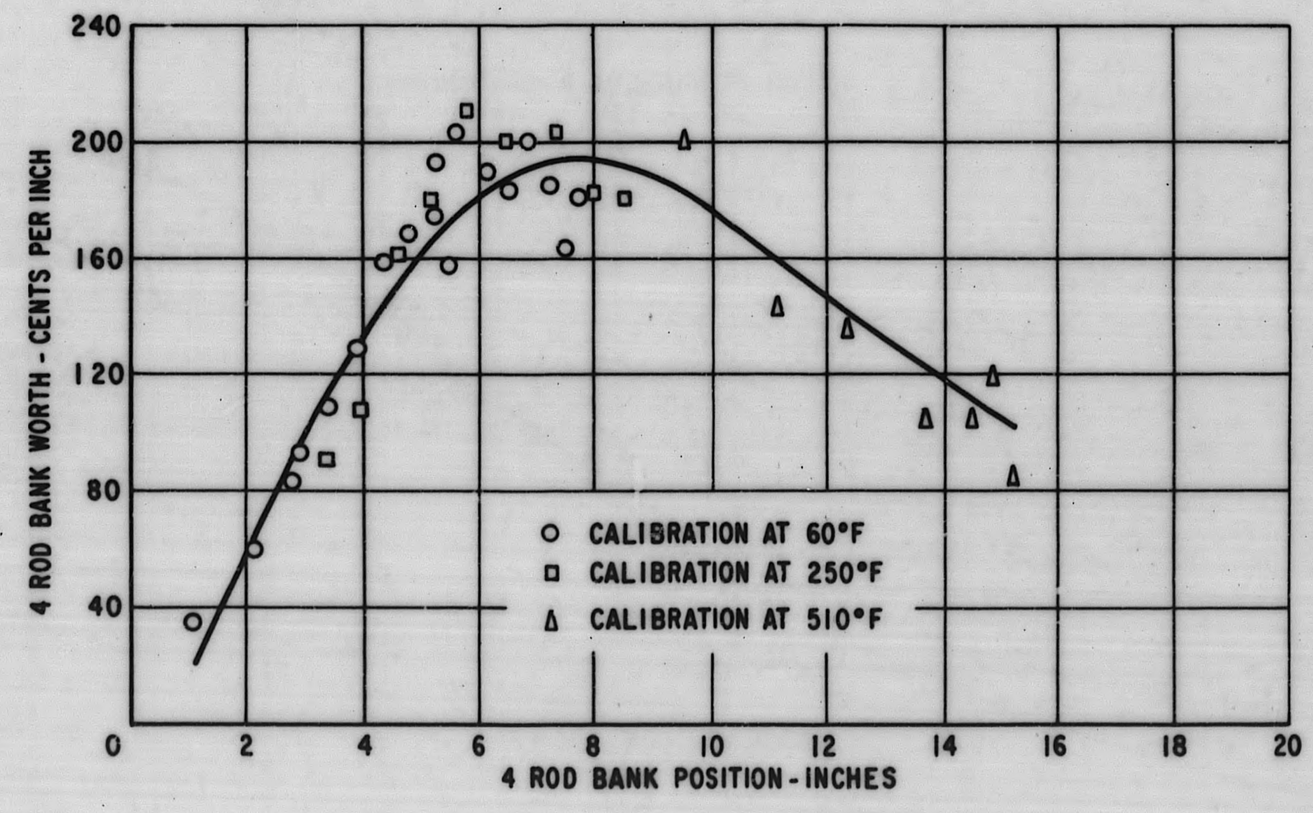

Figure 3. 15. PM-2A Four Rod Bank Worth Vs Bank Position

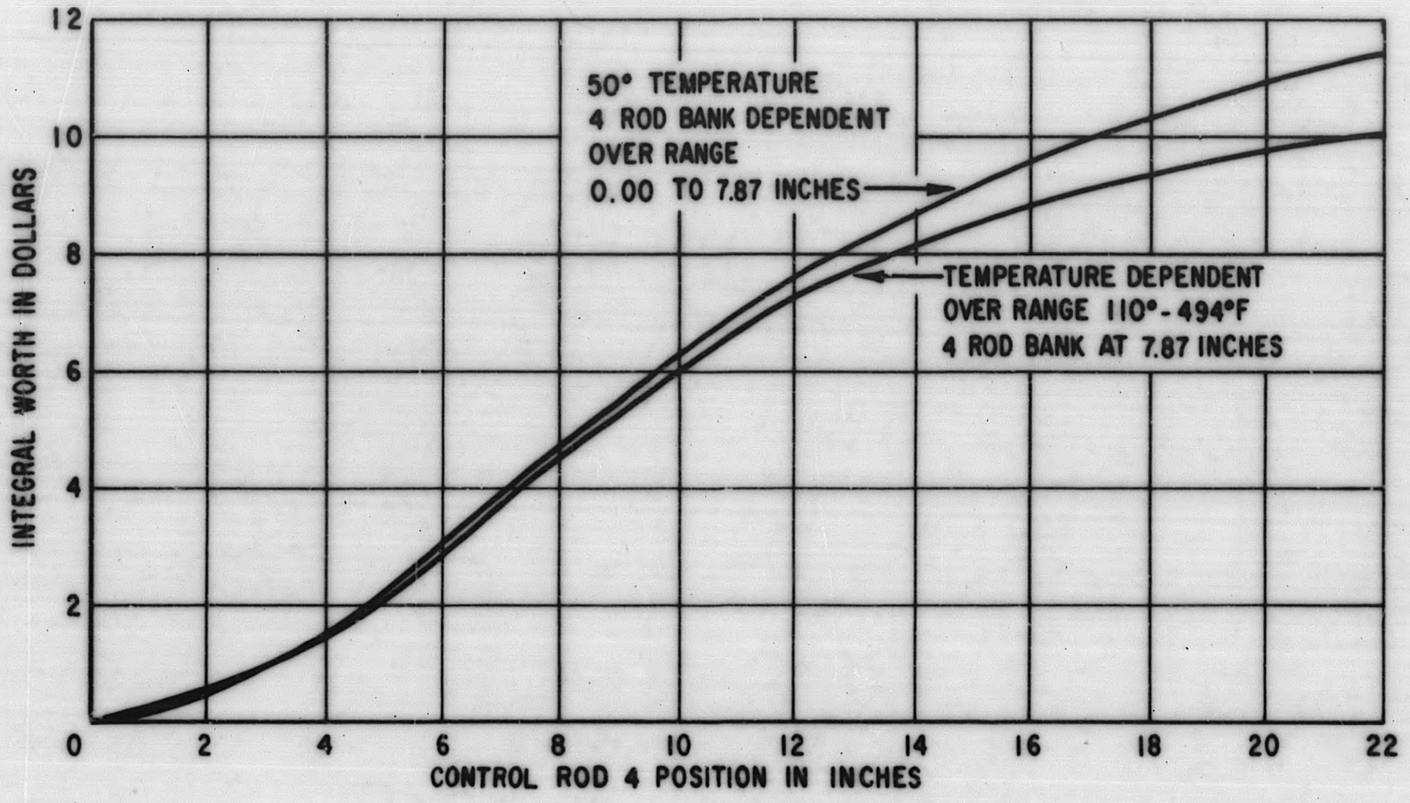

Figure 3.16. PM-2A Integral Control Rod 4 Worth Vs Rod Withdrawal Distance

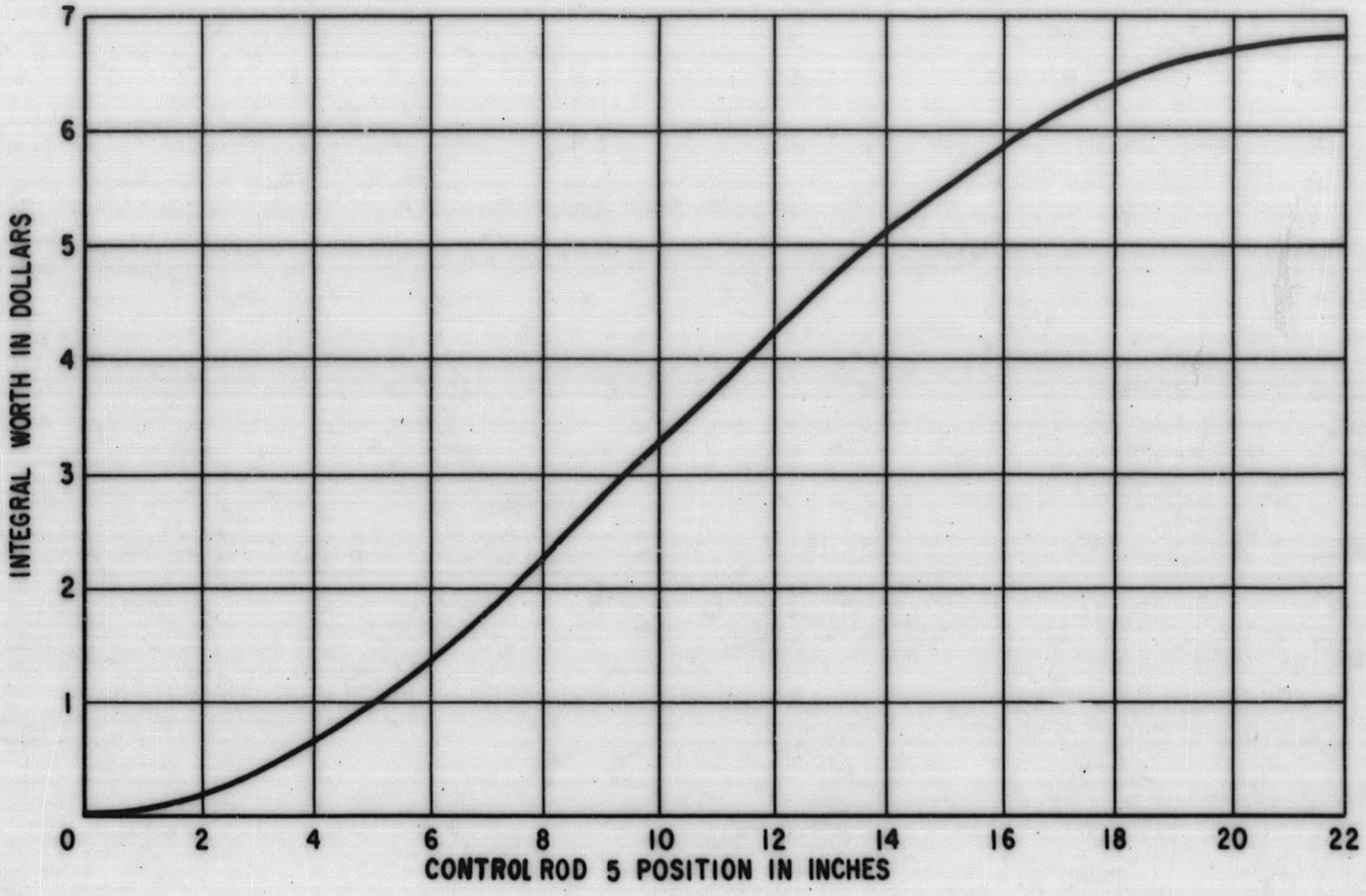

Figure 3.17. PM-2A Integral Control Rod 5 Worth Vs Rod Withdrawal Distance

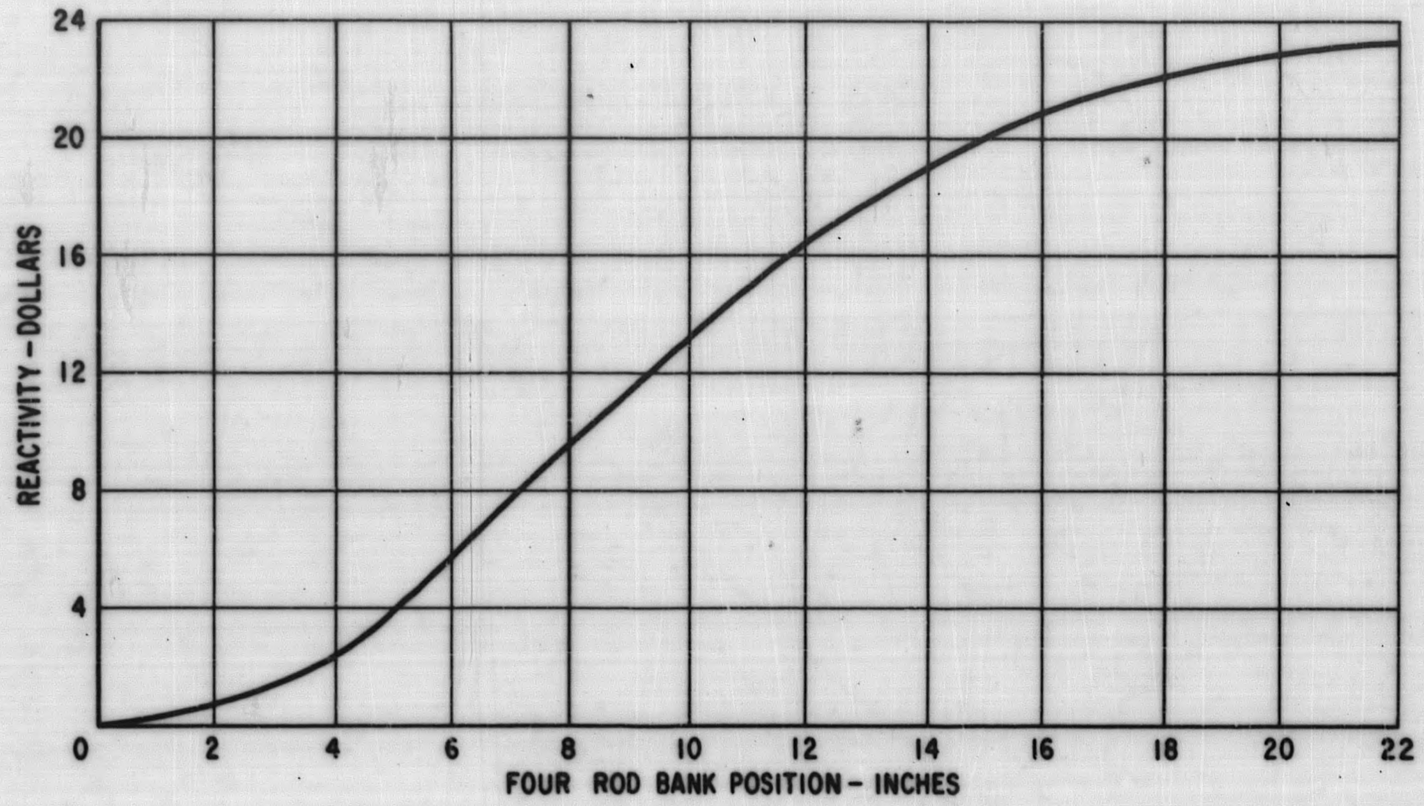

Figure 3.18. PM-2A Integral Four Control Rod Bank Worth Vs Control Rod Bank Withdrawal Distance

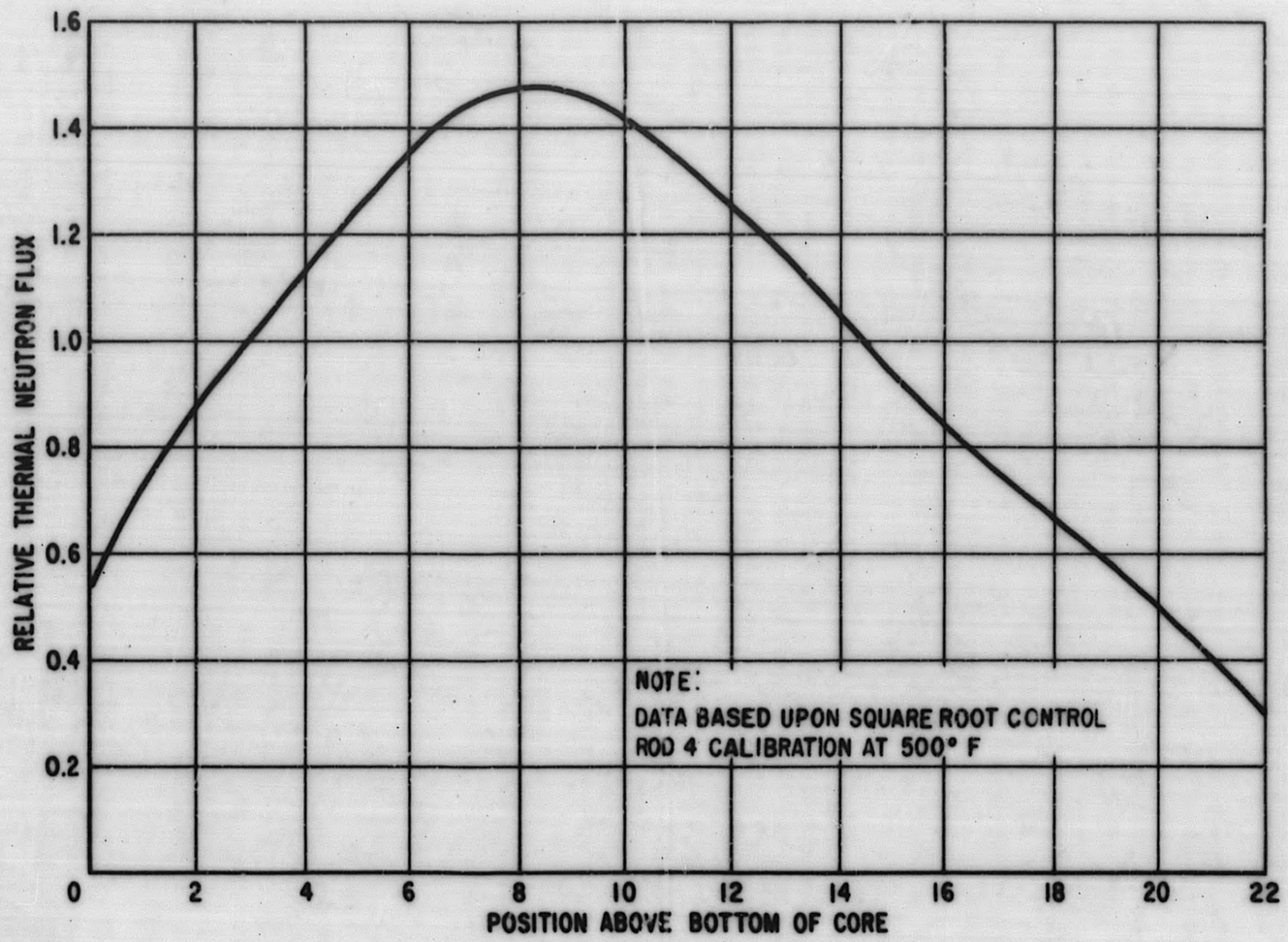

Figure 3.19. Relative Thermal Neutron Flux Vs Distance above Bottom of Active Core

3.6 TEMPERATURE COEFFICIENT OF REACTIVITY

The PM-2A Core I is of lower effective core diameter and is operated at a higher temperature and pressure than any previous small PWR plant; therefore, temperature coefficient measurements were obtained during initial heatup in order to investigate the effect on reactor control at these higher operating conditions. Since no external heat source was available, the core was brought up to temperature by nuclear heating. The four rod bank was maintained at a constant position of 7.87 in. while Control Rod 4 was withdrawn to maintain heatup. The heatup operations were interrupted at intervals of 10-15° F in order to obtain calibrations of Control Rod 4 at the higher core temperature and control rod position. The calibration obtained is presented in Fig. 3.13. The temperature scale at the bottom of Fig. 3.13 is included to indicate the various temperatures at which calibration points were obtained and is not intended to fit any particular scale since the rod worth is not linear with temperature or position.

Figure 3.20 shows the PM-2A Core I startup temperature coefficient data which was calculated by use of the Rod 4 calibration in Fig. 3.13. A curve showing the bulk coefficient of expansion of water normalized to the PM-2A data over the range 150° to 250° F is also presented for comparison. It is well illustrated that the curve shapes agree favorably up to about 400° F and then diverge quite sharply. It is supposed that the temperature coefficient should follow the bulk coefficient curve, and inspection of Figure 3.21 shows that SM-1, PM-2A and SPERT-III data do agree with the bulk coefficient curve up to about 425° F. The divergence beyond that point is not explained although large experimental uncertainty is evident from the scatter of data points.

For comparison purposes, the PM-2A and SM-1 curves were integrated over the range of 100° F to 400° F (since these are the limits of the SM-1 data) and the following results were obtained:

1. SM-1 reactivity change - - $6.50
2. PM-2A reactivity change - - $7.25

It must be noted that the PM-2A values are a result of one series of measurements in a clean core while the SM-1 data is composite data taken over SM-1 Core I lifetime.(6) Other differences which are of note are the core configurations and control rod arrays, operating pressure, and fuel and burnable poison loadings. Considering the differences in the various core parameters, all the curves of Fig. 3.21 agree favorably within the limitations of experimental statistics.

Integration under the PM-2A temperature coefficient curve of Fig. 3.20 over the temperature range of 60° F to 510° F renders a cold to hot reactivity change of approximately minus $11.50.

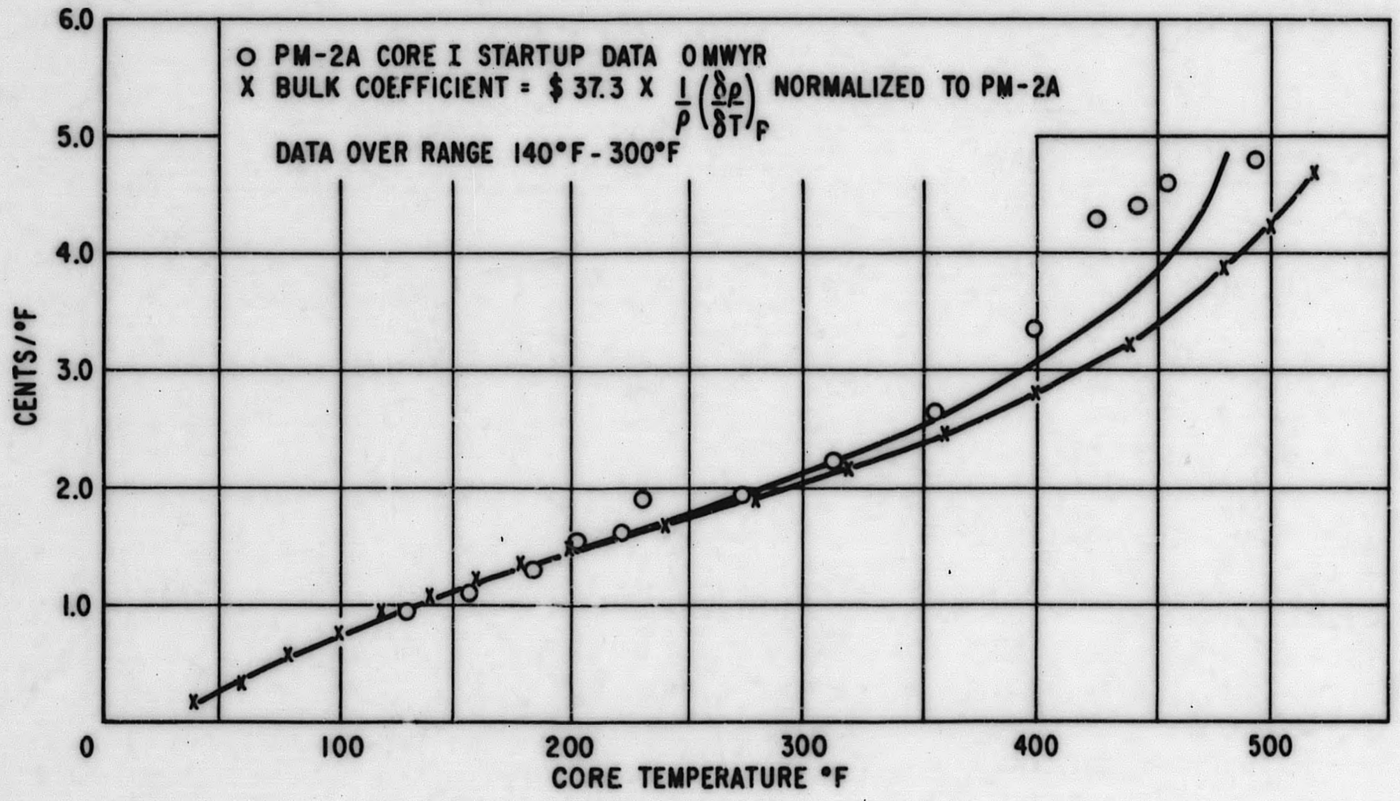

Figure 3.20. PM-2A Temperature Coefficient of Reactivity Vs Core Temperature

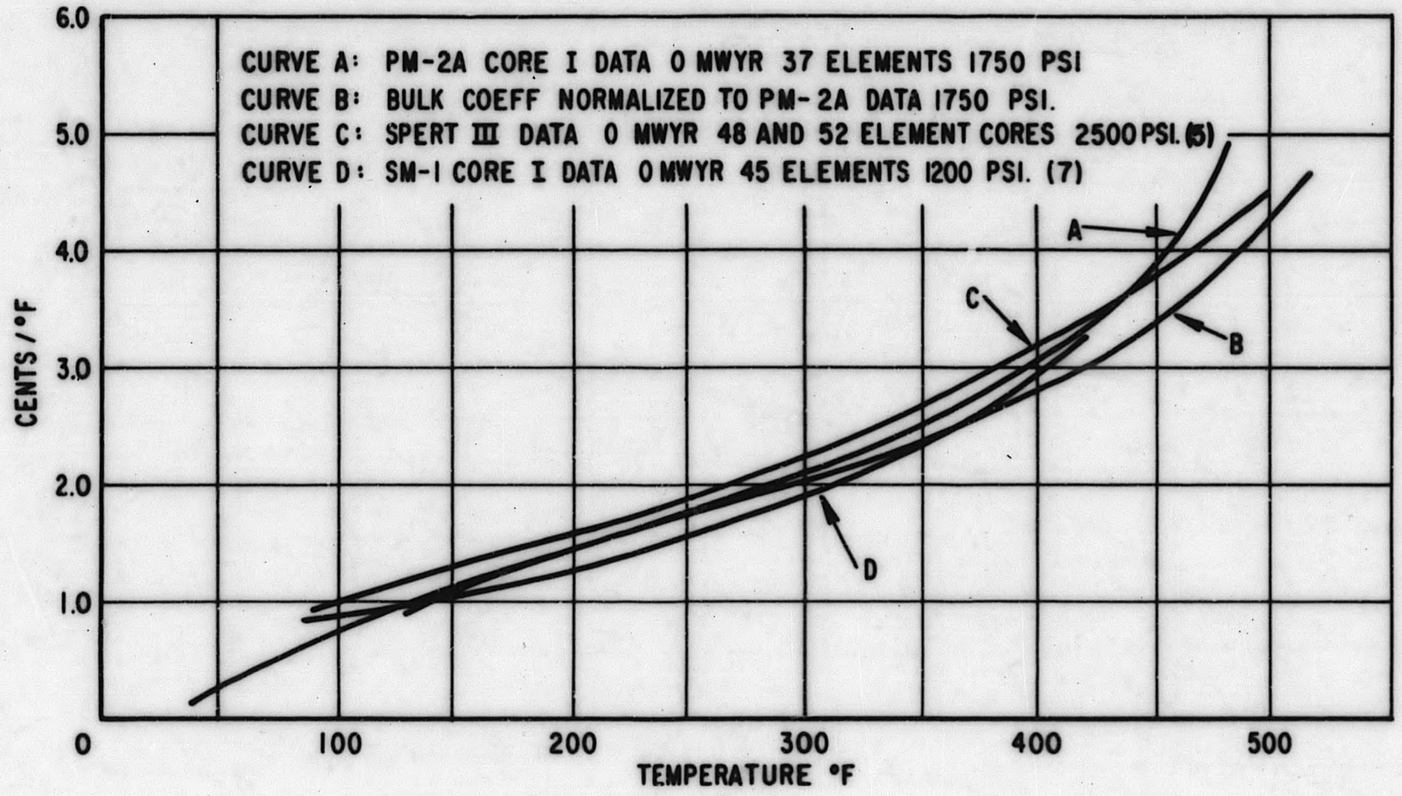

Figure 3.21. Comparative Temperature Coefficients of Reactivity Vs Temperature for Various Reactor Systems

Figure 3.22 shows the Rod 4 movement from which the above data was obtained. Good agreement is obtained from the five rod bank movement: Fig. 3.23 shows the five rod bank moved from 6.25 in. to 10.41 in. during the heatup process. Integration over this range under the curves of Fig. 3.12 (510° F) and 3.15 and adding the results numerically gives a cold to hot change of $11.00 which compares favorably with the value obtained above using control rod 4.

3.7 PRESSURE COEFFICIENT OF REACTIVITY

Pressure coefficients were measured by increasing the pressure and following the associated reactivity change on calibrated Rod 4. The remaining four rods were held at 7.87 in. during these measurements and the average core temperature was 198° F. The results of these measurements are listed in Table 3.6 and agree favorably with data collected at the SM-1 previously. In the range of 80° F - 150° F, the pressure coefficient at the SM-1 is 0.0106 cents/psi [6]. SM-1 data indicates an increase to 0.0335 cents/psi at 440° F. Since data from the two plants agree favorably in the lower temperature regions, it is assumed that the PM-2A pressure coefficient increases at higher core temperatures in a manner similar to that found for the SM-1.

TABLE 3.6

MEASURED PM-2A PRESSURE COEFFICIENT OF REACTIVITY

(CORE TEMPERATURE 198° F)

Pressure Range, Psi	Worth, Cents/psi (+ .001)
130- 800	.0120
130-1750	.0109
800-1750	.0103
300-1750	.0122

3.8 STUCK ROD MEASUREMENTS

Several control rod combinations were checked for criticality with the remaining rods fully inserted in the core. Criticality may be achieved upon withdrawal of any single control rod from the PM-2A Core I, Table 3.7. As a re-

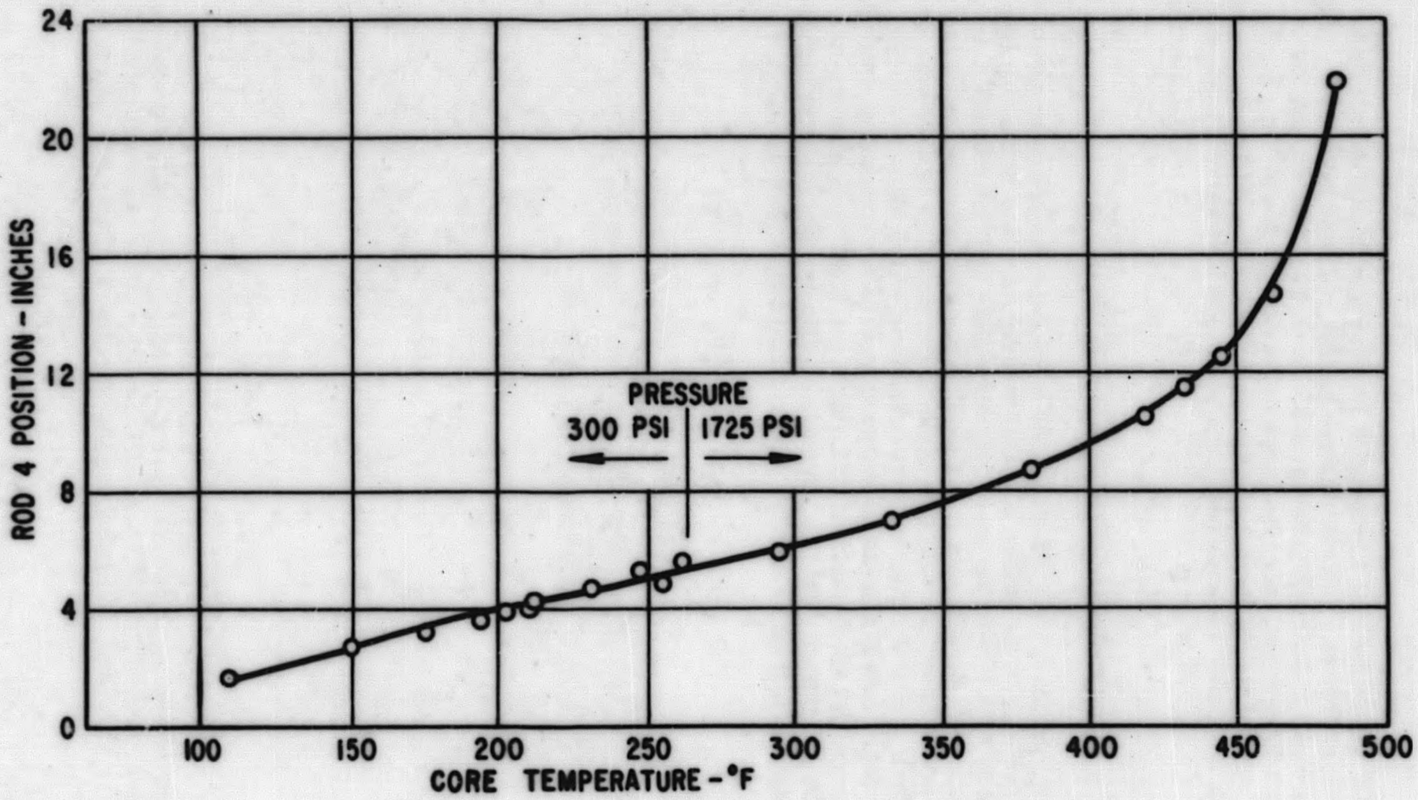

Figure 3.22. PM-2A Control Rod 4 Critical Position Vs Core Temperature

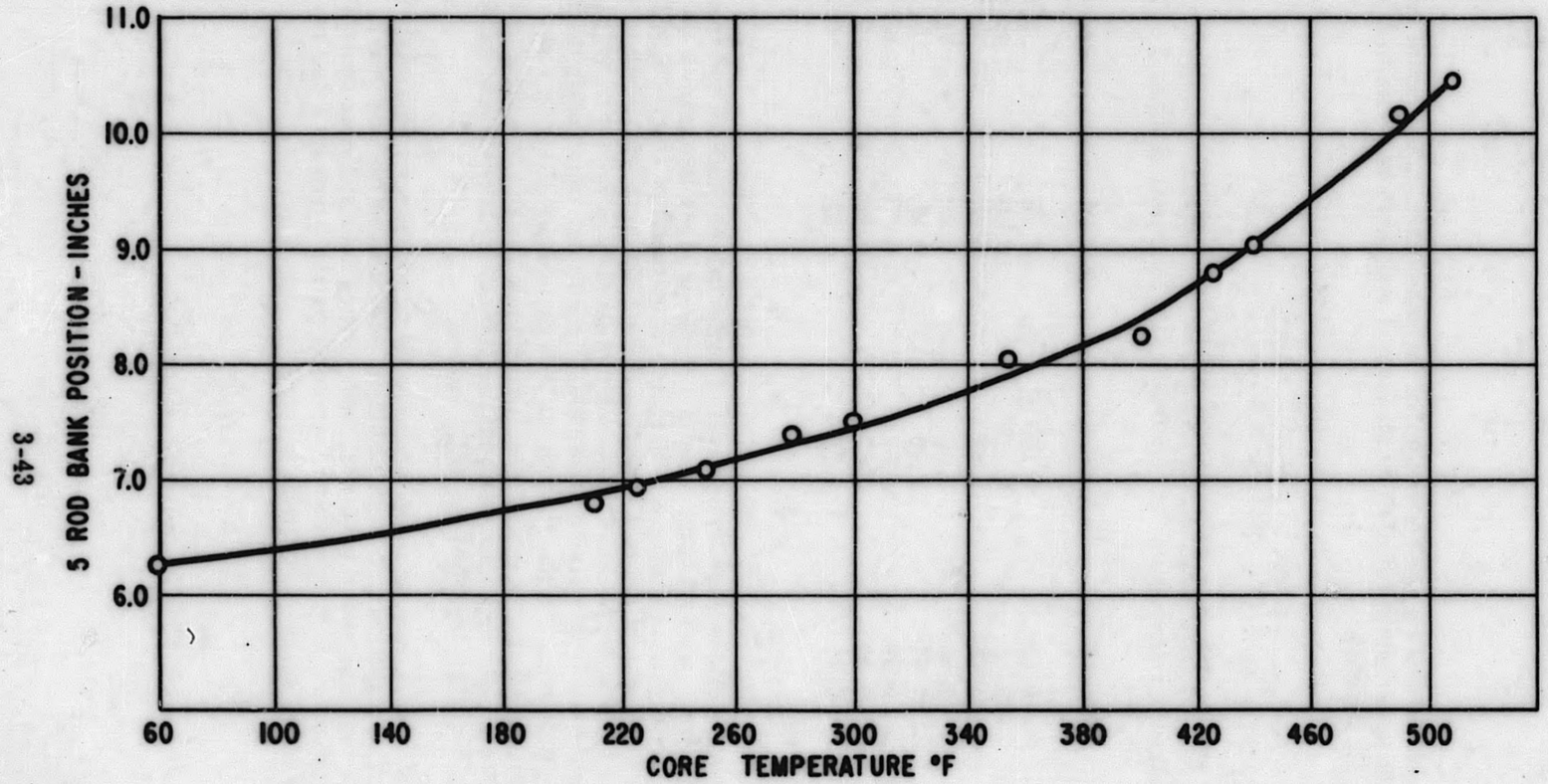

Figure 3.23. PM-2A Five Control Rod Bank Position Vs Core Temperature

sult of these measurements, and to minimize the possibility of accidental rod withdrawal, the upper limit switches on all control rods have been set to arrest rod motion at 15.5 inches.

TABLE 3.7

PM-2A CORE I STUCK ROD MEASUREMENTS

(Core Temperature at 56° F, Control Rod Withdrawal In Inches)

Rod #1	Rod #2	Rod #3	Rod #4	Rod #5
0.00	0.00	0.00	16.28	0.00
0.00	0.00	0.00	0.00	19.50
0.00	19.74	0.00	0.00	0.00
0.00	11.46	0.00	0.00	11.43
7.97	7.97	7.95	0.00	7.96
0.00	0.00	12.50	0.00	12.49
0.00	0.00	0.00	9.86	9.85
6.25	6.25	6.25	6.25	6.25

Instantaneous and complete withdrawal of any eccentric control rod from the cold clean Core I (with all other rods inserted) would put the reactor on a 15 - 20 sec. period; instantaneous and complete withdrawal of control Rod C would cause a near prompt critical condition in the cold clean PM-2A Core I. With the upper limit switches set to stop rod motion at 15.5 in., it is not possible, even under the most reactive (cold, clean) condition, to maintain criticality on any single rod. As the core burns out, the danger of single rod criticality lessens and after the core reactivity has decreased by approximately $1.00, even Rod C fully withdrawn will not maintain criticality and the upper limit switches may then be safely set at 22 inches.

If, for any reason, one or more control rods are withdrawn beyond the operating position and the upper limit switches should also become stuck, then the reactor may be shut down by full insertion of the remaining control rod bank and the subsequent injection of a soluble poison to override the reactivity worth of the stuck rod or rods.

3.9 FIVE ROD BANK POSITIONS

The critical five rod bank positions measured during the startup testing are as follows:

60° F, no xenon	6.25 inches
510° F, no xenon	10.41 inches
510° F, 4.3 MW, equilibrium xenon	11.61 inches

After 387 hr operation at an average power level of 4.84 MWt the five rod bank was at 11.89 in. (510° F equilibrium xenon).

3.10 XENON REACTIVITY MEASUREMENTS

3.10.1 EQUILIBRIUM XENON

Equilibrium xenon measurements were obtained during the initial part of the 387 hr power run and qualification test. Xenon buildup to equilibrium was followed on calibrated Control Rod 4. With the four control rod bank at 14.11 in., Rod 4 traveled from 4.07 in. at no xenon to 7.49 inches. Integration under the Rod 4 calibration curve at 510° F yields an equilibrium xenon worth of $2.60 at an average power level of 4.62 MWt. Figure 3.24 illustrates the Rod 4 movement as a function of time for xenon buildup from no xenon to equilibrium xenon.

The worth of equilibrium xenon on the basis of the five rod bank movement from 10.45 at low xenon to 11.61 at equilibrium xenon (integrating under the curves of Fig. 3.12 and 3.15 at 510° F) rendered the same worth ($2.60) obtained on the basis of the Rod 4 movement described above.

3.10.2 TRANSIENT XENON

The performance of the transient xenon test was interrupted several times because of frequently recurring reactor scrams. As a result, abrupt variations in temperature and in the transient xenon state made it difficult to obtain accurate measurements. However, taking into account variations in Rod 4 movement, the four rod bank movement, and temperature variation, the xenon worth was found to reach its peak value of approximately $3.75 5 hr after reactor shutdown. Due to the uncertainties of these measurements, no quantitative significance should be placed on them. No measurements were obtained for xenon decay from peak since the plant was shut down and the core allowed to cool while maintenance work was being performed.

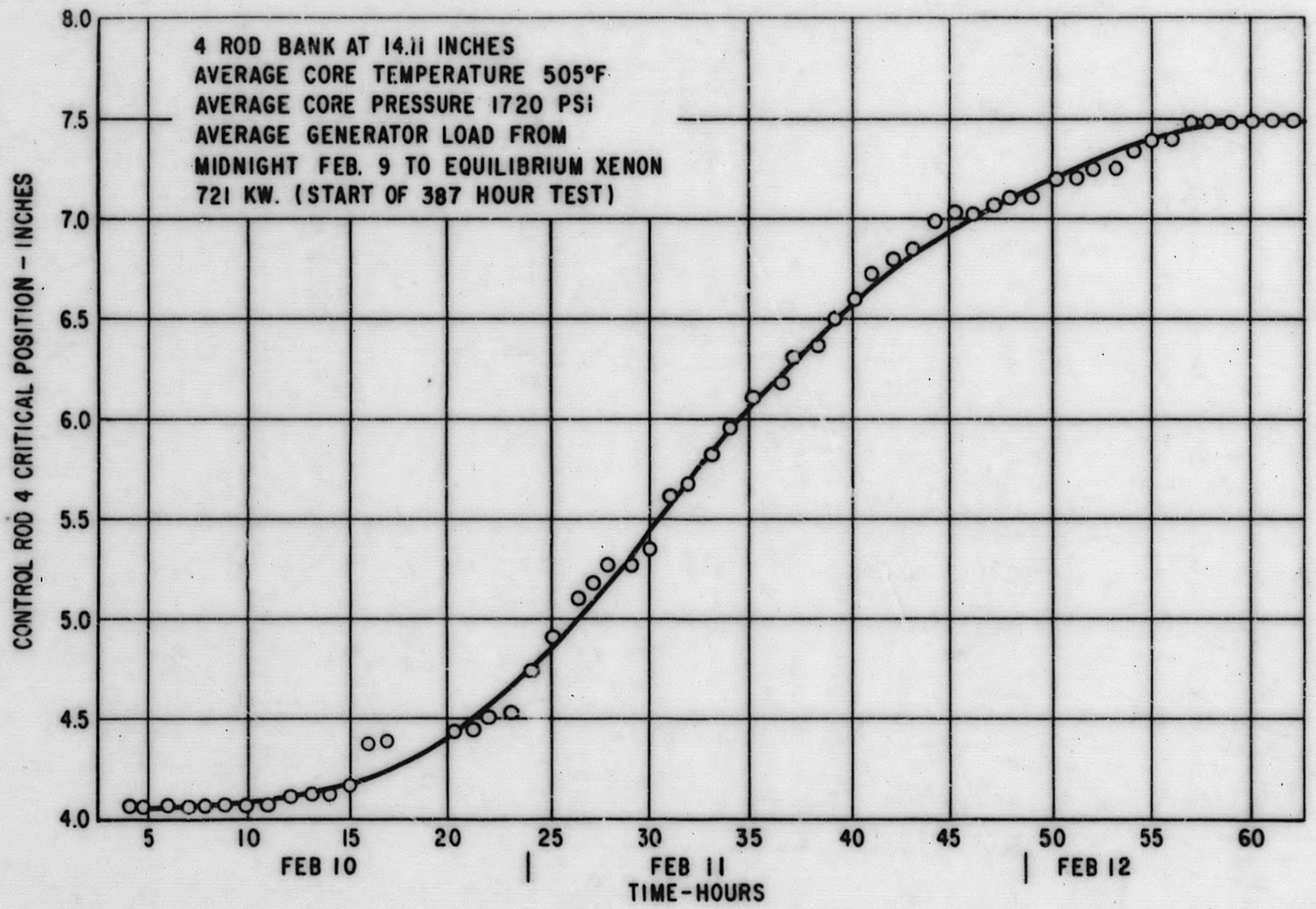

Figure 3.24. PM-2A Control Rod 4 Critical Position Vs Time after Accepting Generator Load

3.11 NEUTRON SOURCE EVALUATION

The PM-2A Core I is provided with a 30 curie polonium-beryllium startup source and an auxiliary beryllium (1/2" x 3" x 12" block) photoneutron source. The beryllium photoneutron source emits neutrons from a (γ, n) reaction with beryllium due to interaction of high energy gamma rays (1.6 Mev or greater) from fission product decay.

Upon completion of the 387 hr power run, shutdown count rates were obtained as a function of time after shutdown. The count rates obtained (after subtracting the Po-Be startup source contribution) are in proportion to the neutrons emitted from the auxiliary photoneutron source as a result of the interaction of fission product gamma rays with the beryllium.

Figure 3.25 presents a comparison of the calculated La^{140} concentration and the measured count rate data from the BF_3, both as a function of time after reactor shutdown. The curves are normalized so that 500 cpm = 1.8×10^{-5} curies La^{140}. The experimental points are count rates obtained from the BF_3 Startup Channel as a function of shutdown time after 387 hr operation at 725 ekw. The calculated lanthanum curve shows the theoretical La^{140} concentration in the core as a function of shutdown time from the same power run, taking into account the La^{140} produced from direct fission and the La^{140} produced as a daughter product from the decay of Ba^{140}. La^{140} is the most likely contributor to the (γ, n) reaction since it emits gamma rays of 1.6, 2.5 and 3.0 Mev and has a high fission yield. The gamma ray energies and yields of other fission products are considerably lower and hence are of no consequence in this calculation. Since the La^{140} concentration is partially dependent on the parent Ba^{140} decay, then, in only partially saturated systems, the decay rate will change with time, depending on the half-lives of both Ba^{140} and La^{140}. The buildup of Ba^{140} and La^{140} was calculated for the 387 hr run according to the method described by Glasstone[7]. Knowing the concentrations of Ba^{140} and La^{140} at the end of the run, the La^{140} concentration as a function of shutdown time was calculated.

The tangent to the curve at 85 hr after shutdown is a linear machine fit to the experimental points taken in the range 60 to 160 hr after reactor shutdown and indicates a 6.04 day effective half-life. Since it is tangent to the calculated La^{140} concentration curve in this region, it demonstrates good agreement between the measured effective half-life and predictions based upon the assumption that the La^{140} fission product is the chief contributor. The gamma ray energy distribution measurements obtained from the spent SM-1 Core I indicated a strong La^{140} gamma ray contribution [8] but did not reveal the presence of a significant contribution from gamma ray emitters of greater than 1.6 Mev. Hence, the preceding assumption that the La^{140} is the principal contributor for the photoneutron emission from the beryllium block is a valid one.

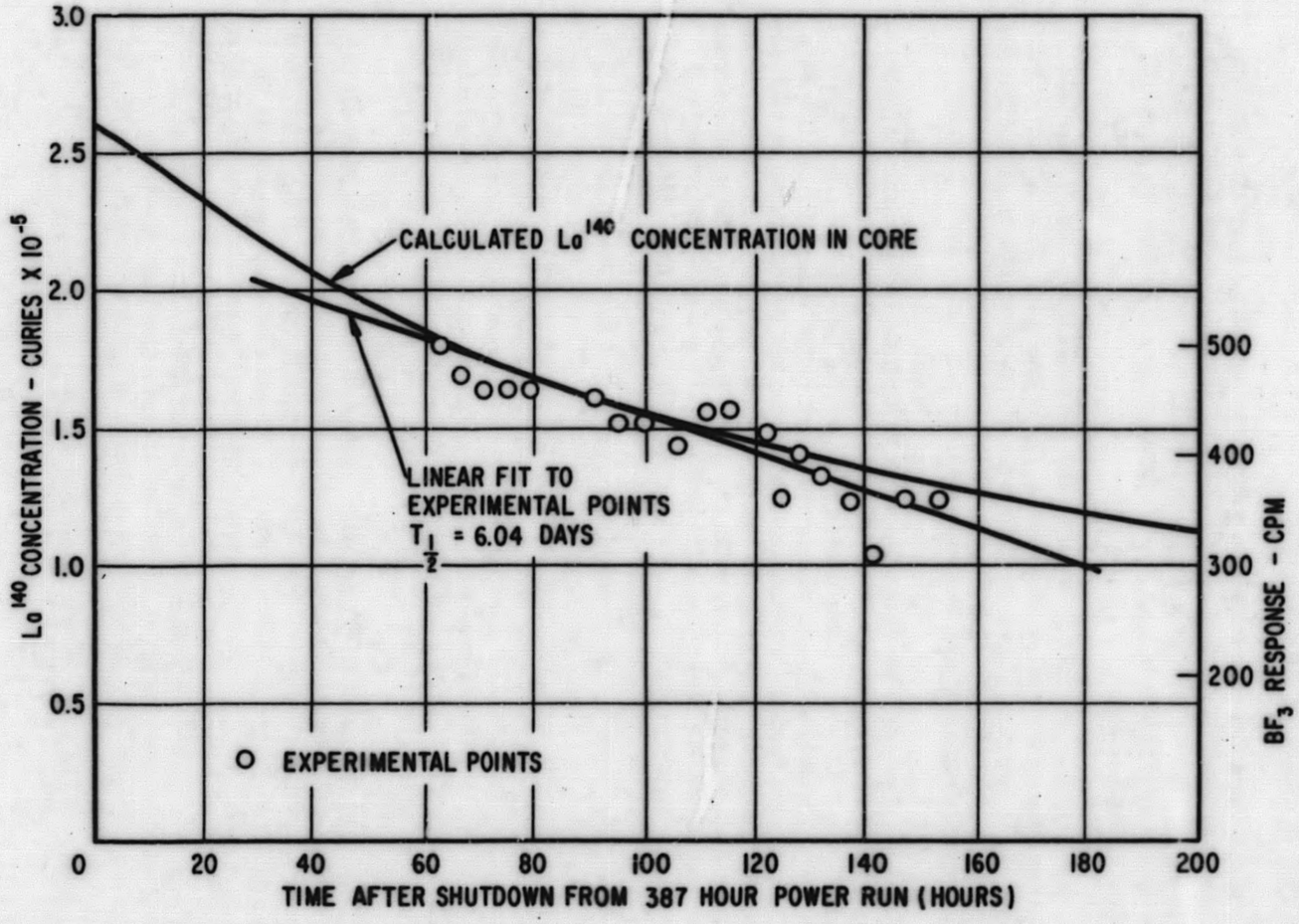

Figure 3.25. Calculated La^{140} Concentration and Measured BF_3 Count Rate Vs Time after Shutdown Following 387 Hours PM-2A Acceptance Test

Measurements obtained before and after the PM-2A, 387 hr operation at 4.65 MWt, indicated that the contribution of the beryllium block was a factor of 3.8 greater than the neutron contribution of the Po-Be startup source (Fig. 3.9). Based upon these measurements, additional calculations indicate that, after 60 days operation at 10 Mw, there will be a factor of four increase in the photoneutron contribution over that measured at startup; this is the case where the Ba-La concentration would be at a saturation level of approximately 10^6 curies La.^{140}

For purposes of comparison, the ratio of "photo" neutrons to "startup" neutrons will be normalized to a startup source strength of 45 curies polonium. At the time of these measurements, the startup source (originally 45 curies) had decreased to 0.425 of its original strength; hence, the ratio must be factored by 0.425. Therefore, in the presence of a 45 curie Po-Be source and with a saturated concentration of the Ba-La activity, the shutdown neutron contribution of the beryllium block from the (γ, n) reaction will be a factor of 3.8 = 4 x .425 = 6.5 greater than the contribution of the Po-Be startup source.

The beryllium blocks of the two cores compare as follows:

SM-1: 3 in. x 3 in. x 0.5 in. (Ref. APAE-2 Rev. 1, Pg. II-14)

PM-2A: 3 in. x 12 in. x 0.5 in. (Ref. Alco Dwg. D9-15-2094)

Thus, the PM-2A block is approximately four times as effective as the SM-1 block for producing photoneutrons through the (γ, n) reaction in beryllium. Therefore, on the basis of beryllium block sizes, the PM-2A auxiliary photoneutron source is four times as effective as that of the SM-1.

The arrangement of the BF_3 chambers, startup sources, and photoneutron sources differed in the two cores; however, these differences do not appear to be significant in this evaluation.

It can be concluded, however, that the PM-2A auxiliary source is a marked improvement over that of the SM-1 and appears to serve its purpose adequately.

3.12 REFERENCES (SECTION 3)

1. "Technical Manual PM-2A Army Nuclear Power Plant," Vols. 12, 13 and 14, Nuclear Instrumentation System, Alco Products, Inc., August 1961.

2. Alco Dwg. A9-30-2001 - Source Container

3. Grid Plates – Spent Fuel Storage Rack – Alco Dwgs. B9-48-2041 and B9-48-2042.

4. Raby, T. M., et al, "PM-2A Core I Zero Power Experiment," APAE No. 75, October 21, 1960.

5. Schroeder, F., et al, "The Spert III Reactor Nuclear Startup," IDO-16586, March 18, 1960.

6. Weiss, S. H., "Summary Report of Physics Measurements on SM-1 Core I," APAE No. 96, February 6, 1962.

7. Glasstone, S., "Principles of Nuclear Reactor Engineering," fourth printing, September 1958, D. Van Nostrand Co., Inc., New York, p. 120.

8 Kemp, S. N., et al, "PWR Research and Development Program Test Report, Gamma Scanning Spent SM-1 Core I Fuel Elements," APAE Memo 281, April 6, 1961.

9. Rosen, S. S., "Hazards Summary Report for the Army Package Power Reactor, SM-1 Task XVII," APAE No. 2, Rev. 1, May 1960.

4.0 PM-2A SHIELDING MEASUREMENTS AND ANALYSIS

The information presented in this Section consists of the initial shielding measurements and radiation surveys performed on the PM-2A during the months of October, November, and December, 1960; the shielding modifications made as a result of the analysis of these measurements; shielding measurements and radiation surveys made subsequent to the shielding modification in February 1961; and the analysis of the PM-2A shielding, as modified.

The shielding data presented was obtained through the use of available foil and film techniques and portable radiation survey instrumentation at the remote PM-2 site.

The PM-2A primary shield prior to the shield modification is illustrated in Fig. 4.1. The structural details of the primary shield as modified, are described in Tables 4.1 and 4.2. These tables indicate the shield composition extending from the core to the outside of the primary shield in the radial and vertical directions, respectively. Figure 4.2 shows the spatial relationship between the PM-2A primary system components.

4.1 SHIELDING MEASUREMENTS MADE PRIOR TO THE PM-2A SHIELD MODIFICATION

4.1.1 INTRODUCTION

Radiation measurements made during the initial startup of PM-2A indicated that radiation levels around the vapor container and on the upper platform of the reactor building were considerably higher than originally predicted. These measurements indicated that the upper level of the reactor building would be inaccessible during full power operation and that access to the vapor container 8 hrs after shutdown would be prohibited. Hence, the need arose for re-evaluation and modification of the PM-2A shield before extensive power operations could begin. Additional radiation surveys were conducted in order to locate the streaming paths and radiation sources; and to estimate the magnitude of the neutron and gamma radiations in the reactor building during full power reactor operation and within the vapor container following reactor shutdown.

TABLE 4.1

DESCRIPTION OF PM-2A PRIMARY SHIELD
IN RADIAL DIRECTION FROM CORE CENTERLINE

Description	Material	Thickness, in.	Outer Radius, in.
Core	--	----	10.08
Reflector	Water	1.68	11.76
Thermal Shield	Stainless Stl.	2.00	13.76
Cooling Passage	Water	5.12	18.88
Pressure Vessel Cladding	Stainless Stl.	0.12	19.00
Pressure Vessel	Carbon Stl.	2.38	21.38
Insulation	Glass Wool	2.00	23.38
Insulation Retainer	Steel	0.12	23.50
Clearance Space	Void	0.55	24.05
P.V. Support Ring	Steel	1.00	25.05
P.V.S.R. Cladding	Boral	0.125	25.175
Cooling Passage	Water	1.25	26.425
Cladding	Boral	0.125	26.550
1st Shield Ring	Steel	3.25	29.800
Cladding	Boral	0.125	29.925
Cooling Passage	Water	1.25	31.175
Cladding	Boral	0.125	31.300
2nd Shield Ring	Steel	3.25	34.550
Cladding	Boral	0.125	34.675
Cooling Passage	Water	1.25	35.925
Cladding	Boral	0.125	36.050
3rd Shield Ring	Steel	3.25	39.300
Cladding	Boral	0.125	39.425
Cooling Passage	Water	1.25	40.675
Cladding	Boral	0.125	40.800
4th Shield Ring	Steel	3.25	44.050
Cladding	Boral	0.125	44.175
Neutron Shield	Water	6.825	51.000
Shield Tank Cladding	Boral	0.125	51.125
Shield Tank Wall	Steel	0.375	51.500
Shield Lead	Lead	2.000	53.500

SUMMARY

Material	Total Thickness, in.
Water (510^{o}F)	6.800
Water (68^{o}F)	11.825
Steel	18.995
Boral	1.250
Insulation	2.550
Lead	2.00

TABLE 4.2

DESCRIPTION OF PM-2A REACTOR SHIELD
IN VERTICAL DIRECTION FROM CORE MIDPLANE

Description	Material	Thickness, in.	Outside Dimen. (in.) Above centerline
Core		11	11
Reflector	Water	34.6875	45.6875
Pressure Vessel Cladding	Stainless Stl.	0.125	45.8125
Pressure Vessel Cover	Carbon Stl.	1.375	47.1875
Insulation	Glass Wool	2.00	49.1875
Insulation Cover	Carbon Stl.	0.1875	49.3750
Gap	Air	0.250	49.6250
Insulation Cover	Carbon Stl.	0.125	49.750
Insulation	Glass Wool	1.750	51.500
Insulation Cover	Carbon Stl.	0.125	51.625
Gap	Water	3.50	55.125
Vapor Container Dome Cap	Carbon Stl.	0.875	56.000
Gap	Water	10.5	66.500
Neutron and Gamma Shield	Water	128	194.5

Summary

Material	Total Thickness, in.
Water (510°F)	34.6875
Water (68°F)	142.00
Steel	2.8125
Insulation	4.000

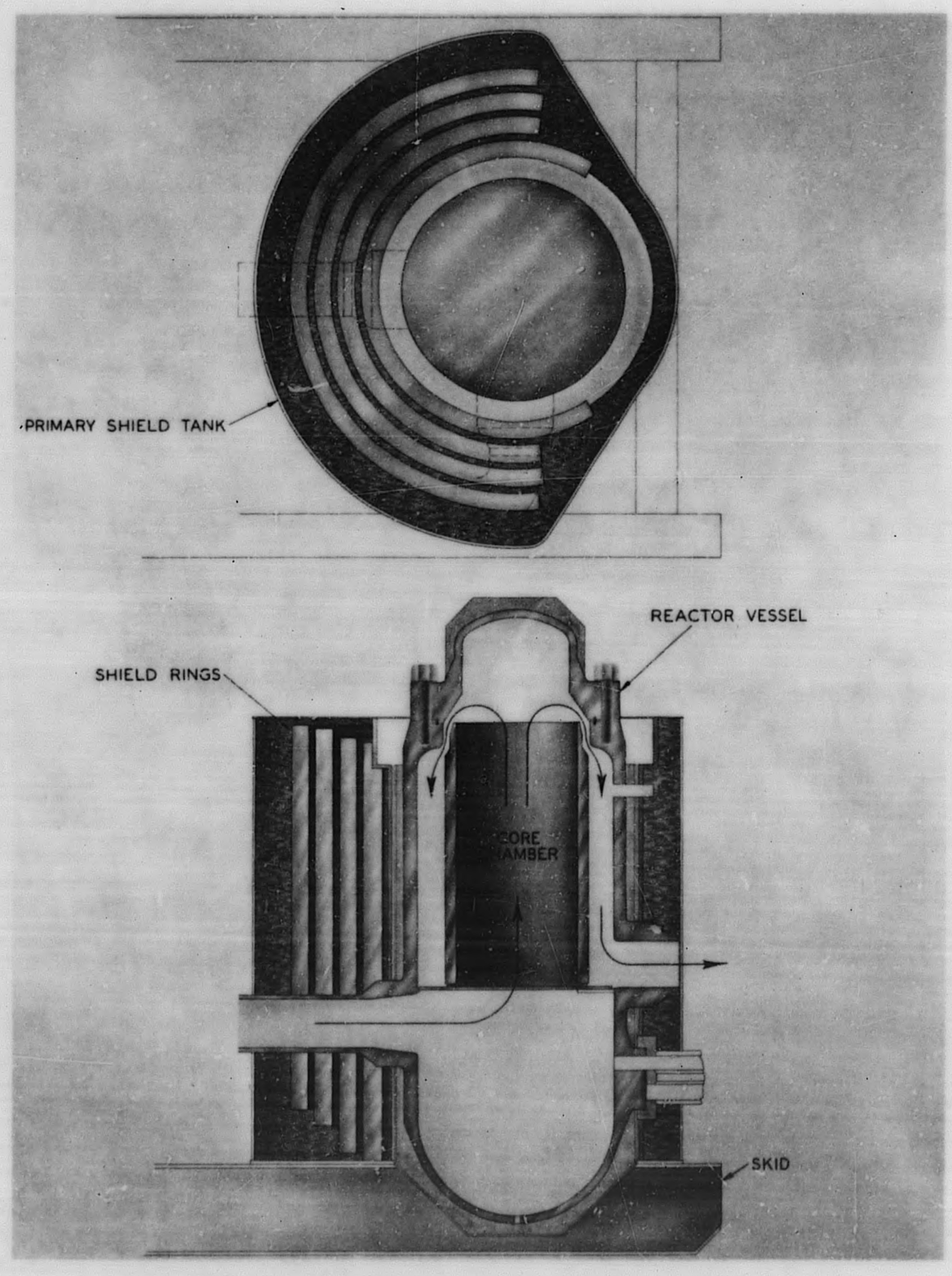

Figure 4. 1. PM-2A Primary Shielding

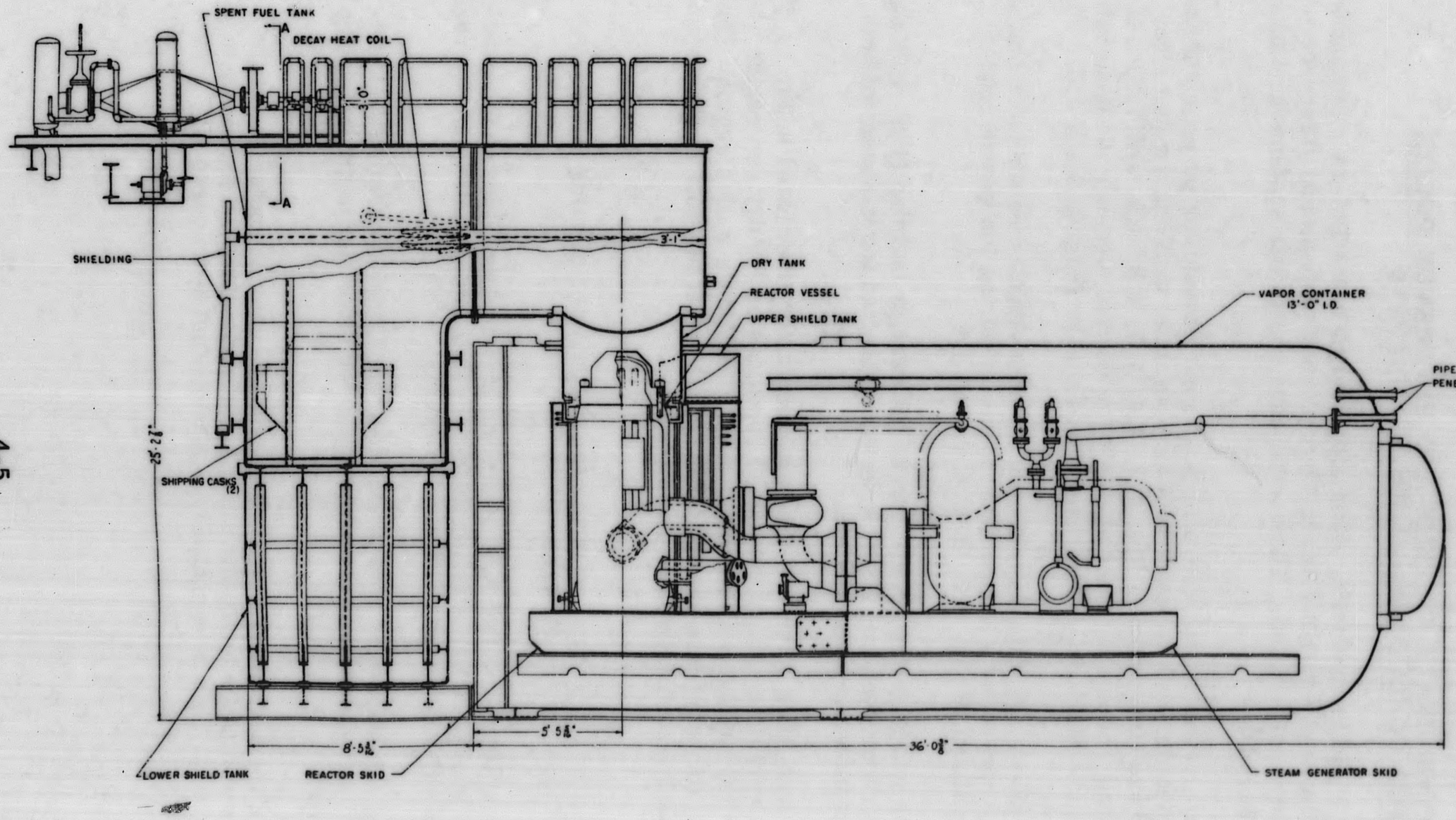

Figure 4.2. PM-2A Primary System Skid Arrangement

4.1.2 COORDINATE SYSTEMS AND REFERENCE POINTS FOR CONDUCTING RADIATION SURVEYS

In order to aid in conducting radiation surveys in the PM-2A plant and in the surrounding area several reference coordinate systems and reference dose points were established. These reference coordinate systems are shown in Figs. 4.3 to 4.10.

Coordinate systems and reference points established for purposes of conducting surveys (during low power reactor operation) utilizing a gamma ray survey meter are illustrated in Fig. 4.3, 4.4, 4.6, 4.8, 4.9, and 4.10. In addition, gamma ray survey instruments were used to measure the dose rates following reactor shutdown at locations illustrated in Figs. 4.3 and 4.6.

The coordinate systems and reference points established for purposes of conducting surveys using a neutron survey meter during low power reactor operation are shown in Fig. 4.3, 4.5, 4.7, and 4.9.

Reference points on the upper level of the reactor building (Fig. 4.7) and outside of the vapor container (Fig. 4.5) were selected for exposure of both neutron and gamma ray sensitive film.

The traverse lines outside of the vapor container illustrated in Fig. 4.5 indicated that particular emphasis should be placed on the dry cap region since most of the leakage radiation appeared to originate in this region. The dose points on the traverses shown in Fig. 4.5 were at one foot intervals and their locations are further defined as follows:

I – Along the top centerline of the vapor container starting at the dry cap and extending forward.

II – Around the starboard side of the vapor container opposite the reactor core centerline starting at the dry cap and extending downward along the vapor container circumference.

III – Along the starboard side of the vapor container on centerline starting at the midpoint of the rear vapor container flange and extending forward.

IV – Along the starboard side of the spent fuel tank at centerline of the vapor container beginning at the front of the tank and extending to the rear. This is essentially a continuation of traverse III.

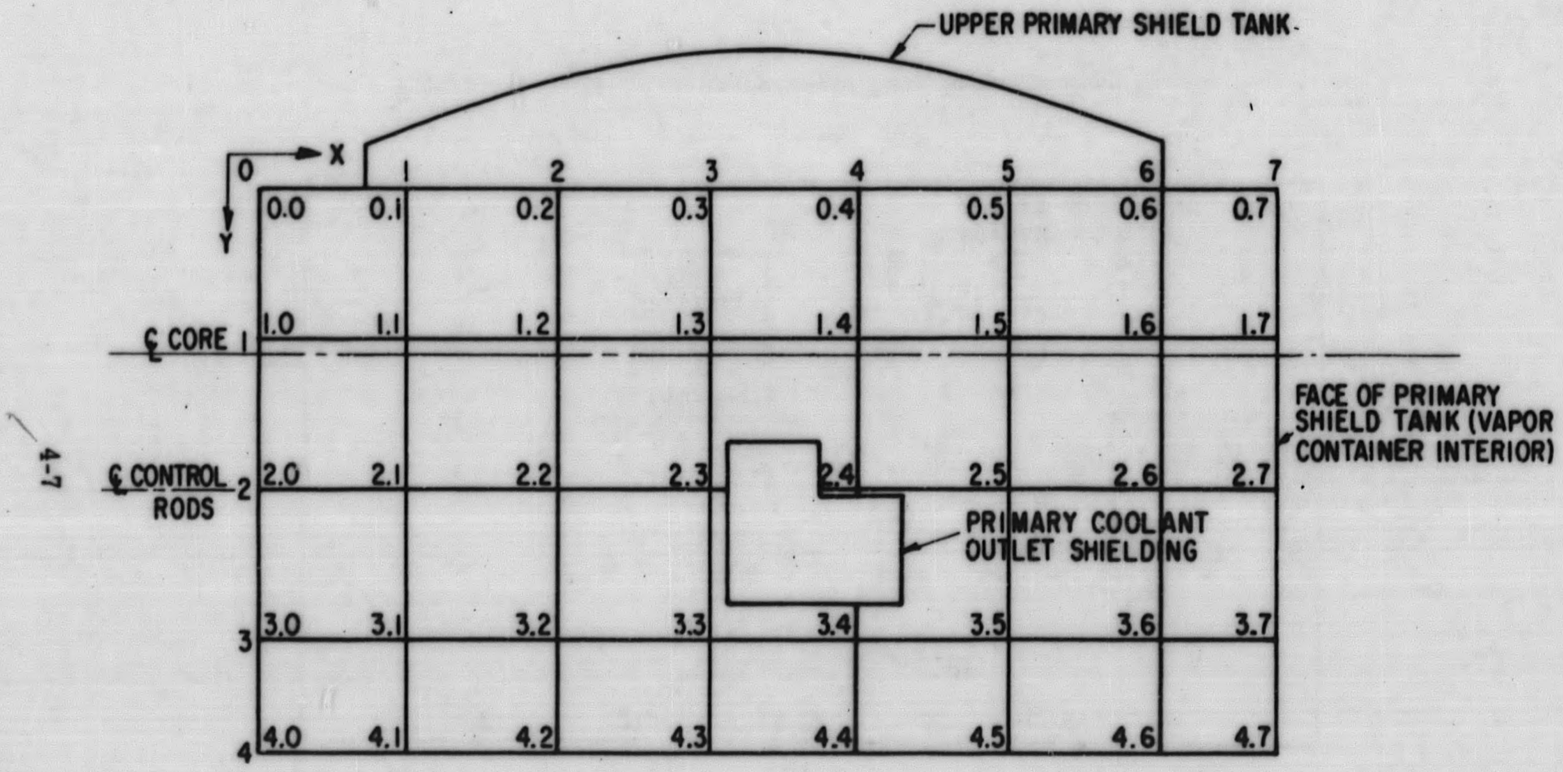

Figure 4.3. PM-2A Primary Shield Tank Coordinates (Radiation Dose Points)

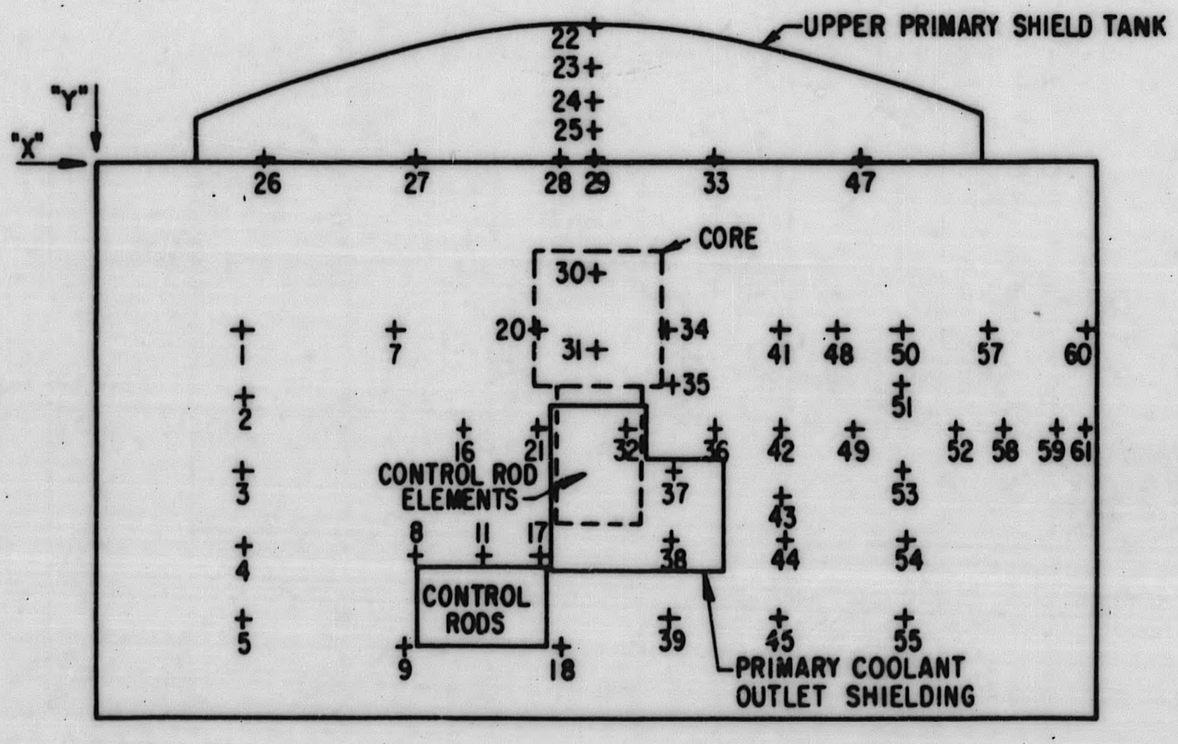

Figure 4.4. PM-2A Primary Shield Tank Radiation Dose Points (Test C-402)

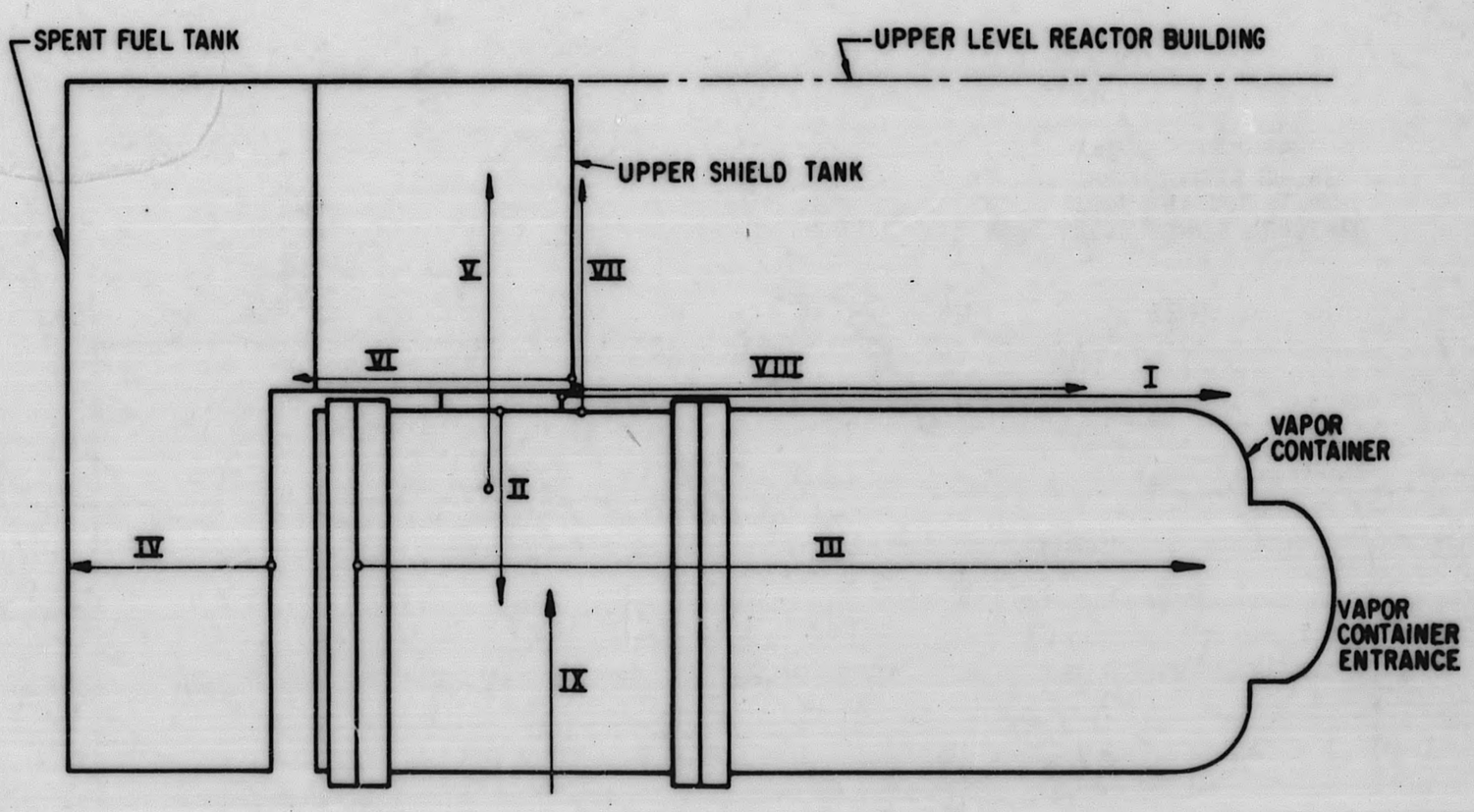

Figure 4.5. Radiation Survey Traverse Locations on PM-2A Vapor Container, Upper Shield Tank and Spent Fuel Tank (Prior to Shield Modification)

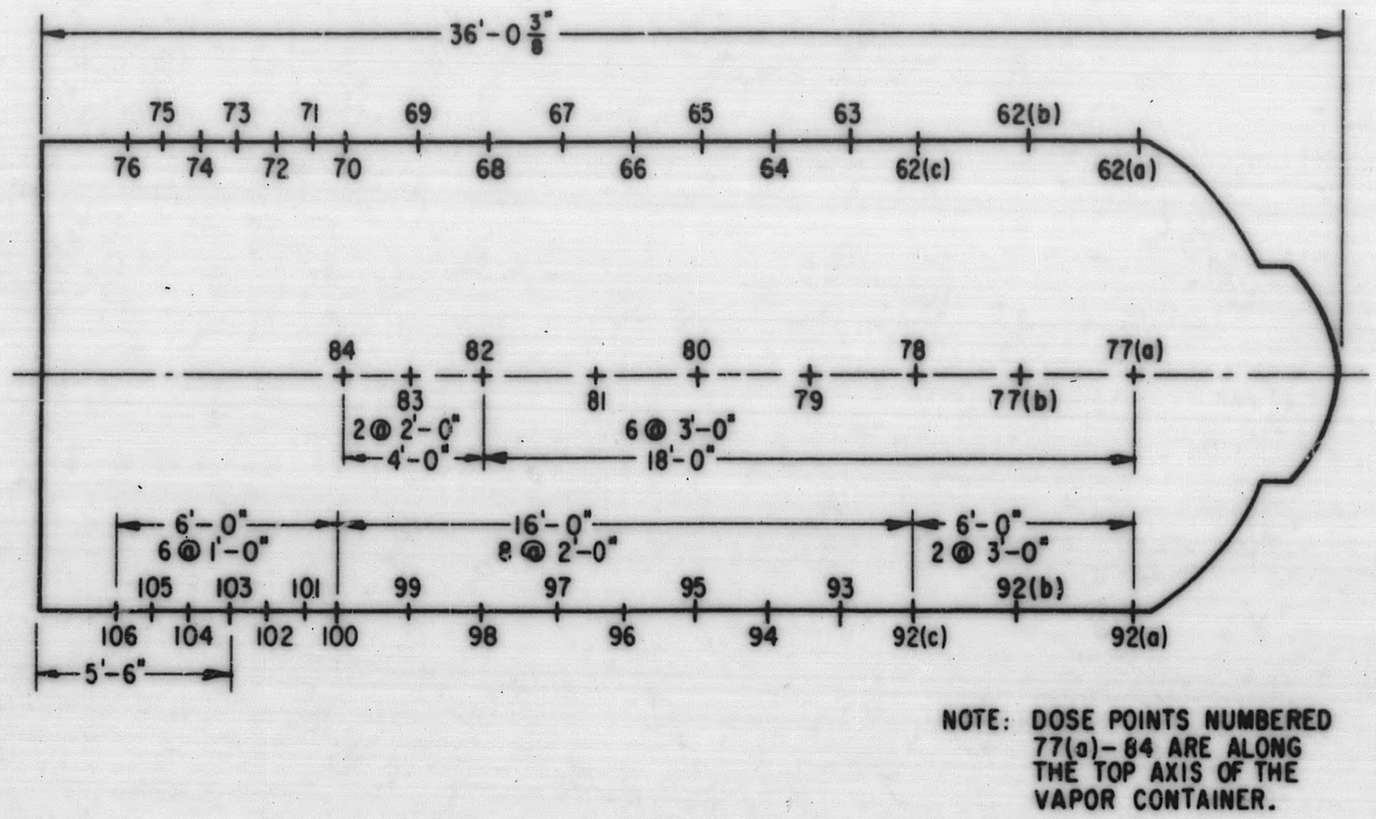

NOTE: DOSE POINTS NUMBERED 77(a)-84 ARE ALONG THE TOP AXIS OF THE VAPOR CONTAINER.

Figure 4.6. PM-2A Vapor Container Exterior (Radiation Survey Dose Points)

NOTES:
POINT 86 DIRECTLY ABOVE CORE ℄.
POINT 91 DIRECTLY ABOVE CENTER OF SPENT FUEL RACK.

(A)

POINTS ON BEAM APPROX 18" TO LEFT OF POINT 88

POINT NO.	ELEVATION
97	FLOOR LEVEL
98	2' ABOVE FLOOR LEVEL
99	4' ABOVE FLOOR LEVEL
100	6' ABOVE FLOOR LEVEL

(B)

POINTS ON FRONT WALL OF REACTOR BUILDING

POINT NO.	ELEVATION
102	6' ABOVE FLOOR
103	3' ABOVE FLOOR
104	3' BELOW FLOOR
105	6' BELOW FLOOR
106	9' BELOW FLOOR
107	12' BELOW FLOOR
108	TOP OF DOOR NEAR V.C.

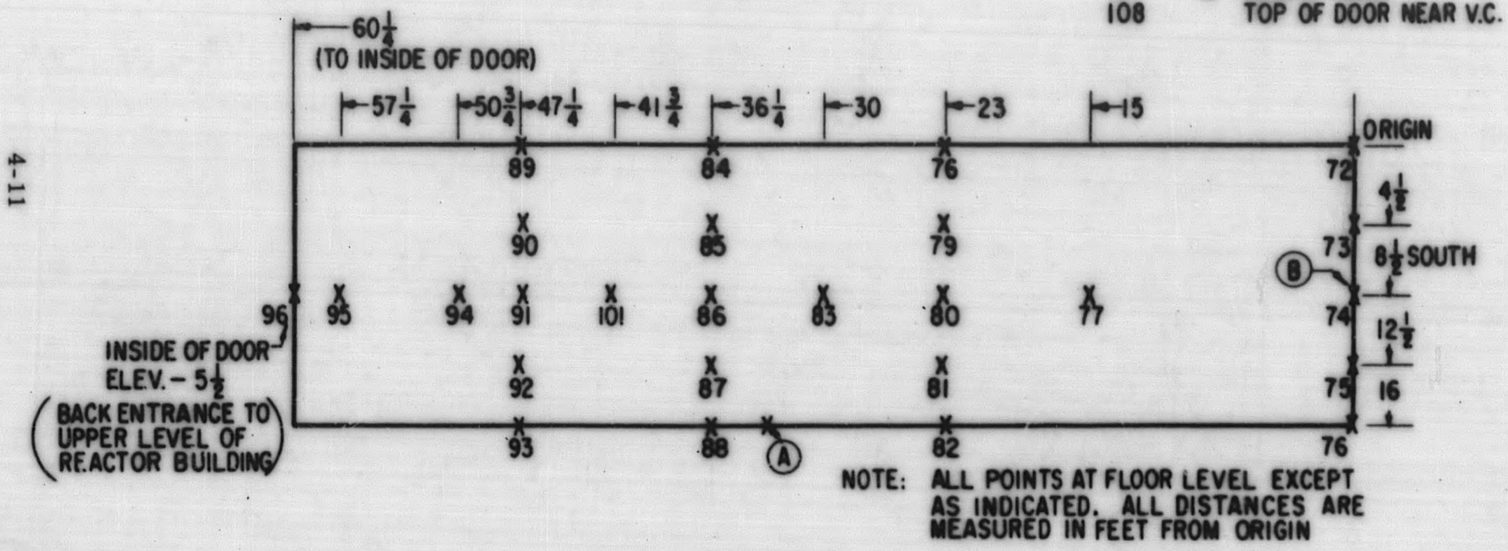

Figure 4.7. Radiation Sensitive Film Survey Points on the Upper Platform of the PM-2A Reactor Building

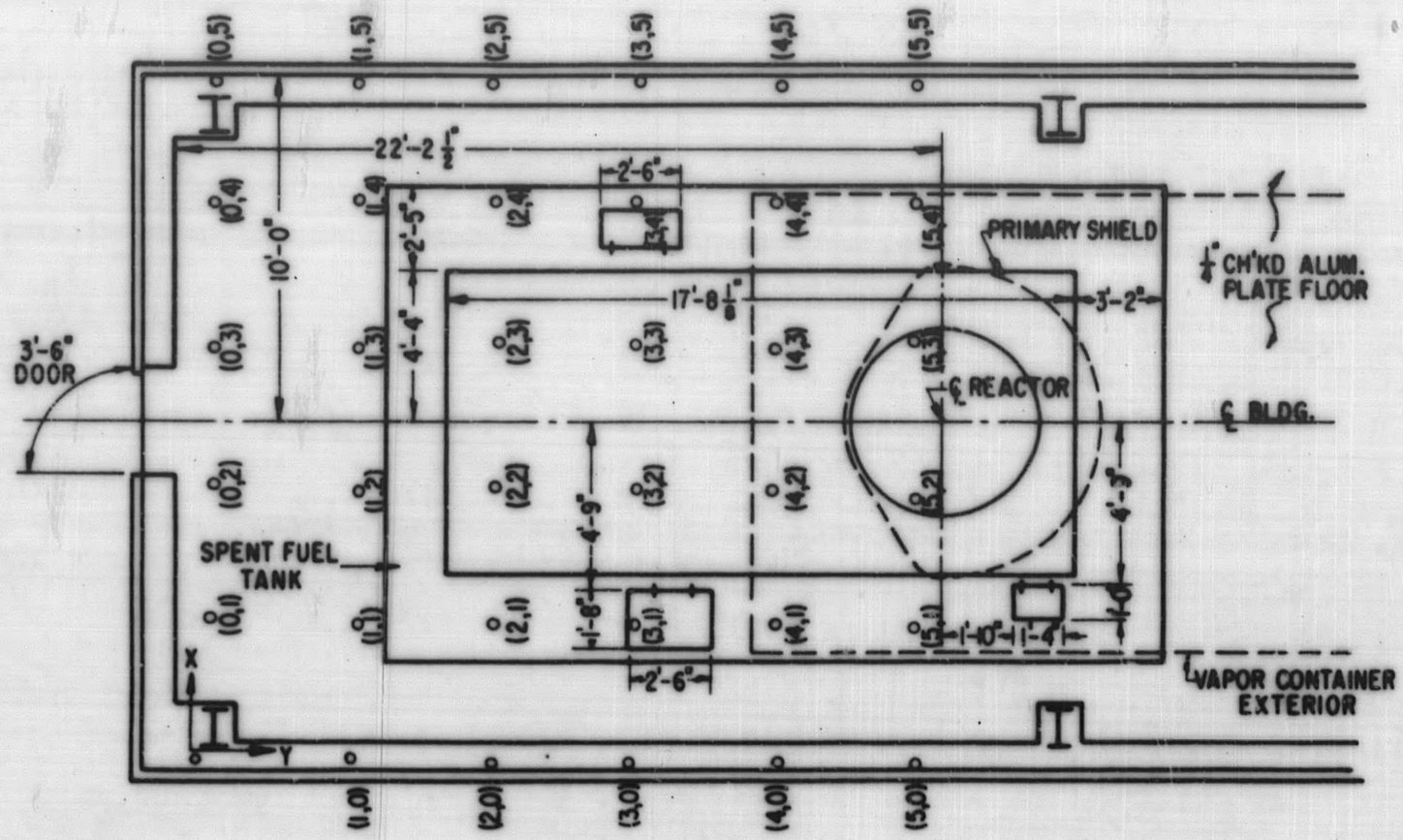

Figure 4.8. Radiation Survey Coordinate System on the Upper Platform of the PM-2A Reactor Building

NOTE: (1) DOSE POINTS ARE AT 4'-0" INTERVALS ALONG THE SIDES OF THE REACTOR BUILDING AND AT QUARTER POINTS ON THE ENDS OF THE REACTOR BUILDING

(2) DOSE POINTS LOCATED 4'-0" OFF SNOW FLOOR, APPROXIMATELY AT THE FLOOR LEVEL OF REACTOR BUILDING

(3) DOSE POINTS 3'-0" FROM REACTOR BUILDING WALLS

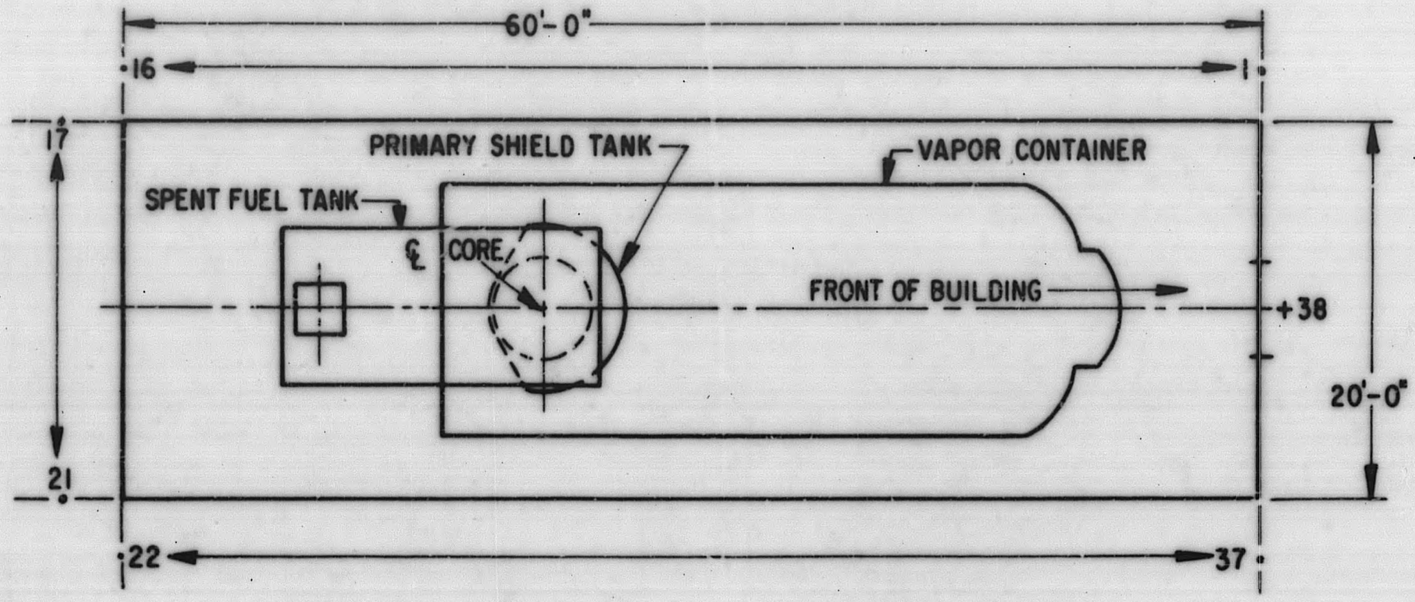

Figure 4.9. PM-2A Reactor Building Exterior (Radiation Dose Points)

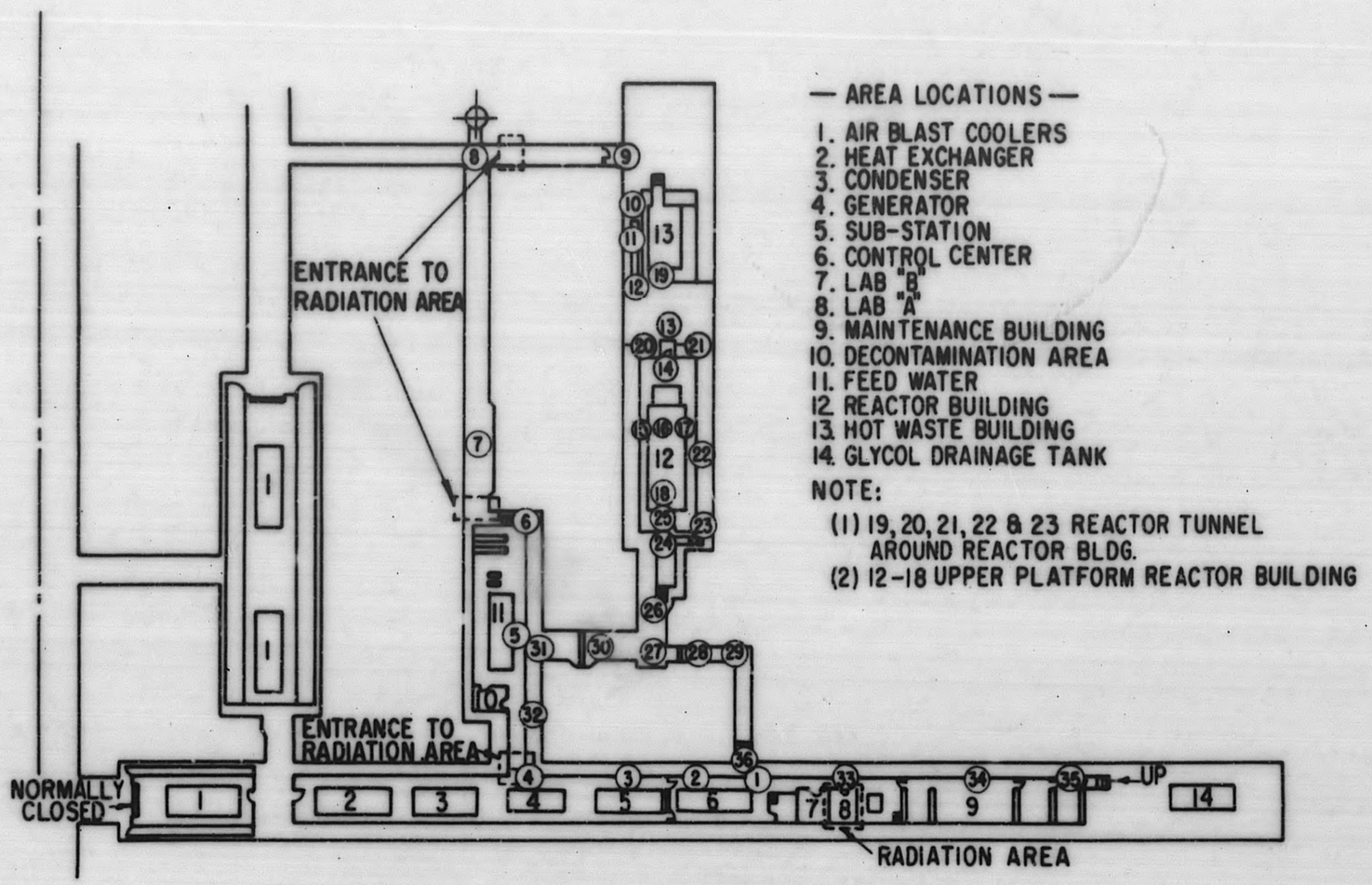

— AREA LOCATIONS —

1. AIR BLAST COOLERS
2. HEAT EXCHANGER
3. CONDENSER
4. GENERATOR
5. SUB-STATION
6. CONTROL CENTER
7. LAB "B"
8. LAB "A"
9. MAINTENANCE BUILDING
10. DECONTAMINATION AREA
11. FEED WATER
12. REACTOR BUILDING
13. HOT WASTE BUILDING
14. GLYCOL DRAINAGE TANK

NOTE:

(1) 19, 20, 21, 22 & 23 REACTOR TUNNEL AROUND REACTOR BLDG.
(2) 12-18 UPPER PLATFORM REACTOR BUILDING

Figure 4. 10. PM-2A Plant Area (Radiation Dose Points)

V – Vertically along the starboard side of the spent fuel tank at the core centerline starting where this plane intersects the side of the vapor container and extending upward.

VI – Along the base of the starboard side of the upper spent fuel tank parallel to traverse III starting at the front of the tank and extending to the rear.

VII – Along the front of the spent fuel tank perpendicular to traverse I at the center of the tank starting at the top of the vapor container and extending upwards.

VIII – On the fill line for the spent fuel tank beginning at the front of the spent fuel tank and extending forward.

IX – Vertically along an I beam on the starboard side of the reactor building and opposite core centerline. The traverse starts at the reactor floor and extends upward.

4.1.3 RADIATION SURVEY TECHNIQUES

A. Radiation Sensitive Films

Gamma and neutron sensitive films used for the radiation measurements were obtained from (and processed by) the Army's Lexington Signal Corps Depot, and Tracerlab Incorporated. The Lexington Signal Corps Depot reported their interpretations of neutron sensitive films in mrem on the basis of 26×10^6 neutrons/cm^2 equal to one rem. This value is set forth in Title 10 Part 20 of the Code of Federal Regulations dated January 1, 1961 for neutrons with energies of approximately 5 Mev (approximate average neutron energy for a Po-Be spectrum). The calibration of the film, to a precalibrated neutron source, resulted in 1 track in 25 fields where a field represents approximately 2×10^{-4} cm^2. This resulted in an exposure equal to 9 mrem. The film used for the surveys was Kodak Type A, which is not energy independent so that a conversion of tracks to radiation dose without determining an energy factor, such as track length, tends to overestimate the dose from the softer neutron energy spectrum that emanates from an iron-water shielded reactor source. However, these measurements do establish distributions and an approximate correction can be applied to account for the "softer" neutron spectrum. Standard film techniques were employed in interpreting the exposed gamma sensitive film.

B. Survey Instruments

Gamma measurements were made with a Jordan Model AGB-10KG-SR radiation survey instrument. This instrument has a built-in source (strontium 90) that is utilized to check the instrument calibration. Additional independent calibration data were obtained by utilizing a Cesium - 137 source. The instrument is considered energy independent for gammas of from 80 kev to 1.2 Mev energies.

Neutron measurements were obtained with a Nuclear Chicago Model 2112 N neutron survey instrument and an Eberline Model FN-1A. The Model 2112N Instrument utilizes a bare boron trifluoride (BF_3) tube, and with filters of cadmium and cadmium covered paraffin for neutron energy discrimination. Because a neutron spectrum similar to the one being measured was not available for calibrating this neutron sensitive instrument, the readings are not interpreted to mrem/hr but are presented as meter readings in counts per minute to render relative neutron spatial distributions. The Model FN-1A utilizes a plastic scintillation phosphor, and is sensitive only to those neutrons with energies greater than about 0.25 Mev.

C. Activation Foils

Gold, cadmium covered gold, and sulfur foils were used to determine neutron levels along the traverses described in Section 4.1.2. The foils are energy dependent and as a result may be employed to generate information on the neutron energies causing the foil activation.

The thermal fluxes were calculated from the equation:

$$\phi_{th} = \frac{C \lambda E P A}{U N_o \sigma_a m (1 - e^{-\lambda t_o}) e^{-\lambda t_w} (1 - e^{-\lambda t})} \qquad (1)$$

where:

t_w = length of time from the end of the irradiation to the start of the counting period (hr)

t_o = length of time of irradiation (hr)

t = counting period (hr)

λ = $\frac{0.693}{T_{1/2}}$ where $T_{1/2}$ is the half life of Au^{179}_{92} in hours

C = total counts recorded in one minute from the bare foil minus the total counts recorded in one minute from the cadmium covered foil as counted with an end window Geiger Mueller tube and scaler counting setup

E = Reciprocal of the counter efficiency for the 1/4-inch diameter gold foils

P = Power level correction factor to full power

A = Atomic weight of gold (197 gms/gm-atom)

U = Conversion factor for hours to seconds ($U = 3.6 \times 10^3$ sec/hr)

N_o = Avagadros number (6.023×10^{23} atoms/gm-atom)

m = mass of foil (gms)

σ_a = Microscopic absorption cross-section for 2200 m/sec neutrons in gold (98×10^{-24} cm^2)

Thermal fluxes at dose points which contained only the bare gold foils were computed using "best values" for the cadmium covered gold foil activity. These "best value" data were obtained by interpolation from graphs of the cadmium covered foil activity vs. dose point location. Thermal activation data were obtained by subtracting the cadmium covered activity from the total (bare foil) activity.

4.1.4 EXPERIMENTAL RESULTS AND PRESENTATION OF RADIATION SURVEY DATA

The data presented in this section was obtained from radiation surveys made at the PM-2A site during October, November and December, 1960. These data were used to identify the problem areas and to provide a basis for design of necessary additional shielding (Sec. 4.2).

All of the data extrapolated to full power was based on a corrected Log N value. The correction to the Log N reading was based on the electrical power output at the time of the survey and a Log N of 100 being equal to 2000 KW(e) or 10 MW(th) (full power). A review of the operating data indicated that up to November 11, 1960 the Log N reading was high and necessitated the use of a correction factor of 0.7. After November 11 the log N chamber was relocated and from November 12, 1960 through January 1, 1961 the Log N reading was low and required a correction factor of 1.33.

More accurate correction factors based on detailed heat balance have since been made available. Measurements made from mid November 1960 to January 1, 1961 indicated that the Log N correction factor based on the reactor plant thermal output was 1.52.

The use of this correction factor would require that:

1. All Log N values recorded in this section for the period mid-November, 1960 to January 1, 1961, be increased by a factor of 1.14.

2. Dose rates scaled to full power in this section for the same period be multiplied by 0.88.

A. Radiation Surveys During Low Power Reactor Operations

Gamma ray and neutron measurements were made on the primary shield during low power reactor operation using portable survey instruments. These measurements were made to determine operating gamma ray dose rates, and to demonstrate that the neutron leakage from the primary shield was sufficiently low to preclude significant activation of primary system components.

Tables 4.3 and 4.4 present the results of a gamma radiation survey on the PM-2A primary shield. This survey utilized the grid system shown in Fig. 4.3. The dose rates are in R/hr scaled to full power. A gamma survey probe was placed at the dose points shown in Fig. 4.4

Table 4.5 presents the neutron survey meter readings for the primary shield survey. The grid system utilized is also as shown in Fig. 4.3, and readings are in counts per minute. A cadmium and paraffin covered BF_3 probe was used to obtain fast neutron flux measurements.

B. Area Surveys - Film

Gamma and neutron sensitive films were placed on the traverse points described below, around the vapor container and at the various dose points on the upper platform of the reactor building to obtain radiation dose rates and distributions during reactor operation.

Three additional film irradiations were made with neutron and gamma sensitive films in order to evaluate the radiation leakage from the dry cap and the rear of the vapor container.

Run 1 - Dry Cap empty (design state)

Run 2 - Dry Cap filled with water

Run 3 - Dry cap filled with water and bags of water soaked sawdust packed in the void between the dry cap and the side and rear of the vapor container.

TABLE 4.3

GAMMA RAY DOSE RATE SURVEY - PM-2A PRIMARY SHIELD DURING LOW POWER REACTOR OPERATION PRIOR TO SHIELD MODIFICATION

Date: October 19, 1960

Reactor Power Level: Operating at a Log N = 0.07 (corrected)

Instrument: Jordon AGB-10K-SR

Note: Dose rates are scaled to R/hr at full power
Primary shield coordinates are shown in Fig. 4.3

Primary Shield Coordinate	Dose Rate (R/hr)	Primary Shield Coordinate	Dose Rate (R/hr)
0.0	530	2.4	
0.1	430	2.5	36
0.2	290	2.6	160
0.3	300	2.7	170
0.4	210	3.0	79
0.5	230	3.1	56
0.6	400	3.2	32
0.7	400	3.3	-
1.0	290	3.4	-
1.1	310	3.5	-
1.2	170	3.6	130
1.3	170	3.7	390
1.4	110	4.0	-
1.5	72	4.1	51
1.6	200	4.2	24
1.7	230	4.3	36
2.0	160	4.4	-
2.1	100	4.5	43
2.2	83	4.6	64
2.3	1150	4.7	79

TABLE 4.4

GAMMA RAY DOSE RATE SURVEY - PM-2A PRIMARY SHIELD DURING LOW POWER REACTOR OPERATION PRIOR TO SHIELD MODIFICATION (TEST C-402 DOSE POINTS)

Date: October 19, 1960

Reactor Power Level: Operating at Log N = 0.07

Instrument: Jordon AGB-10K-SR

Note: Dose points are from test C-402 (Fig. 4.4)
Dose rates are scaled to R/hr at full power

Dose Point	Dose Rate (R/hr)	Dose Point	Dose Rate (R/hr)
1	340	31	230
2	230	32	26
3	100	33	260
4	93	34	100
5	86	35	160
7	93	36	86
8	27	37	210
9	26	39	26
11	72	41	120
16	86	44	43
17	560	45	36
18	140	47	240
20	150	48	200
21	360	49	180
22	860	51	160
23	860	52	140
24	860	54	54
25	390	55	43
26	486	57	200
27	500	58	170
28	300	59	160
29	230	60	200
30	160	61	180

TABLE 4.5

RELATIVE FAST NEUTRON FLUX SURVEY - PM-2A PRIMARY SHIELD DURING LOW POWER REACTOR OPERATION PRIOR TO SHIELD MODIFICATION

Date: November 19, 1960

Instrument: Nuclear Chicago 2112N

Reactor Power Level: Operating at a Log N = 0.0013 (corrected) (Dry Cap empty)

Notes: 1. Fast Neutron Measurements were made with a cadmium - paraffin cover over BF_3 probe.

2. Primary shield coordinates are shown in Fig. 4.3.

3. Relative fast neutron levels are survey instrument reading in cpm.

Primary Shield Coordinate	Relative Fast Neutron Level, cpm
1.2	9000
1.1	13000
2.1	11000
2.2	6500
3.2	6300
1.3	7200
2.3	6600
1.4	7700
2.4	9000
1.5	13500
1.6	Off Scale
3.6	8500
3.5	6500

Table 4.6 lists the results of the interpretation on (Ref. Section 4.1.3) of the gamma ray sensitive films placed on traverse points exterior to the vapor container (Fig. 4.5) and the dose points on the upper platform of the reactor building (Fig. 4.7).

Table 4.7 lists the results of the interpretation (Ref. Section 4.1.3) of the neutron sensitive films placed on traverse points exterior to the vapor container (Fig. 4.5) and the dose points on the upper platform of the reactor building (Fig. 4.7).

C. Area Surveys - Foil

Table 4.8 lists the results of the gold foil irradiation data on the traverse points exterior to the vapor container (Fig. 4.5). Both bare and cadmium covered gold foils were exposed in order to determine the thermal neutron leakage from the dry cap region. These data indicated that the thermal neutron flux could cause significant activation of the vapor container and structural members in the dry cap region.(1)

D. Area Surveys - Survey Instrument

Neutron and gamma ray radiation surveys were made in the general plant area of the PM-2A. The purpose of these surveys were to determine the general radiation spatial distribution and intensities. Radiation levels on the upper platform of the reactor building and in the vapor container were above design target values (Ref. Section 4.2). The data from surveys in the vicinity of the vapor container were used to determine the nature of the sources associated with these high radiation levels.(1)

Table 4.9 presents the dose rates measured on the exterior surface of the vapor container. The dose points are shown in Fig. 4.6. Table 4.10 lists dose rates obtained from a radiation survey made around the exterior of the reactor building. The dose points are shown in Fig. 4.9. Table 4.11 shows the results of a radiation survey on the upper platform of the reactor building utilizing a grid system shown in Fig. 4.8. Table 4.12 presents the recorded results of the PM-2A plant radiation surveys. These surveys were made with the portable health physics survey meters. Dose points are shown in Fig. 4.10. Survey number 1 was made with the dry cap empty (design state). During survey number 2 the dry cap was filled with water and in general indicated lower radiation levels.

Table 4.13 lists the neutron survey meter readings. These surveys were made on the vapor container exterior (Fig. 4.5), on the upper platform of the reactor building (Fig. 4.7), in the general plant area (Fig. 4.9), and at various

TABLE 4.6

GAMMA SENSITIVE FILM SURVEYS PM-2A VAPOR CONTAINER EXTERIOR AND UPPER PLATFORM DURING LOW POWER REACTOR OPERATION

Date: Dec. 6 and Dec. 7, 1960

Reactor Power Level: Reactor operating at Log N = 0.013 (corrected)

Note: (1) Dose points on vapor container exterior (Fig. 4.5)

(2) Dose points on upper platform

Run #1 Dry Cap Empty; 2-hour irradiation

Run #2 Dry Cap Filled; 2-hour irradiation

Run #3 Dry Cap Filled; Wet sawdust behind upper shield; 2-hour irradiation

Dose rates are in rem/hr scaled to full power.

Location		Run 1	Run 2	Run 3
(1) I	0	4700	2100	2100
	1	4810	4880	4700
	2	2700	2625	2550
	3	1420	1425	1500
	4	714	675	790
	5	206	90	101
	6	120	135	135
	7	150	135	135
	8	150	135	135
	9	120	94	135
	10	120	44	101
	11	90	94	101
	12	90	68	101
	13	90	68	101
	14	90	68	67.6
	16	90	68	67.6
	18	90	68	67.6
	20	60	68	67.6
(1) II	0	24000	9200	9000
	1	7690	6950	7140
	2	20200	27400	28500
	3	2880	2100	2020
	4	900	450	356
	5	564	338	262
	6	394	240	131
	7	371	180	169
	8	244	120	135
(1) III	0	270	180	262
	2	620	865	820
	4	225	120	101
	6	262	207	169
	8	262	150	135
	10	244	120	135

Location		Run 1	Run 2	Run 3
(1) V	0	15800	24400	22500
	1	12000	17600	16500
	2	5820	5075	4770
	3	3380	2250	2020
	4	1050	338	262
	5	750	338	300
	6	489	244	202
	7	507	244	202
	8	338	180	135
(1) VI	0	1200	1200	1120
	2	3750	2925	2250
	4	4500	3525	3080
	6	6580	7700	7500
	8	1950	1875	1760
(1) VII	0	--	4925	4960
	1	4800	3375	3380
	2	1390	545	489
	3	790	360	356
	4	600	395	375
	5	338	240	262
(1) VIII	0	790	865	526
	2	564	620	489
	4	394	413	356
	6	300	270	300
	8	210	188	169
	10	180	135	135
	12	120	94	101
	14	94	94	33.8
	16	94	68	67.6
	18	94	94	33.8
	20	60	33.8	33.8
	22	60	68	33.8

Location		Run 1	Run 2	Run 3
(1) IX	0	150	94	101
	2	150	94	101
	4	206	135	101
	6	262	135	135
	7	338	207	168
(2)	72	--	33.8	67.6
	73	60	33.8	33.8
	74	--	64	33.8
	75	33.8	33.8	--
	76	--	33.8	33.8
	77	90	64	33.8
	78	60	60	67.6
	79	150	135	169
	80	90	64	135
	81	180	169	169
	82	90	64	33.8
	83	120	135	101
	84	150	64	67.6
	85	90	33.8	18.8
	86	90	33.8	33.8
	87	120	64	33.8
	89	90	64	33.8
	90	60	64	33.8
	91	60	33.8	--
	92	90	33.8	33.8
	93	60	33.8	33.8
	94	60	33.8	--
	95	60	33.8	--
	97	180	135	135
	98	150	74	101
	99	120	135	67.6
	100	90	84	67.6
	102	60	64	33.8
	103	60	64	33.8
	101	90	64	33.8

TABLE 4.7

NEUTRON SENSITIVE FILM SURVEYS - PM-2A VAPOR CONTAINER AND UPPER PLATFORM DURING LOW POWER REACTOR OPERATION

Date: Dec. 6 and Dec. 7, 1960

Reactor Power Level = Reactor operated at Log N = 0.0133 (corrected)

Note: (1) Dose points located on the vapor container exterior (Fig. 4.5)

(2) Dose points located on the upper platform (Fig. 4.7)

Run #1 Dry cap empty; two hour irradiation

Run #2 Dry cap filled; one hour irradiation

Run #3 Dry cap filled, wet sawdust behind upper shield; 2 hour irradiation

Neutron dose rates are in rem/hr scaled to full power.

Location		Run 1	Run 2	Run 3	Location		Run 1	Run 2	Run 3	Location		Run 1	Run 2	Run 3
(1) I	0	5440	788	525	(1) V	0	6750	--	--	(1) IX	0	75	187	131
	1	1430	27700	11000		1	25100	12000	38600		2	112	150	356
	2	75	24800	15700		2	13900	54000	22500		4	94	112	112
	3	94	338	9390		3	2140	7650	4880		6	52	150	131
	4	75	150	75		4	225	187	488		7	131	112	244
	5	56	150	56		5	75	450	375					
	6	--	187	94		6	112	263	75	(2)	72	75	75	--
	7	--	150	94		7	75	150	112		73	112	75	112
	8	75	112	75		8	75	225	112		74	--	112	--
	9	75	112	--							75	52	112	--
	10	75	150	112	(1) VI	0	940	789	244		76	75	112	52
	11	75	150	--		2	3490	4720	17600		77	75	150	940
	12	75	150	75		4	9000	6000	19100		78	37	187	131
	13	75	112	--		6	11300	13000	15200		79	37	75	112
	14	225	225	--		8	1200	1350	11800		80	75	225	--
	16	94	75	--							81	112	225	--
	18	37	187	--	(1) VII	0	--	38200	14100		82	75	112	112
	20	37	150	--		1	806	35200	14800		83	169	--	--
						2	75	150	75		84	75	225	319
(1) II	0	--	39800	38600		3	37	150	112		85	75	225	206
	1	25500	30000	28200		4	52	225	75		86	75	--	244
	2	38600	67500	--		5	75	150	206		87	112	150	356
	3	5820	4430	3190							89	75	488	112
	4	225	263	2440	(1) VIII	0	806	225	244		90	37	--	75
	5	263	263	1310		2	375	187	94		91	75	112	52
	6	75	187	244		4	94	150	131		92	52	--	206
	7	94	150	112		6	112	112	75		93	75	--	75
	8	75	112	--		8	112	75	75		94	75	--	940
						10	75	150	75		95	75	--	52
(1) III	0	94	112	244		12	75	112	75		97	75	--	112
	2	52	75	--		14	37	--	75		98	52	150	940
	4	--	150	--		16	225	225	75		99	75	112	375
	6	52	187	131		18	112	187	52		100	75	112	131
	8	75	187	244		20	75	150	52		101	75	187	--
	10	52	150	131		22	940	--	94		102	94	112	52
											103	94	150	940

TABLE 4.8

THERMAL NEUTRON FLUX MEASUREMENTS - PM-2A VAPOR CONTAINER EXTERIOR PRIOR TO SHIELD MODIFICATION (GOLD FOIL ACTIVATION)

Date: Nov. 13 & 14, 1960

Reactor Power Level: Reactor operated at a Log N = 0.44 (corrected) for 8.4 hours

Note: Flux is in N/cm^2 sec scaled to full power
Traverse locations are shown in Fig. 4.5

Traverse No. and Foil Location		Thermal Neutron Flux (N/cm^2 sec)	Cadmium Ratio
I	0	$8.65(10^7)$	1.71
	2	$1.90(10^7)$	2.18
	4	$1.15(10^7)$	2.18
II	0	$3.43(10^8)$	1.98
	2	$3.02(10^8)$	2.00
	5	$6.73(10^6)$	1.29
	6	$5.46(10^6)$	1.29
	8	$7.14(10^6)$	1.29
III	1	$6.1(10^6)$	1.58
	3	$1.25(10^6)$	1.74
	4	$1.25(10^6)$	1.74
	6	$1.19(10^6)$	1.74
	7	$7.93(10^6)$	1.58
	9	$7.85(10^6)$	1.58
	10	$5.04(10^6)$	1.32
	12	$4.49(10^6)$	1.32
IV	0	$1.20(10^7)$	2.65
	1	$1.25(10^7)$	2.65
	3	$1.31(10^7)$	2.71
	4	$1.16(10^7)$	2.67
	6	$1.53(10^7)$	2.67
V	0	$5.90(10^7)$	1.27
	1	$6.20(10^7)$	1.26
	3	$3.04(10^7)$	1.26
	4	$1.51(10^7)$	1.27
	5	$6.57(10^6)$	1.27
	6	$8.67(10^6)$	1.27
	7	$8.84(10^6)$	1.27
	9	$7.59(10^6)$	1.27
	10	$3.80(10^6)$	1.27
VI	0	$1.47(10^7)$	1.76
	1	$3.87(10^7)$	1.76
	3	$5.41(10^7)$	1.76
	4	$5.97(10^7)$	1 51
	7	$4.40(10^7)$	1.76
	9	$2.90(10^7)$	1.76
VII	0	$6.42(10^7)$	1.63
	1	$1.08(10^7)$	1.63
	3	$5.86(10^6)$	1.63
	4	$6.01(10^6)$	1.63
	6	$2.18(10^6)$	1.20
	7	$2.33(10^6)$	1.20
	9	$2.97(10^6)$	1.20
	10	$1.05(10^6)$	1.20

TABLE 4.9

GAMMA RAY DOSE RATE SURVEY - PM-2A VAPOR CONTAINER EXTERIOR DURING LOW POWER REACTOR OPERATION PRIOR TO SHIELD MODIFICATION

Date: October 19, 1960

Reactor Power Level: Reactor Operating at Log N = 0.07 (corrected)

Instrument: Jordan AGC-10K-SR

Note: Dose Rate are in R/hr scaled to full power
See Fig. 4.6 for dose point location

Dose Point	Full Power (R/hr)	Dose Point	Dose Rate (R/hr)
62 (a)	2.3	80	30.0
62 (b)	6.3	81	42.8
62 (c)	9.3	82	214
63	12.8	83	643
64	15.7	84	1570
65	22.8	92 (a)	5.7
66	27.1	92 (b)	7.1
67	27.1	92 (c)	11.4
68	37.1	93	14.3
69	57.1	94	17.1
70	71.5	95	22.9
71	92.8	96	25.7
72	100	97	27.1
73	214	98	42.9
74	843	99	57.1
75	2140	100	78.5
76	3570	101	100
77 (a)	7.1	102	114
77 (b)	12.1	103	286
78	17.1	104	1280
79	22.8	105	3430
		106	3570

TABLE 4.10

GAMMA RAY DOSE RATE SURVEY - PM-2A REACTOR BUILDING EXTERIOR DURING LOW POWER REACTOR OPERATION PRIOR TO SHIELD MODIFICATION

Date: Oct. 19, 1960

Instrument: Jordan AGB-10K-SR

Reactor Power Level: Reactor Operating at Log N = 0.028 (corrected)

Note: Dose Rates are in R/hr scaled to full power.

Survey Location		Dose Rate R/hr
Entrance to Reactor Building		10.7
Dose Point (2, 3) on Primary Shield (Fig. 4.3)		5350
Measurements made at 4 foot intervals along starboard side of reactor building from front to rear (Fig. 4.9)	1	21.4
	2	28.6
	3	32.2
	4	42.9
	5	53.5
	6	64.2
	7	75.0
	8	92.9
	9	146
	10	179
	11	179
	12	143
	13	122
	14	107
	15	89.3
	16	89.3
	17	64.3

Survey Location		Dose Rate R/hr
Measurements made along rear of reactor building at quarter points	18	64.3
	19	46.4
	20	42.9
	21	39.3
	22	39.3
Measurements made along port-side of reactor building at 4 foot intervals from rear to front	23	57.1
	24	82.1
	26	92.9
	27	123
	28	143
	29	115
	30	89.3
	31	75
	32	57.1
	33	42.9
	34	32.2
	35	26.8
	36	17.9
	37	16.1
	38	12.5

TABLE 4.11

GAMMA RAY DOSE RATE SURVEY - UPPER PLATFORM IN PM-2A REACTOR BUILDING DURING LOW POWER REACTOR OPERATION PRIOR TO SHIELD MODIFICATION

Date: November 7, 1960

Reactor Power Level: Reactor Operating at Log N = 0.175 (corrected)

Instrument: Jordan AGB-10K-SR

Note: Dose rates are in R/hr scaled to Full Power
Dose point locations are shown in Fig. 4.8

Dose Point	Dose Rate (R/hr) (3'-0" Off Deck)	Dose Point	Dose Rate (R/hr) (3'-0" Off Deck)
0.0	57.1	2.0	97.0
0.1	48.5	2.1	85.5
0.2	48.5	2.2	68.5
0.3	48.5	2.3	68.5
0.4	45.6	2.4	85.5
1.1	58.1	3.0	137
1.2	58.1	3.1	114
1.3	57.1	3.2	80
1.4	57.1	3.3	80
1.5	57.6	3.4	114
		3.5	143

Dose Point	Dose Rate (R/hr) (3'-0" Off Deck)	Dose Rate (R/hr) (6'-0" Off Deck)
4.0	143	120
4.1	114	91.3
4.2	80	74.1
4.3	80	68.5
4.4	137	120
4.5	137	120
5.0	114	91.3
5.1	85.5	62.7
5.2	62.7	51.4
5.3	57.1	51.4
5.4	91.1	62.7
5.5	114	68.5
Entrance to Reactor Building	456	

TABLE 4.12

GAMMA RAY DOSE RATE SURVEY - PM-2A PLANT AREA DURING LOW POWER REACTOR OPERATION PRIOR TO SHIELD MODIFICATION

Date: November 11, 1960

Reactor Power Level: Reactor Operating at Log N = 12.5 (corrected) and 0.125 (corrected) as indicated in the table.

Instrument: Jordan Model AGB-10K-SR

Note: For dose point location see Fig. 4.10

Dose rates are survey instrument readings in mr/hr at the indicated corrected Log N reading.

Dose Point	Survey #1 mr/hr	Survey #2 mr/hr	Remarks	Dose Point	Survey #1 mr/hr	Survey #2 mr/hr	Remarks
1	0.082	0.05	Log N=12.5 (corrected)	19	0.65	0.60	Log N=0.125 (corrected)
2	0.080	0.05	"	20	42	40	"
3	0.085	0.05	"	21	65	--	"
4	0.09	0.05	"	22	81	--	"
5	0.25	0.19	"	23	14	17	"
6	0.15	0.10	"	24	23	30	"
7	0.13	0.07	"	25	32	45	"
8	0.18	0.12	"	26	9	12	"
9	33	29	"	27	2	2.7	"
10	43	45	"	28	0.30	0.22	"
11	55	53	"	29	0.22	0.21	"
12	650	600	"	30	1.20	0.9	Log N=12.5 (corrected)
13	28	25	Log N=0.125 (corrected)	31	0.21	0.16	"
14	52	50	"	32	0.074	0.08	"
15	160	150	"	33	0.085	0.05	"
16	88	82	"	34	0.086	0.05	"
17	150	180	"	35	0.085	0.05	"
18	52	60	"	36	0.075	0.05	"

points inside the vapor container. The readings are in counts per minute (See Section 4.1.3) and were not converted to neutron flux, since the purpose of the survey was to determine relative distribution and since the conversion factors are quite uncertain when this instrument is employed, under these test conditions.

E. Radiation Surveys Following Reactor Shutdown

Gamma ray dose rate measurements were made following shutdown at locations both inside and outside of the PM-2A vapor container.

Dose rate measurements were made at approximately 8 hr following reactor shutdown. These measurements indicated that the dose rate on the primary shield exceeded the design target value of 50 mr/hr 8 hr after reactor shutdown.(1) Gamma ray dose rate decay measurements were made for purposes of identifying the sources of the high dose rates following reactor shutdown.

Table 4.14 is a compilation of dose rate decay measurements made on the surface of the primary shield. The dose point coordinate system is illustrated in Fig. 4.3.

The data from these measurements were used to identify the activated corrosion inhibitor as the predominant source of after shutdown radiation levels.(1)

Table 4.15 presents the decay data as indicated by a Tracerlab TA-6 probe placed at dose point 84 shown in Fig. 4.6. The data was read off the master meter at the radiation monitoring panel in the control console room following 10 hr of reactor operation at approximately 700 ekw.

Table 4.16 and Table 4.17 are compilations of the PM-2A plant dose rate decay measurements. Readings were taken both inside the vapor container and around the reactor building.

4.2 MODIFIED PM-2A SHIELD DESIGN

The shielding measurements made at the PM-2A site and presented in Section 4.1 indicated that the radiation levels on the upper platform of the reactor building on the surface of the primary shield tank and in the vapor container were above the design target values. Design targets were:

a. The shielding be adequate to permit access to the rear 4 ft of the Spent Fuel tank on the upper platform of the reactor building, for

TABLE 4.13

Date: November 19, 1960
Instrument: Nuclear Chicago 2112N

PM-2A PLANT NEUTRON SURVEYS DURING LOW POWER REACTOR OPERATION PRIOR TO SHIELD MODIFICATION

Reactor Power Level: Variable as noted in Table.
Fast - Cadmium and paraffin cover over BF_3 probe
Thermal - Bare BF_3 probe
Epi-Cadmium - Cadmium cover over BF_3 probe

Note:
(1) Log N = 0.013 (corrected)
(2) Log N = 0.0013 (corrected)
(3) Dry Cap filled with water.
(4) Dry Cap empty of water
(5) Dose points on vapor container exterior (Fig. 4.5)
(6) Dose points on upper platform (Fig. 4.7)
(7) Dose points in area around reactor building (Fig. 4.9)

		Relative Neutron Levels (Instrument Reading cpm)		
Dose	Point	Fast	Thermal	Epi-Cadmium
(1)	I-25	2400	1400	150
(3)	I-24	2500	1600	120
(5)	I-23	3400	1900	150
	I-22	3500	1600	130
	I-21	3100	1500	150
	I-20	4700	2100	180
	I-19	5000	1800	260
	I-18	5600	2200	250
	I-17	6200	2300	250
	I-16	6500	2400	250
	I-15	7000	2500	300
	I-14	7500	2700	250
	I-13	8000	3000	300
	I-12	8600	3000	350
	I-11	9000	3100	300
	I-10	9600	3400	---
	I-9	9900	3500	---
	I-8	----	3600	---
	I-7	----	3700	---
	I-6	----	3100	---
	I-5	----	4100	---
	I-4	----	4700	---
	VIII-6	----	5200	---
	VIII-8	10400	4500	---
	VIII-10	8600	4200	---
	VIII-12	7600	3500	---
	VIII-14	6400	3100	---
	VIII-16	5600	2800	---
	VIII-18	5000	2500	---
	VIII-20	4400	2300	---
	VIII-22	3600	2200	---
	III-30	2000	----	---
	III-28	2500	1500	120
	III-26	2600	1600	120
	III-24	3100	2000	200
	III-22	3400	2000	200
	III-20	4300	2200	180
	III-18	5200	2600	200
	III-16	6300	3500	250
	III-14	7600	4000	350
	III-12	8500	4800	400
	III-10	10500	4800	450
	III-8	12500	4200	450

		Relative Neutron Levels (Instrument Reading cpm)		
Dose	Point	Fast	Thermal	Epi-Cadmium
(1)	72	1050	900	90
(3)	73	1800	1050	100
	74	1500	1150	200
(6)	75	1600	1200	60
	76	1100	950	60
	102	1600	1150	30
	103	1700	1200	30
	77	4500	2400	120
	78	4200	2500	150
	79	5500	2700	150
	80	5100	2700	150
	81	5500	3000	150
	82	4000	2600	150
	83	4700	3100	150
	84	9000	4000	260
	85	6500	3000	200
	86	2400	2200	150
	87	6500	3300	200
	88	8500	5200	400
	97	6500	7700	300
	98	5400	6400	300
	99	4400	5000	300
	100	3200	3500	150
	101	2300	2400	160
	89	4300	2700	150
	90	3900	2300	190
	91	1700	2000	100
	92	4300	2500	90
	93	4500	3200	140
	94	2100	2300	100
	95	2000	2300	120
	96	1200	1800	60
(1)	20	1000	3100	45
(3)	21	1400	3200	80
(7)	22	4000	4600	250
	23	250	650	15
(1)	I-25	12200	7200	600
(4)	I-24	12200	7200	580
(5)	I-23	14500	6500	600
	I-22	pegged		

		Relative Neutron Levels (Instrument Reading cpm)		
Dose	Point	Fast	Thermal	Epi-Cadmium
(2)	I-25	1400	1400	100
(4)	I-24	1400	1400	90
	I-23	1800	1500	90
(5)	I-22	2000	1400	110
	I-21	2000	1300	50
	I-20	3400	1600	150
	I-19	3400	1900	170
	I-18	3800	----	130
	I-17	4100	1900	150
	I-16	4600	2000	200
	I-15	5100	2100	210
	I-14	5500	2100	250
	I-13	5800	2300	280
	I-12	6300	2400	200
	I-11	6800	2500	200
	I-10	7100	2600	250
	I-9	7900	2600	260
	I-8	7300	2900	230
	I-7	7100	2900	280
	I-6	6000	2300	330
	I-5	pegged	3300	400
	I-4	----	3900	600
(1)	9	10	150	5
(4)	10	25	150	0
(7)	11	50	250	0
	12	500	1500	25
	19	25	350	0
	20	4300	10000	250
	21	6000	11500	400
	22	pegged	pegged	850
	24	2200	5000	170
	26	1000	3000	45
	27	250	400	0
	30	0	0	0

		Relative Neutron Levels (Instrument Reading cpm)
Dose	Point	Fast
(1)	72	6500
(4)	74	8500
	76	6000
(6)	102	7500
	103	7300
	86	10000
	91	7000
	94	8500
	95	8500

All other points on the upper platform pegged the survey instrument.

		(Fast)
Door to V.C.	(2)	1100
Portside pressurizer	(4)	5200
Rod drives motors		5600
Starboard P.C. pump		10200
All point at void between upper and lower primary shield tanks		pegged
Rod Drives		6000

TABLE 4.14

GAMMA RAY DOSE RATE DECAY SURVEYS - PM-2A PRIMARY SHIELD SURFACE PRIOR TO SHIELD MODIFICATION

Instrument: Jordan AGB-10K-SR
Note: Dose rates are survey instrument readings in mr/hr. See Fig. 4.3 for dose point locations.

Primary Shield Coordinates	Shutdown for 14 hrs. 48 min. following 2 hr. 13 min. operation at Log N = 31.7 (corrected) - November 12, 1960														
	Survey at 0400 prior to starting 10-hr. power run - November 20, 1960														
			Time after shutdown (0402, Nov. 22, 1960) following 10 hrs. of reactor operation at Log N = 35 (corrected)												
			4 hrs.	6 hrs. 15 min.	9 hrs. 15 min.	11 hrs. 30 min.	14 hrs.	18 hrs.	22 hrs.	30 hrs.	38 hrs.	46 hrs.	54 hrs.	62 hrs.	70 hrs. 25 min.	86 hrs. 35 min.
0,0	140	2.1	900	1100	500	550	450	380	220	170	95	65	52	40	18	11
0,1	65	0.75	290	400	500	180	350	140	50	110	70	50	30	18	5	4
0,2	70	0.45		250		150	250	140	50	90	70		40	22	3.5	3
0,3	65	0.44	150	300	650	130	260	65	38	100	90	40	40	25	0.4	3.5
0,4		0.45	180	300		120	400	50	49	160	150	17	58	36	4	3.5
0,5	50	0.55	180	250	280	160	200	45	25	90	60	12	35	25	2.5	3.0
0,6	200	3.5	750	900	500	450	250	240	170	100	100	80	40	32	23	11
0,7		5	850	1000		600	300	250	140	110	90	50	45	35	18	11
1,0	210	1.4	650	1000	500	700	500	540	400	240	140	125	75	65	30	16
1,1	220	1,3	600	1000	1000	700	550	510	400	230	150	120	85	62	29	16
1,2	250	1.2	560	900	950	620	500	520	370	200	150	120	75	60	25	17
1,3	240	1.5	450	900	950	750	500	490	350	220	180	110	75	52	26	16
1,4	240	1.5	450	800	900	600	450	450	350	210		120	75	50	22	16
1,5	190	1.2	420	700	800	500	400	420	250	170	150	120	60	52	22	13
1,6	140	1.4	410	800	800	550	400	410	280	175	150	100	70	55	23	13
1,7	200	1.3	450	800		600	400	410	270	180	1150	90	70	52	23	14
2,0	250	1.3	650	1000		750	550	600	400	250	145	120	82	62	30	16
2,1	250	1.4	600	1000	1000	750	575	590	420	250	155	130	85	69	29	16
2,2	220	1.2	480	900	900	600	500	500	360	190	150	120	75	60	23	16
2,3	300	17	1000	1600	1400	1000	575	580	390	220	175	120	90	100	42	40
2,4	200	3.0	500	900		500	360	360	290	190	160	90	70	50	22	17
2,5																
2,6	100	1.0	300	500	500	300	225	220	140	95	85	50	37	30	12	7
2,7	190	1.5	400	700	500	500	350	340	140	150	135	80	60	45	20	12
3,0	300	1.6	650	1100		900	625	650	480	300	180	140	90	70	33	17
3,1	290	1.6	600	1000	1000	800	625	650	450	280	165	140	100	72	30	17
3,2	240	1.6	500	900	900	600	500	510	360	210	150	125	80	69	25	16
3,3	220	1.8	410	820	1400	620	360	450	300	160	140	80	75	52	25	16
3,4			450													
3,5	240	1.3	500	900	900	750	450	510	330	200	210	140	80	60	27	15
3,6	260	2.9	550	900	900	600	450	510	325	200	190	120	80	68	27	18
3,7	350	12	900	1500	900	900	550	520	350	220	210	125	96	90	45	32
4,0	10	0.13	35	45		20	18	20	15	8	6	3.5	3	2.1	1	0.6
4,1	7	0.13	35	49		22	32	17	11	7	4	3.4	2.5	2.0	1	0.6
4,2	13	0.18	50	60		37	30	26	18	11	9	6	4	3.5	1.4	0.6
4,3	16	0.30	45	60		37	25	20	17	10		6	4.5	4.6	1.5	1
4,4		0.26	40	55		35					10			6		1
4,5	15	0.44	50	70		40	25	19	17	7	5	7	4	3	1.7	1
4,6	8	0.20	35	50		20	18	18	13	6.5	5	3	2.9	2	1	0.7
4,7	7	0.20	35	45		20	15	20	10	5.5	4.8	2.5	2.4	1.8	1	0.8

TABLE 4.15

GAMMA RAY DOSE RATE DECAY SURVEY - PM-2A VAPOR CONTAINER EXTERIOR PRIOR TO SHIELDING MODIFICATION

Date: November 22, 1960

Reactor Power Level: Reactor Scrammed at 0402 Following 10 Hr Operation at Log N = 35 (corrected)

Instrument: Tracerlab Probe Model TA-6

Note: Probe located at dose point 84 on Vapor Container exterior (Fig. 4.6)

Time	Dose Rate (mr/hr)	Time	Dose Rate (mr/hr)
0400	---	1730	42
0430	1500	1830	38
0530	600	1930	29
0630	400	2030	21
0730	290	2130	19
0830	240	2230	18
0930	190	2330	17
1030	150	November 23, 1960	
1130	125	0030	16
1230	95	0130	16
1330	85	0230	15
1430	75	0330	15
1530	60	0430	15
1630	52	0530	14
		0630	14

TABLE 4.16

GAMMA RAY DOSE RATE DECAY SURVEYS - PM-2A REACTOR AREA
PRIOR TO SHIELD MODIFICATION (NOV. 12, 1960)

Date: Nov. 12, 1960

Reactor Scram at 0742 following 2 hr-13 min. Operation at Log N - 31.7 (corrected)

Instrument: Jordan AGB-10K-SR

Note: Dose Rates are survey instrument readings in mr/hr.

	TIME												
Survey Location	0745	0800	0830	0900	1000	1015	1100	1115	1300	1440	1600	1730	2230
Top of Stairway to Reactor Building	1.2												
Reactor Building Door to Upper Platform	8.0					5.2		4.8	2.9	2.1	1.3	1.0	
Upper Platform over Spent Fuel Rack	17.0					8.5		7.5	4.5	3.8	1.8	1.3	
Vapor Container Entrance		10			11		80		6.0	4.9	4	3.8	0.4
Port Side of Pressurizer		60			95				55	50	33	33	15
Starboard Side Primary Coolant Pump	110												25
Dose Point (2.3)	2600		2400	2500		2200		1400	1200	700	800	300	
Control Rod Drives	350		350	400		400		300	300	240	240	110	
Control Rod Drive Motors	100			140		130		90	80	65	55		
Seal Leakage Pump	140												
Upper Platform over Spent Fuel Rack		11											
Upper Platform 15 feet forward of Reactor		19			16		14	8.4	6	3.7	2.6		

TABLE 4.17

GAMMA RAY DOSE RATE DECAY SURVEYS - PM-2A REACTOR AREA
PRIOR TO SHIELD MODIFICATION
(NOV. 22-24, 1960)

Date: Nov. 22-24, 1960

Instrument: Jordan AGB-10K-SR

Reactor Power Level: Reactor Scrammed at 0402 Nov. 22 following 10 Hours Operation

At Log N=35 (corrected)

Note: Dose rates are survey instrument readings in mr/hr

	22 November						23 November			24 November	
Location of Survey	0645	1015	1315	1530	1800	2200	0200	1000	1800	0200	1000
Vapor Container Entrance	14	6.5	2.4	2.4	2.0	2.5	1.7	0.6	0.55	0.5	0.32
Control Rod Drives	--	500	500	300	250	280	250	125	58	80	34
Pressurizer, Port Side	--	90	60	60	35	40	--	21	9.5	6	4.5
BF_3 Chamber Wall	2500	1100	250	--	100	80	--	22	20		17
Chamber Wall #3 (Upper Platform - Reactor Bldg.)	--	--	250	--	120	90	--	22	26	12	18
Chamber Wall #4 (Upper Platform - Reactor Bldg.)	2000	700	400	--	110	79	--	18	18	13	12
Chamber Wall #5 (Upper Platform - Reactor Bldg.)	2300	800	500	--	110	62	--	18	17	12	10
Primary Coolant Pump, Starboard Side	--	110	150	55	70	60	--	23	26		10

loading spent fuel elements in shipping casks during full power operation. A dose rate of 100 mrem/hr was used as a target value to meet this desired objective. A dose rate on approach to this position may be somewhat higher.

b. The shielding be adequate to permit access to the primary skid 8 hr after reactor shutdown. The design target value was set at 50 mrem/hr.

c. The shielding be adequate to permit operating personnel working an 84 hr week to conform to government established radiation tolerance standards which allows an average integrated total dose of 300 mrem per week.[2] A maximum permissible integrated total body exposure of 3 rems may be received in a period of short duration within a thirteen consecutive week period and the annual exposure may not exceed 5 rems per year.

Analysis of the measurements made prior to shield modification indicated high neutron and gamma ray leakage in the region between the vapor container and the bottom of the spent fuel tank. It was believed that scattering of this leakage and gamma rays associated with neutron capture by hydrogen atoms in the snow walls were the principal sources of the high radiation levels encountered above the rear of the spent fuel tank. The "above-target" values on the surface of the primary shield tank in part were due to the presence of sodium in the corrosion inhibitor "NALCO" in the primary shield tank.

Modifications to the PM-2A shielding were designed and installed. The analysis leading to these modifications is presented in the literature.[1]

4.2.1 DESCRIPTION OF THE MODIFICATIONS

A. Within the Dry Cap (Fig. 4.11)

To permit the dry cap to be operated flooded, an insulated cover was designed for the top of the reactor vessel. This cover maintains a steam jacket over the studs and nuts. The presence of water in the dry cap is primarily for the reduction of neutron leakage from the dry cap region.

B. Above the Primary Shield Tank (Fig. 4.12)

The shielding in this area consists of interconnected water tanks on top of the primary shield tank in the region between the small upper shield tank and the vapor container tank. This additional shielding is primarily for reduction of neutron leakage. Concrete cylinders were placed in the regions not filled by the water tanks. Cadmium was placed on top of these shielding additions.

C. Primary Shielding Water Additives

The corrosion inhibitor in the primary shield tank (Nalco 39) which contains sodium was replaced by a compound containing potassium.

D. On Surface of Primary Shield (Fig. 4.13)

Two inches of lead were added to the surface of the primary shield in order to substantially reduce the gamma radiation level within the vapor container after shutdown following full power operation. This lead was strapped to the surface of the primary shield tank.

E. External to the Vapor Container (Fig. 4.14)

Additional shielding, consisting of cadmium, lead, wood, boral, and boric acid crystals was placed in the region between the vapor container and the upper shield tank. Cadmium was placed on the surface of the vapor container in the areas of the highest neutron leakage. A blanket of boric acid crystals was placed between the layers of wood shielding during installation. The purpose of the boric acid is to capture thermal neutrons, thus reducing gamma rays arising from captures by hydrogen in the wood.

F. On Surface of Snow Walls

A saturated boric acid solution, colored for easy identification, was sprayed and frozen on the walls in the vicinity of the reactor for purposes of reducing hydrogen capture gamma rays in the tunnel snow wall. The walls were treated in this manner from near the snow tunnel floor level to the approximate height of the spent fuel platform. The boric acid spray extended from a position opposite the middle of the vapor container to a position opposite the spent fuel rack.

4.3 SHIELDING MEASUREMENTS MADE SUBSEQUENT TO PM-2A SHIELD MODIFICATION

4.3.1 INTRODUCTION

Radiation measurements were made in February, 1961 subsequent to modification of the PM-2A shielding. These measurements were made for purposes of evaluating the effectiveness of the "as modified" PM-2A shielding to verify that radiation levels in areas where access is required to not exceed the design target values.

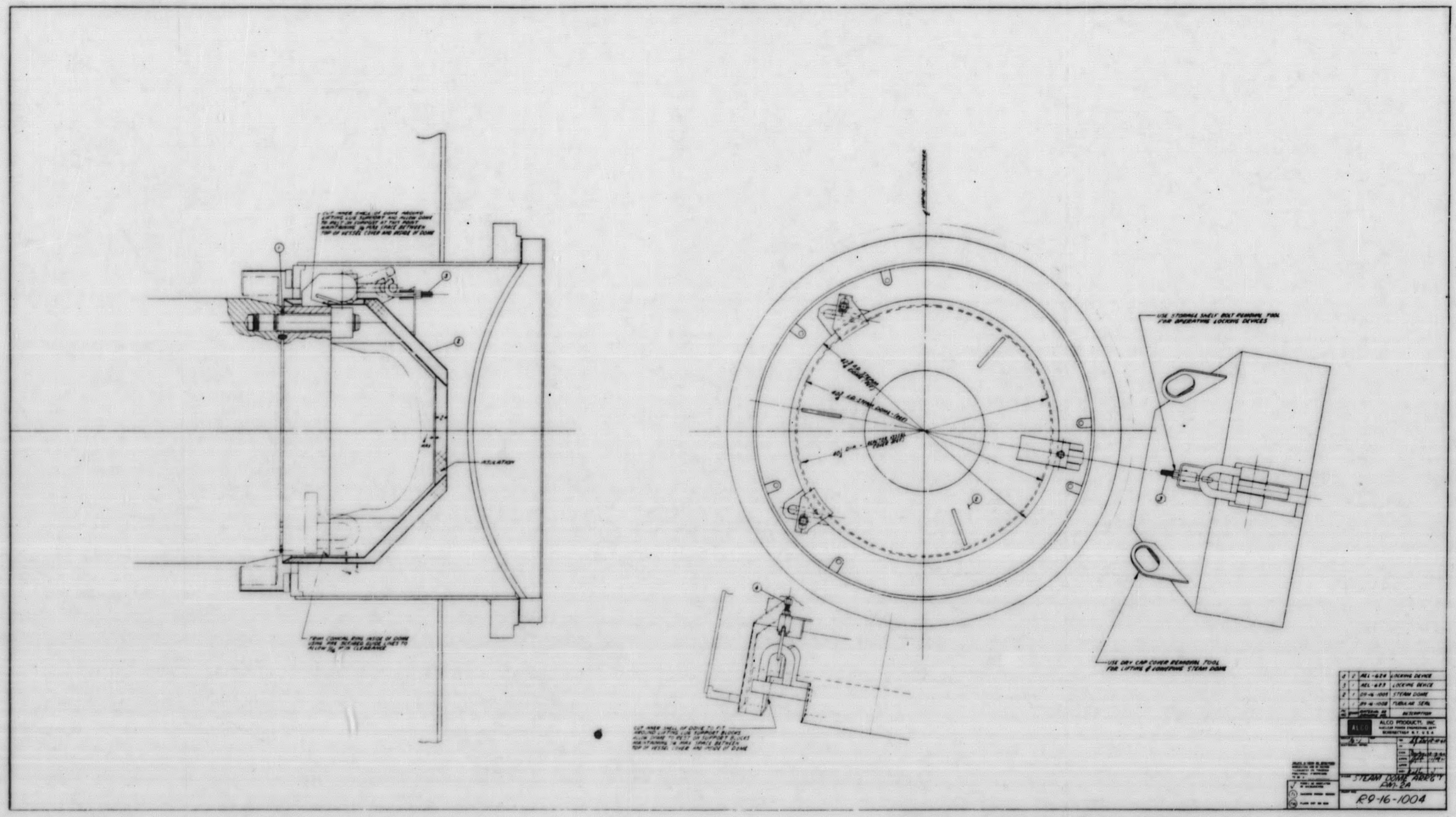

Figure 4.11. PM-2A Shielding Modification-Steam Dome Arrangement to Permit Operation with Dry Cap Filled with Water

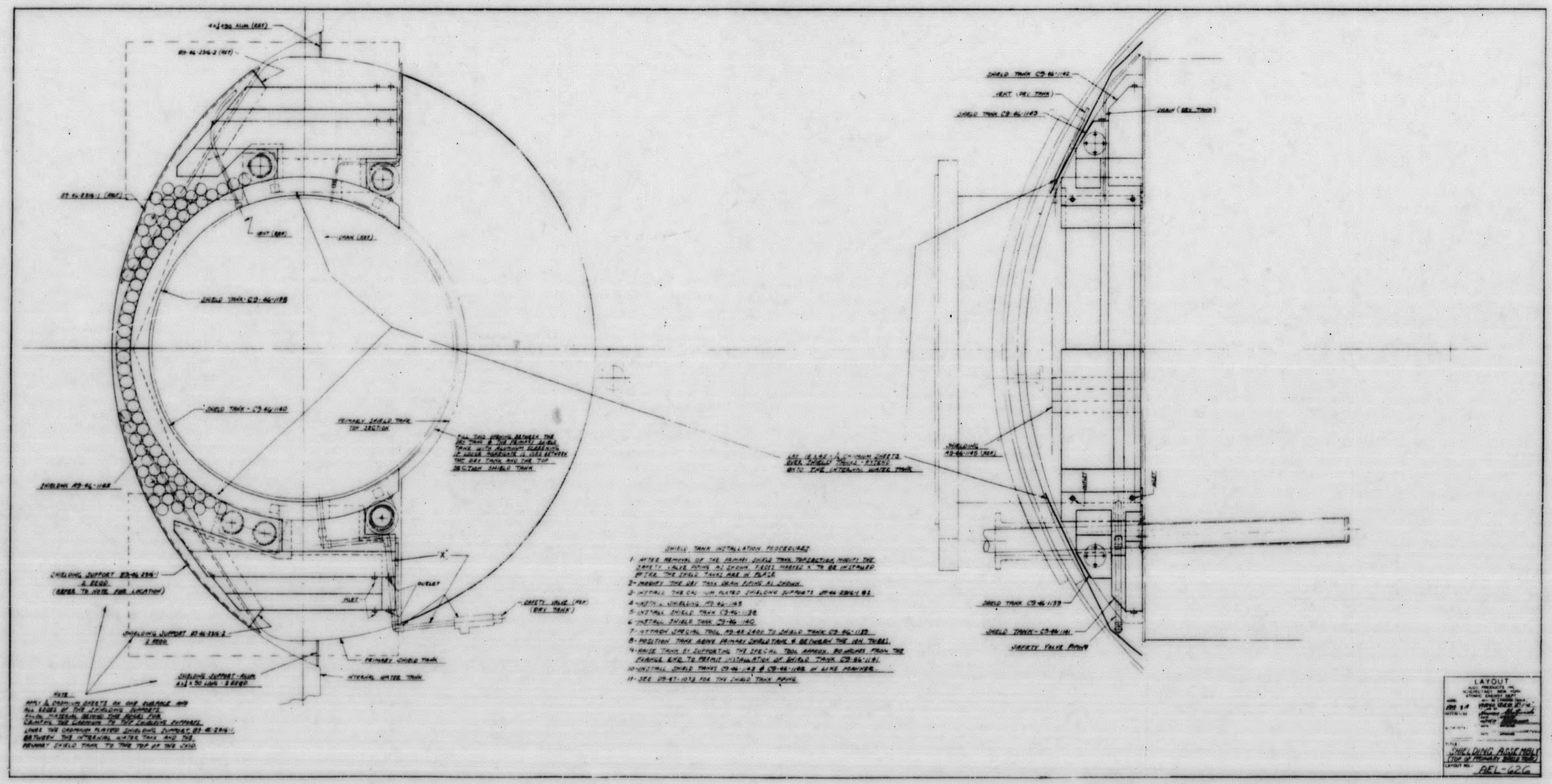

Figure 4.12. PM-2A Shielding Modification-Top of Primary Shield Tank

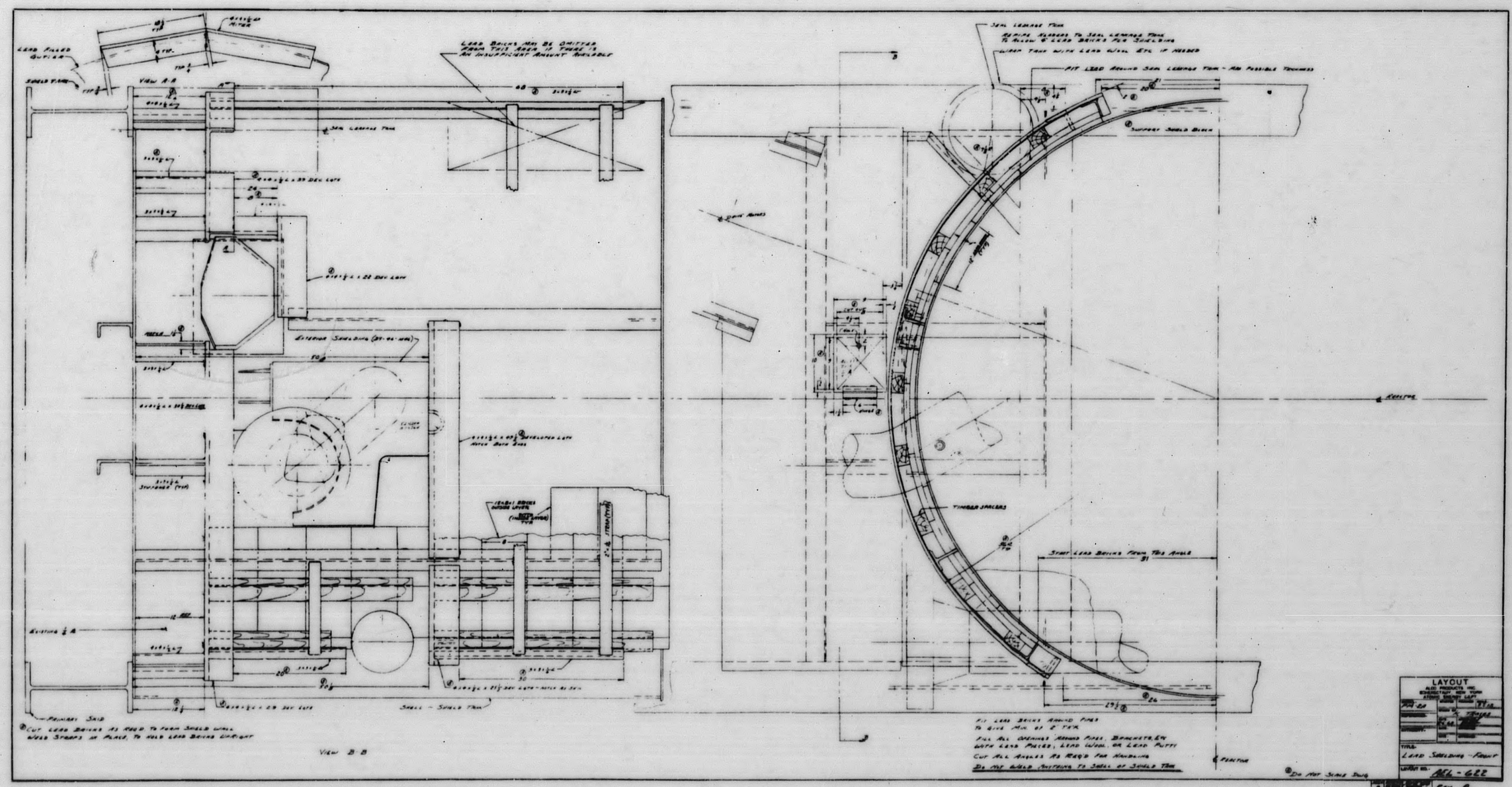

Figure 4.13. PM-2A Shielding Modification-Lead Shielding Added to Front of Primary Shield Tank

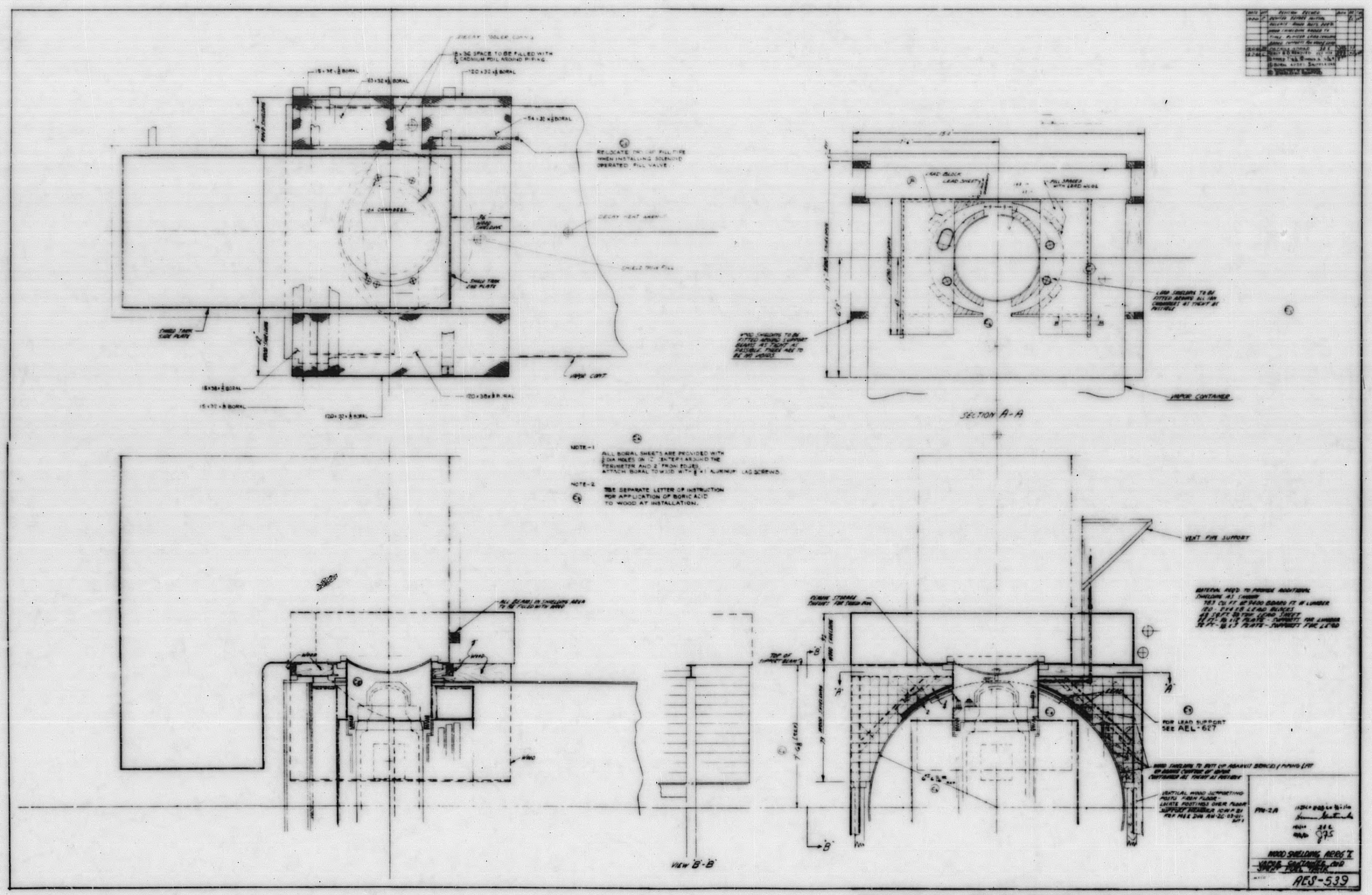

Figure 4. 14. PM-2A Shielding Modification - Vapor Container and Spent Fuel Tank

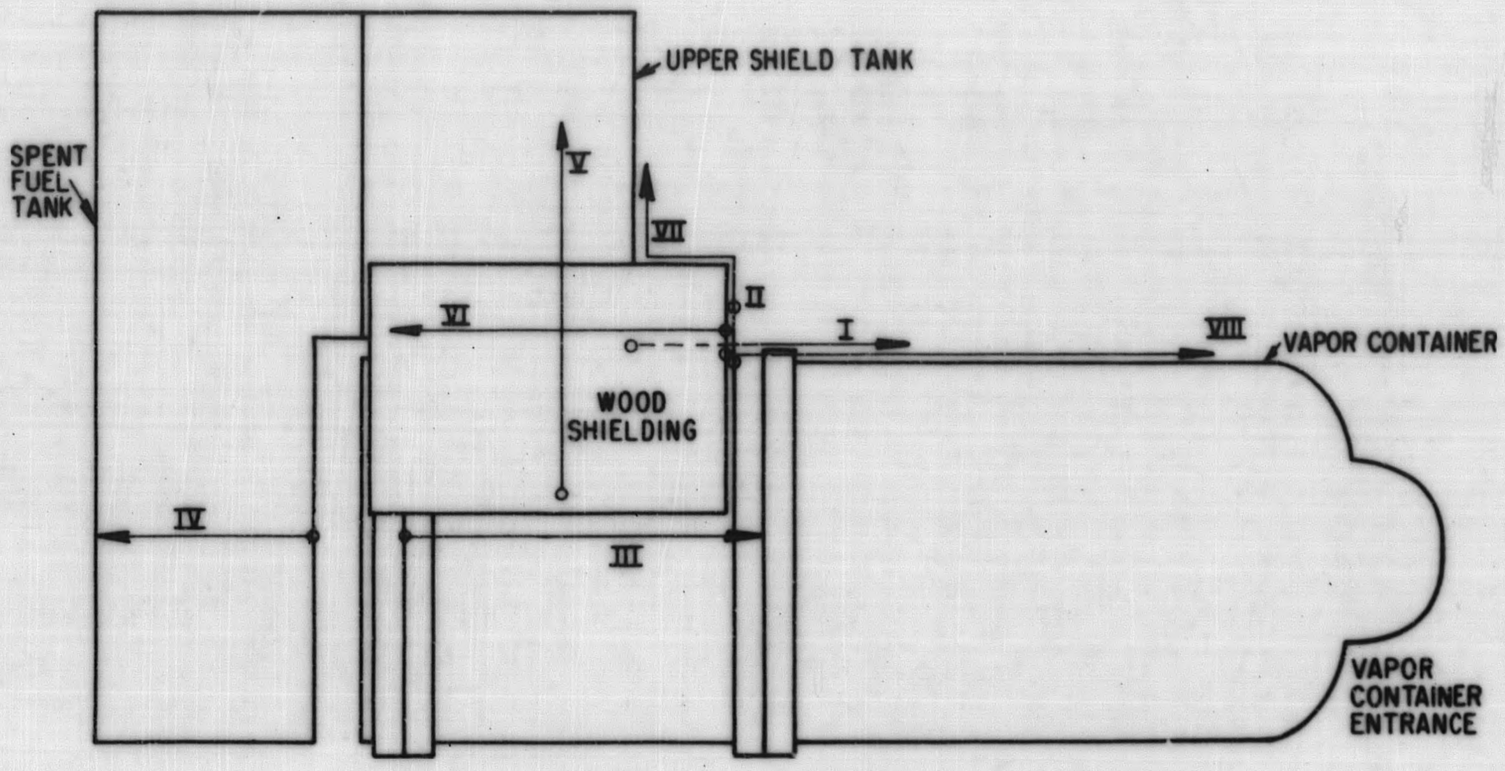

Figure 4. 15. Radiation Survey Traverse Locations on the Starboard Side of the PM-2A Vapor Container, Upper Shield Tank, and Spent Fuel Tank (Subsequent to Shield Modification)

4.3.2 COORDINATE SYSTEMS AND REFERENCE POINTS FOR CONDUCTING RADIATION

In order to permit direct comparison of radiation measurements made before and after shield modification, the dose points established previously were used wherever possible.

A survey grid, similar to that described in Section 4.1.2 was marked off on the surface of the primary shield tank which had been covered by 2 in. of lead during the modification. These dose points would then be extended 2 in. radially outward, but in the same location as shown in Fig. 4.3. The dose points on the deck of the upper spent fuel platform remained the same. The system of traverses placed around the vapor container exterior and shield tanks were outside of the shield modifications, and deviated from those described in Section 4.1.2. The dose points were at one foot intervals and their locations shown in Fig. 4.15 are described as follows:

I – Along the top centerline of the vapor container starting at the "dry cap" and extending forward. Points 1, 2, and 3 were covered by the shield modification and were not accessible.

II – Along the front surface of the modification starting at the center and extending, horizontally, to the starboard side.

III – Along the starboard side of the vapor container, on the mid-plane, starting at mid-point of the rear vapor container flange and extending forward.

IV – Along the starboard side of the spent fuel tank at the centerline of the vapor container beginning at the front of the tank and extending to the rear. This is essentially a continuation of traverse III described above.

V – On the vertical surface of the wood modification on the starboard side, lying in a plane parallel to the axis of the vapor container. Points 8a, 8b and 8c lie in the horizontal plane on top of the surface of the wood modification between the vertical points 8 and 9 of the traverse.

VI – On the starboard side of the reactor, beginning at the front of the wood modification and extending backward along the side of the modification at an elevation approximately one (1) foot above the top of the vapor container.

VII - On the front surface of the wood modification in front of the spent fuel tank perpendicular to the vapor container axis, starting at the vapor container and extending upwards. Points 3a, 3b, and 3c lie in a horizontal plane on the top surface of the wood modification between the traverse points 3 and 4.

VIII - On the fill line for the spent fuel tank beginning at the front surface of the wood modification and extending forward.

4.3.3 EXPERIMENTAL RESULTS AND PRESENTATION OF RADIATION SURVEY DATA

Radiation surveys were again made using the available portable instrumentation, gamma and neutron sensitive film, and gold foils. These surveys were made to determine the effectiveness of the shield modification.

A correction factor was applied to the Log N readings for extrapolation of the survey data to full reactor power. A review of the operating data indicated the Log N readings were low by a factor of 2.1 and had to be corrected. All the data extrapolated to full power were based upon the above correction factor and the value of the Log N of 100 being equal to 10 MW(th) at full power. The extrapolations were made from the corrected power levels recorded for each survey.

The Log N correction factor based on a detailed heat balance is 3.43. This is an average correction factor for the six day period, February 10 - February 15, 1961. Use of this correction factor would necessitate:

1. All corrected Log N values reported in this section being increased by a factor of 1.63.

2. All radiation measurements scaled to full power in this section being multiplied by 0.615.

The following tables present the data obtained as a result of the radiation surveys and the film and foil irradiations during February of 1961. These data established the effectiveness of the shield modifications described in Par. 4.2.

A. PRIMARY SHIELD SURVEYS

Gamma ray and neutron measurements were made on the PM-2A primary shield during reactor operation.

Table 4.18 presents the gamma ray dose rate survey of the PM-2A primary shield utilizing the coordinate system shown in Fig. 4.3. During this survey the reactor was operated at log N = 0.53 (corrected).

Table 4.19 presents fast neutron flux measurements made with a cadmium paraffin covered BF_3 probe. Dose point locations are shown in Fig. 4.3. This survey was made during reactor operation at log N = 0.021 (corrected)

Table 4.20 lists thermal neutron flux data obtained on the primary shield dose points illustrated in Fig. 4.4. Bare and cadmium covered gold foils were irradiated at these points for 387 hours at an average power level of 725 kw(e). The full power thermal neutron fluxes were obtained by the method of Par. 4.1.3. These data were used to demonstrate that neutron induced activation of primary system components would not be a problem.

Table 4.21 presents neutron flux measurements made in the instrument wells and on the primary shield surface subsequent to the shield modification. Cobalt foils were irradiated in instrument wall #1 and #2 at the elevation of the core midplane for purposes of measuring the thermal and epithermal neutron flux at these locations. A cadmium ratio of 10 was assumed in order to reduce the foil readings to thermal and epithermal flux values.

Sulfur foils were irradiated in instrument wall #1 at approximately the elevation of the core midplane and at several points on the primary shield. These foils were used to measure the fast flux above 2.9 Mev by means of the S^{32} (n, p) P^{32} reaction.

The irradiation time for the cobalt and sulfur foils was 387 hrs at an average corrected leg N of 36.3.

B. Area Surveys - Film

Table 4.22 lists the results of gamma sensitive film surveys made outside of the vapor container (Fig. 4.15) and on the upper platform of the PM-2A reactor building (Fig. 4.7). These data, scaled to full reactor power, were obtained by irradiating the films for approximately 17 hr at a corrected log N of 0.53. These data were used to indicate the gamma ray leakage from the dry cap region, and to establish the gamma ray intensity on the second level of the reactor building following the shield modification.

C. Area Surveys - Foil

Table 4.23 presents thermal neutron flux data obtained on the PM-2A vapor container. Bare and cadmium covered gold foils were irradiated for 387 hr at a log N = 36.3 (corrected). The fluxes have been corrected to full power by the method of Par. 4.1.3. The purpose of these measurements was

TABLE 4.18

GAMMA RAY DOSE RATE SURVEY - PM-2A PRIMARY SHIELD DURING LOW POWER REACTOR OPERATION AFTER SHIELD MODIFICATION

Date: February 8, 1961

Reactor Power Level: Reactor Operating at Log N = 0.53 (corrected)

Instrument: Jordan AGB-10K-SR

Note: Dose rates are in R/hr scaled to full power
See Figure 4.3 for dose point location

Dose Point	Dose Rate (R/hr)	Dose Point	Dose Rate (R/hr)
0.0	625	2.4	---
0.1	63	2.5	188
0.2	48	2.6	675
0.3	125	2.7	---
0.4	50	3.0	113
0.5	90	3.1	---
0.6	450	3.2	12
0.7	----	3.3	450
1.0	525	3.4	---
1.1	35	3.5	28
1.2	30	3.6	500
1.3	40	3.7	---
1.4	35	4.0	68
1.5	38	4.1	---
1.6	625	4.2	15
1.7	----	4.3	45
2.0	425	4.4	---
2.1	----	4.5	25
2.2	20	4.6	
2.3	2000	4.7	

TABLE 4.19

RELATIVE FAST NEUTRON FLUX SURVEY - PM-2A PRIMARY SHIELD DURING LOW POWER REACTOR OPERATION AFTER SHIELD MODIFICATION

Date: February 8, 1961

Reactor Power Level: Reactor Operating at Log N = 0.021 (corrected)

Instrument: Nuclear Chicago Model 2112N

Note: Readings in cpm with cadmium covered paraffin over BF_3 Probe. Dose point locations are shown in Fig. 4.3.

Dose Point	Instrument Reading (cpm)	Dose Point	Instrument Reading (cpm)
0.0	12,500	4.3	14,000
1.0	14,500	0.4	Off Scale
0.1	9,500	1.4	8,200
1.1	8,500	2.4	Off Scale
2.1	6,500	3.4	Off Scale
3.1	6,300	4.4	Off Scale
4.1	14,000	0.5	12,000
0.2	10,000	1.5	9,000
1.2	6,500	3.5	11,500
2.2	5,500	4.5	14,500
3.2	6,200	0.6	Off Scale
4.2	11,800	1.6	Off Scale
0.3	6,800	2.6	Off Scale
1.3	6,000	3.6	Off Scale
2.3	13,500	4.6	Off Scale
3.3	Off Scale		

TABLE 4.20

THERMAL NEUTRON FLUX SURVEY - PM-2A PRIMARY SHIELD
AFTER SHIELD MODIFICATION (GOLD FOIL ACTIVATION)

Date: February 9-26, 1961

Reactor Power Level: Reactor Operated for approximately 387 hours at an Average Log N = 36.3 (corrected)

NOTE: Foil locations are shown in Figure 4.4
Neutron fluxes were corrected to full power.

Foil Location	Thermal Neutron Flux Neutrons/cm^2sec	Cadmium Ration	Foil Location	Thermal Neutron Flux Neutrons/cm^2sec	Cadmium Ration
1	1.35 (10^5)	1.35	34	1.71 (10^5)	1.37
2	1.33 (10^5)	1.40	35	1.98 (10^5)	1.34
3	1.17 (10^5)	1.44	36	1.21 (10^5)	1.22
4	1.32 (10^5)	1.53	37	1.57 (10^5)	1.21
5	1.25 (10^5)	1.38	39	9.20 (10^5)	1.21
21	1.02 (10^5)	1.27	40	8.00 (10^5)	1.18
23	2.25 (10^5)	1.26	47	1.35 (10^5)	1.14
25	2.58 (10^5)	1.37	49	1.39 (10^5)	1.16
26	2.44 (10^5)	1.25	50	1.52 (10^5)	1.32
27	2.90 (10^5)	1.33	51	1.61 (10^5)	1.32
29	3.44 (10^5)	1.36	52	2.93 (10^5)	1.37
30	1.79 (10^5)	1.54	54	1.14 (10^5)	1.22
31	1.22 (10^5)	1.36	58	1.62 (10^5)	1.30
32	1.12 (10^5)	1.16	59	1.18 (10^5)	1.20
33	2.34 (10^5)	1.25			

TABLE 4.21

NEUTRON FLUX SURVEY - PM-2A INSTRUMENT WELLS AND PRIMARY SHIELD DURING HIGH POWER OPERATIONS SUBSEQUENT TO SHIELD MODIFICATION (COBALT AND SULFUR FOIL ACTIVATION)

Date: March 2, 1961

Reactor Power Level: Reactor operated for 387 hours at a Log N = 36.6 (corrected)

Note: The neutron flux was corrected to full power.

See Fig. 3.1 for instrument well locations.

See Fig. 4.4 for primary shield dose point locations.

Location	Neutron Flux (neutrons/cm^2 sec) Thermal*	epi-cadmium*	fast**	Foil Type
Instrument Well #1 at the elevation of the core midplane	$9.35(10^7)$	$8.73(10^6)$		Co
Instrument Well #2 at the elevation of the core midplane	$2.06(10^8)$	$1.93(10^7)$		Co
Instrument Well #1 at the elevation of the core midplane			$4.16(10^8)$	S
#24 (primary shield)			$1.05(10^5)$	S
#27 (primary shield)			$2.19(10^4)$	S
#29 (primary shield)			$3.78(10^5)$	S
#39 (primary shield)			$5.29(10^4)$	S
#43 (primary shield)			$3.67(10^6)$	S
#59 (primary shield)			$3.70(10^4)$	S

* Assumed Cadmium Ratio = 10

** E > 2.9 Mev

TABLE 4.22

GAMMA SENSITIVE FILM SURVEYS - PM-2A VAPOR CONTAINER EXTERIOR AND UPPER PLATFORM OF THE REACTOR BUILDING AFTER SHIELD MODIFICATION

Date: February 6 & 7, 1961

Reactor Power Level: Reactor operated at Log N=0.53 (corrected) for 17 hours 4 minutes

Note: Dose Rate in R/Hour scaled to Full Power

The following measurements were made on the PM-2A Vapor Container Exterior.
Film Locations are shown in Fig. 4.15.

Film Location		Dose Rate R/Hour
III	0	56
	2	379
	4	22
	6	33
	8	22
	10	15
I	4	403
	5	173
VII	0	322
	1	279
	2	145
	3	78
	4	60
	5	45
	6	33
	7	22
	8	26
	3a	56
	3b	67
	3c	123
V	10	33
	11	33
	12	22
	13	14
	0	67
	1	67
	2	67
	3	56
	4	22
	5	33
	6	12
	7	10
	8	8
	8a	6
	8b	13
	8c	28
	9	22
II	0	280
	1	240
	2	269
	3	200
	4	134
	5	67
	6	33
	7	16
IV	0	436
	2	56
	4	22
	6	92
VI	0	7.0
	1	5.2
	2	4.8
	3	5.5
	4	8.4
	5	8.9
	6	8.4
	7	9.1
	8	9.5
	9	8.9
	10	8.4
	11	16.8
VIII	0	4.3
	2	5.5
	4	14
	6	22
	8	22
	10	19
	12	10.6
	14	7.7
	16	6.4
	18	5.0
	20	4.1
	22	3.4

The following measurements were made on the Upper Platform of the PM-2A Building. Film Locations shown in Fig. 4.7.

Film Location	Dose Rate R/Hour
73	1.1
74	2.3
75	2.1
76	0.6
77	12.0
78	1.6
79	10.0
80	4.1
81	1.6
82	4.1
83	8.9
84	2.2
85	1.1
86	6.0
87	1.2
88	1.9
89	0.3
90	0.2
91	0.1
92	0.6
93	3.3
94	0.2
95	0.6
96	0.3
97	1.3
98	2.2
99	3.0
100	2.1
101	1.5
102	4.1
103	2.7
104	2.1
105	1.6
106	1.0
107	1.4
108	8.7

TABLE 4.23

THERMAL NEUTRON FLUX SURVEYS - PM-2A
REACTOR AREA AFTER SHIELD MODIFICATION
(GOLD FOIL ACTIVATION)

Date: February 9 through February 26, 1961

Note: Neutron Fluxes were corrected to full power.

Reactor Power Level: Reactor Operated for approximately 387 hours at an average power level of 725 KW(e) Log N = 36.3 (corrected)

The following measurements were made on the PM-2A Vapor Container exterior. Foil locations are shown in Fig. 4.15.

Foil Location		Thermal Neutron Flux Neutrons/cm^2sec	Cadmium Ratio
II	4	1.41 (10^6)	4.15
	5	6.76 (10^5)	
III	0	4.21 (10^5)	
	1	4.21 (10^5)	
	2	3.70 (10^5)	
	3	3.19 (10^5)	2.6
	5	2.94 (10^4)	
	6	7.91 (10^4)	1.6
	7	2.78 (10^4)	
III	0	3.15 (10^4)	
	2	3.86 (10^4)	2.12
	4	5.42 (10^4)	
	6	8.31 (10^4)	
	8	1.035 (10^5)	1.53
	10	7.43 (10^4)	
IV	0	2.02 (10^4)	3.02
	2	2.42 (10^4)	
	4	2.20 (10^4)	
	6	1.60 (10^4)	2.70

The following measurements were made on the PM-2A Vapor Container exterior. Foil locations are shown in Fig. 4.15.

Foil Location		Thermal Neutron Flux Neutrons/cm^2sec	Cadmium Ratio
V	0	7.90 (10^4)	2.65
	1	4.97 (10^4)	
	3	4.97 (10^4)	3.81
	4	4.85 (10^4)	
	5	4.31 (10^4)	
	6	3.38 (10^4)	3.98
	7	1.185 (10^4)	
	8	1.295 (10^4)	
	8c		2.04
	10	7.81 (10^3)	
	12	1.065 (10^4)	2.66
VI	0	3.03 (10^4)	1.68
	1	2.07 (10^4)	
	2	2.01 (10^4)	
	3	1.22 (10^4)	2.05
	4	9.15 (10^3)	
	5	1.28 (10^4)	
	6	1.31 (10^4)	2.58
	7	1.452 (10^4)	
	8	1.527 (10^4)	
	9	1.231 (10^4)	2.60
	12	7.61 (10^3)	2.17

The following measurements were made on the PM-2A Vapor Container exterior. Foil locations are shown in Fig. 4.6.

Foil Location	Thermal Neutron Neutrons/cm^2sec	Cadmium Ratio
62 b	3.69 (10^4)	2.11
71	2.02 (10^5)	1.97
72	2.33 (10^5)	2.04
73	9.55 (10^5)	2.63
74	5.74 (10^5)	2.86
82	3.26 (10^5)	1.41
101	2.28 (10^5)	1.70
102	2.21 (10^5)	1.71
103	1.00 (10^5)	1.57
104	6.05 (10^4)	2.46
105	2.99 (10^4)	2.56

to determine whether the neutron flux leaking from the dry cap region was contributing to the dose rate above the spent fuel tanks by means of the n, γ reaction in the tunnel snow walls.

D. Area Surveys - Survey Instruments

Neutron and gamma ray surveys were made in the general PM-2A plant area for purposes of determining whether radiation levels were below government established radiation tolerance standards.

Table 4.24 is a compilation of the PM-2A Plant radiation surveys. Four of these surveys were taken of the entire plant and were made with the gamma sensitive radiation survey meters. Figure 4.10 shows the dose point locations. The dose rates presented in this table are survey meter readings and were not scaled to full power.

Table 4.25 presents the results of a gamma ray dose rate survey of the PM-2A vapor container exterior. This survey was made during low power reactor operation (corrected log N = 0.53). Dose points are illustrated in Fig. 4.6.

Table 4.26 lists the results of the neutron flux survey made on the PM-2A vapor container exterior during low power reactor operation. These data are presented as instrument readings in cpm and are indicative of the fast neutron flux. The survey was performed using a cadmium-paraffin cover over a BF_3 probe. During the survey the reactor was operated at a log N = 0.021 (corrected). Dose point locations are illustrated in Fig. 4.6.

Table 4.27 is a compilation of gamma ray dose rate decay measurements made on the PM-2A primary shield subsequent to shield modification. These measurements were made from 9 to 66 hr following shutdown from 387 hr of reactor operation at a corrected log N = 36.3. These survey data were used in evaluating the effect of altering the corrosion inhibitor in the primary shield tank. The dose point coordinate system shown in Fig. 4.3 was utilized for this survey.

Table 4.28 presents gamma ray decay data taken on various primary system components within the vapor container. These data were obtained following shutdown from 387 hours of reactor operation at an average corrected log N = 36.3. The survey point locations are identified in the table. These data indicated that the radiation levels in the PM-2A vapor container eight hours following shutdown from full power reactor operation will be less than 50 mr/hr. Therefore safe access to the vapor container for operating and maintenance duties is possible at this time.

TABLE 4.24

GAMMA RAY DOSE RATE INSTRUMENT SURVEYS - PM-2A PLANT AREA
DURING LOW POWER REACTOR OPERATION AFTER SHIELD MODIFICATION

Date: February 7, 1961 Reactor Power Level: (a) Log N-0.53 (corrected) for Survey #1 & #2

Instrument: Jordan Model AGB-10K-SR (b) Log N-32.5 (corrected) for Survey #3 & #4

Note: Dose Point Locations are shown in Figure 4.10
Dose rates are survey Instrument Readings in mr/hr.

Dose Point	Survey #1 (mr/hr)	Survey #2 (mr/hr)	Survey #3 (mr/hr)	Survey #4 (mr/hr)
1	0.04	0.065	0.04	0.055
2	0.038	0.065	0.038	0.055
3	0.038	0.055	0.038	0.055
4	0.038	0.038	0.065	0.053
5	0.14	0.09	0.14	0.087
6	0.06	0.075	0.06	0.065
7	0.051	0.065	0.051	0.06
8	0.048	0.07	0.048	0.056
9	0.052	0.07	0.45	0.26
10	0.058	0.07	1.4	0.6
11	0.07	0.065	0.32	0.2
12	0.13	0.15	5.2	2.6
13	0.48	0.4	25	34
14	0.58	0.4	48	33
15	8.2	5.5	950	800
16	10	6	1200	720
17	5.2	6.5	1000	800
18	6	3.5	1500	1000
19	0.12	0.13	--	5.0
20	3.8	3.7	240 (Streaming)	1300 (Streaming)
21	22	15	480	2000
22	62	26	--	--
23	0.5	0.32	--	--
24	2.2	1.2	--	--
25	4	2.2	--	--
26	0.5	0.36	--	--
27	0.34	0.06	--	--
28	0.06	0.055	--	--
29	0.5	0.25	--	--
30	0.55	0.3	--	--
31	0.045	--	--	--
32	0.045	--	--	--
33	0.09	--	0.09	--
34	0.095	0.07	0.095	--
35	0.095	0.07	0.095	--
36	0.085	--	0.085	--
37	0.54	--	60	46
38	36	--	3500	3200

TABLE 4.25

GAMMA RAY DOSE RATE SURVEY - PM-2A VAPOR CONTAINER EXTERIOR DURING LOW POWER REACTOR OPERATION AFTER SHIELD MODIFICATION

Date: February 8, 1961

Reactor Power Level: Reactor Operating at Log N = 0.53 (corrected)

Instrument: Jordan AGB-10K-SR

Note: Dose point locations are shown in Fig. 4.6
Dose rates are in R/hr scaled to full power

Dose Point	Dose Rate R/hr	Dose Point	Dose Rate R/hr
77 (a)	0.55	95	5.27
77 (b)	2.26	96	6.8
78	3.2	97	6.03
79	4.7	98	12.3
80	9.04	99	33.9
81	7.9	100	60.5
82	340	101	85.0
92 (a)	0.83	102	114
92 (b)	1.17	103	85.0
92 (c)	2.64	104	414
93	3.39	105	602
94	4.52	106	142

TABLE 4.26

FAST NEUTRON FLUX SURVEY - PM-2A VAPOR CONTAINER EXTERIOR DURING LOW POWER REACTOR OPERATION AFTER SHIELD MODIFICATION

Date: February 8, 1961

Reactor Power Level: Reactor operating at Log N = 0.021 (corrected)

Instrument: Nuclear Chicago Model 2112N

Note: Readings are in cpm with cadmium covered paraffin over BF_3 probe. Dose Points locations are illustrated in Fig. 4.6.

Dose Point	Instrument Reading (cpm)
77 (a)	200
77 (b)	450
78	550
79	650
80	1,100
81	1,300
82	3,000
92 (a)	140
92 (b)	250
92 (c)	450
93	550
94	900
95	800
96	1,100
97	1,100
98	3,500
99	2,000

TABLE 4.27

GAMMA RAY DOSE RATE DECAY SURVEY - PM-2A PRIMARY SHIELD SURFACE FOLLOWING REACTOR SHUTDOWN AFTER SHIELD MODIFICATION

Date: February 26-28, 1961

Reactor Power Level: Reactor Scrammed at 0522 on Feb. 26, 1961 following 387 hours operation - at an average Log N = 36.3 (corrected)

Instrument: Jordan AGB-10K-SR

Note: Dose Rates are survey instrument readings in mr/hr

See Fig. 4.3 for Dose Point Location

	TIME AFTER SHUT DOWN						
Dose Point	9 Hours	17 Hours	27 Hours	34 Hours	42.5 Hours	56.5 Hours	66 Hours
0.0	--	35	18	14	16	9.5	9.0
0.1	10	3.6	1.9	1.7	2.6	1.3	1.3
0.2	14	3.5	1.7	1.5	0.2	1.4	1.8
0.3	--	5.2	2.1	2.4	3.6	1.6	1.2
0.4	--	6.0	3.9	2.8	2.9	1.5	1.2
0.5	--	5.5	2.4	2.2	3.0	1.5	--
0.6	--	22	15	15	10	5.9	--
0.7	--	--	--	--	--	--	--
1.0	--	45	19	16	10	7.5	4.9
1.1	6.2	2.7	1.2	1.2	1 1	0.72	0.62
1.2	7.0	3.0	1.2	1 4	1.2	0.92	0.78
1.3	15	6.5	2.6	2.4	2.7	2.1	1.6
1.4	22	12	5.5	4.0	2.7	2.7	2.5
1.5	--	10	1.5	2.5	3.1	1.6	--
1.6	52	35	16	16	10	6.5	--
1.7	--	--	--	--	--	--	--
2.0	--	39	16	14	9	4.8	3.4
2.1	4.8	3.8	1.6	1.4	21	0.75	0.59
2.2	11	3.5	1.3	1.6	1.3	1.2	0.95
2.3	180	25	40	32	37	35	35
2.4	85	--	14	18.0	20	16	--
2.5	--	21	--	7.5	7.0	5.8	--
2.6	160	70	24	24	20	20	--
2.7	--	--	--	--	--	--	--
3.0	--	45	14	12	9.9	5.5	4.0
3.1	10	5.5	1.7	1.7	1.5	0.95	0.79
3.2	14	8.0	3.8	4.0	3.7	3.1	2.8
3.3	30	15	9	11	7.5	7.8	8.0
3.4	--	--	7	3.8	3.6	2.6	2.7
3.5	--	9.5	3.8	2.5	3.0	2.2	--
3.6	200	170	82	70	55	55	--

TABLE 4.28

GAMMA RAY DOSE RATE DECAY SURVEY - PM-2A VAPOR CONTAINER INTERIOR FOLLOWING REACTOR SHUTDOWN AFTER SHIELD MODIFICATION

Reactor Power Level: The reactor was shutdown at 0522 on February 26, 1961 following 387 hr of operation at an average log N-36.3 (corrected).

Date: February 26 - March 1, 1961

Note: Dose rates are survey instrument readings in mr/hr.

	Hours after Shutdown						
Dose Point Location	9.3	16.8	27.3	33.8	43.3	56.7	65.8
Blowdown line discharge cooler	13		7	8	7	7.5	5.8
Blowdown cooler	10	13	6	5.5	6.2	5.0	4.1
Seal coolant tank discharge	6		2.1	2	1.9	1.8	1.2
Seal coolant tank	7		1.6	1.8	2.1	1.2	0.89
Seal coolant tank inlet	8.5		2.5	2	1.5	1.9	1.2
Pri. coolant at outlet of reactor			16.0	14	13	16	7.0
Pri. coolant at inlet to stm. generator	16		3.1	2.9	3.4	2.5	1.8
Outlet of stm. gen. below P.C. pump	29	14	3.1	2.6	2.9	2.8	1.7
Pri. coolant pump	42	8.8	3.8	3.2	3.9	4.2	2.5
P.C. pump disch. at shield tank	60	20	8	7	10	6.5	5.8
Bottom of pressurizer	5	2	2.4	2.5	2.9	2.8	1.6
Pressurizer recirculation line	7		6.1	4.5	4.4	3.6	2.5
Stm. gen. shell	42	17	6	7	8.5	7.5	7.0
Stm. gen. dome	5	3.1	1.2	1.3	1.6	1.1	1.2
Stm. Gen. Stm. Dome head	1.7	0.75	0.4	0.36	0.39	0.36	0.28

TABLE 4.29

GAMMA RAY DOSE RATE DECAY SURVEY - PM-2A VAPOR CONTAINER EXTERIOR FOLLOWING REACTOR SHUTDOWN AFTER SHIELD MODIFICATION

Date: February 26, 27, and 28, 1961 Reactor Power Level: Reactor Shutdown at 0522 on 2/26/61 following 387 hr of power operation at an average Log N-36.3

Instrument: Jordan Model AGB-10K-SR

Note: Dose rates are survey meter readings in mr/hr. Dose Point locations are shown in Fig. 4.6

	Hours After Shutdown					
Dose Point	9 Hr	27 Hr	34 Hr	56 1/2 Hr	66 Hr	78 Hr
77 (a)	0.65	0.13	0.13	0.12	0.17	0.15
77 (b)	2.3	0.26	0.28	0.27	0.32	0.32
78	3.5	0.37	0.42	0.38	0.41	0.45
79	4.9	0.55	0.55	0.50	0.60	0.62
80	9.9	0.8	0.85	0.70	0.85	0.95
81	17	1.4	1.4	0.85	0.90	1.0
82	6.2	7.2	7.5	6.5	9.0	10.
92 (a)	0.7	0.09	0.1	0.12	0.13	0.12
92 (b)	0.9	0.11	0.11	0.14	0.15	0.14
92 (c)	2.2	0.17	0.17	0.18	0.19	0.18
93	4.6	0.24	0.25	0.29	0.31	0.32
94	5.2	0.32	0.33	0.38	0.41	0.41
95	7.3	0.43	0.4	0.45	0.56	0.60
96	7.8	0.42	0.42	*	0.50	0.58
97	8.0	0.35	0.35	*	0.48	0.45
98	12	0.52	0.49	*	0.52	0.45

* - Not taken due to radioactive surface contamination on vapor container surface.

TABLE 4.30

GAMMA RAY DOSE RATE DECAY SURVEY - PM-2A PLANT AREA FOLLOWING REACTOR SHUTDOWN SUBSEQUENT TO SHIELD MODIFICATION

Date: February 20, 1961

Instrument: Jordan AGB-10K-SR

Reactor Power Level: Reactor Scrammed at 0522 on Feb. 26, 1961 following 387 hours of reactor operation at an average Log N = 36.3 (corrected)

Note: Dose point locations are noted in Table.
Dose rates are survey meter readings in mr/hr.

Dose Point	Hours After Shutdown	Dose Rate (mr/hr)	Dose Point	Hours After Shutdown	Dose Rate (mr/hr)
(2.3)	9.3	180	(1.4)	9.3	22
Primary Shield	16.8	75	Primary Shield	16.8	12
Figure 4.3	27.4	40	Figure 4.3	27.4	5.5
	33.9	32		33.9	4.0
	42.4	37		42.4	2.7
	56.5	35		56.5	2.7
	65.9	35		65.9	2.5
	78.4	32		78.4	3.1
	141.1	27		141.1	3.0
(3.6)	9.3	200	#98	9.3	12
Primary Shield	16.8	170	Upper Platform	27.4	0.52
Figure 4.3	27.4	82	Reactor Building	33.9	0.49
	33.9	70	Figure 4.7	65.9	0.52
	42.4	55		78.4	0.45
	56.5	55		141.1	0.30
	78.4	105*	#82	9.3	62
	141.1	30	Upper Platform	27.4	7.2
			Reactor Building	33.9	7.5
			Figure 4.7	141.1	2.1

* Removed Pb Shield for repairs to decay heat line.

Table 4.29 lists the results of dose rate decay surveys made on the vapor container exterior subsequent to shield modification. These surveys are made following shutdown from 387 hr of reactor operation at an average corrected log N = 36.3 Dose point locations are shown in Fig. 4.6.

Table 4.30 presents gamma ray surveys made following shutdown at locations both inside of and exterior to the PM-2A vapor container. These data were obtained following shutdown from 387 hr of reactor operation at an average corrected Log N = 36.3.

4.4 ANALYSIS OF RADIATION MEASUREMENTS ON THE PM-2A PRIMARY SHIELD TANK SURFACE

4.4.1 REVIEW OF ROC CODE CALCULATIONS

The primary shield analysis was accomplished using the ROC codes developed at Alco and is presented in APAE-39[3]. The ROC codes calculate the gamma flux distribution radially through the shield at the height of the core midplane. The codes calculate, at designated locations within the shield, both the dose rate due to the core gamma rays and the dose rate due to secondary gamma rays originating in materials outside of the core. Core gamma rays were assumed to have an average energy of 1.65 Mev. Gamma sources in the regions outside of the core are divided into 5 energy groups. In both cases, the gamma ray source strengths are calculated from a two group neutron flux distribution. The input required for the codes is as follows:

1. Volume fractions of all materials in core.
2. Core geometry - radius and height.
3. Average thermal and fast neutron flux in core.
4. Description of all regions external to the core as to position, region thickness and region material.
5. Thermal and fast neutron flux distribution through the region outside of the core.
6. Description of radial distance at which dose rate is to be calculated.

All other necessary parameters are contained within the codes. The output of the ROC codes gives the dose rate in mr/hr at each designated position within the shield and on the outside surface of the shield. These dose

rates are given separately for the core gamma rays and the secondary gamma rays.

The ROC code values for the SM-1 have been compared to SM-1 experimental values. Agreement within a factor of two was obtained through most of the shield for the operating dose rates. In all cases, the calculated results were higher than the measured values originally obtained on the SM-1 and were therefore conservative.[4]

Complete details of the machine calculation are contained in APAE 35[4] and APAE Memo 142.[5]

A. Operating Dose Rate Calculation

Use of the ROC codes in calculating PM-2A operating dose rates gave a value of 247 R/hr on the shield tank surface. The contribution from the core was 73.8 R/hr and that from capture and activation sources in the shield was 173.3 R/hr. The dose rate in the SM-1 outside a shield thickness corresponding approximately to the total thickness of the PM-2A was 86.4 R/hr. In that the PM-2A shield rings are boral coated it would appear that 86.4 R/hr would be an upper limit for the PM-2A. Nevertheless, the 247 R/hr was accepted as the design target value of the operating dose on the shield tank surface because the radiation level eight hours after reactor shutdown met the design target value (Ref. Section 4.2).

B. Shutdown Dose Rate Calculations

The ROC codes rendered a value of 110 mr/hr on the surface of the primary shield tank 2.5 hr after an infinite operation at 10 Mw. Of this value, 44 mr/hr was due to core gamma rays and 66 mr/hr was due to gamma rays from activated shield materials. A hand calculation for the dose rate due to core gamma rays rendered 24.3 mr/hr.

Past experience (on the SM-1) had indicated that the machine calculations consistently gave dose rates higher than measured values.[4] Therefore, the surface dose rate from the PM-2A core and activated shield materials was estimated to be about 50 mr/hr rather than the calculated 110 mr/hr.

In addition to the radiation from the primary shield tank, there are two other sources of radiation which contribute to the dose rate on the shield tank surface. These are:

1) Activated corrosion products distributed throughout the primary system.

2) Activated components in the vapor container.

Based on the earlier experience with the SM-1, it was concluded that these two sources would give a dose rate of 30 mr/hr on the shield tank surface. Consequently, a total design gamma ray dose rate of 80 mr/hr from all sources was predicted on the PM-2A primary shield tank surface 2.5 hr after infinite operation at 10 Mw.

4.4.2 EVALUATION OF THE RESULTS OF THE ROC CODE SHIELDING CALCULATION FOR THE PM-2A PRIMARY SHIELD

The usefulness of the ROC code shielding calculations for the PM-2A primary shield was evaluated by comparing the calculated values to the measured values scaled to full power. The average of the dose rates measured at points (1.0) and (1.6) were chosen for comparison to the calculated value. As may be seen from Fig. 4.3 which shows the location of the dose points and Fig. 4.13 which shows the position of the lead shielding added to the primary shield tank surface, these dose points are unaffected by the lead shielding. A comparison of the measured dose rates at these points with the calculated values is appropriate as no lead was considered in the design calculations.

The dose rates at points (1.0) and (1.6) were obtained from Table 4.27 which presents the gamma ray dose rate decay data for the PM-2A primary shield subsequent to shield modification. These dose rates were multiplied by the factor $\frac{2000}{725} = 2.76$ in order to scale to a full power reactor operating history.

The measured dose rate decay on the primary shield scaled to full power is illustrated in Fig. 4.16. This gamma ray decay curve consists of the sum of contributions from the following sources:

1. The core and shield tank

2. The activated corrosion inhibitor in the pirmary shield tank

3. The activated corrosion products in the primary coolant

Decay curves for the activated corrosion inhibitor and activated corrosion products in the primary coolant are plotted for comparison with the measured total dose rate. The decay curve for the activated corrosion inhibitor was obtained by fitting a 12.5 hr half life curve for potassium - 42 through the value of 66 mr/hr calculated for 8 hours after shutdown. (See section 4.4.4)

The decay curve for the activated corrosion products was obtained by normalizing the decay data for an average of several points on the primary piping to the mean value of 9 mr/hr for the radiation field which exists in the vapor container 9 hr after shutdown. This curve was also multiplied by 2.76 to correct to a full power reactor operating history. (See Sec. 4.4.6)

The difference between the sum of the decay curves for the activated corrosion inhibitor in the shield tank and the activated corrosion products in the primary coolant, and the curve for the measured total dose rate on the surface of the primary shield is due to gamma rays originating in the core and shield rings. The resulting curve is presented in Fig. 4.17. In Fig. 4.17 the following decay curves are plotted for comparison:

1. Decay curve on surface of PM-2A primary shield following 387 hr reactor operation based on altering experimental measurements in order to:

   a) Correct to a full power operating history.

   b) Account for dose rate contributions from the activated corrosion inhibitor and from activated nuclides in the primary coolant.

2. Calculated Dose Rate Decay on PM-2A Primary Shield

3. Dose Rate Decay between the 7th and 8th shield rings of the SM-1. This position corresponds most closely to the surface of the PM-2A primary shield tank.

Comparison of curves (1) and (2) indicates that the calculated values are a factor of 3 lower than the values based on experimental measurements at 8 hours after shutdown and a factor of 1.8 at 24 hr after shutdown.

Results from the machine calculation indicated a dose rate on the PM-2A shield surface of 110 mr/hr for infinite operation at 10 Mw and 2.5 hr shutdown time. However, the machine calculation had been found to give dose rates consistently higher than those measured at the SM-1.[4] Between the 7th and 8th shield rings of the SM-1 where total shielding is approximately equal to that of the PM-2A, the machine calculated dose rate is about six times the measured dose rate for the SM-1. At this position in the SM-1

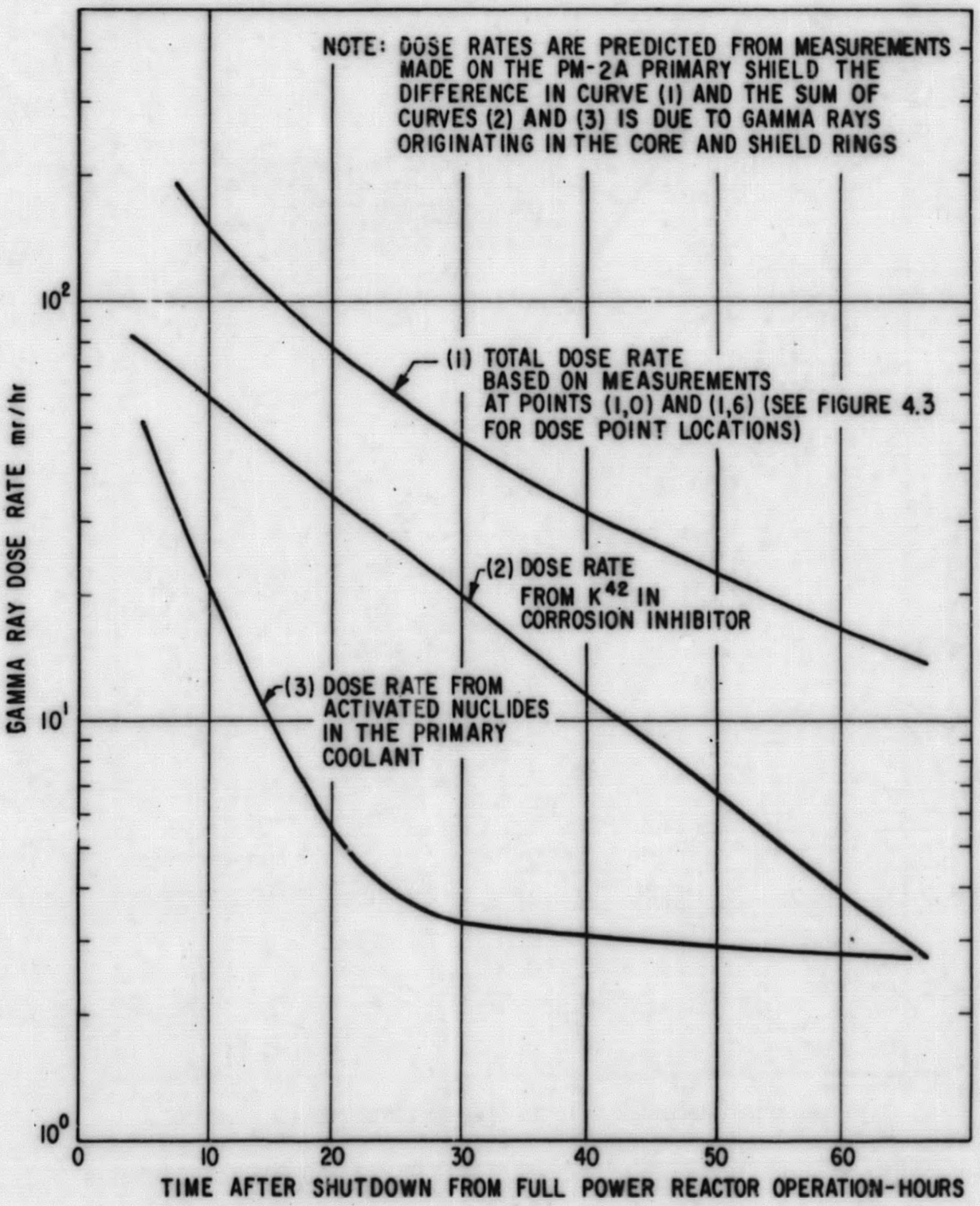

Figure 4.16. Gamma Ray Dose Rate Decay on PM-2A Primary Shield Following Shutdown from Full Power Reactor Operation

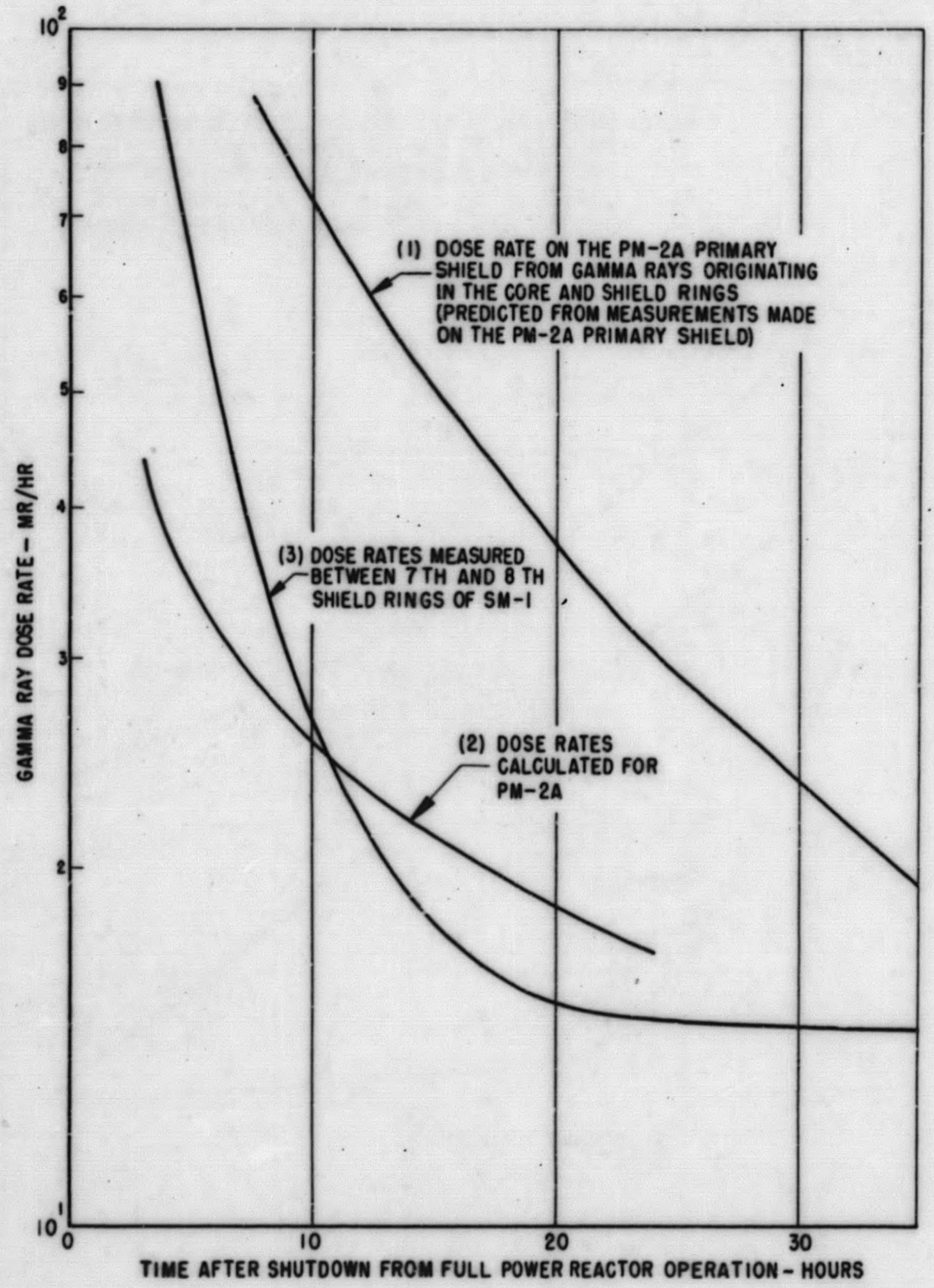

Figure 4.17. Comparison of Shutdown Dose Rates Predicted from Measurements on the PM-2A Primary Shield with Calculated Shutdown Dose Rates on the PM-2A Primary Shield and Measured Shutdown Dose Rates in the SM-1 Primary Shield

shield, the contribution to the total dose rate due to backscattering and sources at greater radial distances is negligible. Therefore, it was estimated that the dose rate on the PM-2A shield tank surface 2.5 hr after shutdown would be 50 mr/hr from the primary shield rather than the 110 mr/hr calculated by the machine program.

It appears that the results of the ROC code uncorrected to the SM-1 measurements more closely approximated measurements at the PM-2A. This will be considered in future uses of the ROC code.

More recent tests at the SM-1 indicate that operating gamma ray dose rates are higher by a factor of three than previous measurements.[6] A detailed analysis of data obtained from these tests has not yet been performed, however it appears possible that the magnitude of the difference between the ROC code calculations and measured SM-1 dose rates may have been overestimated.

The effectiveness of the lead added to the primary shield tank surface was observed by comparing the operating gamma ray dose rates before and after the shielding modification. These dose rates were normalized so that the same values were obtained in regions unaffected by the addition of the lead. In this manner, the effect of the modified corrosion inhibitor and variations in reactor operating history or power level was minimized. The reduction factor of from 0.09 to 0.17 is in agreement with the predicted attenuation of the operating gamma flux escaping the primary shield.

4.4.3 EVALUATION OF THERMAL NEUTRON FLUX CALCULATIONS FOR THE PM-2A PRIMARY SHIELD

Thermal neutron flux measurements on the primary shield are presented in Table 4.20. Foil locations for the primary shield survey are shown in Fig. 4.4. A thermal flux of approximately 2.2×10^5 n/cm^2 sec is uniformly distributed over the surface of the shield.

The neutron flux distribution through the primary shield tank was calculated using two-group diffusion theory.[3] The machine calculations yielded the following values for thermal and fast neutron flux on the surface of the primary shield tank. The difference in the magnitude of the thermal and fast neutron flux may be attributed to the presence of boral on the inner surface of the shield tank.

$$\phi_{th} = 1.62 \times 10^4 \ \frac{n}{cm^2\text{-sec}}$$

$$\phi_f = 3.38 \times 10^6 \frac{n}{cm^2\text{-sec}}$$

In order to properly evaluate the machine calculation, it is necessary to know what portion of the total thermal flux at the surface is due to thermal neutron leakage from the shield tank, and what part results from slowing of the fast flux in the snow walls and subsequent scattering back in the direction of the primary shield. This information could possibly be obtained by exposing foils which have cadmium covers on one side only (Ref table 4.38).

4.4.4 DETERMINATION OF DOSE RATES FROM ACTIVATED WATER ADDITIVES IN THE PM-2A PRIMARY SHIELD TANK AFTER SHIELD MODIFICATION

Measurements on the primary shield tank surface before shield modification demonstrated that there were higher than anticipated radiation levels on the surface following reactor shutdown. It was contended that Na^{24} contained in the corrosion inhibitor Nalco 39 was largely responsible for the higher radiation levels since that material was not accounted for in the original shielding calculations.(1) Upon modification of the PM-2A shield the Nalco 39 was replaced by a corrosion inhibitor containing potassium. The predicted dose rate contribution on the PM-2A primary shield due to the presence of potassium in the corrosion inhibitor was based on data obtained prior to modification of the shielding. These data were altered to account for the replacement of sodium by potassium in the corrosion inhibitor.

The surface dose rate from the activated corrosion inhibitor was due to the presence of radioactive Na^{24} in the Nalco. The dose from this activation was due principally to the activity contained in the last water gap of the primary shield (See Fig. 4.1). The thickness of the water gap is 6.825 in. and it is shielded by 3/8 in. of steel and 1/8 in. of boral (Ref Table 4.1). Na^{24} emits two gammas per disintegration. One has an energy of 2.75 Mev and the other has an energy of 1.37 Mev. Previous calculations(1) have shown that for Na^{24} the material properties of the shield are such that the surface dose rates were divided in the ratio of the two gamma energies. Consequently in order to minimize the errors due to uncertainties in the magnitude of the activating neutron flux and uncertainties in the selection of a geometrical model to approximate the actual source, the surface dose due to 1.37 Mev gammas was used to estimate the dose from the potassium inhibitor. The dose from the 1.37 Mev gammas was used to estimate the dose from the potassium inhibitor. The dose from the 1.37 Mev gammas from sodium is as follows:

$$D_{1.37} = (S_v)_{Na} (1.37)\, A(T, E) \qquad (2)$$

where: $(S_v)_{Na}$ = Na^{24} Activity

$A(T, E)$ = factor which accounts for attenuation of materials and effect of distance.

$(S_v)_{Na}$ for any reactor history is evaluated as follows:

$$(S_v)_{Na} = (S_{sat})_{Na} (1 - e^{-\lambda_{Na} T_{Na}})\, e^{-\lambda_{Na} t_{Na}} \frac{P_{Na}}{2000} \qquad (3)$$

where: $(S_{sat})_{Na}$ = saturated full power activity of Na^{24}

λ_{Na} = decay constant for Na^{24} = 0.0465 hr^{-1}

T_{Na} = operating time of reactor, hours

t_{Na} = shutdown time of reactor, hours

P_{Na} = operating power level of reactor, ekw

The surface dose due to the potassium inhibitor may be calculated in a similar manner. The only activation reaction of significance in elemental potassium is the K^{41} thermal neutron capture producing radioactive K^{42} with a 12.5 hr half life. K^{42} emits a 1.53 Mev gamma in 18% of its decays. The dose due to K^{42} is given by

$$D_K = (S_v)_K (1.53)\, B(T, E) \qquad (4)$$

$(S_v)_K$ is evaluated for any reactor history as follows:

$$(S_v)_K = (S_{sat})_K (1 - e^{-\lambda_K T_K})\, e^{-\lambda_K t_K} \frac{P_K}{2000} (0.18) \qquad (5)$$

Parameters in the above two equations are defined for K^{42} similar to the parameters of equations (2) and (3). The ratio of the dose rate from K^{42} to that of the 1.37 Mev gamma of Na^{24} is

$$\frac{D_K}{D_{1.37}} = \frac{(S_v)_K \;\; 1.53\, B(T, E)}{(S_v)_{Na} \;\; (1.37) \;\; A(T, E)} \qquad (6)$$

If no accounting is made for the 2 inches of lead placed on the shield surface during modification, the geometry assumed in the K^{42} dose equation will be identical with that assumed in the dose equation for the 1.37 Mev gamma. Material attenuation properties for a 1.37 Mev gamma are essentially the same for a 1.53 Mev gamma ray. Therefore, the factors which account for material attenuation and the effect of distance may be equated:

$B(T, E) = A(T, E)$. The ratio of the dose rates then becomes

$$\frac{D_K = (S_v)_K (1.53)}{D_{1.37} (S_v)_{Na} (1.37)} \tag{7}$$

Substituting from equations (2) and (4) we get

$$\frac{D_K}{D_{1.37}} = \frac{(S_{sat})_K \left(1-e^{-\lambda_K T_K}\right) e^{-\lambda_K t_K} P_K (0.18)}{(S_{sat})_{Na} \left(1-e^{-\lambda_{Na} T_{Na}}\right) e^{-\lambda_{Na} t_{Na}}} \tag{8}$$

The saturation full power activity for any isotope is $\sigma N \phi$

where σ = thermal activation cross section (cm^2)

ϕ = full power activating thermal neutron flux (N/cm^2 sec)

N = number density of the isotope (cm^{-3})

The ratio of the saturated activities of potassium and sodium is then

$$\frac{\sigma_K N_K \phi_K}{\sigma_{Na} N_{Na} \phi_{Na}}$$

The full power thermal activation flux will be the same for both isotopes. The ratio of the saturated activities then becomes

$$\frac{\sigma_K N_K}{\sigma_{Na} N_{Na}}$$

With the sodium replaced in equivalent atomic concentration with potassium the ratio N_K/N_{Na} is merely the ratio of the isotopic abundances of K^{41} and Na^{23}. K^{41} is present in the amount of 6.9% in natural potassium and has a thermal activation cross section of 1 barn. Na^{23} is of 100% isotopic abundance and has a thermal activation cross section of 0.53 barn. The ratio of the saturation activities is then

$$\frac{(1)\quad(.069)}{(.53)\quad(1.00)} = 0.13$$

The ratio of the dose rates then becomes

$$\frac{D_K}{D_{1.37}} = \frac{(1 - e^{-\lambda_K T_K})\, e^{-\lambda_K t_K} (P_K)\,(.026)}{(1 - e^{-\lambda_{Na} T_{Na}})\, e^{-\lambda_{Na} t_{Na}} (P_{Na})} \qquad (9)$$

By using the above relation, the dose rate on the surface of the shield tank due to replacing sodium with potassium may be determined if the dose rate of Na^{24} is known. From measurements taken before the shield modification the dose due to the 1.37 mev gamma of Na^{24} may be obtained. Table 4.14 shows the dose rate decay data on the surface of the primary shield tank before modification. Based on these decay data, it was assumed that Na^{24} was the source of the surface radiation [1] From Table 4.14 it is seen that a point (1.1) the total measured dose rate is 1000 mr/hr 9.25 hours after reactor shutdown. It was noted that dose rates due to Na^{24} are in the ratio of the two gamma energies. The surface dose due to 1.37 mev gammas only is then

$$D_{1.37} = \frac{(1.37)}{(1.37 + 2.75)}\,(1000) = 332 \text{ mr/hr}$$

The reactor history to which this dose pertains is for $T_{Na} = 10$ hr, $t_{Na} = 9.25$ hr, and $P_{Na} = 700$ KW(e). Substituting these numerical values into equation VIII we get

$$D_K = (.051)\ (1 - e^{\lambda_K T_K})\ (P_K)\, e^{-\lambda_K t_K} \qquad (10)$$

Eight hours after shutdown from 400 hours of full power operation, the anticipated value of the surface dose rate is:

$$D_K = 66 \text{ mr/hr}$$

Adjusting this value to account for the dose rate reduction resulting from the 2 inch thickness of lead on the primary shield surface gives a dose rate of 7 mr/hr.

Subsequent to the shield modification a dose rate measurement was made at point (1.1) on the primary shield 9 hr following shutdown from 387 hr of reactor operation at approximately 725 kw(e) (Table 4.27). This measurement may be compared with the calculated value if;

1. The measured value is multiplied by 1.14 to account for the difference in shutdown times.

2. The measured value is multiplied by 2.76 to extrapolate to a full power reactor operating history.

The dose rate at point (1.1) on the primary shield is 19.5 mr/hr based on altering the measured value as described above.

It thus appears that about 13 mr/hr at point (1.1) is due to sources other than the potassium in the corrosion inhibitor.

4.4.5 ESTIMATION OF DOSE RATE LEVELS ON THE PRIMARY SHIELD SURFACE ACTIVATED PM-2A PLANT COMPONENTS

Figure 4.18 illustrates the decay of activated Type 1030 carbon steel for various reactor operating histories. These curves are based on materials activation data of Bopp and Sisman.[7] Surface dose rates may be obtained from these curves by the following relationship:[8]

$$Da = \frac{\text{A fraction Specific Activity from Curve)} \times \rho \times \lambda}{C} \qquad (11)$$

Where Da = Specific dose rate mr/hr per unit thermal neutron reaction

ρ = Density of steel = 7.7 gm/cm^3

λ = Relaxation length for the given radiation within the steel-cm

C = Conversion factor - $\frac{\text{photons}}{\text{cm}^2 - \text{sec}}$ to R/hr

The above equation was developed for an infinitely large volume distributed source with no buildup. However since the activated materials encountered in the PM-2A are at most a few centimeters thick, these two

assumptions tend to cancel each other and the equation should yield a good approximation for the surface dose rates on these materials.

Each component in activated Type 1030 steel omits a gamma ray of about 1 Mev energy.[7] Based on this energy, the values for λ and C are:[9]

$$\lambda = 2.17 \text{ cm}$$

$$C = 5.2 \times 10^5 \ \frac{\text{photons/cm}^2 \text{ sec}}{\text{R/hr}}$$

The relationship between specific activity and specific dose becomes:

$$Da = 3.22 \times 10^{-5} \times \text{(Specific Activity from Curve)} \qquad (12)$$

The thermal neutron flux has been measured on the primary shield surface. These measurements are presented in Table 4.20 and the foil locations are shown in Fig. 4.4. A full power thermal flux of approximately 2.2×10^5 n/cm^2-sec was uniformly distributed over the primary shield surface. The size of the primary shield surface is large compared to distances from this surface to primary system components. Therefore it may be assumed that a uniform thermal flux field of 2.2×10^5 n/cm^2 sec exists in the vapor container in the vicinity of the primary shield.

With this assumption, the surface dose rate due to activated plant components is:

$$D = 3.22 \text{ (Specific Activity from Curve)} \ \frac{R}{hr} \qquad (13)$$

This relationship gives the surface dose rate following full power reactor operation. Reactor operating history and shutdown times are determined by the selection of an appropriate specific activity.

The surface dose rates for Type 1030 carbon steel for several reactor operating histories and at several times after shutdown are shown in Table 4.31.

Data from Bopp and Sisman [7] has also been used to calculate the surface dose rates for Type 304 stainless steel.

The surface dose rates shown were obtained using the factor 3.22 derived above and are presented in Table 4.31.

The surface dose rates listed in Table 4.31 indicate that for the full power thermal neutron flux which exists in the vicinity of the primary shield, no significant activation problem is present. Activated components contribute a negligible portion of the dose rates on the primary shield.

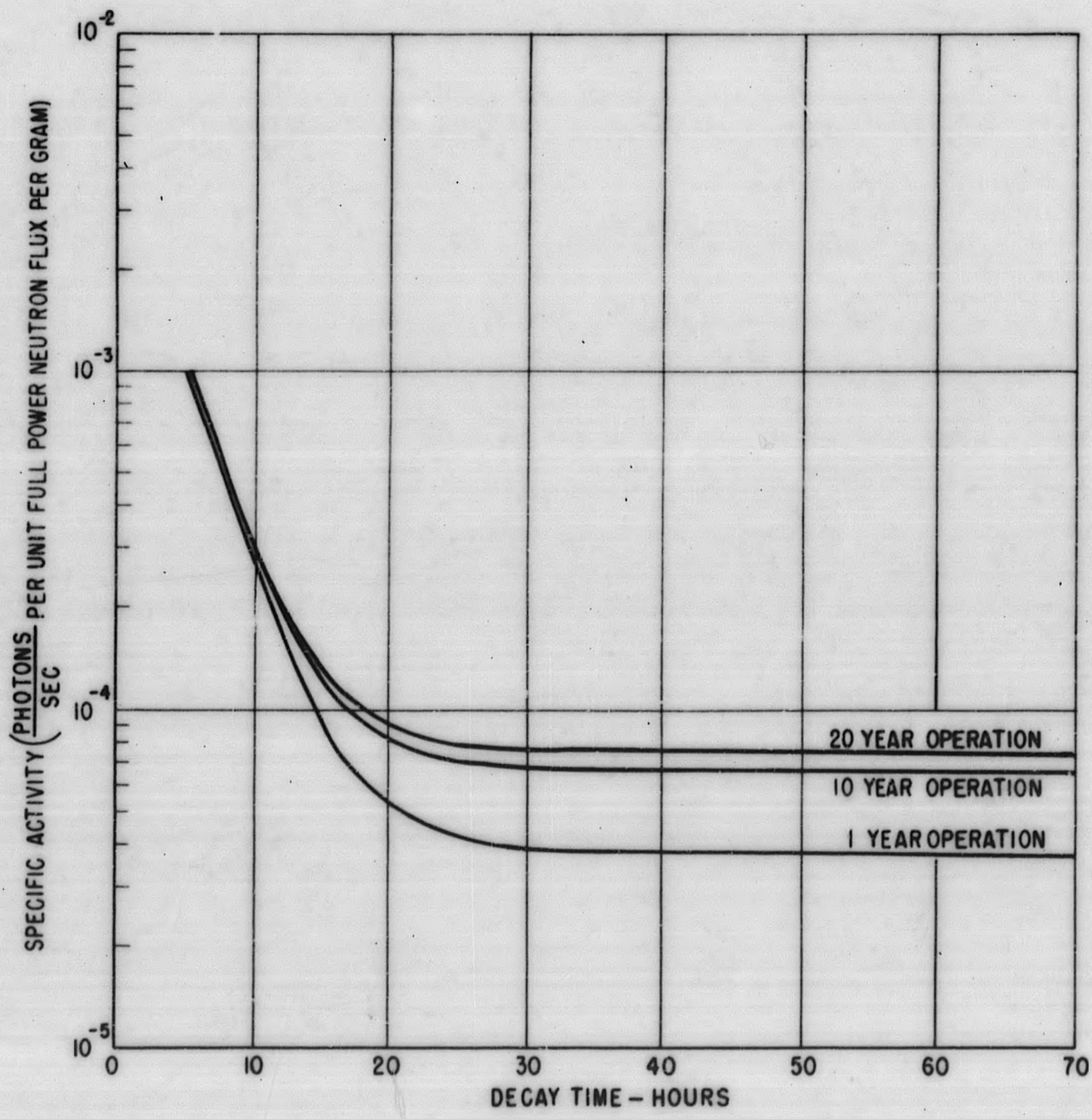

Figure 4.18. Decay of Activated Type 1030 Carbon Steel

TABLE 4.31

SPECIFIC ACTIVITY AND SURFACE DOSE RATES FOR TYPE 304 STAINLESS STEEL AND TYPE 1030 CARBON STEEL

Steel		Type 304 SS		Type 1030 CS	
Activation time, years	Shutdown time, hours	Specific Activity*	Surface Dose Rate** mr/hr	Specific Activity*	Surface Dose Rate** mr/hr
1	0	$9.52(10^{-4})$	6.76	$1.44(10^{-3})$	9.23
	8	$2.38(10^{-4})$	1.67	$1.91(10^{-4})$	1.42
	24	$1.51(10^{-4})$	1.07	$3.98(10^{-5})$	0.284
	36	$1.49(10^{-4})$	1.06	$3.78(10^{-5})$	0.268
10	0	$1.25(10^{-3})$	8.90	$1.46(10^{-3})$	9.91
	8	$5.42(10^{-4})$	3.85	$2.19(10^{-4})$	1.49
	24	$4.55(10^{-4})$	3.24	$6.78(10^{-5})$	0.484
	36	$4.52(10^{-4})$	3.21	$6.58(10^{-5})$	0.466
20	0	$1.35(10^{-3})$	9.61	$1.47(10^{-3})$	9.91
	8	$6.41(10^{-4})$	4.53	$2.28(10^{-4})$	1.56
	24	$5.53(10^{-4})$	3.92	$7.69(10^{-5})$	0.540
	36	$5.51(10^{-4})$	3.89	$7.49(10^{-5})$	0.540

* Specific Activity in $\left(\frac{\text{photons}}{\text{sec-gm - unit full power neutron flux}}\right)$

** For an activating flux of $2.2 \times 10^5 \frac{n}{cm^2\ sec}$

4.4.6 ESTIMATION OF DOSE RATE LEVELS ON THE PM-2A PRIMARY SHIELD SURFACE DUE TO ACTIVATED NUCLIDES IN THE PRIMARY SYSTEM

The contribution to the dose rate on the primary shield following reactor shutdown is estimated from measurements made at various points on the primary coolant system. The gamma dose rate measurements made within the PM-2A vapor container after reactor shutdown and subsequent to the shield modification are listed in Table 4.28. Of the dose point locations listed in this table, four were chosen as being representative of locations on the primary system piping. The radiation levels at these four locations were assumed to be due entirely to the presence of activated nuclides within the primary system piping. The dose points on the primary coolant piping were:

Primary coolant at outlet of reactor
Primary coolant at inlet to steam generator
Outlet of steam generator below primary coolant pump
Primary coolant pump discharge at shield tank

The dose rates at these locations were averaged in order to obtain a single set of dose rate decay data which is representative of the decay at several points within the vapor container. Also, by averaging these data, errors in the data are minimized. Table 4.32 presents these average dose rates normalized to the dose rate on the primary coolant pump discharge.

TABLE 4.32

Gamma Dose Rate Decay on PM-2A Primary System Components (Normalized to Dose Rate on Primary Coolant Pump Discharge)

Time after Shutdown (hr)	Average Dose Rate (mr/hr)
9.3	58
16.8	20
27.3	8.6
33.8	7.4
43.3	8.6
56.7	8.2
65.8	5.5
78.3	7.0

From Table 4.28, it is seen that a radiation field of from 5 to 13 mr/hr excluding localized extremes exists in the vapor container 9.3 hr after shutdown. The dose rate is somewhat higher near the primary coolant piping, steam generator and primary coolant pump. From the curve of the decay data for the averaged dose rates in Table 4.32, the dose rate 8 hr after shutdown was found by extrapolation to be a factor of approximately 1.2 higher than the dose rate 9.3 hr after shutdown. The decay data was obtained after a 387 hr reactor operation at an average power level of 725 ekw. As an estimate of the radiation field 8 hr after shutdown following full power operation, the dose rates were multiplied by the ratio

$$\frac{2000 \text{ ekw}}{725 \text{ ekw}} = 2.76$$

The estimated radiation field in the vapor container due to corrosion product activated nuclides in the primary coolant system was thus found to be from 16 to 43 mr/hr excluding localized extremes 8 hr after shutdown.

Surveys made on previous occasions at the SM-1 plant lead to the following conclusion:[3]

1. The dose rate from vapor container activation is small compared to the dose rate from deposited activated corrosion products.

2. A general radiation field exists in the SM-1 vapor container from activated corrosion products which gives a dose rate of about 30 mr/hr at 2.5 hr after shutdown and about 6 mr/hr at 24 hr after shutdown.

It may be noted from Table 4.27 that a non uniform gamma radiation field exists on the shield tank surface. This apparently results from the presence of the primary coolant pump, steam generator and primary system piping on that side of the primary skid. The primary coolant and deposited crud in these components constitutes a major source of radiation.

Dose measurements indicate that there is a high radiation area at point (2, 3). This is due to localized streaming through the primary shielding, or due to activated nuclides in the primary coolant.

4.4.7 COMPARISON OF MEASURED AND CALCULATED DOSE RATES ON THE PM-2A PRIMARY SHIELD TANK

The following is a summary of the Operating dose rate contributions to the full power gamma dose rate on the surface of the primary shield.

Contributing Source	Calculated Dose Rate (R/hr)
Core Gamma Rays (ROC Code)	73.8 (Par. 4.4.1)
Capture and Activation Sources Within the Primary Shield (ROC Code)	173.3 (Par. 4.4.1)
Total (Before Shield Modification)	247
Total (After Shield Modification)	25
Measured Values(R/hr)* - Scaled to full power operations	
Before Shield Modification	72-310 (Table 4.3)
After Shield Modification	30-40 (Table 4.18)

Dose Rates After Shutdown

The dose rates which were calculated in the previous sections for a shutdown time of 8 hr following infinite reactor operation at full power are summarized in the following table.

Contributing Source	Calculated Dose Rate after Shield Modification (mr/hr)
Core and shield tank (ROC Code)	2.8 (Par. 4.4.1)
Activation of Components	1 (Par. 4.4.5)
Activated Corrosion Products in Primary Coolant System	16 - 43(Par. 4.4.6)
Activated Corrosion Inhibitor	7 (Par. 4.4.4)
Total	27 - 54

Measured Values (mr/hr)**after Shield Modification 15 - 60 (Table 4.27)

*Range of dose rates on primary shield opposite core midplane in region affected by the addition of lead.

** Range of dose rates on primary shield opposite core midplane on surface of lead.

4.5 ANALYSIS OF THE GAMMA RAY DOSE RATE ON THE UPPER PLATFORM OF THE PM-2A REACTOR BUILDING

Radiation surveys made prior to shield modification at the PM-2A reactor site indicated that the radiation level on the upper platform above the spent fuel tank was greater than the desired objective of 100 mr/hr.

The effectiveness of the shielding modifications in reducing the radiation levels above the spent fuel tank was analyzed and compared to measurements made subsequent to these modifications.

The total dose rate on the upper platform consists of contributions from the following sources:

1. Gamma ray scattering off the tunnel snow wall.
2. Gamma rays from neutron capture by hydrogen in the tunnel snow wall.
3. Gamma rays from N^{16} in the primary coolant
4. Gamma rays from direct penetration from the reactor core.

An estimate of the magnitude of each of these contributing sources is contained in the paragraphs that follow.

4.5.1 ESTIMATION OF DOSE RATES FROM GAMMA RAY SCATTERING OFF THE TUNNEL SNOW WALLS

The contribution to the dose rate above the spent fuel tank due to scattering from the snow wall was estimated by:

1. Obtaining a gamma intensity distribution on the snow wall from film measurements made exterior to the vapor container in the dry cap region.
2. Assuming that the equation from Stephenson[10] for scattering from a thick slab applies.

This equation which gives the dose rate, I, due to scattering from a thick slab is:

$$I = I_o \frac{C}{X^2} \frac{3.015 \times 10^{23}}{\mu_1 + \mu_2 \frac{\cos\theta_1}{\cos\theta_2}} \frac{d\sigma}{d\Omega} \quad \text{(R/hr)} \quad (14)$$

where:

I and I_o must have identical units

C and X^2 must have identical units

μ_1 = Mass absorption coefficient for incident gamma rays - cm^2/gm

μ_2 = Mass absorption coefficient for scattered gamma rays - cm^2/gm

$\frac{d\sigma}{d\Omega}$ = Differential scattering cross section - cm^2

C = Area of scattering region-ft^2

I_o = Dose Rate (R/hr)-assumed constant within region.

θ_1 = Angle of radiation incident on snow wall with respect to the normal.

θ_2 = Angle of radiation scattered from snow wall with respect to the normal.

X = Distance from scattering point to detector point-ft.

Dose rate measurements on the surface of the wood shielding were projected, on the snow wall by extrapolating the line segments connecting the geometric center of the core and the detector positions. The geometric attentuation was accounted for by applying a $1/R^2$ factor. This was accomplished by simply drawing the lines connecting core center, dose point and snow wall on the appropriate scale drawing, and measuring distances along these ray lines.

The gamma ray measurements which were projected to the snow wall are listed in Table 4.22. The locations of these traverses are shown in Fig. 4.15

The gamma intensity distribution on the snow obtained from the projected measurements is shown in Fig. 4.19.

The region on the snow wall from which single scattering to a point 3 ft above the spent fuel tank can occur extends to about 2 ft above the vapor container midplane. Radiation scattered from below this region would be attenuated by the upper shield tank water.

Three regions of uniform source intensity were assumed, i.e.; 2.26 R/hr, 11.3 R/hr, and 22.6 R/hr. The area of each of these regions was obtained from Fig. 4.19. It was further assumed that each region could be approximated by a point source on the snow wall in the vertical plane through the detector point above the spent fuel tank. The point sources were located approximately 10, 4, and 2.5 ft above the core midplane for regions 1, 2, and 3, respectively.

The mass absorption coefficient used was $\mu = 0.07$ cm^2/gm for a 1 Mev gamma ray in water or snow.

Table 4.33 contains numerical values used with the scattering equation. Scattering data was obtained from Stephenson.[10]

TABLE 4.33

PARAMETERS FOR CALCULATING THE DOSE RATE ABOVE THE SPENT FUEL TANK FROM SCATTERING OF GAMMA RAYS OFF THE TUNNEL SNOW WALLS

Region	I_o R/hr	X ft.	C_2 ft	θ_{1_o}	θ_2	Total Angle of Scatter	E_1 mev	E_2 mev	μ_1	μ_2	$\frac{d\sigma}{d\Omega}$
1	2.26	18.5	157	41°	30°	134°	1	.24	0.07	0.13	0.85 (10^{-26})
2	11.3	22	122	34°	44°	134°	1	.24	0.07	0.13	0.86 (10^{-26})
3	22.6	25	15	32°	50°	134°	1	.23	0.07	0.13	0.84 (10^{-26})

The total dose rate due to scattering is the sum of the dose rates from each scattering region.

This calculation rendered a dose rate of 54.3 mr/hr during full power operation at a point 3 ft above the top of the spent fuel tank. Scattering from both walls was considered.

It is apparent from the geometrical model used that the dose rates would increase nonlinearly with distance above the surface of the upper platform. A dose point located on the surface would have a negligible contribution from

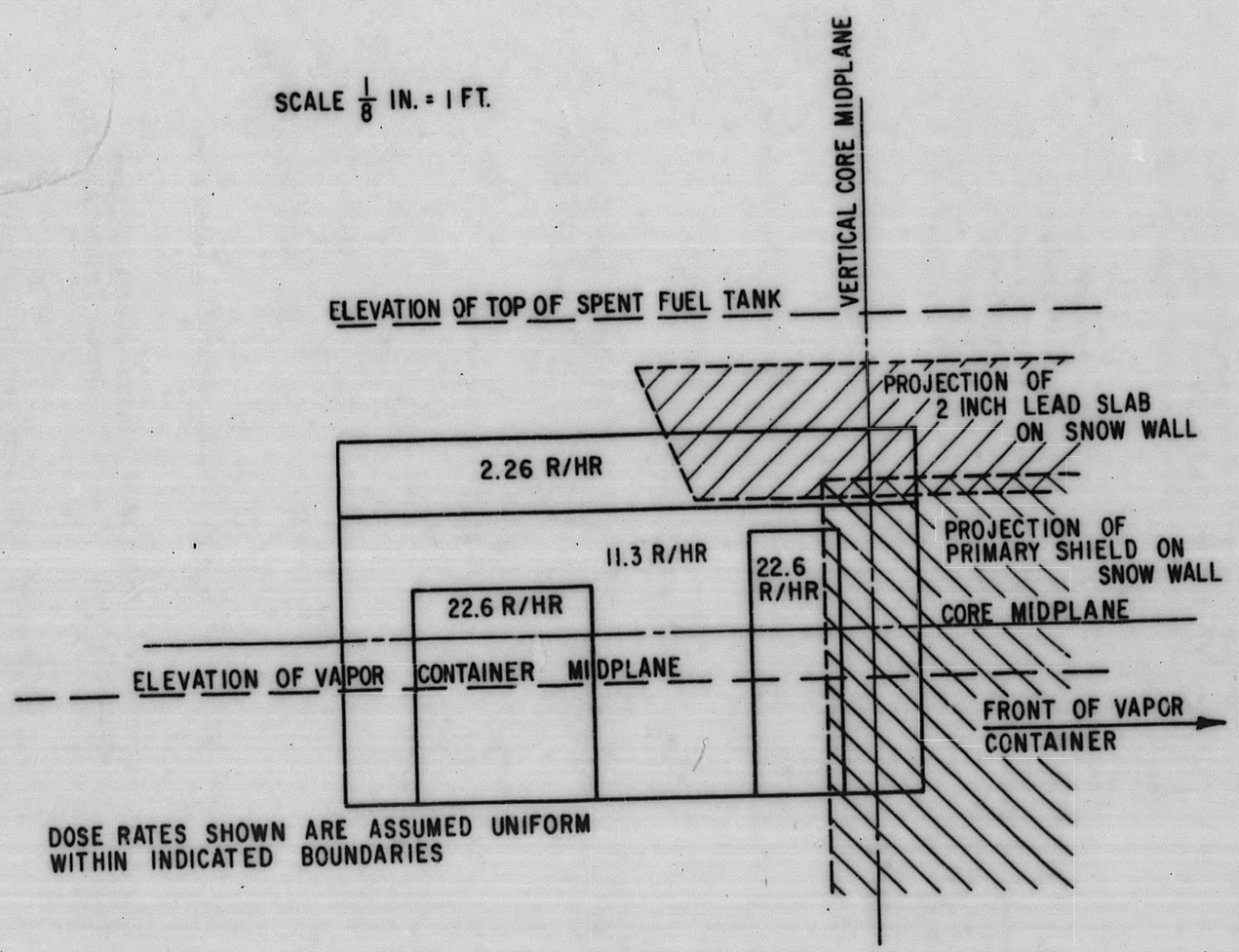

Figure 4. 19. Full Power Gamma Ray Dose Rate Distribution on the PM-2A Tunnel Snow Wall Predicted from Measurements Made on the PM-2A Vapor Container

single scattering from the snow walls. Very little of the scattering source would be visible to a detector at this location.

A detector located at a point 6 ft above the surface of the spent fuel tank can "see" the part of the snow wall which is above a point 4 ft below the vapor container centerline. In this case, the equation for thick slab scattering yielded a dose rate of 320 mr/hr.

The accuracy of the calculated values presented in this section is strongly dependent on the accuracy of the representation of the dose rate distribution on the snow wall. Therefore the flux distribution on the snow wall shown in Fig. 4.19 is at most, an estimation based on the available experimental data.

4.5.2 ESTIMATION OF DOSE RATES FROM NEUTRON CAPTURE IN THE TUNNEL SNOW WALLS

An estimation of the contribution to the dose rate above the spent fuel tank due to neutron capture in the tunnel snow wall was based on neutron measurements made subsequent to shield modification. These measurements were obtained on the vapor container exterior in the vicinity of the dry cap. Foil traverse locations are illustrated in Fig. 4.15.

The procedure for extrapolating the neutron flux data to the snow wall was the same as used to obtain the gamma dose rate distribution on the snow wall. The following assumptions were made:

1. An inverse square attenuation factor may be applied to the flux on the vapor container to obtain the flux on the snow wall.

2. The epithermal leakage from the vapor container is the same order of magnitude as the thermal leakage.

The thermal neutron traverses which were projected to the snow wall are listed in Table 4.23. Extrapolation of these data rendered the neutron distribution shown in Figure 4.20.

The attenuation of the neutron flux in the snow is approximately defined by

$$\phi = \phi_o \Sigma e^{-\Sigma X} \qquad (15)$$

where

ϕ = Neutron flux at distance x (cm) within the snow. - n/cm^2 sec

ϕ_o = Incident epithermal flux - n/cm^2 sec

Σ = Effective removal cross section - cm^{-1}

All neutrons incident on the wall are assumed to be captured with the emission of a 2.2 Mev gamma ray per capture. The gamma source distribution in the snow is therefore:

$$I = 2.2\ \phi_o\ \Sigma e^{-\Sigma X} \quad \frac{\text{Mev}}{\text{cm}^3\ \text{sec}} \tag{16}$$

The total emergent gamma flux at the surface of the snow is given by: (8)

$$S = 2\pi \int_0^{\infty} \int_0^{\pi/2} IG(R)R^2 \sin\theta\, d\theta\, dR \tag{17}$$

where:

$$I = 2.2\ \phi_o\ \Sigma e^{-\Sigma X} = 2.2\phi_o\ \Sigma e^{-\Sigma R \cos\theta}$$

$$G(R) = \frac{e^{-R/\lambda}}{4\pi R^2}$$

λ = Relaxation length for 2.2 Mev gamma ray in snow

The geometrical model used is shown below. A unit buildup factor is assumed in the calculation.

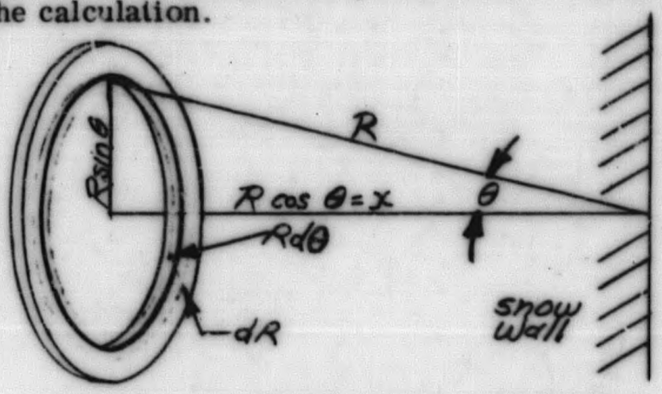

Geometry for Gamma Source Calculation

Integration of the above equation yields the following expression for the surface source strength. A factor of 2 has been included so that the expression will represent an isotropic surface source.

$$S = 2.2\ \phi_o\ \ln(1 + \lambda\,\Sigma)\ \frac{\text{Mev}}{\text{cm}^2\ \text{sec}} \tag{18}$$

The effective removal cross section for epithermal neutrons in water is approximately 0.1 cm^{-1}. [8] Assuming a snow density of 0.5 gm/cm^3, the removal cross section for the snow wall is approximately 0.05 cm^{-1}. The mass attenuation coefficient for 2.2 Mev gamma rays in water is μ = 0.047 cm^2/g [9]

Multiplying by the snow density yields a linear attenuation coefficient

$\mu = 0.0235\ cm^{-1}$. The relaxation length is therefore:

$\lambda = 42.6$ cm

Use of the above values for Σ and λ in the previously developed equation gives an expression which relates the gamma source strength on the snow surface to the epithermal neutron flux incident on the surface.

$$S = 2.5\ \phi_o \quad \frac{\text{Mev}}{\text{cm}^2\ \text{sec}} \tag{19}$$

Calculation of the dose rate above the spent fuel tank was done in the following manner:

1. A portion of the snow wall was divided into 22 sections each having an area of 22.5 ft^2. This region extended from the plane of the upper platform to the lowest point on the snow wall "visible" to a detector placed three feet above the spent fuel tank surface. This point is about 4 ft above the core midplane. In the horizontal direction, the region began at a point 15 ft behind the projection of the core axis and extended 18 ft forward of the projection of the core axis. The manner in which the snow wall was divided into sections is shown in Fig. 4.20.

2. An area averaged dose rate for each section was estimated using the flux distribution shown in Fig. 4.20 and the relationship between neutron flux and capture gamma source intensity previously developed.

3. Each section was approximated by a point source located in the geometrical center of the section.

4. Distances from the point source to the detector were calculated for each source, and an inverse R^2 attenuation factor was applied. The dose rate from one wall at the detector is the sum of the contributions from the 22 point sources, i.e.:

$$D = \sum_i \frac{Si}{R^2 i} \qquad (20)$$

From both walls

$$D = 2 \sum_i \frac{Si}{R^2 i} \qquad (21)$$

Table 4.34 shows values of R^2 and S for each section on the snow wall. The source strengths presented in this table are based on estimated full power epithermal neutron fluxes.

The calculated total gamma flux at the detector position is 1.81×10^4 Mev/cm^2-sec. A factor of 6.2×10^2 $\frac{\text{Mev/cm}^2 - \text{sec}}{\text{mr/hr}}$ was used to convert the 2.2 Mev gamma ray energy flux to a dose rate in mr/hr. The estimated full power dose rate 3 ft above the spent fuel tank due to neutron capture in the snow walls is:

$$D = 29.2 \text{ mr/hr}$$

This value is an estimate of the actual contributions from capture gamma rays in the snow wall. The greatest uncertainty occurs in the magnitude and distribution of the epithermal neutron flux on the snow wall.

4.5.3 RE-ASSESSMENT OF ANALYSIS OF N^{16} ACTIVITY IN PRIMARY COOLANT

During reactor operation, activation of the primary coolant results in all parts of the primary water system becoming severe gamma sources. This activity is due to the decay of N^{16} which results from the O^{16} (n,p) N^{16} reaction. The reaction has a threshold of 10.2 Mev.

The N^{16} activity of the PM-2A coolant was calculated in APAE-39[3]. As the primary water is activated in both the core and reflector it was necessary to determine the collided and uncollided flux in these regions. Values of the activating flux for neutron energies from 10 to 17 Mev were obtained with the use of Watt's semi-empirical relation for the fission spectrum: $f(E) = 0.48e^{-E} \sinh \sqrt{2E}$ [3].

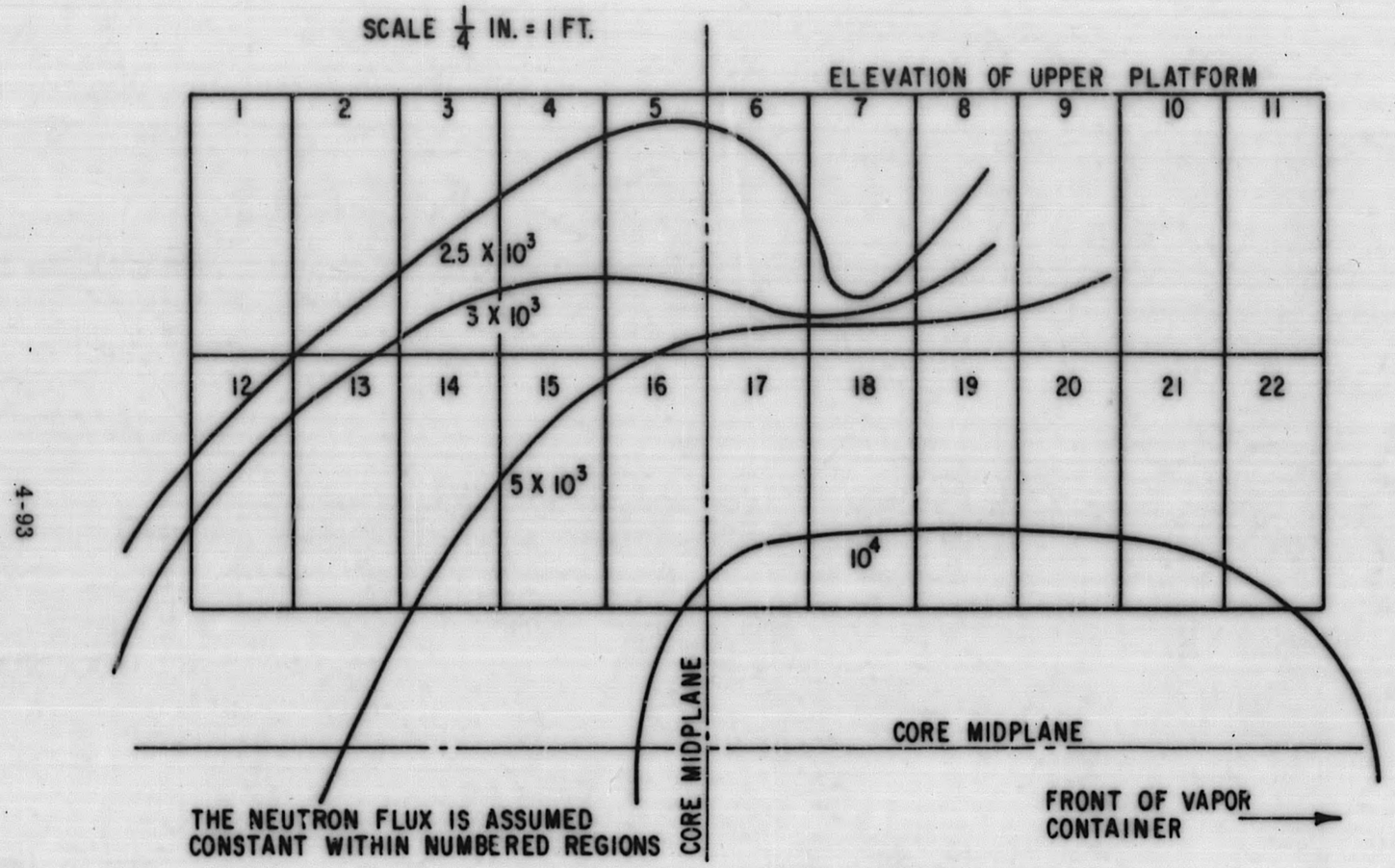

4-93

Figure 4.20. Full Power Epithermal Neutron Flux Distribution on the PM-2A Tunnel Snow Wall Predicted from Thermal Neutron Flux Measurements Made on the PM-2A Vapor Container

TABLE 4.34

PARAMETERS USED IN THE CALCULATION OF THE DOSE RATE ABOVE THE SPENT FUEL TANK FROM NEUTRON CAPTURE IN THE PM-2A TUNNEL SNOW WALLS

SECTION	S(Mev/cm^2 sec)	R^2(ft^2)
1	2.5 (10^3)	282
2	2.5 (10^3)	270
3	6.26 (10^3)	276
4	6.75 (10^3)	300
5	7.02 (10^3)	342
6	7.02 (10^3)	402
7	5.50 (10^3)	480
8	6.26 (10^3)	576
9	6.26 (10^3)	690
10	7.51 (10^3)	822
11	7.51 (10^3)	973
12	7.24 (10^3)	396
13	7.51 (10^3)	384
14	1.00 (10^4)	390
15	1.20 (10^4)	414
16	1.25 (10^4)	456
17	1.50 (10^4)	516
18	1.75 (10^4)	594
19	1.75 (10^4)	690
20	1.75 (10^4)	804
21	1.50 (10^4)	936
22	1.25 (10^4)	1087

The 0^{16} activation cross section used was $\Sigma_a = 4.274 \times 10^{-4}$ cm^{-1}. This calculation rendered a value of 4.098×10^6 disintegrations/sec-cm^3 of primary coolant.

A rough comparison was obtained from measured N^{16} activity and known coolant cycle times in the SM-1. From the scaling of the measured activity in the SM-1, the activity in the PM-2A would be 2.504×10^6 dis/sec-cm^3. This value is 39% lower than the calculated value, however, the secondary shielding calculations were based on the calculated value of 4.098×10^6 dis/sec-cm^3.

Calculation of the attenuation of N^{16} gamma rays was done by the RAS-1 code.[3] RAS-1 takes the source due to the N^{16} activity and attenuates it through shields within the vapor container and the secondary shield. To obtain the source geometry, the primary coolant piping and steam generator are divided into sections about one foot in length. These sources are then approximated by a point source at the center of these sections. The point sources are then located in a three-dimensional coordinate system. Essentially, the same setup is used to determine the shadow shields within the vapor container. The code input consists of the properties of the sources, piping, steam generator and other components in the vapor container. The points at which the dose rates are to be calculated are also included in the input.

The computer calculates the self absorption of the source, the attenuation due to the distance from the source to the selected dose point; and, if the gamma ray passes through a shadow shield, calculates the attenuation due to the intervening material. For secondary shielding, the machine code uses two shields of specified thicknesses for which the code computes slant attenuation and buildup. The dose rate at the selected dose point from all sources is summed by the machine which then prints the dose rate as output.

The method used to calculate the gamma dose rate from the primary coolant is described in RAS-I[11] and AP Note 63.[12]

Use of the RAS-1 code gave a dose rate value of 132 mr/hr at a point 36.2 ft above the axial centerline of the PM-2A vapor container. This value was chosen as a basis for comparison with PM-2A measured dose rates (See next section)

During the shielding task conducted at the SM-1, measurements were performed to determine the dose rate at various positions outside of the secondary shield [4]. In all cases, the dose rate calculated by RAS-1 was between a factor of 1.25 and 3 greater than the measured dose rate.

According to Ref. (11) the machine calculation has been checked against the STR Mark I shield test and the calculated dose rates were consistently higher than the measured dose rates. Therefore, the dose rate of 132 mr/hr at a point 36.2 ft above the axial centerline of the vapor container, calculated by the RAS-1 code, may be considered as a conservative (high) value.

4.5.4 EXTRAPOLATION OF CALCULATED N^{16} OPERATING DOSE RATES TO THE UPPER PLATFORM

Radiation surveys at the PM-2A before modification of the shield indicated that operating gamma dose rates on the upper platform were prohibitively high. Modification of the shield reduced the upper platform dose rates considerably. Operating gamma dose levels on that part of the platform to which access is desired during operation are now about 125/mr/hr. However, dose levels increase rapidly as one proceeds along the platform toward the front of the reactor building. Measured dose rates at points on the platform after shield modification are shown in Fig. 4.21. In that N^{16} activity of the primary coolant is a source of gamma radiation during operation, it is necessary to know the contribution this source makes to the platform dose levels.

In the PM-2A design analysis dose rates due to N^{16} activity were calculated at 33 locations.[3] Three dose points were chosen directly above the vapor container at an elevation 36.2 ft above the axial centerline of the vapor container. One of these dose locations is above the center of the vapor container, and the highest calculated N^{16} dose rate is at this location. A value of 132 mr/hr was estimated for this point. It is expected that this point will be a maximum, as it is almost directly above the steam generator. The steam generator has a relatively large water volume and is, therefore, a large source of N^{16} dose rate on the upper platform, it was assumed that all N^{16} activity is concentrated in a homogeneous right circular cylinder located at the position of the steam generator as shown in Fig. 4.21. The dose rate equation for a dose point on the midplane of a finite cylindrical source is

$$D = \frac{BS_v R_o^2 F(\theta, b_2)}{2(a + Z)} \qquad (22)$$

where:

B = Buildup Factor

S_v = Volumetric Source Strength - Mev/cm^3 sec

R_o = Radius of Cylinder - cm

a = Distance from surface of cylinder to dose point - cm

Z = Effective self-attenuation distance - cm

$\theta = \tan^{-1} \dfrac{h}{2(a + Z)}$ where h = height of cylinder.

b_2 = Total number of relaxation lengths of shielding (including self-attenuation)

$$F = (\theta, b_2) = \int_0^{\theta} e^{-b_2 \sec \theta} \, d\theta$$

The source material is water and a source attenuation coefficient of .0275 cm^{-1} is used.

Using the above equation to calculate the dose rate on the cylinder midplane at a point 36 ft away, the following values are applicable:

$\theta = 11.25^{o}$

$b_2 = .29$

$F(\theta, b_2) = 1.4 \times 10^{-1}$

$B = 1.25$

$a = 36$ ft

$z = 0.346$ ft

Substituting, we get

$$D_{36} = S_v R_o^{2} (2.4 \times 10^{-3}) \qquad (23)$$

For calculating the dose rate at a point on the cylinder midplane at the upper platform 18.5 ft. away, applicable values are as follows:

$\theta = 21.25^{o}$

$b_2 = .29$

$F(\theta, b_2) = 2.7 \times 10^{-1}$

$B = 1.25$

$a = 18.5$ ft

$z = 0.346$ ft

Again substituting we get

$$D_{18.5} = S_v R_o^2 \ (8.95 \times 10^{-3}) \tag{23}$$

S_v and R_o are constants. The ratio of the two dose rates is then

$$\frac{D_{18.5}}{D_{36}} = \frac{8.95 \times 10^{-3}}{2.4 \times 10^{-3}} = 3.7 \tag{24}$$

The previously calculated value of D_{36} is 132 mr/hr. The N^{16} dose on the upper platform directly above the steam generator is then 490 mr/hr. This is obviously a conservative estimate which may be considered a maximum value for N^{16} dosage at the platform.

In Fig. 4.21 it is shown that the measured gamma dose rate above the steam generator on the upper platform is 4100 mr/hr after shield modification. The access area is well removed from N^{16} sources and intervening material shields this area from such sources.

The point on the upper platform directly above the spent fuel tank is approximately 32 ft from the geometric center of the assumed cylinderical source. The materials encountered by a gamma ray directed toward the upper platform above the spent fuel tank are approximately 16 ft of water and 4 ft of wood. The attenuation due to 16 ft of water alone is on the order of 10^{-6}. Therefore the N^{16} contribution to the dose rate above the spent fuel tank is negligible.

4.5.5 ESTIMATION OF DOSE RATES ON THE UPPER PLATFORM OF THE PM-2A REACTOR BUILDING DUE TO DIRECT GAMMA RAY PENETRATION FROM THE CORE

The direct beam gamma dose rate on the upper platform of the reactor building prior to shield modification were calculated in AP Note 316[1] These dose rates were found to contribute a negligible fraction of the total dose rates on the platform before shielding modification. Since the direct beam dose rates on the upper platform are unaffected by the modifications, the analysis presented in AP Note 316 is also applicable after the shielding modification.

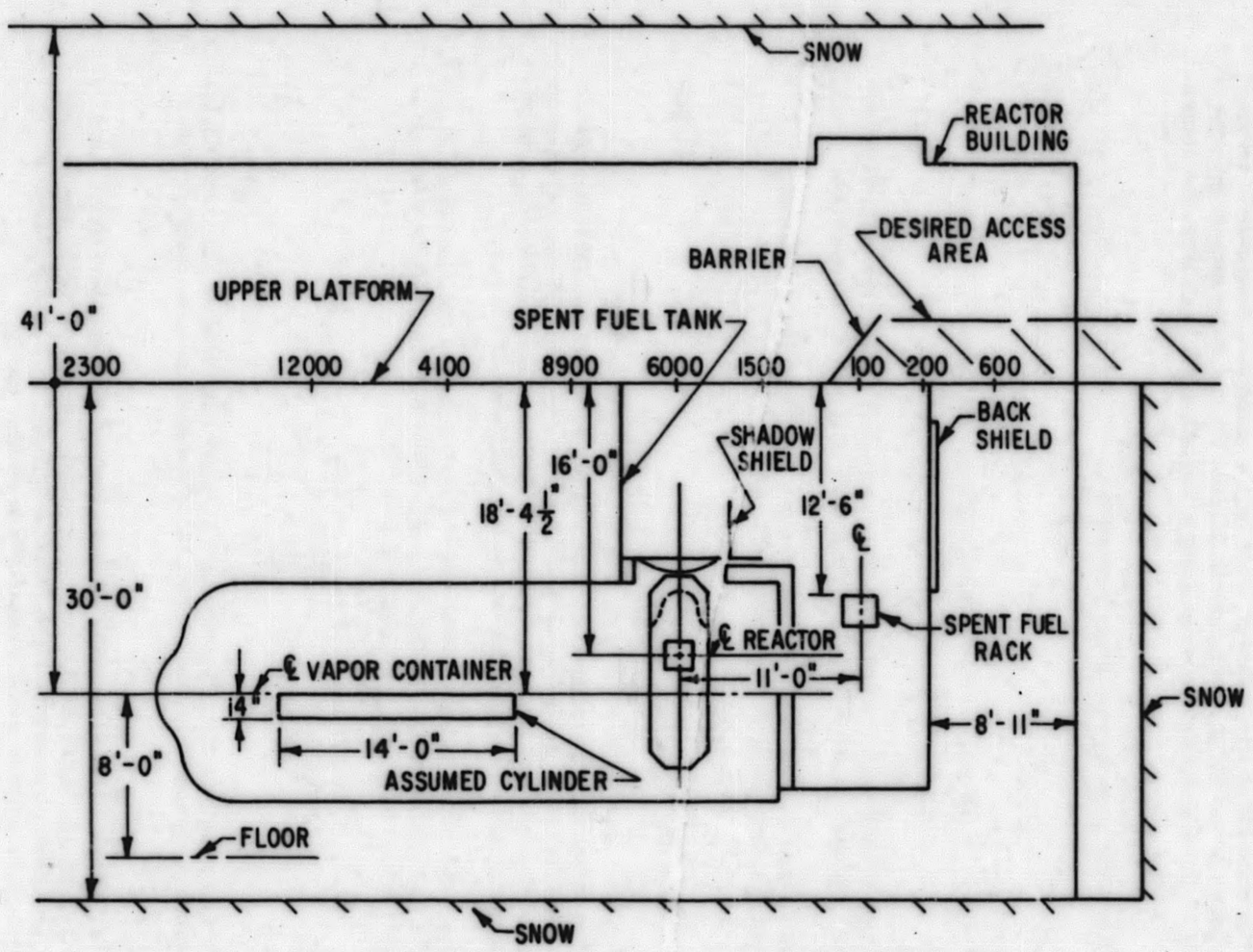

Figure 4.21. Full Power Operating Gamma Ray Dose Rate on the Upper Platform in the PM-2A Reactor Building

The calculation was based on altering the measured dose rate[4] on the top surface of the SM-1 shield tank to account for the difference in the materials in the PM-2A encountered along a "line of sight" ray from the center of the core.

The point geometry equation was used.

$$D = \frac{S_a A(T, E)}{4 \pi R^2} \tag{25}$$

where S_a = Gamma ray source strength - Mev/sec

R = Distance from source point to detector - cm

and attenuation due to materials is expressed as A (T, E), i.e. a function of both the gamma ray energy and the thickness of a specified material.

For equal source strengths and gamma energies, the relationship between the dose rates at two points is:

$$\frac{D_1}{D_2} = \frac{A(T_1)}{A(T_2)} \frac{(R_2)^2}{(R_1)^2} \tag{26}$$

The full power operating dose rate at the surface of the SM-1 upper shield tank has been measured to be 232 mr/hr.[4] The distance between the center of the core and the water surface is 202 in. The thicknesses of intervening materials are equivalent to a water thickness of 221 in.

Since the full power operating source strengths and the core gamma spectra are essentially identical in the SM-1 and PM-2A, PM-2A dose rates may be found from the SM-1 measured value by

$$D_1 = 232 \frac{A(T_1)}{A(221)} \frac{(202)^2}{R_1^2} \text{ mr/hr}$$

In this equation, the unknown quantities are the distance, R_1, and equivalent water thickness between the PM-2A core center and the distance dose point.

The values, A(T), are obtained from curves of attenuation (for 7 Mev gamma rays) vs. water thickness. A preponderance of the dose penetrating to the positions of interest arises from the prompt (n, γ) reactions in steel which produce capture gamma rays of 6 to 10 Mev energy.

The use of this technique whereby the measured dose is perturbed by differences in intervening materials allows an expedient solution, and it reduced any error involved with the uncertainty of the source strength.

The equivalent water thicknesses for the materials between source point and dose points were obtained from the following relationship:

$$T_{water} = \frac{(\rho\mu)_{material}}{(\rho\mu)_{water}} T_{(material)} \qquad (27)$$

where:

T = thickness (cm)

ρ = density (gm/cm^3)

μ = mass attenuation coefficient for 7 Mev gamma rays (cm^2/gm)

The use of this equation implies the assumption that the ratio of the buildup factors is essentially unity for the materials and relaxation length of interest.

TABLE 4.35

WATER EQUIVALENCE FACTORS USED
IN CALCULATING THE DOSE RATE ON THE UPPER PLATFORM
DUE TO DIRECT GAMMA RAY PENETRATION

Material	T(water) T(material)
Core	2.2
Core water	0.8
Steel	6.95
Lead	11.47
Snow	0.6
Wood	0.5

Data for the dose points on the surface of the shield tanks are contained in Table 4.36.

TABLE 4.36

MATERIALS ENCOUNTERED ALONG RAYS CONNECTING THE PM-2A CORE CENTER AND DOSE POINTS ON THE UPPER PLATFORM

Dose Point Location	R (Inches)	X (feet)	Core	Vessel Water	Steel	Lead	Water	Snow	T (inches)
Top of stairs on back of snow barrier	192	0	11	22	1.5	0	126	0	188
Rear door of reactor building	226	10.9	13	22	6	4	148	0	282
Above spent fuel rack	336	23.2	15	11	9	0	157	0	263
Above reactor	624	49.2	11.5	9	6	5	136	276	437
SM-1	202	0	11.5	48	3.25	0	134	0	221

where: R = distance from source point to dose point.

X = horizontal distance from core axis to dose point.

T = equivalent water thickness between source point and dose point.

The results of this analysis are plotted in Fig. 4.22. The full power dose rate at the point of interest directly above the spent fuel tank is approximately 3 mr/hr due to direct penetration from the core.

4.5.6 COMPARISON OF ESTIMATED AND MEASURED GAMMA RAY DOSE RATES ON THE UPPER PLATFORM OF THE PM-2A REACTOR BUILDING

The following is a summary of calculated contributions to the gamma ray dose rate at a point approximately 3 ft above the PM-2A spent fuel tank. Calculated and measured values obtained both before and after shield modification are presented for comparison. Estimated dose rates applicable to the unmodified shield were obtained from AP Note 316.(1)

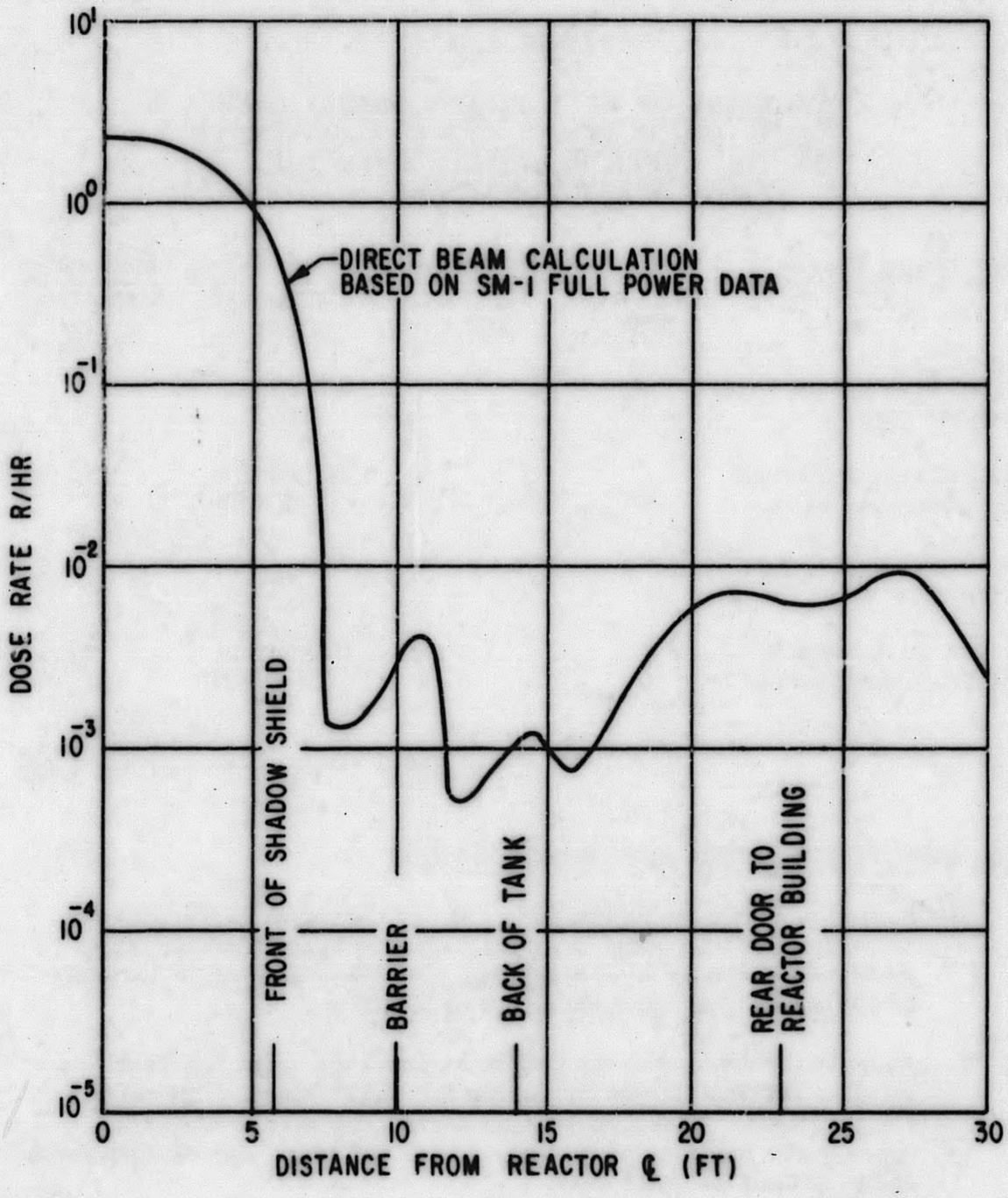

Figure 4.22. Calculated Gamma Ray Dose Rate on the Upper Platform in the PM-2A Reactor Building Due to Direct Penetration from the Reactor Core

TABLE 4.37

SUMMARY OF FULL POWER GAMMA DOSE RATE CALCULATIONS AND MEASUREMENTS ON THE UPPER PLATFORM OVER THE PM-2A SPENT FUEL TANK

Contributing Source	Before Shield Modification		After Shield Modification	
	Calculated, R/hr	Measured R/hr	Calculated, mr/hr	Measured, mr/hr
Direct Penetration from the core	0		3 (Section 4.5.5)	
Gamma rays scattered off of the snow walls	9		54 (Section 4.5.1)	
Captured gamma rays in the snow walls	13		29 (Section 4.5.2)	
Gamma rays from N^{16} in the primary coolant	0		0 (Section 4.5.4)	
Total	22	60(Table 4.6)	86	100-200 (Table 4.22)

4.6 CONCLUSIONS AND RECOMMENDATIONS

1. Radiation levels measured show that an individual can work an 84 hr week in PM-2A Plant in areas requiring access. The values measured indicate that the reactor operating crew would normally be subjected to an exposure of 20 to 30 mr/wk.

2. Radiation levels in the working area above the spent fuel tank are between 100 and 200 mr/hr during full power reactor operation i.e., 10 Mwt. These values will permit limited access to the upper spent fuel tank platform to check and adjust the building level and to unload the spent core.

3. Dose rate measurements made within the vapor container indicate the radiation level will be from 4 to 60 mr/hr, 8 hr after shutdown following full power reactor operation, i.e., 10 Mwt. This will permit safe access to the vapor container for operating and maintenance duties.

4. The effect of the boral cladding on the primary shield rings cannot be estimated with any certainty from the available data.

The following information is presented in support of this contention:

A. The measured shutdown gamma dose rates on the primary shield tank surface were extrapolated to full power and corrected to account for the presence of sources other than the core and steel shielding. These corrected dose rates were approximately a factor of three higher than both the dose rates measured at a corresponding position in the SM-1 and the machine calculated dose rates for the PM-2A as modified to account for past experience gained at the SM-1. However the PM-2A measurements scaled to full power were in fair agreement with the unmodified machine calculated dose rates.

Recent shielding tests at the SM-1 have rendered dose rates which are approximately a factor of three higher than those previously measured. Further analysis of SM-1 primary shield test data should provide a comparison of SM-1 and PM-2A dose rates.

B. The activation of long-lived components in the steel shielding had not reached saturation during the 400 hr of operation after which the dose rate measurements were obtained. As the buildup of these activities progress it may be possible to isolate this contribution to the total dose rate on the primary shield surface.

5. A need for additional experimentation exists. The radiation measurements recommended in Table 4.38 are intended to complement the existing data. These measurements should serve to:

A. Further evaluate the accuracy of existing design methods.

B. Define areas for potential improvement in the PM-2A shielding

TABLE 4.38

RECOMMENDED ADDITIONAL RADIATION MEASUREMENTS FOR THE PM-2A

Location	Type of Measurements	Purpose
Primary Shield Tank Surface	1. Thermal neutron current 2. Epithermal neutron leakage. 3. Gamma ray energy and angular distribution	Provide data for evaluating effectiveness of boral cladding in primary shield.
	4. Periodic neutron and gamma ray flux measurements.	Insure continued adequacy of Primary shielding by following buildup of fission product and materials activation.
On Snow wall	1. Thermal and epithermal neutron flux mapping of snow wall (Before and after shaving the snow wall)	Provide a firmer estimate of the contribution to the dose rates on the upper platform due to gamma scattering and neutron capture in the snow.
	2. Thermal and epithermal neutron current at snow wall.	
	3. Gamma ray mapping of snow wall	
On Upper Platform of reactor building	1. Gamma dose rate as a function of height above the platform	Identify the radiation sources contributing to the dose rate on the upper platform.
	2. Gamma ray energy and angular distribution.	
In Snow Wall	1. Gamma ray and neutron dose rates as a function of snow thickness	Evaluate snow attenuation data to verify the behavior of snow as water having a reduced density.

4.7 REFERENCES (SECTION 4)

1. Coombe, J.R. et al, "PM-2A Shielding Problem and the Solution," AP Note 316, Alco Products, Inc., December, 1960.

2. Code of Federal Regulations, Title 10, Atomic Energy, Chapter 1, Part 20.

3. "Design Analysis of a Prepackaged Nuclear Power Plant for an Ice Cap Location," APAE No. 39, Alco Products, Inc., January, 1959.

4. Rosen, S.S., "APPR-1 Shielding Experiments and Analysis," APAE No. 35, October, 1958.

5. Rosen, S.S. et al, "Primary Shield Calculations on the IBM 650 (ROC CODES)," APAE Memo No. 142, October, 1958.

6. Moote, F.G., Obrist, C.H., "Shielding Measurements at the SM-1 Reactor (June 1961)," Alco Products, Inc. APAE-35 Supplement 2, March 16, 1962.

7. Bopp, C.D. and Sisman, O., "How to Calculate Gamma Radiation Induced in Reactor Materials, "Nucleonics Vol. 14, No. 1, January, 1956

8. Glasstone, S., "Principles of Nuclear Reactor Engineering," D. Van Nostrand Co., Inc., Princeton, N.J., 1955.

9. Rockwell, Theodore, "Reactor Shielding Design Manual," USAEC, March 1960.

10. Stephenson, R., "Introduction to Nuclear Engineering," McGraw-Hill Book Co., Inc., New York, 1954.

11. Czapek, E. et al, "Gamma Shield Design for Primary Coolant Sources Using the IBM Type 650 Computer, RAS-I, "Electric Boat Div. of General Dynamics Corp., September, 1956.

12. Rosen, S.S., "Supplement to RAS-I," AP Note 63, Alco Products, Inc., June 1957.

5.0 THERMAL AND HYDRAULIC TESTING AND ANALYSIS

Four test procedures were conducted in order to furnish data on the thermal and hydraulic behavior of the primary system for checking design methods and calculations, and for developing improvements in the design and operating procedures. These tests consisted essentially of taking certain portions of the basic startup and checkout procedures and expanding these to include more data. Also included were oscillograph recordings of major variables during rapid transient tests.

The four test procedures were -

C-603 Primary System Warm-up

C-602 Primary System Thermal Survey - Steady State Operation

C-601 Load Transient Test

C-604 Decay Heat Removal System Test

Because of the urgent need to put the power plant into regular operation as quickly as possible, approval for this increase in the scope of the acceptance test was obtained on the basis that this would not cause any delay in the primary objective of fulfilling contract tests.

Because of the problem encountered with the shielding, it was not possible to perform the 400-hr run of the acceptance test directly following the initial checks at full camp load in November, 1960, as originally planned. A representative set of data for the steady state thermal survey was obtained during a 10-hr run on November 21-22, 1960, as well as some data on the response to a loss of flow in the primary loop. These earlier results are incorporated with those from the final tests which were run in February 1961.

The following is a summary of the PM-2A testing that provided data for the C-600 series of test procedures described above.

Date	Plant Operation	Test
Nov. 5, 1960	Primary System Pressure Check	TP-C603
Nov. 8, 1960	1 hr of plant Operation	TP-C603 TP-C602

Date	Plant Operation	Test
Nov. 21-22, 1960	10 hr of Plant Operation	TP-C602 TP-C604
Feb. 8-26, 1961	400 hr of Plant Operation	TP-C603 TP-C602
March 7, 1961	Transient T&H Test Data Taken	TP-C601
March 7-8, 1961	Decay Heat Data Taken	TP-C604

5.1 PM-2A PRIMARY SYSTEM WARM-UP TEST (TP-C-603)

This test is intended to establish an understanding of the thermal and hydraulic behavior of the primary system as it is brought up to operating temperature and pressure. Power input rates for the reactor core and the pressurizer, associated pressurizer temperature and pressure, and response of flow rate to loop temperature are among the variables observed.

5.1.1 GENERAL TEST PROCEDURE AND OPERATING CONDITIONS

In order to pressure test the primary system connections and fittings after reassembly at the site, the pressure was first brought up to design value while the primary loop temperature was maintained at 225 to 253°F. Subsequently the primary loop was brought up to its operating temperature of 500 to 516° F. The second heat-up before the shielding revisions, as well as the two which followed it, were performed in the normal manner, with pressurizer and loop temperatures raised simultaneously.

Direct indication of primary loop flow rate is not provided by the standard PM-2A plant instrumentation. Initially, auxiliary equipment in the form of a milliampere ammeter was provided to measure the flow signal transmitted to the Btu/hr meter. This was initially set for 50 milliamp full scale at a flow tube differential of 200 in. of water. The primary system is equipped with a Gentile flow tube (see Fig. 5.1) for measuring flow rate. The differential pressure from this tube is connected to a differential pressure (DP) cell whose transducer's output signal is used for the low flow scram and for the flow rate input to the Btu/hr meter. Subsequently, for convenience, the output of the DP cell (without square root treatment) was connected directly to the actual panel indicating instrument of the Btu/hr meter (see Sec. 5.3.3). Fig. 5.2 shows the relationship of the ammeter signal to flow and Fig. 5.3 shows the relationship between the ammeter signal and meter scale reading.

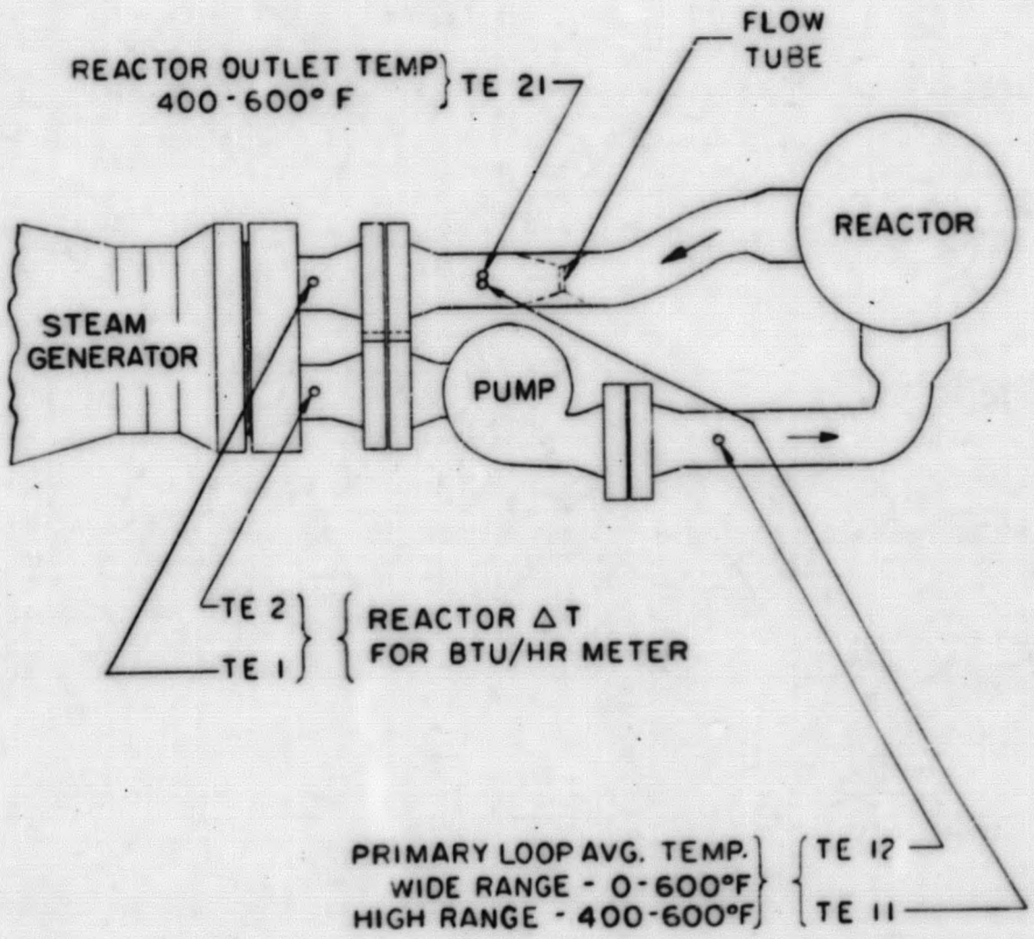

Figure 5.1. Schematic of PM-2A Primary Loop Temperature and Flow Instrumentation

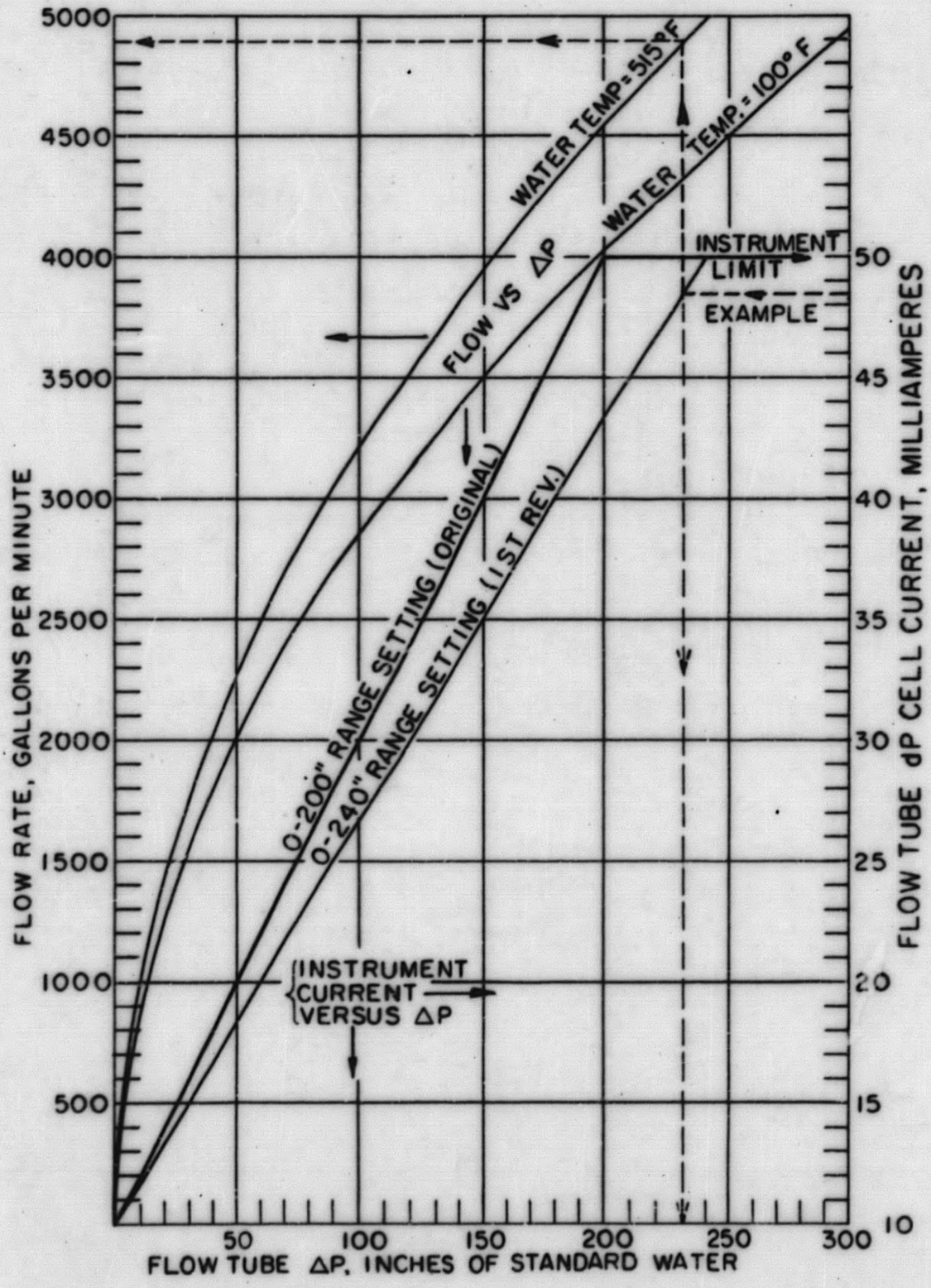

Figure 5.2. Calibrations of Primary Loop Flow Measuring Equipment for the PM-2A

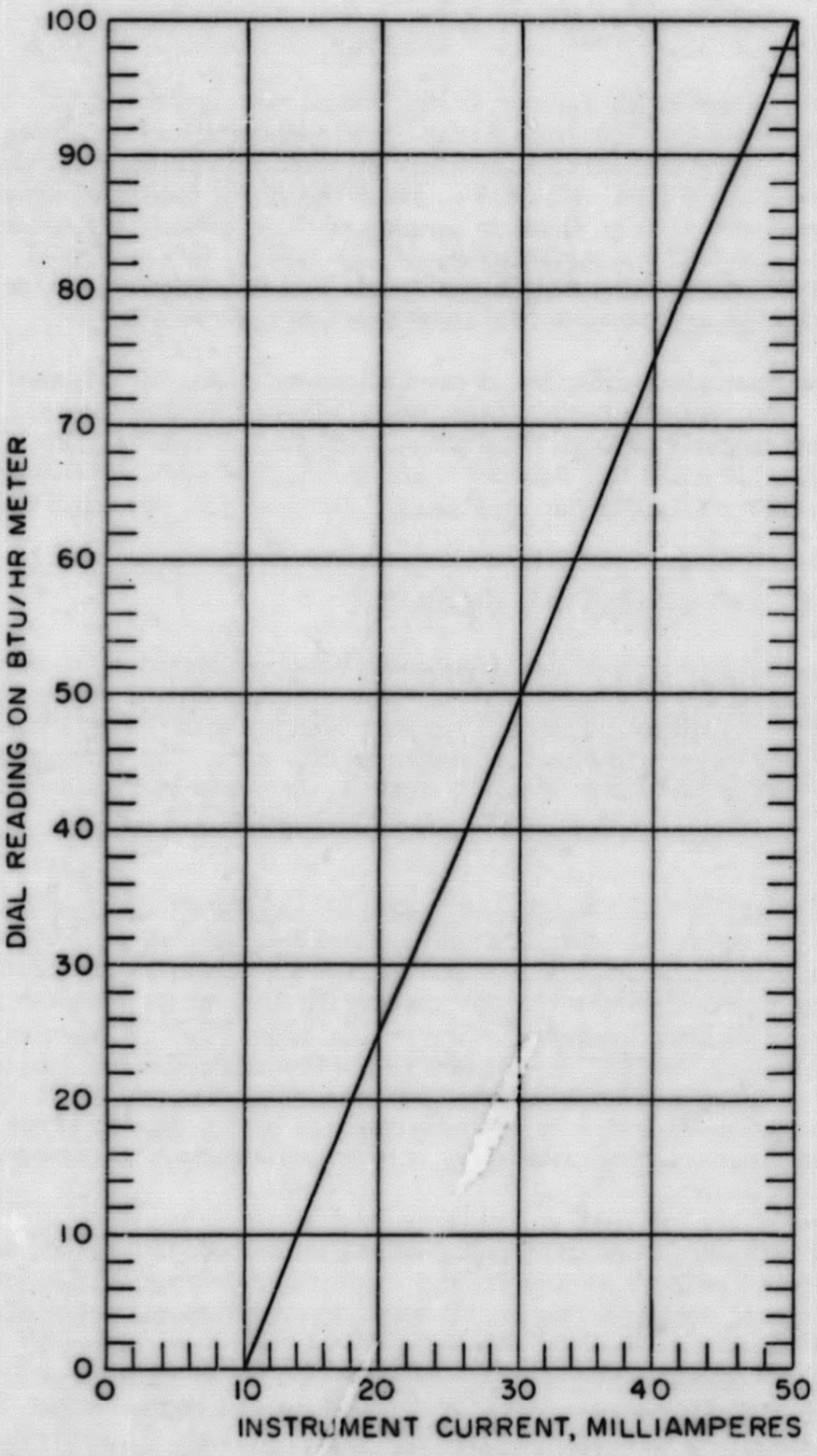

Figure 5.3. Relationship of Reading on Btu/hr Meter to Instrument Current, when dP Cell Output is Wired Directly to the PM-2A Control Console Indicator

Power output of the reactor during initial heat-ups could only be measured by the Log N nuclear instrument since the temperature rise across the reactor is too small to be measured accurately by plant instrumentation which has a tolerance of $\pm 3^{o}$ F (Ref. Sec. 5.3). Since the Log N meter measurements are a relative rather than an absolute measurement of power, subsequent calibration by the thermal instrumentation, at high power, was required. During power operations, output of this reactor is measured by the Btu/hr meter, which indicates a product of loop flow rate and reactor ΔT_o .

Primary system pressure is maintained by manual or automatic control of the water temperature in the pressurizer. During system heat-up it is necessary to use manual control. The water is heated by twenty 1-kw, 110 to 120-volt heaters, divided into 5 banks, each having four series-connected heaters with 440-480 volts applied to each bank. Current flow per bank was measured.

5.1.2 EXPERIMENTAL RESULTS

The graphic presentation of the initial heat-up in which the pressurizer alone was first brought to operating temperature is shown in Fig. 5.4 (Heat up #1 - Nov. 5, 1960). The primary loop was heated at constant pressure on Nov. 8, 1960 (Heat up #2) and is shown in Fig. 5.5. The subsequent composite heat-ups of the entire primary system are shown in Fig. 5.6, (Heat up #3 Nov. 21, 1960), 5.7(Heat up #4 Feb. 7, 1961) and 5.8 (Heat up #5 - Mar. 4-5, 1961).

In the second heat-up (Nov. 8, 1960) the primary loop flow rate was measured at 4870 gpm at 455^{o} F coolant temperature, increasing to 4890 gpm at design operating temperature (500^{o} -514^{o} F). The DP cell was set at 240 in. of standard water at 50 ma for the second heat-up as shown in Fig. 5.5. Final design calculation rates[1] were 4570 gpm at 500^{o} F inlet temperature and 4475 gpm at 70-100^{o} F. Review of the test setup used during the pump acceptance tests indicates that the test performance curve for the pump,[2] on which the as-built flow rate prediction was based, was in error. Accordingly, the measured high flow rates are credible and are believed correct (see Sec. 5.3).

This difference between predicted and measured flow rates, combined with the effect of high coolant density, generated flow signals in excess of the instrument range setting for all coolant temperatures below 455^{o} F even after the range setting of the flow tube DP call had been changed from 200 to 240 in. The operating crew concluded that 250 in. of water was the upper cell limit and adjusted the cell to this value for full signal output. When the plant was started up again (#3 heat-up, Fig. 5.7, Feb. 7, 1961) the indicated flow rate was even higher than during the November operations. At the end

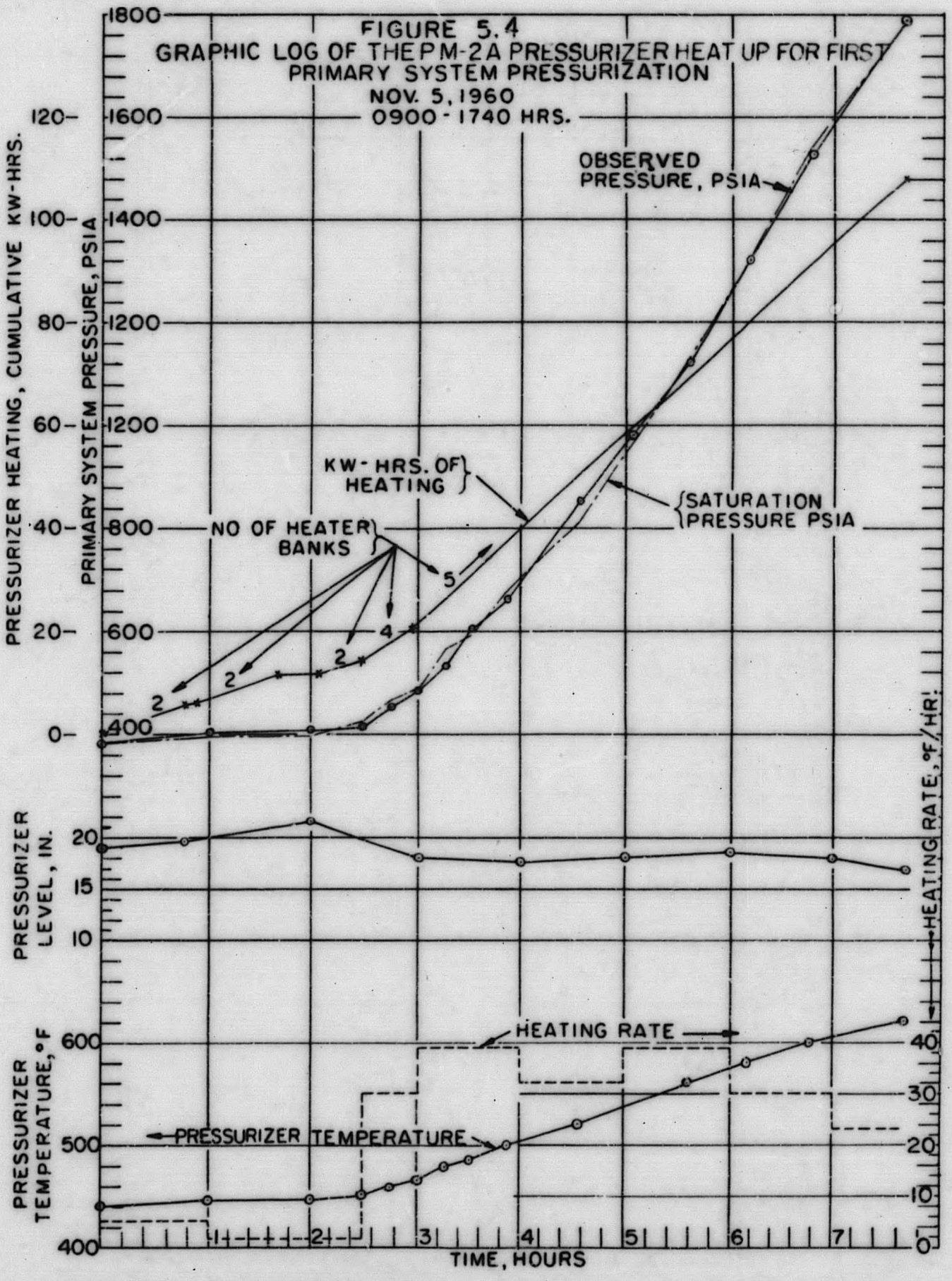

Figure 5.4. Graphic Log of the PM-2A Pressurizer Heat-up for First Primary System Pressurization

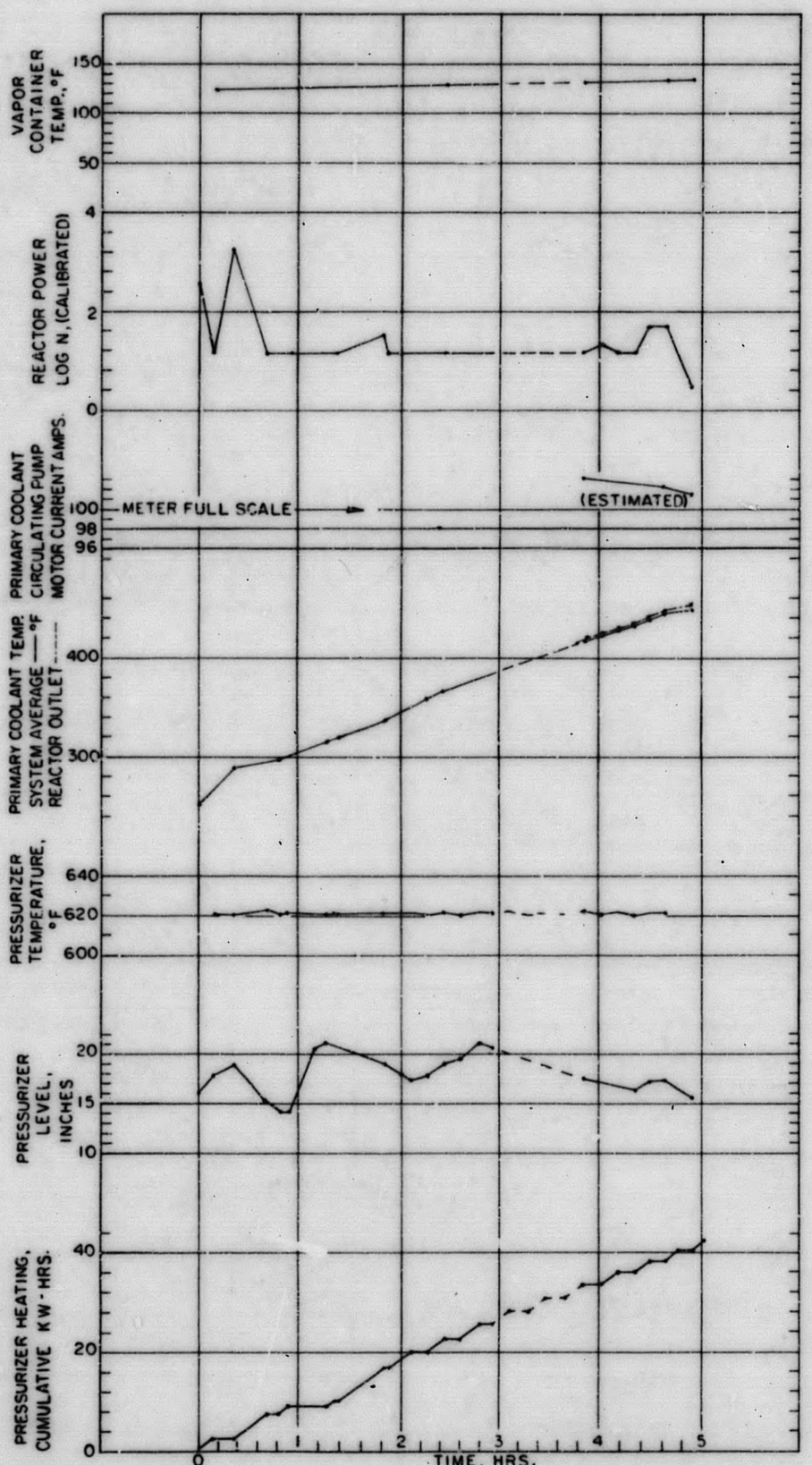

Figure 5.5. Graphic Log of the PM-2A Primary Loop Heat-up at Constant System Pressure

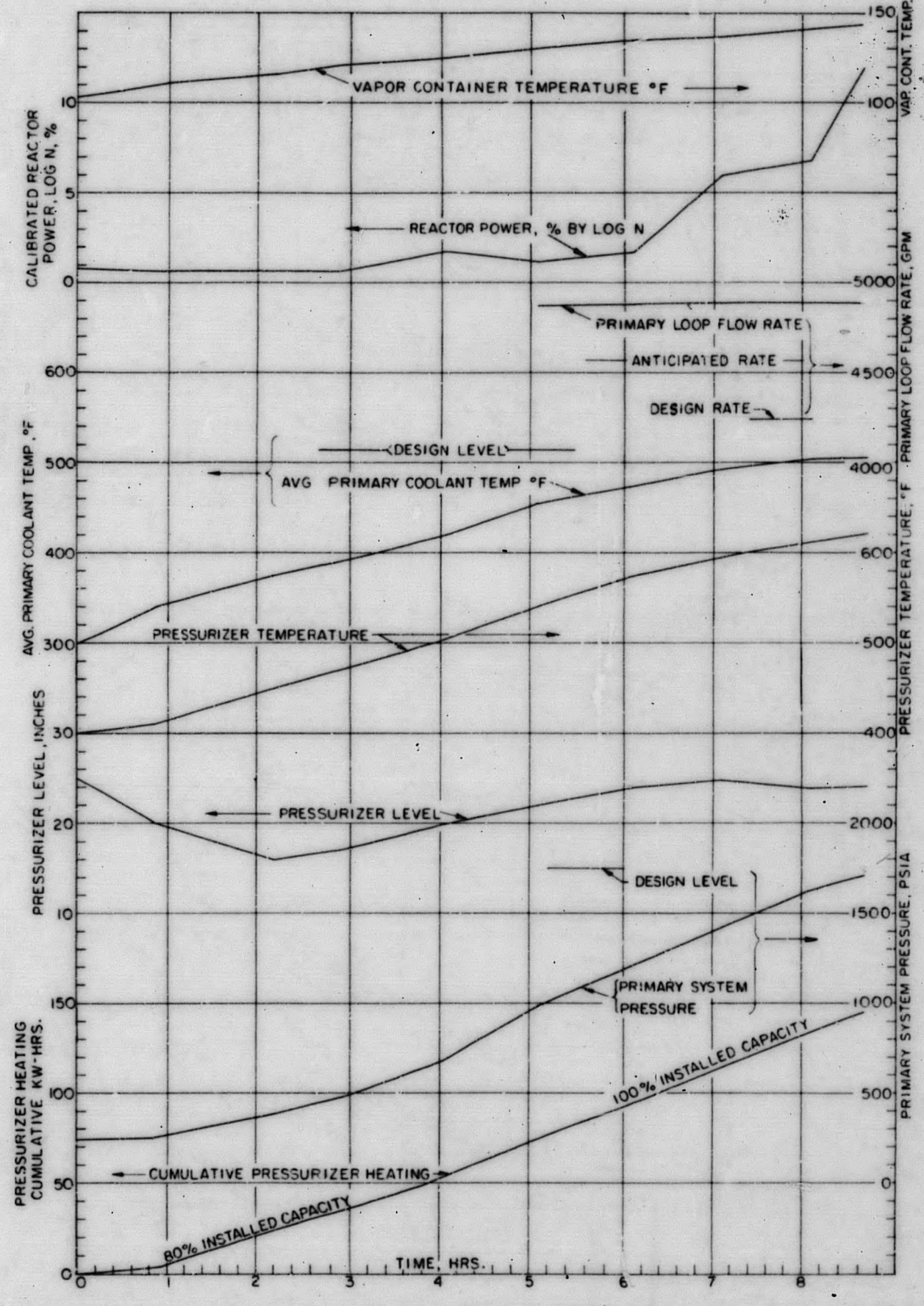

Figure 5.6. Graphic Log of First Unified Primary System Heat-up for the PM-2A

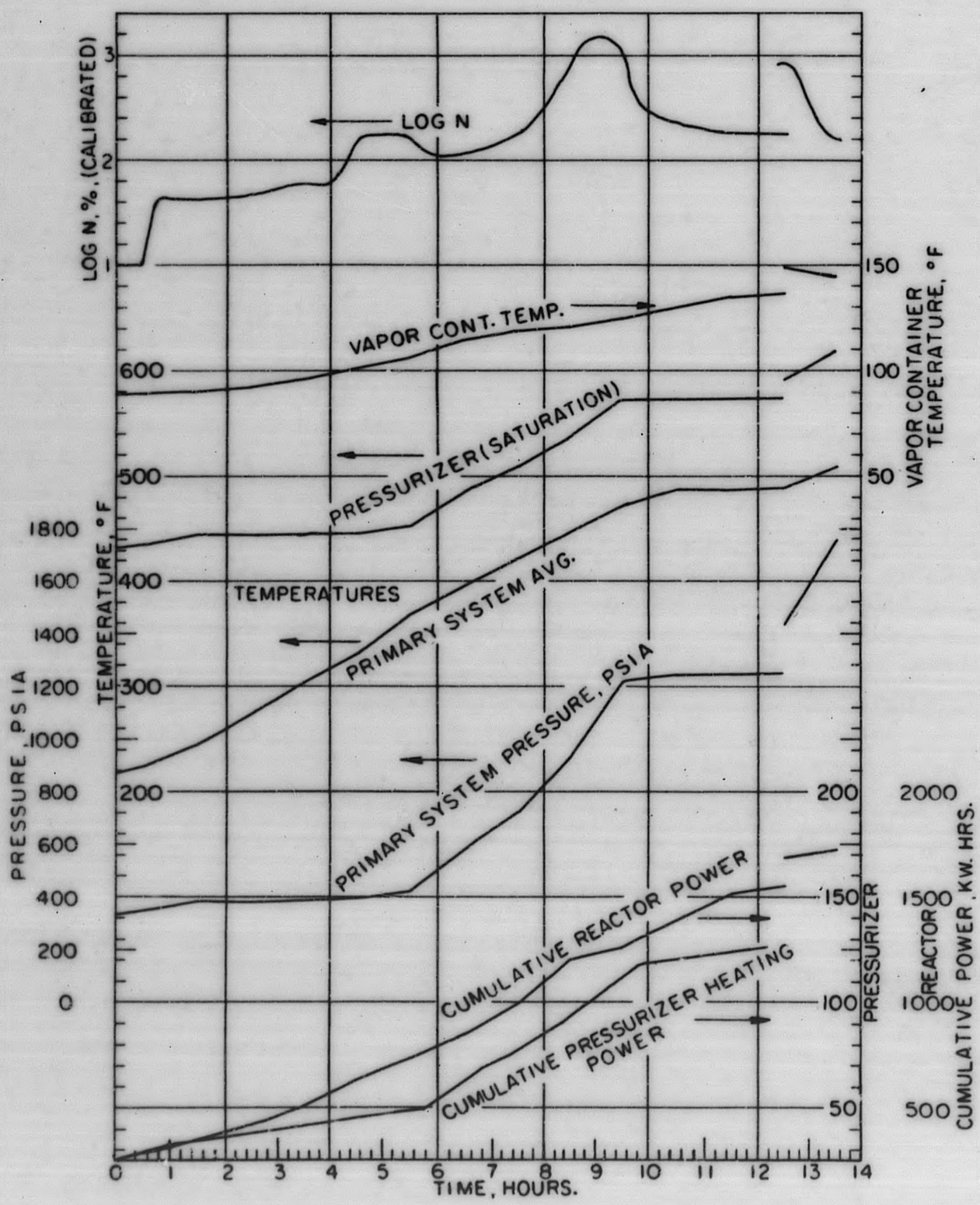

Figure 5.7. Graphic Log of the PM-2A Primary System Heat-up Before 400 Hour Test

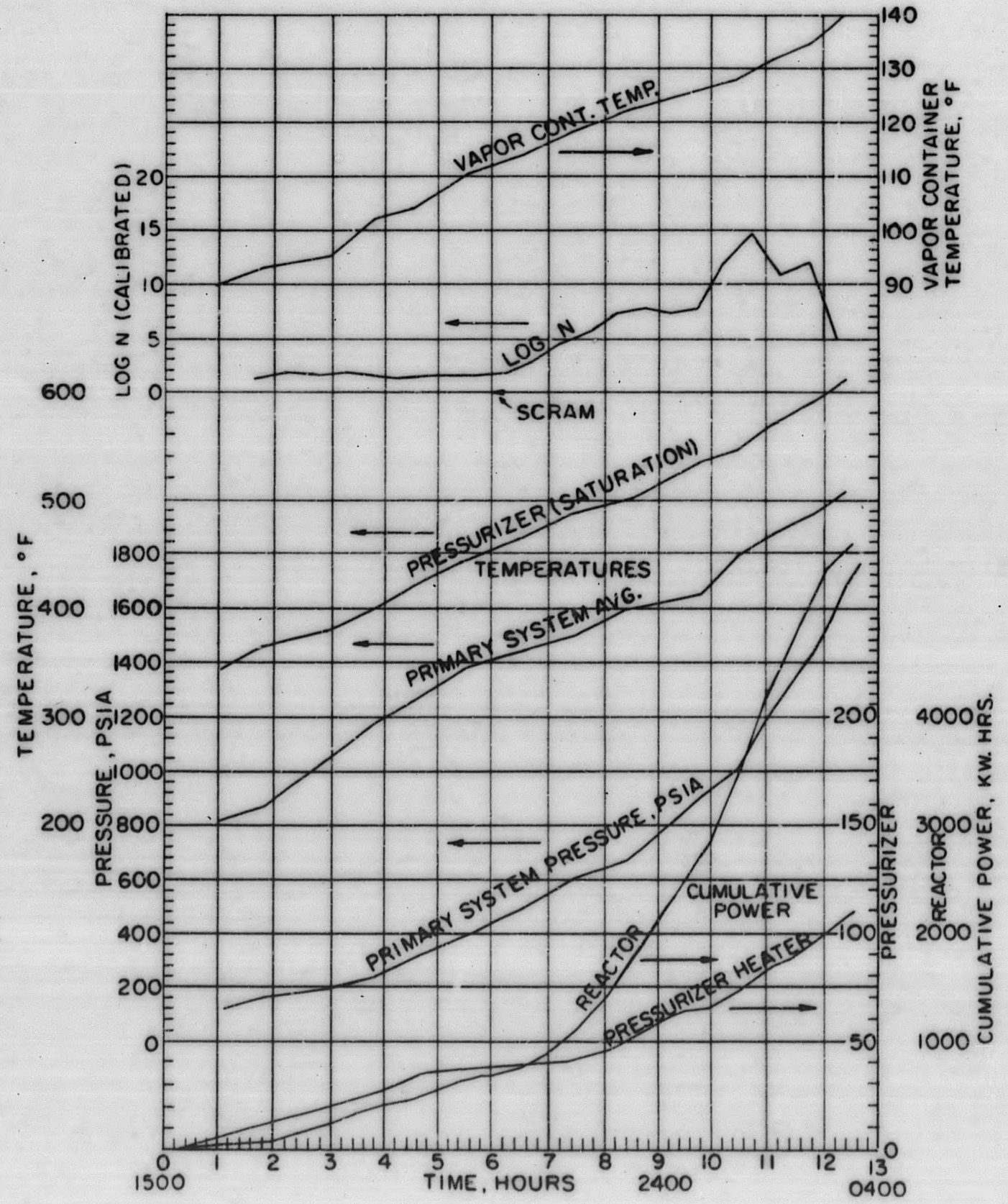

Figure 5.8. Graphic Log of the PM-2A Primary System Heat-up After 400 Hour Test

of the 400-hr test it was found that the DP cell was definitely out of order. In view of this it is felt that none of the flow readings obtained during the period from February to March 1961 are valid, since they indicate higher flow than previous readings.

During the November 1960 operations previously reported,[3] intermittent leakage from a faulty pressure relief valve on the pressurizer caused enough leakage of steam to require full heater capacity operation for almost 60% of the heat-up period, and a total power consumption of 85.4% of the maximum available pressurizer heater capacity (20 kw) during the period.

The measured power consumption of the pressurizer heaters during the November heatup operations of the heater banks is tabulated in Table 5.1.

TABLE 5.1

PM-2A PRESSURIZER HEATER CAPACITY

Heater Bank No.	Current, Amp	Power, Kw
1	7.5	3.60
2	7.7	3.70
3	7.8	3.65
4	7.6	3.74
5	7.7	3.70
Total	38.3	18.39

During the operations in February and March 1961, the full available heater capacity was called for less than 25% of the time during heat-up and pressurization. The total power used was less than 50% of the maximum available in the elapsed time of the heat-up.

5.1.3 ANALYSIS AND DISCUSSION

5.1.3.1 Flow Rate Measurement and Evaluation

The original minimum design requirement for coolant flow rate, determined by the core thermal analysis[4] was 4219 gpm at 500° F inlet temperature. As a result of conservatism in the initial calculations of core and loop pressure drop, final predicted ΔP values were lower than the pump specification values. Similarly, conservatism on the part of the pump manufacturer resulted in a delivered pump head slightly above the specification.

Figure 5.9 shows the operating point anticipated for the PM-2A primary loop prior to these tests, based on the equilibrium between the performance curve of the pump and the calculated pressure drop of the primary system. The latter was prepared after completion of the distribution flow tests in the air-flow model.[1] The predicted primary system flow rate based on pre-shipment testing was 4570 gpm at operating temperature (a 7.8% favorable margin), and 4475 gpm at 70-100°F. The observed operational flow rate was 4870 gpm at 455° and 4890 gpm at operating temperature. The latter is an additional 7% above the predicted rate. Although this difference is not excessive, it reflects a substantial departure in terms of delivered or required head, or both, at a given flow rate.

After review of the derivations of the two curves it is concluded that:

1. The observed flow rate is correct within normal tolerances.

2. The pump manufacturer furnished a pump that develops a head in excess of the contract requirement and is even substantially greater than shown on the performance curve. This latter difference was due to the following test conditions during the pump tests:

   (a) A long radius elbow at the inlet to the pump above was immediately preceded by a two-joint 90° miter elbow, with the single tap for pump inlet static pressure located in the final section of the mitered elbow, on the mean centerline of the elbow less than 1/4 pipe diameter downstream of the second joint. The location of the inlet pressure tap would undoubtedly cause some error in measurement, but its direction and magnitude are uncertain. The pressure drop due to the long radius elbow was included as part of the over-all pump performance, and also included in the calculation of loop pressure drop; thus it was accounted for twice.

   (b) Similarly the single tap for static pressure at the pump discharge was located in the first section of a mitered elbow immediately following the pump flange, less than 1/2 diameter downstream of the flange and less than 1/4 diameter from the first joint of this second mitered elbow. Again, this use of a single tap is almost certain to introduce some error, and its location immediately adjacent to the scroll prevents it from sensing the static pressure recovery associated with the return to normal pipe velocity profile.

   (c) The close proximity of the upstream mitered elbow, resulting in a compound bend preceding the pump, can be expected to have produced an abnormal swirl at the impeller entrance and

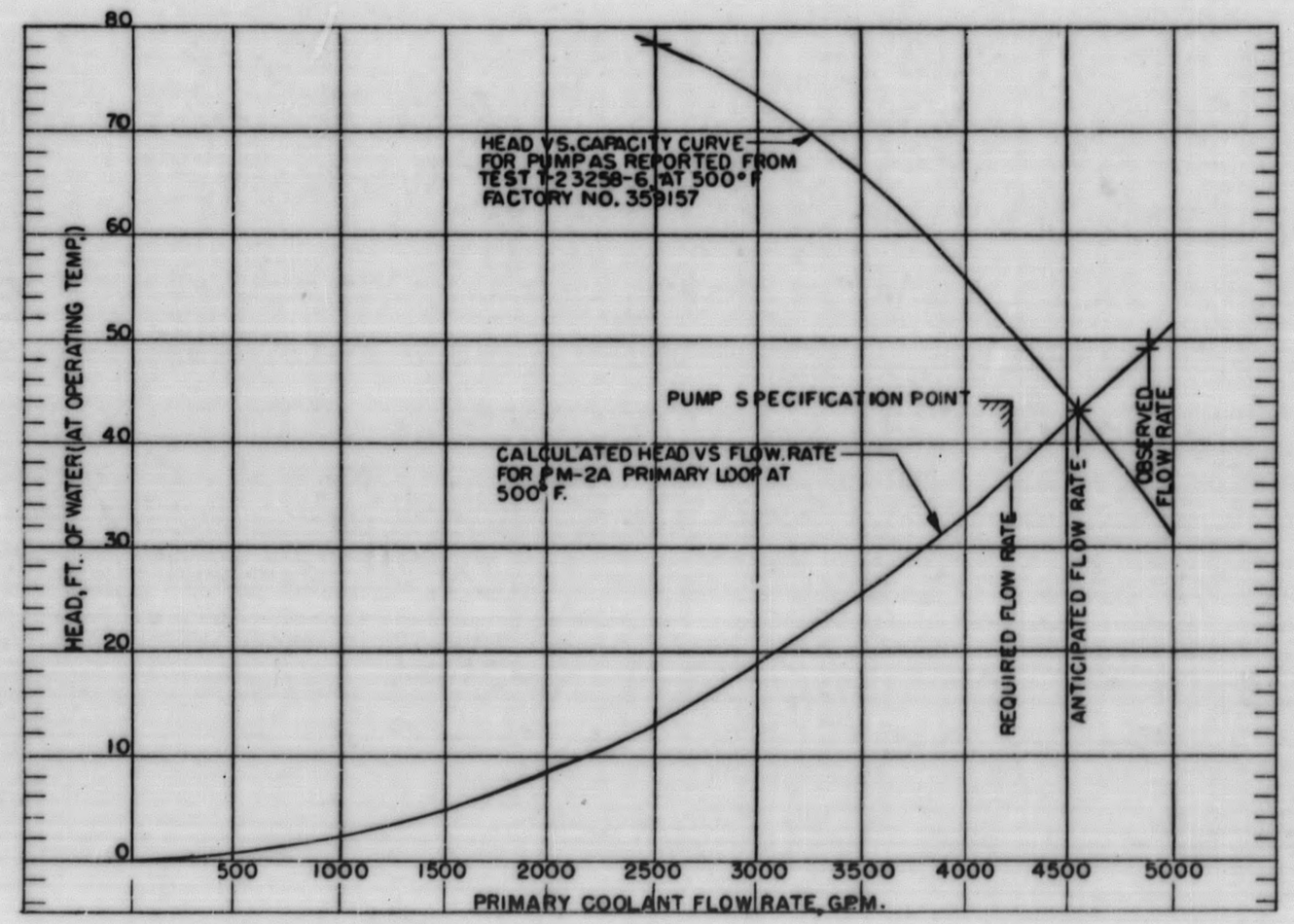

Figure 5.9. Head Vs Flow Characteristics of the PM-2A Primary Loop and Circulating Pump

this impaired actual pump performance in the tests. The PM-2A installation itself is a much more favorable arrangement.

Some of the sections of the Standards of the Hydraulic Institute [5] that cover the discrepancy in pump testing described above are "Methods of Head Measurement" (page B-VII-13, para. B-112-b and para. B-112-3) and "Effect of Operating Conditions" (page B(V-III)-4, para. B-90, C).

The flow tube and its associated instrument circuit for measuring the primary system flow rate was selected and designed prior to final pumping head requirements and manufacture and test of the pump. The allowance for possible excess flow (hot) was only 6%, which was insufficient during these plant tests.

5.1.3.2 Operation of the Log N Meter

Under steady state operation (see Sec. 5.2) following the reactor heat-ups in November, a log N meter reading of 26(%) was obtained when the steam generator output was 44.6% of rated power. Neglecting primary system heat losses and pump power input to the coolant, calibration of the Log N readings required that they be multiplied by the ratio 44.6 : 26, or 1.71. Turbo-generator output at this time was only 37 1/2% of rated output but this difference is the normal result of the reduced turbine efficiency when operating at less than half load, compared to full load performance.

The log N chamber calibration was the same for all heat-ups in November, shown in Fig. 5.4, 5.5 and 5.6. The calibration of the Log N chamber was changed by movement of the chamber before the heatup of February 7, shown in Fig. 5.7 which preceded the 400-hr test and before the heatup of March 4 shown in Fig. 5.8 which preceded the transient load tests. In the case of the heatup shown in Fig. 5.8, the values of core power as determined by the Log N meter were considerably higher than values obtained in previous heatups. This was due in part to the use of a chamber not properly compensated for gamma radiation buildup which occurred as a result of the 387 hr acceptance testing run.

5.1.3.3 Primary Loop ΔT and Power Measurements

To evaluate the temperature differential to be expected in the primary loop during startup, the following rough derivation of the temperature rise across the reactor is given. The values below were derived for a reactor heat-up rate of 30° F/hr.

Wt of primary liquid exclusive of pressurizer, mean temp.	3,350 lb
Wt of primary equipment experiencing essentially full temperature rise	42,000 lb
Wt of secondary water to be heated (in steam generator), mean temp. 400°F	3,450 lb
Vol. of steam in steam generator and line, normal operating level	24 cu ft

Total heat input required from 300° to 500° is computed by the equations -

$$Q = W_f(h_{g',2} - h_{f,1}) + W_m \cdot c_p \cdot (T_2 - T_1) + \Delta W_g - h_{fg}$$

$$\text{and } W_g = \frac{Vol_g}{v_{g,2}} - \frac{Vol_g}{v_{g,1}}$$

where:

Q = heat input, Btu

W = weight of material, lb

h = enthalpy, Btu/lb.

c_p = specific heat, Btu/lb, °F

T = temperature, °F

Vol = volume, ft^3

v = specific volume, ft^3/lb

with the following subscripts

f = of the liquid

m = of the metal

g = of the vapor

fg = of evaporation, taken at intermediate temperature

1 = initial condition

2 = final condition

$$Q = (3350 + 3450)(488-269) + 42,000 \times 0.12 \times 200 +$$

$$\left(\frac{24}{.67} \times 1201 - \frac{24}{6.5} \times 1180\right) + \left(\frac{18}{.67} - \frac{18}{6.5}\right)(1202-270)$$

$$= 14.9 \times 10^5 + 10 \times 10^5 + 0.47 \times 10^5 = 25.3 \times 10^5 \text{ Btu.}$$

At 30^o/hr, power required = $\frac{25.3 \times 10^5 \text{ Btu}}{200^o + 30^o/\text{hr}} = 0.38 \times 10^5$ Btu/hr

Full reactor power = 34.13×10^6 Btu/hr

Average power for 30^o/hr heating = $\frac{.38 \times 10^5}{34.13 \times 10^6} = 1.1\%$ of rated power

The family of curves in Fig. 5.19 shows reactor power output per degree of primary coolant temperature rise vs. primary flow rate, in the range of interest. The single line in the lower portion of the graph shows the temperature rise, for 10 MWt, vs. flow rate of water at 508^o F average temperature. Both parts of this figure are calculated directly from standard thermal properties of water.(6) From the single curve in the lower portion of Fig. 5.10, it is seen that based on an average flow rate of 4850 gpm over this heat-up temperature range, full power temperature rise is 14.95^o F for 508^o F water. For 300^o F water based on the ratio shown by the family of lines in Fig. 5-10, this would be 15.0^o F. Thus the calculated temperature rise across the reactor at 1.1% of full power is $15 \times 0.011 = 0.165^o$ F, requiring $\pm 0.01^o$ F over-all accuracy for the data to be within ± 6%.

To this might be added steady state heat loss from the primary system to the surroundings, but much of this occurs between the core and the nearest measuring stations, so that it would not show on the instruments.

The normal tolerance for the temperature sensing resistance bulbs is $\pm 1/2^o$ F, ranging up to $\pm 1^o$ in the upper part of the temperature range. Calibrations at room temperature and in boiling water, performed at the site, substantiated the former tolerances. To this must be added the tolerances of the resistance-to-current converters and of the indicating milliammeters. These are ± 1/2% and ± 1% of span, respectively. Altogether, this amounts to ± 3 1/2 to 4^o F for the two installed temperature indicators and 1 1/2 to 2^o F for the input to the Btu/hr meter.

The Btu/hr meter for measurement of reactor power was not operative during this test and unsatisfactory meter components had been removed from service and returned to the manufacturer for repair and modification. The over-ranging of the flow tube also would have prevented its use here.

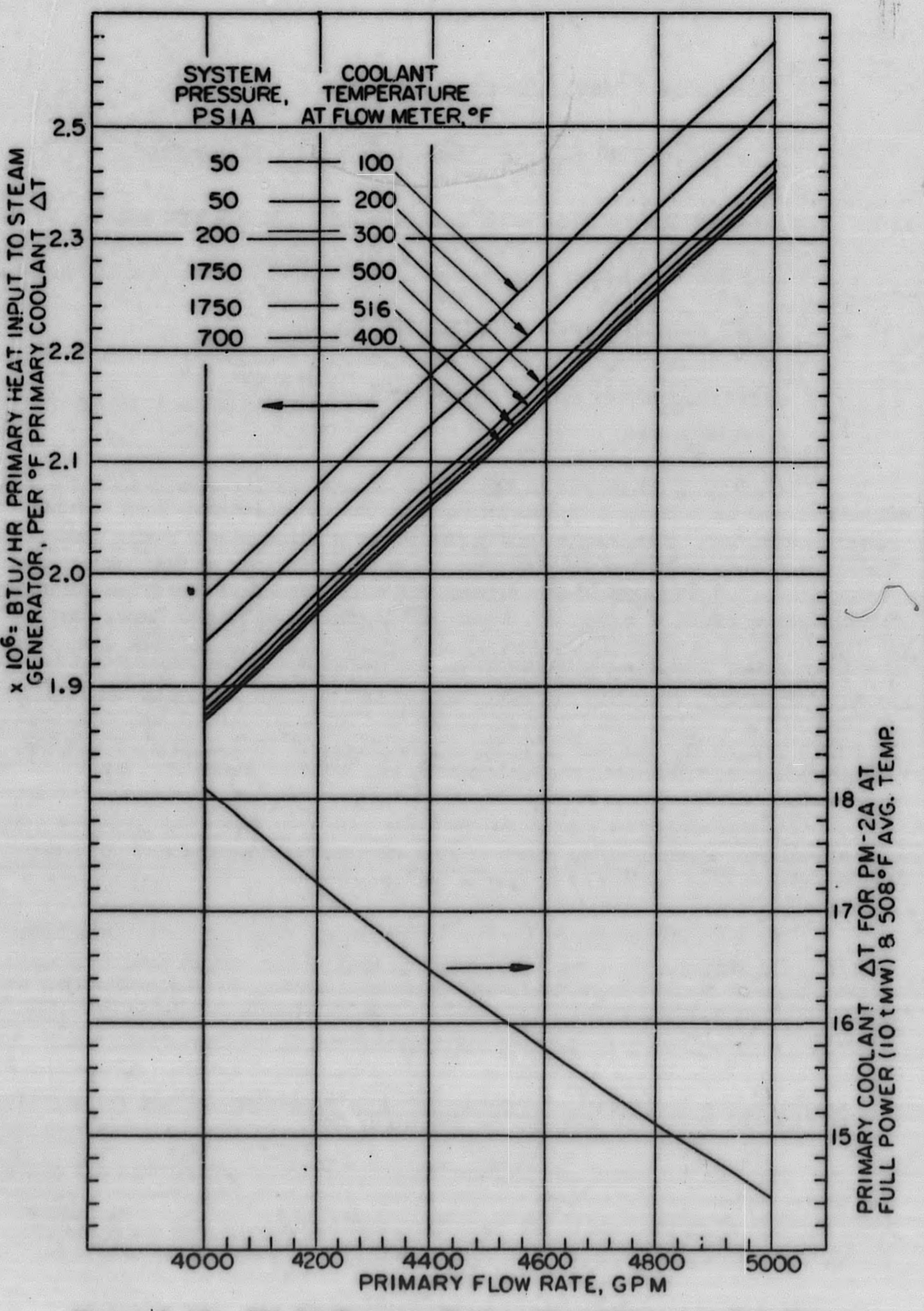

Figure 5. 10. PM-2A Primary System Heat Output and Full Power Temperature Difference Vs Flow Rate

One of the two installed temperature indicators shows reactor outlet temperature, on a dial covering only 400 to 600° F (Ref. Fig. 2.13, Table 2.2). The other shows primary loop average, based on two bulbs located one upstream and one downstream of the reactor, and is a dual range instrument with one scale running from 0 to 600° F, and the other from 400 to 600° F. In keeping with the above tolerances the visual scales of the dials are not designed to be read more closely than one whole degree. Accordingly, derivation of temperature rise across the reactor from these two independent measuring circuits, based on taking the difference between them and doubling it, is impossible below 400° F and would yield a total possible error of 2 [+ 3 1/2 - (-3 1/2)] ° = 14° F for the temperature range of 400 to 600° F.

5.1.3.4 Pressurizer Heater Performance Evaluation

To evaluate the performance of the pressurizer heaters during the high demand portion of the heat-up, the rate of increase of stored energy is calculated as follows, for heating from 545 to 612° F: (This calculation assumes a constant pressurizer level for normal steady state operation.)

Wt of water at 545° : $5.1\ ft^3 / 0.0216 \frac{ft^3}{lb} = 235.5$ lb

Wt of water at 612° : $5.1\ ft^3 / 0.0242 \frac{ft^3}{lb} = 210.0$ lb

change in mass of water in pressurizer = 25.5 lb (decrease)

Increase in water enthalpy = 210 x 634.6 - 235.5 x 542.9 = 6000 Btu

Wt of steam at 612° : $13.8\ ft^3 / 0.238 \frac{ft^3}{lb} = 58.0$ lb

Wt of steam at 545° : $13.8\ ft^3 / 0.444 \frac{ft^3}{lb} = 31.1$ lb

Change in mass of steam in pressurizer = 26.9 lb (increase)

Increase in steam enthalpy = 58.0 x 1156.8 - 31.1 x 1191.7 = 30,040 Btu
Heat load due to water intake (26.9-25.5) (588-458) = 182 Btu
Where 588 and 458 are mean values of enthalpy for pressurizer and primary loop liquid, respectively.

Vessel wt = 3,900 lb at 0.12 Btu/lb° F specific heat

Increase in metal enthalpy = 3900 x 0.135 x (612-545) = 35,200 Btu
Total heat addition required: 71,422 Btu.

This portion of the fourth heat-up reported was accomplished in 1.9 hr. Therefore, the average calculated demand was:

$$71,422/1.9 = 37,591 \text{ Btu/hr} = 11.0 \text{ kw}$$

The average metal temperature would not be quite as high as that of the contained fluids, at either temperature, with a greater difference apparent at the higher temperature. Thus the increase in heat content of the metal is slightly less than shown. But this is partly offset by the fact that enthalpy increase in the insulation has been ignored. In Test C-602 (see Sec. 5.2), it was found that approximately 5 kw would just balance the steady state heat losses from the pressurizer. Adding this to the 11.0 kw demand derived above for 35°/hr yields a calculated heater requirement of about 16.0 kw.

Actual power consumption during this period was 18.4 kw for 1.6 hr and 11 kw for 0.3 hr, averaging 17.4 kw. This is 8.75% higher than the calculated requirement. The measured power consumption is in fair agreement with the calculated value. Differences may be attributed to unaccountable heat losses from the pressurizer to the primary system as well as instrument errors in measuring the power consumed. Variations in pressurizer liquid level impose an added load on the heaters.

5.2 PRIMARY SYSTEM THERMAL SURVEY (STEADY STATE - TEST TP C-602)

This test is intended to provide as complete information as plant instruments can furnish on the normal steady state operation of the primary system, in the field of thermal and hydraulic performance. This data will be used for evaluation of design methods, studies of plant operation, and in replacement core development. It is limited to observations at zero plant load and to observations under normal operation at full available camp load.

5.2.1 GENERAL TEST PROCEDURE AND OPERATING CONDITIONS

5.2.1.1 General Method and Conditions

Two primary system thermal surveys were performed, one prior to the shield modification and one with more detailed measurements subsequent to the shield modification. Steady state design conditions were maintained. Limitations were imposed by the camp, which required only 35 to 45% of the design steam generator load. In order to reduce the resulting variability, most of this data was recorded at night. At this time the demand was fairly stable and only slightly smaller than the day load. The test con-

sisted of obtaining general thermal and hydraulic data such as reactor thermal power from an installed Btu/hr meter, heat losses from the pressurizer by determining heater power consumption, primary loop flow rate, primary loop ΔT and pertinent data necessary for performance of a primary system heat balance.

The basic instrumentation of the primary loop and its location is shown on the schematic drawing of the primary loop, Fig. 5.1 (Ref. Sec. 2.8, 5.1, and Fig. 2.9).

5.2.1.2 Power Measurement

The original test plan called for determining reactor thermal power by reading it directly from an installed Btu/hr meter. This instrument receives temperature signals from resistance bulbs TE-1 and TE-2 (Fig. 5.1) (Ref. Sec. 2.8 and Fig. 2.9) mounted in the inlet and outlet primary nozzles of the steam generator and a $\Delta\rho$ signal from the Gentile flow tube. Because two components of the Btu meter had been returned to the factory for repair, an alternate method was required to obtain a measure of reactor heat output. This consisted of independently measuring the resistance of the two temperature bulbs which provided the input to the inoperative Btu meter. In the November operations this was done by a portable potentiometer. Attempts were made to determine the error differential between them by observations at zero power. In the later tests, the regular resistance-to-current converters were left in the active circuit, so that the signal was read as milliamperes on the 10 to 50 ma scale. Sustained running at zero load provided an error calibration.

5.2.1.3 Pressurizer Heater Performance

The heat losses from the pressurizer were obtained by measuring the number and frequency of heaters in operation and the current drawn by each heater bank. During the 400-hr test different heater bank arrangements were used.

5.2.2 EXPERIMENTAL RESULTS

5.2.2.1 Over-all Plant Data

Plant thermal survey uncorrected log sheet data recorded during the preliminary 10-hr run on November 21 and 22, 1961 are shown in Table 5.2. Table 5.3 presents the no load readings obtained prior to the 400-hr test. Part of the data taken at the available camp load during the 400-hr run is shown in Table 5.4.

5.2.2.2 Primary Loop Flow Rate

During the November test, the primary loop flow was measured as 4890 gpm at operating temperature (Ref. Sec. 5.1)

The measurements obtained during the 400-hr test indicate a flow ranging from 5000 to 5100 gpm. This represents an even greater departure from the anticipated flow. However, subsequent to these tests it was found that the instrument was out of calibration, hence these measurements are not considered valid.

5.2.2.3 Primary Loop ΔT.

At no-load on the steam generator (zero steam flow), direct measurements of the temperature drop of the primary coolant across the steam generator rendered substantial values of ΔT, ranging from 5.8 to 12.2° F, and averaging 7.7° F. The value obtained by comparing console readings for reactor outlet and reactor average was 4.8° F, ranging from 0 to 10° F. During the 400-hr test the camp electrical load ranged from 655 to 810 ekw (gross), or 32.8 to 40.5% of design electrical load. The ΔT measured across the steam generator ranged from 15.0 to 22.5° F. When the averages of the values at no-load were taken as a "zero" error, and subtracted, they yielded net readings of 7.3 to 14.8° for the direct measurements, and 5.2 to 11.2 for the results using the reactor outlet and average readings. Figure 5.11 shows that these readings were highly erratic and inconsistent.

5.2.2.4 Secondary System Flow Rates

The log data readings of the secondary steam, feedwater and blowdown flow rates shown in Tables 5.2, 5.3, and 5.4 are in reasonable agreement. Actually in more than half of the log data readings there was a large discrepancy between these measurements. Hunting on the part of the feedwater control system at this low power may be an explanation for this discrepency.

5.2.2.5 Pressurizer Heater Operation

Table 5.5 shows the percentages of the elapsed time during the 400-hr test which the pressurizer heaters were on in response to the automatic pressure regulator, as a function of the number of heaters set to respond to the controller. These have been multiplied by the measured power consumption of the heaters, to yield values of equivalent continuous demand, from which an over-all average of 5.01 kw was obtained.

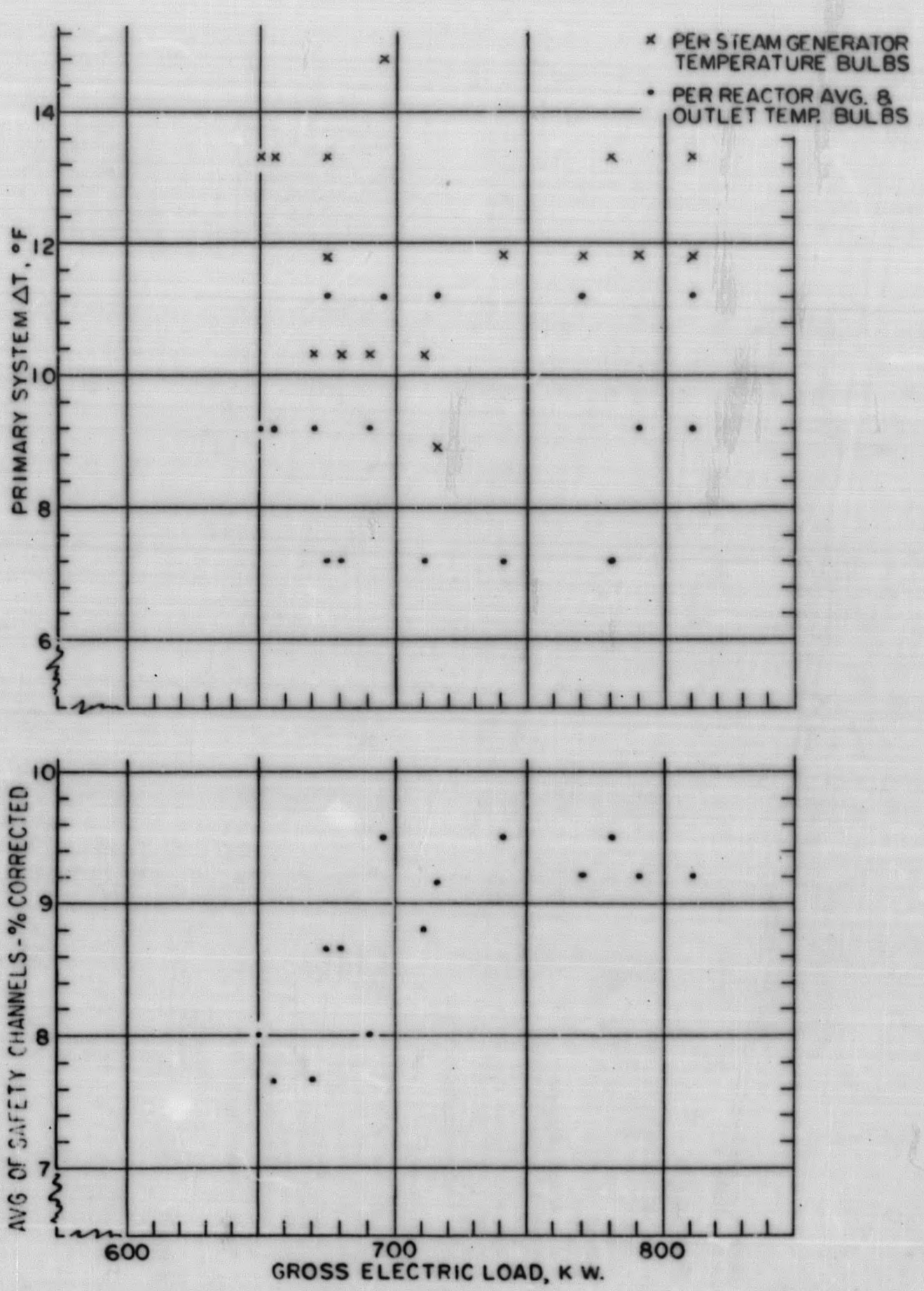

Figure 5. 11. Primary Loop ΔT and Nuclear Channel Reading Vs Electric Generator Load for the PM-2A

TABLE 5.2

TEST NO. C-602

PRELIMINARY PRIMARY SYSTEM THERMAL SURVEY ON PM-2A REACTOR OPERATING AT THE AVAILABLE CAMP ELECTRICAL LOAD

LOG SHEET DATA — CAMP CENTURY, GREENLAND

DATE: Nov. 20-22, 1960 TIME (HOURS)		18:00	19:00	20:30	22:00	23:00	24:00	01:10	02:00	03:00
Primary System										
Average Reactor Temp., °F.		507	510	510	510	510	507	507.5	510	510
Reactor Outlet Temp., °F.		512	517	516	515	515	513	512.5	516	516
Steam Gen. Inlet Temp., °F.		523.1	---	522.9	---	---	---	---	---	---
Steam Gen. Outlet Temp., °F.		513.25	---	513.5	---	---	---	---	---	---
Log N %		30	30	30	30	30	30	28	30	30
Avg. of Safety Channels		23	23.8	23.5	---	---	---	22.3	23	21.5
Primary Coolant Flow (Meas. % of 240" ΔP)*		95.5	95.5	95.5	95.5	95.5	95.5	95.5	95.5	95.5
Pressurizer Pressure, psig		1,705	1,740	1,730	1,740	1,730	1,700	1,750	1,705	1,710
Pressurizer Temp., °F.		620	622	620	625	620	620	622	620	625
Pressurizer Level, in.		20	17.2	17.1	17.5	15.4	15.2	18.2	16.5	20.0
D.C. Pump Motor Current, amp		---	95	96	96	96	96	96	97	96
Secondary System										
Main Steam Flow, lb/hr.**		16,400	19,800	14,000	13,800	14,000	13,000	13,200	13,000	13,500
Feedwater Flow, lb/hr.**		15,500	16,200	15,500	15,000	15,500	10,000	13,900	15,000	17,000
Main Steam Press., psig		560	575	590	595	590	595	595	600	600
Main Steam Temp., °F.		---	477	475	480	480	480	480	480	480
Feedwater Pressure, psig		555	568	580	590	580	590	595	590	595
Feedwater Temp., °F.		---	147	150	151	153	154	156	---	---
Secondary Blowdown Rate, gpm		---	0.2	0.3	---	---	---	0.43	---	---
Electrical Gen. Load, kw		560	575	760	725	725	725	715	700	715
Vapor Container Temp. °F.***		145	147	148	150	150	150	150	150	151
External	Thermocouple Number									
Primary (inner)	39	77	80	81	84	85	85	85	86	85
Shield Tank	38	78	80	81	84	85	85	85	86	85
Temps, °F	37	79	81	81	84	85	86	86	87	86
Spent Fuel Pit	36	43	44	50	43	44	43	--	43	44
Support Tank	35	51	51	56	51	51	51	--	51	50
Temps, °F	34	56	56	68	56	56	56	--	56	57
Spent Fuel Outer	33	67	68	67	68	68	67	67	67	67
Shield Tank	32	93	93	95	97	98	99	100	100	101
Temps, °F	31	104	104	102	102	102	102	102	101	101

*See Fig. 5.2 for conversion to gpm.

**Both of these flow rates are recorded as read, without corrections for off-design densities. Observed feedwater rate should have exceeded observed steam flow rate by about 2000 lb/hr.

***Temperature bulb located above primary coolant pump, about 1 ft. below vapor container wall.

TABLE 5.3

TEST NO. C-602

FINAL PRIMARY SYSTEM THERMAL SURVEY ON PM-2A REACTOR OPERATING WITH NO ELECTRICAL LOAD

LOG SHEET DATA — CAMP CENTURY, GREENLAND

DATE: Feb. 8-9, 1961 TIME (HOURS)	21:10	21:32	22:30	23:00	00:25	01:02	01:42	02:00	02:41
Primary System									
Average Reactor Temp., °F.	490	492	483	494	508	509	508	508	508
Reactor Outlet Temp., °F.	495	---	---	495	510	511	511	511	511
Steam Gen. Inlet Temp., °F.	488	480	480	483	503	503	501.5	503	500
Steam Gen. Outlet Temp., °F.	495.2	488	488	495.2	508.8	510	509.8	506.8	510
Steam Gen. △T °F.	7.2	8.0	8.0	12.2	5.8	7.0	7.3	5.8	10.0
Log N %	0.38	0.0001	1.0	1.0	1.2	0.35	0.38	0.39	0.32
Avg. of Safety Channels	---	---	---	---	---	---	---	---	---
Primary Coolant Flow, ma	49.5	49.5	49.5	49.5	48.5	48.5	48.5	48.5	48.5
Primary Coolant Flow, gpm	5020	5020	5020	5020	5000	5000	5000	5000	5000
Primary Coolant Press., psig	1730	1670	1720	1730	1730	1740	1730	1730	1710
Pressurizer Temp., °F.	615	610	615	615	615	618	618	618	615
Pressurizer Level, in.	25	18	17.5	18.5	17.2	17.1	17.1	17.1	17.1
P. C. Pump Motor Current, amp	100	100	100	100	100	100	100	100, 110	102
Primary Blowdown Rate, gpm	1.1	0.5	1.0	0.7	0.8	0.8	1.0	0.7	1.0
Secondary System									
Main Steam Flow, lb/hr.	---	---	---	---	---	---	---	---	---
Feed Water Flow, lb/hr.	---	---	---	---	---	---	---	---	---
Main Steam Pressure, psig	670	600	595	630	740	735	718	718	718
Main Steam Temperature °F. **	300	250	300	300	500	500	510	510	510
Steam Generator Level	11	9	7	8.5	13.8	13.3	12.4	12.1	11.2
Feed Water Pressure, psig	650	590	500	620	500	***	---	---	---
Feed Water Temperature, °F.	110	110	130	130	130	128	126	126	123
Secondary Blowdown Rate, gpm	2.0	2.0	0.12	0.12	0.12	0.12	0.12	0.30	0.12
Electrical Gen. Load, kw	---	---	---	---	---	---	---	---	---
Vapor Container Temp., °F.	148	149	148	149	150	151	153	152	153
External	Thermocouple Number								
Primary (inner) Shield Tank Temperature, °F	39	95	95	97	97	97	99	98	99
	38	95	95	97	97	98	99	99	99
	37	98	99	100	100	102	103	104	103	104
Spent Fuel Pit Support Tank Temp., °F.	36	40	40	40	40	40	40	40	40	40
	35	45	45	45	45	46	44	44	45	44
	34	47	47	46	47	47	46	46	46	46
Spent Fuel Outer Shield Tank Temp., °F.	33	56	56	55	56	56	54	54	56	54
	32	88	88	88	88	90	90	91	92	92
	31	88	88	88	91	91	91	92	92	92

* See text in regard to faulty instrument operation.

** Based on "Main Steam Temp." bulb which is downstream of the (closed) trip valve.

*** Valve closed.

TABLE 5.4

TEST NO. C-602

FINAL PRIMARY SYSTEM THERMAL SURVEY ON PM-2A REACTOR OPERATING WITH THE AVAILABLE CAMP ELECTRICAL LOAD

LOG SHEET DATA — CAMP CENTURY, GREENLAND

DATE. Feb. 10-11, 1961 TIME (HOURS)		22:11	23:00	23:37	00:45	01:48	02:57	04:01	05:06	06:00
Primary System										
Average Reactor Temp., °F.		504	504	504	504	504	503	503	503	503
Reactor Outlet Temp., °F.		510	510	509	509	510	510	510	510	510
Steam Gen. Inlet Temp., °F.		482	494.9	488.3	492	487.3	490.3	488.3	487.3	490.3
Steam Gen. Outlet Temp., °F.		502.4	510	502.4	510	507	510	508.5	507	508.5
Steam Gen. ΔT, °F		19.5	15.0	15.0	18.0	19.5	19.5	21.0	19.5	19.5
Primary Coolant btu/hr.		---	98	98	97	97.5	97	98	97	---
Log N %		15	13	12	12	12	13	14	13	13
Avg. of Safety Channels		9.5	10	9.7	9.5	9.7	10	10.2	10	10
Primary Coolant Flow, ma.		48.0	48.5	48.5	48.0	48.5	48.5	49.0	48.5	48.5
Primary Coolant Flow, gpm		---	---	---	---	---	---	---	---	---
Primary Coolant Press., psig		1720	1710	1710	1710	1710	1730	1710	1710	1730
Pressurizer Temp., °F.		618	615	615	615	615	618	618	618	620
Pressurizer Level, Inches		17	17	17	17	17	17	17	17	17
Heater Banks Connected		2*	2	2	2	3	3	4	4	5
P. C. Pump Motor [illegible], amps.		102	102	102	102	102	102	102	102	102
Primary Blowd[illegible], gpm.		0.80	0.9	0.9	0.9	0.9	0.8	0.9	0.9	0.9
Secondary System										
Main Steam Flow, lbs/hr.		15,500	15,000	14,800	14,000	14,500	15,000	14,000	15,200	14,900
Feed Water Flow, lbs/hr.		17,500	16,000	16,000	15,000	17,400	18,000	15,000	17,000	16,200
Main Steam Pressure, psig		560	565	570	575	570	565	565	562	565
Main Steam Temp. °F.		472	465	475	475	470	470	475	470	470
Steam Gen. Level, Inches		13.5	13.3	13.2	14.2	14.2	14.2	14.2	14.1	14.2
Feed Water Press. psig		550	550	560	570	565	560	565	555	555
Feed Water Temp., °F.		272	275	273	272	273	274	272	272	275
Secondary Blowdown Rate gpm		1.03	1.04	1.00	0.92	0.91	0.91	0.90	0.90	1.11
Electrical Gen. Load, kw		740	795	740	710	710	725	730	790	790
Vapor Container Temp. °F.		140	137	135	133	135	135	133	134	132
External	Thermo-couple Number									
Primary (inner) Shield	39	86	86	86	85	86	85	84	84	84
Tank Temp., °F.	38	86	86	85	85	86	85	84	84	83
	37	94	94	94	94	94	94	93	93	92
Spent Fuel Pit Support	36	44	44	45	45	45	44	44	44	44
Tank Temp., °F.	35	48	48	48	48	48	48	48	48	48
	34	50	50	50	50	50	50	50	50	50
Spent Fuel Outer Shield	33	57	57	58	57	57	58	57	58	57
Tank Temp., °F.	32	129	130	130	130	131	131	132	132	132
	31	130	131	132	132	132	132	132	132	132

TABLE 5.5

PM-2A PRESSURIZER HEATER OPERATION

No. of Heater Banks Used	2	3	4	5
Power Consumption, kw	7.36	11.03	14.72	18.39
Total Time On, min.	215	146	114	90
Total Time Off, min.	113	181	174	281
Total Elapsed Time, min.	328	327	288	371
Percentage of Time Used, %	.655	.446	.396	.242
Equiv. Continuous Demand, kw	4.82	4.93	5.83	4.45

Equiv. Continuous Demand, Overall Average, kw 5.01

5.2.3 ANALYSIS AND DISCUSSION

5.2.3.1 Primary Loop Flow Rate

The observed flow rate of 4890 gpm is 7% higher than predicted[1] and 15.4% higher than required by the core thermal analysis. This difference is beneficial for future potentialities of this reactor although at the cost of a very slight loss in present plant efficiency.

Figure 5.9 shows the operating point predicted for the PM-2A primary loop prior to these tests, based on the equilibrium between the performance curve of the pump and the calculated pressure drop of the primary system. The latter was prepared after completion of the distribution flow tests in the airflow model. The flow rate thus predicted was 4570 gpm at operating temperature, compared to the observed rate which was 4890 gpm.

The original thermal analysis was based on the requirement that there should be no nucleate boiling during steady state operation, and this in turn was interpreted to call for keeping the maximum fuel plate surface temperature, including all allowances for instrument error or control tolerances, below saturation temperature.

New experimental data from tests performed for Type 3 Cores Single Element Flow Testing [7] of this contract, show individual channel flow deficiencies, compared to the average velocity, ranging up to 11% in

stationary elements and 22% in control rods vs. the 3% and 6%, respectively, postulated at the time of this thermal analysis.

Analyses of the effects of maldistribution[8] under AEC Contract AT(30-1)-2639 indicate that this criterion is relatively unimportant.

In a negative load transient, theoretically some small increase in primary system pressure must take place before the negative temperature coefficient initiates the shutdown of core power, but actually the volume of water in the return from the steam generator to the core, and the associated transport time, are so small that the average coolant temperature in the core begins to rise at exactly the same time that the system pressure does. Thus, for this type of transient there is no danger of poor control due to collapse of bubbles preceding or overriding the decrease in liquid density due to increase in its temperature. This has been amply demonstrated in the SM-1, in which the load transient response is completely automatic and satisfactory. Furthermore, the transit time from the steam generator to the core is much shorter in the PM-2A than in the SM-1.

From these observations it is concluded that with the existing flow rate the PM-2A can be operated at a primary system pressure lower than the design value of 1750 psia. This would extend the life or improve the performance of packings, pumps, safety valves and such components or accessories. It would permit wider tolerances for operating and some relaxation in the requirements for certain automatic control equipment. The required pressure for hydro-testing future modifications can be lowered, possibly to the point that it no longer requires special protection by isolation or removal from the system for such parts as control rod seals, which would be damaged by excess pressure. Fewer pressurizer heaters would be required to accomplish a heat-up in a given time.

Based on present understanding of irradiation damage to reactor vessels, the reduction in operating pressure will reduce reactor vessel stress and as a result probably offset the effect of an increase in nil-ductility transition temperature of the reactor vessel.

An alternate way to exploit this advantage would be to operate the primary system at slightly higher than design temperatures, at least until near the end of life of each core, at which time it should be restored to design temperatures. This would provide higher turbine inlet temperature and thus a slight improvement in thermal efficiency. The limitation would be the corresponding increase in peak transient secondary system pressure. Based on the small increase in observed steam pressure during Test C-601, following an abrupt loss of load from 45% of design to 0 output, it would appear that 25^{o} F increase in temperatures would not cause excessive pressures, even

when the reactor can be loaded to full design power level. However, if this temperature were maintained throughout, a decrease in core life due to the negative temperature coefficient would be experienced and must be evaluated.

5.2.3.2 Determination of the Reactor Thermal Load

Initially reactor power must be measured thermally to calibrate the intermediate and power range channels. Normally the primary system data should be used, and a comparison of the primary system data made with that from the secondary by performing a heat balance that would indicate the losses in the system. During these tests, however, calculated coolant temperature rise through the reactor was 6.8° F, or less, due to reduced load operations. The smallest increment observed on the readings from temperature bulbs TE-1 and TE-2 via the current converter and the milliameters was 0.1 ma, which corresponds to 1.5° F on the temperature readout scale based on the respective zero and full scale values. Thus the smallest increment of power detected from the milliameters was 1.5/7.4 or 22% of maximum available plant load. As previously stated and shown on the plots of the results, the observed values for coolant temperature rise, were apparently in error as much as 7° F.

In view of this the reactor thermal power could not be calculated from the measurements in the primary loop and it was necessary to go directly to secondary system data. Thus it was also necessary to use calculated figures for the difference between steam generator output and reactor output to determine the latter, and consequently no experimental heat balance was achieved.

Within a small variation in load span, a close proportionality should exist between reactor power and electric power output. The observed data points shown in Fig. 5.11, however, do not show this proportionality. For an actual evaluation of reactor load, it was necessary to evaluate the thermal output of the steam generator, as a measure of the output of the primary system, instead of using the turbo-generator electric output simply as read from the wattmeter.

Table 5.6 shows the observed and corrected values for the feedwater, and blowdown flow rates during part of the 387 hr acceptance run. These meter corrections for feedwater rate were necessary since the instruments were calibrated for full load temperatures and pressures. Consequently the readings at part load must be compensated for the attendant changes in these conditions.

Figure 5.13 presents the results of this data reduction. In order to overcome the erratic behavior of the individual readings as shown by Fig. 5.11, it would be desirable to obtain an integration of steam and feedwater

flow and of all power or ΔT readings. True integration, however, cannot be accomplished on the basis of nominally instantaneous readings separated by at least half an hour. The whole series should not be averaged either, because the power level did vary significantly. Accordingly, the points were grouped into four power ranges and the readings within these ranges were averaged. On this basis, a satisfactory +2.8 to -0% balance of outflow vs. inflow for the steam generator is achieved, as well as logical relationships among all the variables. Correction factors for the nuclear instrument readings have been derived from this work.

The calculations for the miscellaneous minor heat flow quantities which comprise the differences between steam generator output, measured primary loop performance, and reactor core output are given below.

In order to derive the correct values for primary loop ΔT, it is necessary to add to the values of steam generator output the heat losses to the surroundings from the steam generator and the loss due to secondary system blowdown. From this total, the heat equivalent of the portion of the primary loop pump energy which is converted to friction in the steam generator must be subtracted.

To obtain values for reactor core power, in order to derive correction factors for the nuclear power instruments, the remainder of the pump input energy must be subtracted, and the heat loss due to primary system blowdown, plus the remaining heat leakage, must be added. These calculations are given below.

A. Steam Generator Output Correction

Steam generator input = output + 41,000 + 6,700 - 60,400 = output - 12,700 Btu/hr. where

41,000 Btu/hr = secondary system blowdown

6,700 Btu/hr = heat loss from steam generator to surroundings

60,400 Btu/hr = energy input from primary system work.

This represents a negligible correction to steam generator outputs of 14,500,000 to 16,680,000 Btu/hr in Table 5.6.

B. Frictional Heat Acquired in the Pump

In order to estimate the frictional heat acquired in the pump, it is necessary to apply the hydraulic efficiency of the pump. The over-all measured power consumption was 54 kw. The useful pump output was

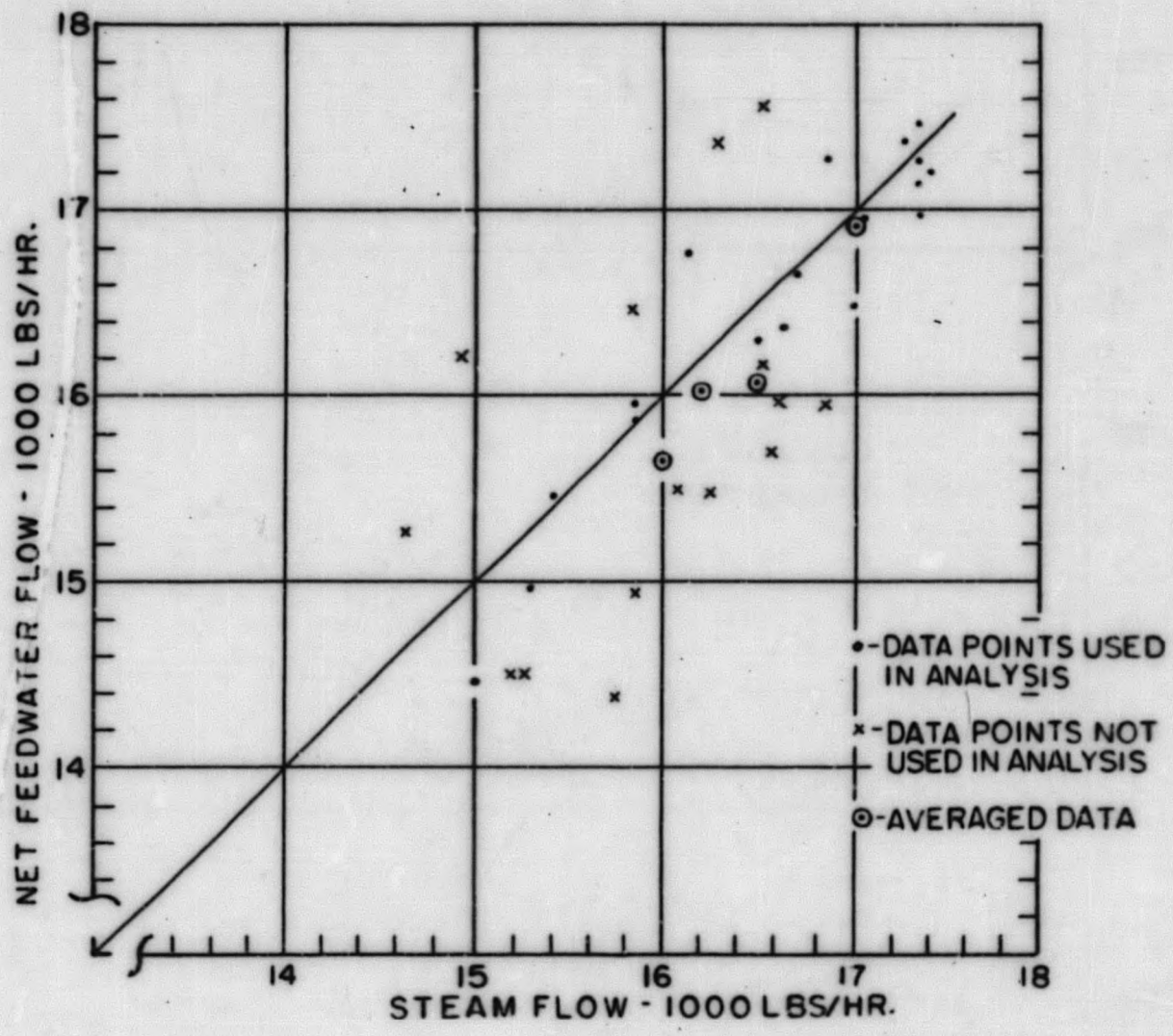

Figure 5. 12. Fluid Balance for the PM-2A Steam Generator at Full Camp Load

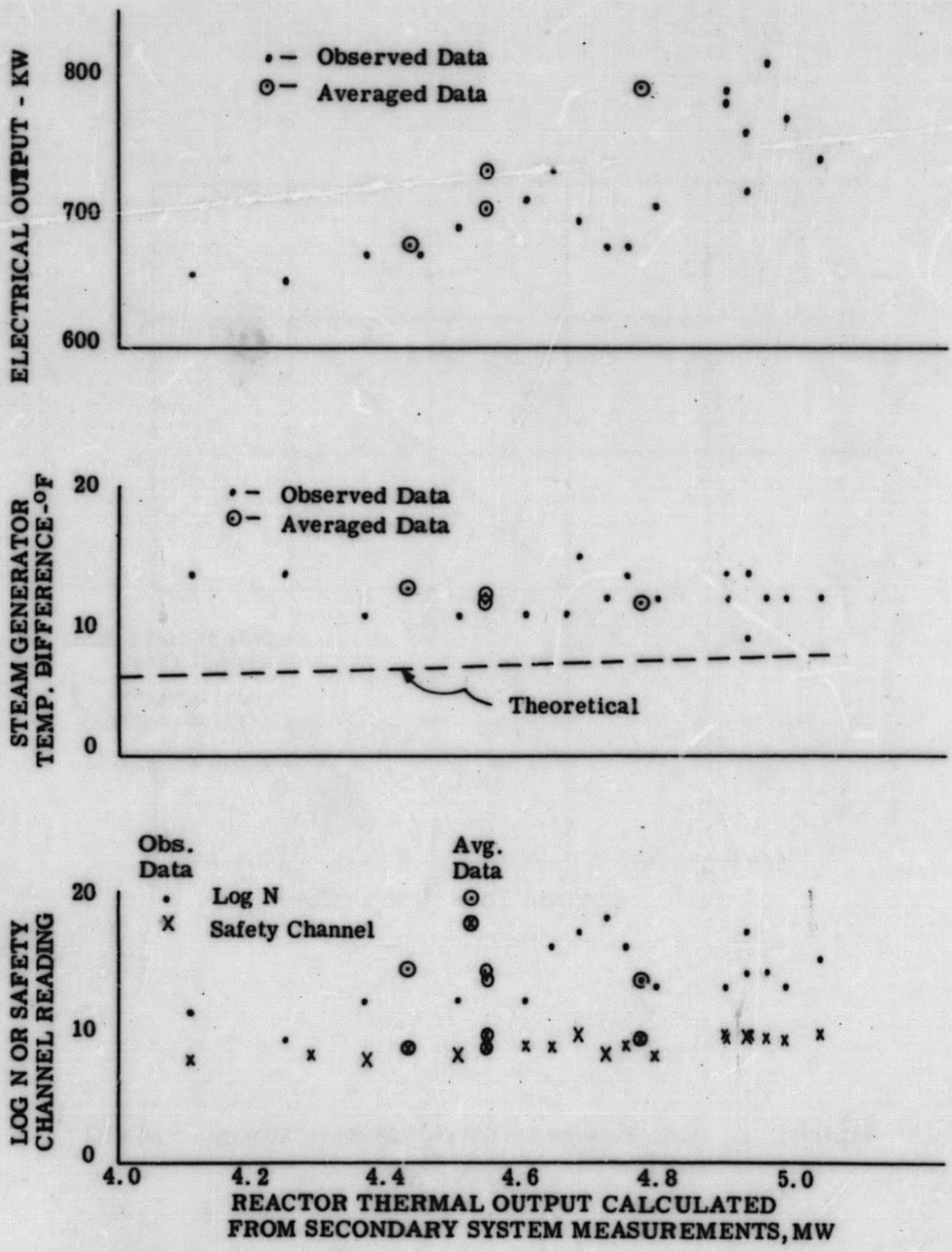

Figure 5.13. Comparison of Power Measurements for the PM-2A Plant

calculated as 35.4 kw, thus the efficiency obtained was $\frac{35.4}{54} = 65.6\%$. The closest that the published curves for this pump come to this is 64% at which the pump alone is 80% efficient.

Taking this value, frictional heat

$$= \frac{1 - .80}{.80} \times 35.4 \text{ kw} = 8.85 \text{ kw} = 30,000 \text{ Btu/hr}$$

Of the over-all power input, data from the original tests on the pump show a heat rejection to the auxiliary coolant of 26 kw. Electric motor losses are 54 - (35.4 + 8.9) = 9.7 kw. Thus, the net heat flow is a removal of 26 - (8.9 + 9.7) = 7.4 kw. or 26,000 Btu/hr.

C. Heat Loss from Primary System Blowdown

Primary system blowdown rate was 0.9 gpm. Primary system liquid loss, or "net make-up", averaged 4.1 gal/hr. Make-up water is received at the room temperature of the feedwater skid, approximately 60° F. Blowdown takes place at 500° F, though the flow is measured at low pressure and at about 100° F. Specific volume and enthalpies are therefore, 0.01616 ft^3/lb and 487.4 and 33.0 Btu/lb, respectively. Heat loss is thus:

$$(.9 \times 60 + 4.1) \frac{0.01604}{0.01616} \times 8.33 \frac{\text{lb}}{\text{gal}} \times (487.4 - 33) = 218,000 \frac{\text{Btu}}{\text{Hr}}$$

D. Secondary System Blowdown

The flow rate was reported at 0.4 gpm for all readings during the 400-hr test.

Temperature of blowdown - 470° F (steam temperature)

Temperature of makeup - 270° F (feedwater temperature)

Heat loss per lb., $h_{out} - h_{in} = 453 - 239 = 214$ Btu/lb.

Actual heat loss = .4 gpm x 60 $\frac{\text{min}}{\text{hr}}$ x 8 $\frac{\text{lbs}}{\text{gal}}$ x 214 $\frac{\text{Btu}}{\text{lb}}$ =

$$41,000 \frac{\text{Btu}}{\text{hr}}$$

E. Radiation Heat Loss from the Steam Generator

The natural convection and radiation losses to the surroundings have been estimated at 6,700 $\frac{\text{Btu}}{\text{hr}}$

F. Energy Input from the Primary System Pump Work

The conversion of this energy into sensible heat in the primary system is distributed throughout the primary loop. It will take place in direct proportion to the frictional and acceleration pressure drops in the components and piping. At the pump itself, there will be a slight temperature drop because the losses to the auxiliary coolant exceed the total inefficiency, electric plus hydraulic, of the pump.

Useful pump output at 4890 gpm, 49 ft H_2O = 35.4 kw, where 49 ft H_2O occurs at the observed flow rate, Fig. 5.9

The calculated pressure drop for the steam generator was 21.4 ft H_2O out of a total drop for the primary loop of 42.3 ft H_2O or 50% of the total, where 42.3 ft H_2O occurs at the anticipated flow rate Fig. 5.9.

35.4 kw x 50% = 17.7 kw = 60,400 Btu/hr.

G. Remaining Heat Losses from Primary Loop to the Surroundings

The remaining heat loss from the primary loop to the surroundings = 38,910 - 6,700 + 8,700 = 40,910 Btu/hr, where 38,910 Btu/hr was the total load that a space cooler would have carried, 8,700 Btu/hr is the heat loss to the primary shield tank carried off by the cooling coil in the tank [4] and 6,700 is the heat loss from the steam generator.

H. Summary of Heat Losses to Determine Reactor Thermal Power

Steam generator input = Q_1

Net heat exchange in pump = Q_2 = 26,000 Btu/hr

Primary system blowdown = Q_3 = 218,000 Btu/hr

Heat losses from primary loop to surroundings = Q_4 = 40,910 Btu/hr

Steam generator output = Q_5

Reactor power = $Q_1 + Q_2 + Q_3 + Q_4 = Q_5 + [(Q_2 + Q_3 + Q_4) - 12,700)]$

Reactor power = Q_5 + 26,000 + 218,000 + 40,910 - 12,700 = Q_5 + [(284,910 - 12,700)]

Reactor power = Steam generator output + 272,200 Btu/hr

In Table 5.6 a heat balance correction of ~ .1 Mu (272,200 Btu/hr = 74.7 kw) is added to the steam generator output to obtain the reactor output.

5.3 PM-2A RESPONSE TO LOAD TRANSIENTS - (TEST TP C-601)

The purpose of this test was to record the transient behavior of the primary loop immediately following a change in plant load. The test response data obtained was used to check the reactor alarm and scram settings and to evaluate the analytical methods used as a basis for plant design.

5.3.1 DESCRIPTION OF NORMAL PLANT RESPONSE

The PM-2A reactor core, through the presence of its negative temperature coefficient, adjusts core power to correspond with changing plant load without control rod movement. Mean primary temperatures before and after a transient are necessarily the same, while the temperature rise between inlet and outlet coolant is proportional to the power level.

During the transient, the changing coolant temperatures along the primary loop produce net volumetric changes which are absorbed or supplied by the pressurizer acting as an accumulator. The pressurizer is sized to limit the extremes of associated pressure variations within satisfactory operating limits.

5.3.2 GENERAL TEST PROCEDURE AND OPERATING CONDITIONS

The PM-2A was subjected to the most severe load changes possible at the time of the tests. Only 760 kw of the design gross load of 2000 kw was available, and 320 kw of this was station load. Due to difficulties which resulted in a reactor scram when all the available load was instantaneously transferred to or from the diesel generator, a total load transfer had to be accomplished in two steps.

With the nuclear plant stabilized at full available load, and the standby generator synchronized with the nuclear plant, camp feeders were opened, dropping camp load from the nuclear plant. With the nuclear plant re-stabilized at station load, and synchronized with the standby generator, camp feeders were closed, transferring camp load back to the plant.

In a subsequent test, with the nuclear plant at full available load, camp load and then station load were dropped from the plant, the steps were performed in rapid sequence and almost simultaneously to simulate a combined

TABLE 5.6

PM-2A HEAT BALANCE DATA

	Feb. 10				Feb. 11			Feb.12		Feb. 13			Feb. 14			Feb. 15	
	22:11	22:46	02:26	05:06	05:31	06:58	07:30	05:43	02:44	04:32	05:01	02:58	03:31	04:11	02:12	02:50	05:56
Steam Pressure - psia	572	573	587	574	572	572	572	592	587	592	587	592	602	587	572	570	570
Feedwater Temperature ^{o}F	272	273	273	272	273	277	275	265	268	268	270	270	269	268	268	270	270
Feedwater Flowmeter Corr. Ratio, i.e. $\sqrt{\text{Density Ratio}}$	1.009	1.009	1.009	1.009	1.009	1.009	1.009	1.012	1.011	1.011	1.010	1.010	1.011	1.011	1.011	1.010	1.010
Observed Feedwater Flow lb/hr x 10^3	17.5	17.0	16.0	17.0	17.3	17.3	17.2	16.8	15.9	14.5	15.5	16.8	16.4	15.0	16.5	17.4	16.7
Corrected Feedwater Flow lbs/hr x 10^3	17.66	17.16	16.14	17.14	17.47	17.45	17.32	17.04	16.07	14.66	15.65	16.97	16.56	15.16	16.68	17.57	16.87
Secondary Blowdown Rate lbs/hr x 10^3	0.19	0.19	---	---	---	0.19	0.19	0.19	0.19	0.19	0.19	0.19	0.19	0.19	0.19	0.19	0.19
Net Feedwater Flow lbs/hr x 10^3	17.47	16.97	15.95	16.95	17.28	17.26	17.13	16.85	15.88	14.47	15.46	16.78	16.37	14.97	16.49	17.38	16.68
Enthalpy of Steam Leg Btu/lb	1203.6	1203.6	1203.4	1203.6	1203.6	1203.6	1203.6	1203.4	1203.4	1203.4	1203.4	1203.4	1203.2	1203.4	1203.6	1203.6	1203.6
Enthalpy of Feedwater, h Btu/lb	241	242	242	241	242	246	244	233.8	236.8	236.8	238.8	238.8	237.8	236.8	236.8	238.8	238.8
Enthalpy Gain, Δh, Btu/lb	962.6	961.6	961.4	962.6	961.6	957.6	959.6	969.6	966.6	966.6	964.6	964.6	965.4	966.6	966.8	964.8	964.8
Steam Generator Output $W_{fw} \times \Delta h$, Btu/hr x 10^6	16.82	16.32	15.33	16.32	16.62	16.53	16.44	16.34	15.35	13.99	14.91	16.19	15.80	14.47	15.94	16.77	16.09
Steam Generator Output Megawatts	4.92	4.78	4.49	4.78	4.87	4.84	4.81	4.73	4.49	4.10	4.36	4.74	4.63	4.24	4.67	4.91	4.71
Calculated Primary ΔT Across Steam Generator, ^{o}F (From Figure 5-10)	7.22	7.22	6.60	7.10	7.01	7.20	7.11	6.93	6.65	6.29	6.44	6.75	6.96	6.41	7.12	7.22	6.99
Net Observed Primary ΔT Across Steam Generator	11.8	13.3	10.3	11.8	11.8	11.8	13.3	11.8	10.3	13.3	10.3	13.3	10.3	13.3	14.8	8.8	11.8
Reactor Output, TMW	5.02	4.88	4.59	4.88	4.97	4.94	4.91	4.88	4.59	4.20	4.56	4.84	4.73	4.34	4.77	5.01	4.81
Log N Reading %	15	13	12	13	13	14	14	13	12	11	12	16	16	14	17	17	18
Electrical Output, EKW	740	780	710	790	770	810	810	705	690	655	670	675	680	650	695	715	675
Log N Correction Ratio	3.3	3.8	3.8	3.8	3.8	3.5	3.5	3.7	3.7	3.7	3.6	3.0	2.9	3.0	2.7	2.9	2.6
Avg. of Linear Power Channels	9.5	9.5	8.8	9.0	9.0	9.2	9.2	7.8	8.0	7.7	7.7	8.7	8.7	8.0	9.5	9.2	8.7
Corr. Ratio for Linear Power	5.3	5.1	5.2	5.4	5.5	5.4	5.3	6.1	5.6	5.3	5.7	5.4	5.3	5.3	4.9	5.3	5.4

AVERAGE DATA FOR POINTS GROUPED BY POWER LEVEL

Reactor Output, TMW	4.42	4.53	4.53	4.76
Electrical Output, EKW	677.5	702.5	730	791
Log N Reading %	14.3	13.4	14.0	13.63
Log N Correction Ratio	3.1	3.4	3.2	3.5
Avg. of Linear Power Channels	8.25	8.58	9.14	9.14
Corr. Ratio for Linear Power	5.4	5.3	5.0	5.2
Calc. Primary ΔT across Steam Generator (see Fig. 5-10)	6.70	6.77	6.88	7.10
Corr. Ratio for Net ΔT Signal	0.54	0.59	0.61	0.63

step transfer. With the nuclear plant re-stabilized, but carrying no electrical load, station load and then camp load were applied to the plant, the steps again were performed almost simultaneously.

Three methods were employed to record PM-2A plant load transient data at Camp Century:

1. Visicorder traces of operating parameters

2. 35 mm still photographs of console instrumentation

3. Visual observation and recording of data

The visicorder was connected to the output of the sensing probe and in parallel with the normal console indicating instrumentation. Table 5.7 is a listing of parameters that were monitored during the transient load tests plus a listing of the appropriate references for instrument locations, indicator and sensing probe locations and instrument range of response. Each sensing probe provides a signal of 10 to 50 milliamps from minimum to full scale deflection of the indicating dial.

The still cameras photographed the control console dials during each test. These photographs offered a check on the visicorder data.

5.3.3 EXPERIMENTAL RESULTS

The three variables of greatest interest were plotted as a function of time after a step change in load:

1. Pressure change vs. time after step load change (Fig. 5.14)

2. Volume change vs. time after step load change (Fig. 5.15)

3. Primary coolant average temperature change vs. time after step load change (Fig. 5.16).

The tests show that for a drop in load from 600 kw to 0 kw, the pressurizer responds to a 0.58 cu ft (calculated from pressurizer level change) insurge with an increase in primary system pressure of 120 psia (1750 to 1870 psia). During this transient the average core temperature rises 5.4° F. and returns to the initial reading. For the drop from camp load to station load (760 kw to 320 kw) the volume surge, which has been calculated from the pressurizer level change, is 0.3 cu ft, pressure surge is +14 psia and the temperature rise 2° F.

TABLE 5.7

SUMMARY OF TEST PARAMETERS FOR THE PM-2A TRANSIENT LOAD TESTING

Parameter	Reference Fig. No.	Instrument Ref. No.	Indicator* Code No.	Instrument Range	Instrument Tolerance
1. Log N	2.13	5	MUR-13		
2. Reactor Outlet Temperature	2.14	12	TI-31	400°-700°F	± 3°F
3. Primary Coolant Avg. Temp.	2.13	6	MTI-31	(a) 0°-600°F	± 6°F
				(b) 400°-600°F	± 2°F
4. Steam Generator Inlet Temp.	(Not monitored on Control Panel)		TE-1	---	---
5. Steam Generator Outlet Temp.	(Not monitored on Control Panel)		TE-2	---	---
6. Pressurizer Liquid Level (Volume)	2.14	9	LIC-11	0-34 in. H_2O	±1/3 in. H_2O
7. Pressurizer Temperature	2.14	14	TI-1	0-700°F	± 7°F
8. Primary System Pressure	2.14	11	PIC-11	0-2200 psig	± 22 psig

* Refer to Figure 2.9 for location of sensing probes.

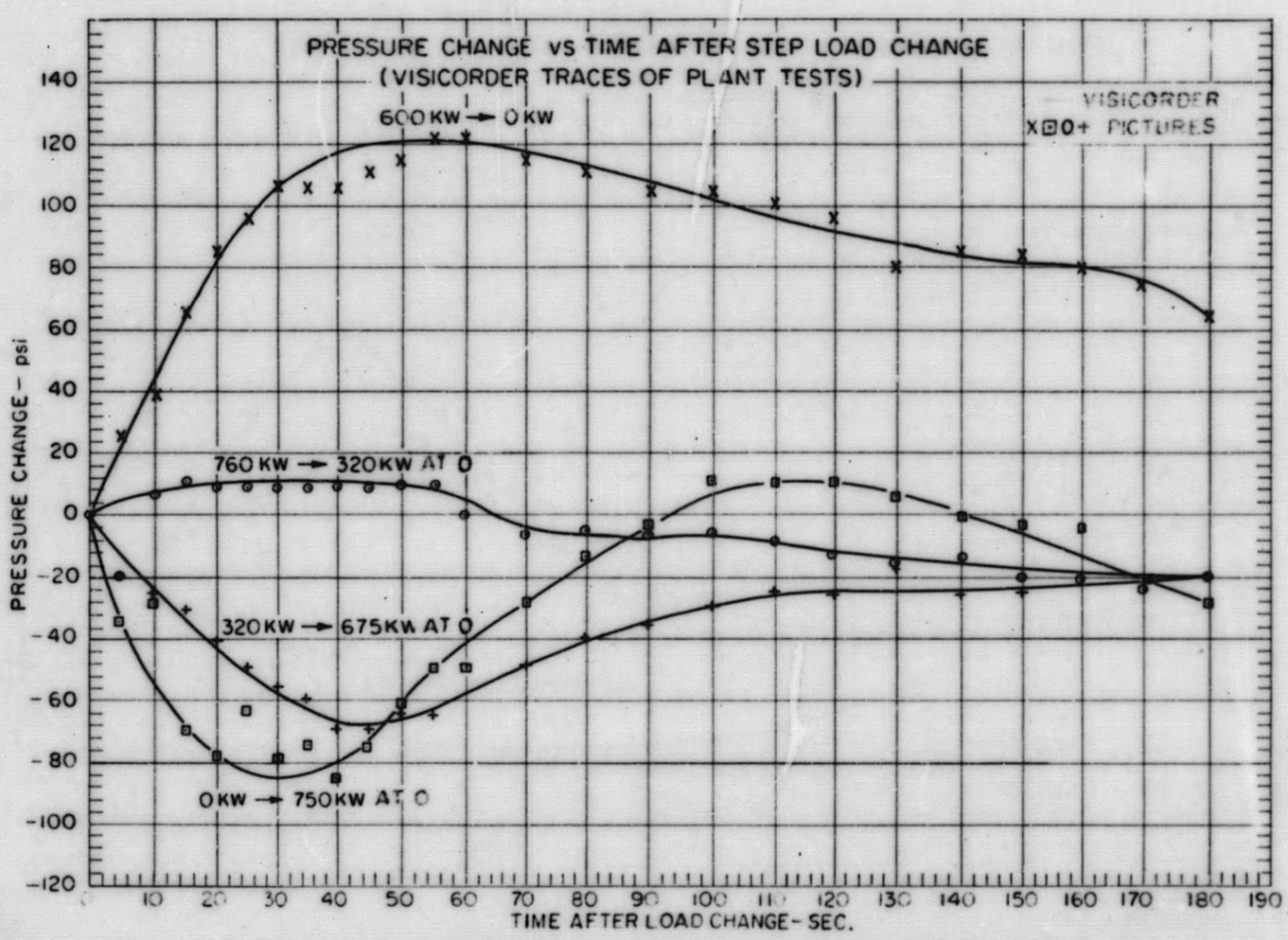

Figure 5. 14. PM-2A Primary System Pressure Change Vs Time After a Step Load Change

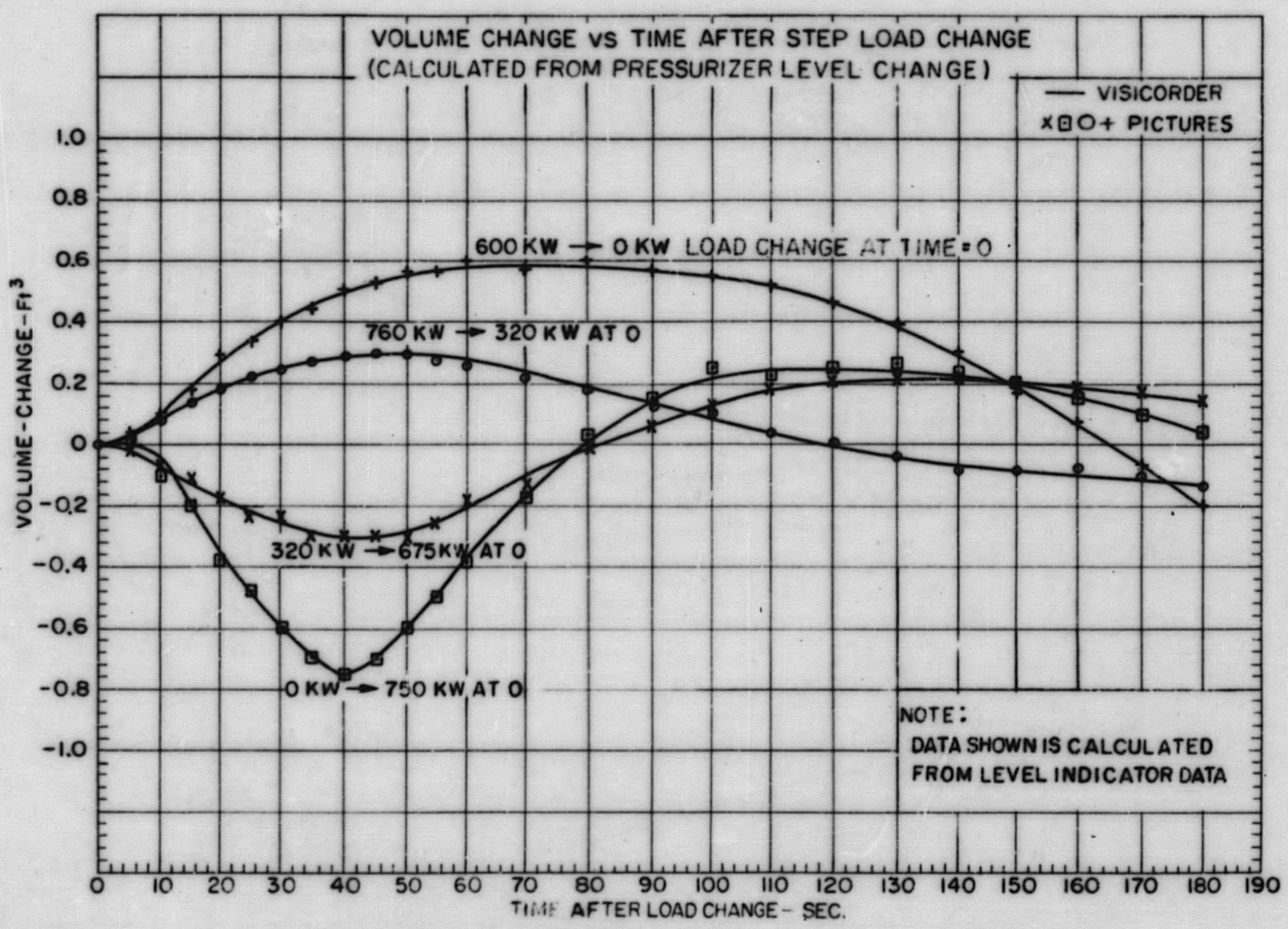

Figure 5.15. PM-2A Primary Coolant Volume Change Vs Time After a Step Load Change

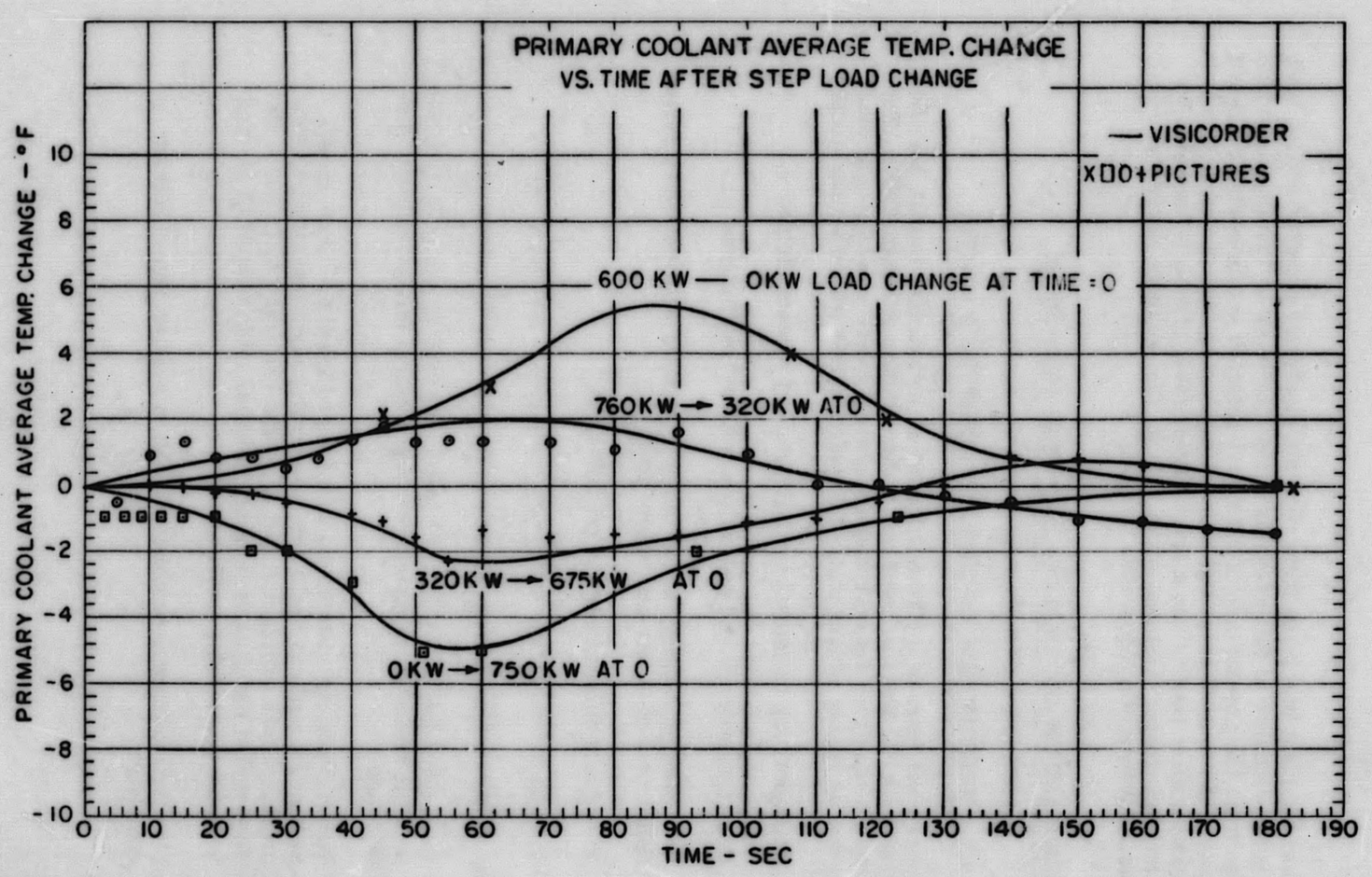

Figure 5.16. PM-2A Primary Coolant Average Temperature Vs Time After a Step Load Change

When the plant was taken from zero net electrical output to station load and in quick sequence to full available camp load (0 kw to 750 kw) the volume outsurge from the pressurizer of 0.75 cu ft resulted in a pressure decrease of 85 psia (1750 to 1665 psia) and an average temperature decrease of 5^{o}. When camp load is added from a stable power level of station load (320 kw to 675 kw) the volume outsurge was 0.3 cu ft, the pressure surge was -69 psia and the temperature decrease was 2.3^{o} F.

5.4 COMPARISON OF ANALOG AND TEST RESPONSES

5.4.1 DESCRIPTION OF ANALOG COMPUTER MODEL

The general form of the kinetic model of the primary loop is derived analytically for the SM-1 pressurized water reactor in APAE-38[9]. The simultaneous equations representing component behavior are programmed for solution by analog computer, and include the following considerations.

1. Transport lag of coolant through primary system piping.
2. Core temperature and pressure reactivity coefficients.
3. Heat storage capacity of fuel plates, primary and secondary system liquid, and of steam generator tubes.
4. Five group delayed neutron contributions.
5. Portion of core power generated outside fuel plates.

The significant assumptions made in the derivation include:

1. Core considered as a lumped system. Uniform power distribution, uniform fuel plate temperature, and uniform coolant velocity distribution.
2. Steam generator considered as a lumped system. Basic model assumes a uniform shell-side temperature corresponding to saturation, and a constant steam film heat transfer coefficient. Refined model recognizes superheat of shell-side temperatures and variable steam film coefficient.
3. Slug flow in piping, complete mixing in reactor vessel plenum chambers.

The applicability of this model form in representing the PM-2A is assumed because of the basic similarity between the SM-1 and PM-2A plants.

The analog circuit diagram for the PM-2A kinetic model is shown in Fig. 5.17. The derivation of the plant constants and the corresponding circuit potentiometer settings is presented in APAE-39.[4]

5.4.2 ANALOG RESULTS

In examining the discrepancies between model and plant response, the limitations of the PM-2A plant recording instrumentation should be remembered. This instrumentation is of the station operation type, designed for rugged use and nominal precision of measurement at steady state operation. The large size of thermocouple beads dictate a relatively large temperature response lag; thus the recording of a temperature change and return over a short time interval is displaced and foreshortened in relation to the actual variation. On the other hand, no allowances are necessary for measurement of analog model parameters since response lag of the computer recorder is insignificant.

Traces from the analog model for the PM-2A were made by the Sanborn recorder and are shown in Fig. 5.18. The load perturbations examined were:

Run 1	760 kw	- 320 kw
Run 2	600 kw	- 0 kw
Run 3	320 kw	- 675 kw
Run 4	0 kw	- 750 kw
Run 5	100%	- 5% of Design Power
Run 6	0%	- 100% of Design Power

5.4.3 COMPARISON OF TEST DATA WITH ANALOG RESULTS

A comparison is made between the analog calculations and test data (Fig. 5.19) for the load change from available camp load (760 kw) to station load (320 kw). Peak test values of temperature, pressure and volume change are shown and compared with analog calculations in Table 5.8.

The analog trace shows that the average primary coolant temperature starts at an initial temperature and rises to a maximum of 3^{o} in 55 sec. The temperature then starts to return to the initial reading at the rate of 1.2^{o}/min. The test data for the average primary coolant temperature shows the temperature starts at a reference level and rises to a peak of 2^{o} in 65 sec. The temperature then decreases at the rate of 1.7^{o}/min.

The peak temperature measurements are expected to be less than the analog traces because of the time lag in the thermocouple.

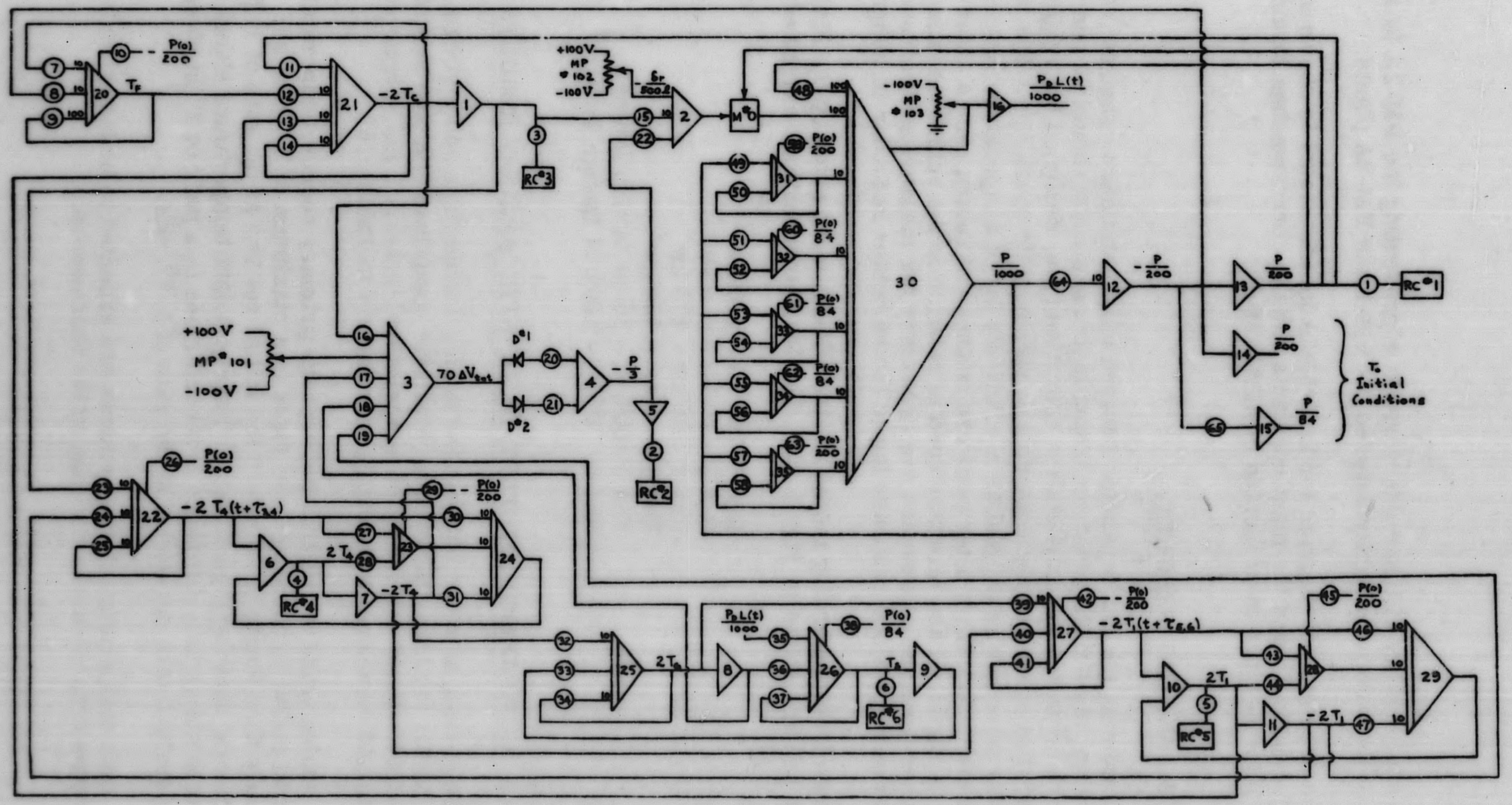

Figure 5.17. Electronic Analog Computer Circuit Diagram for Plant Kinetic Model of the PM-2A

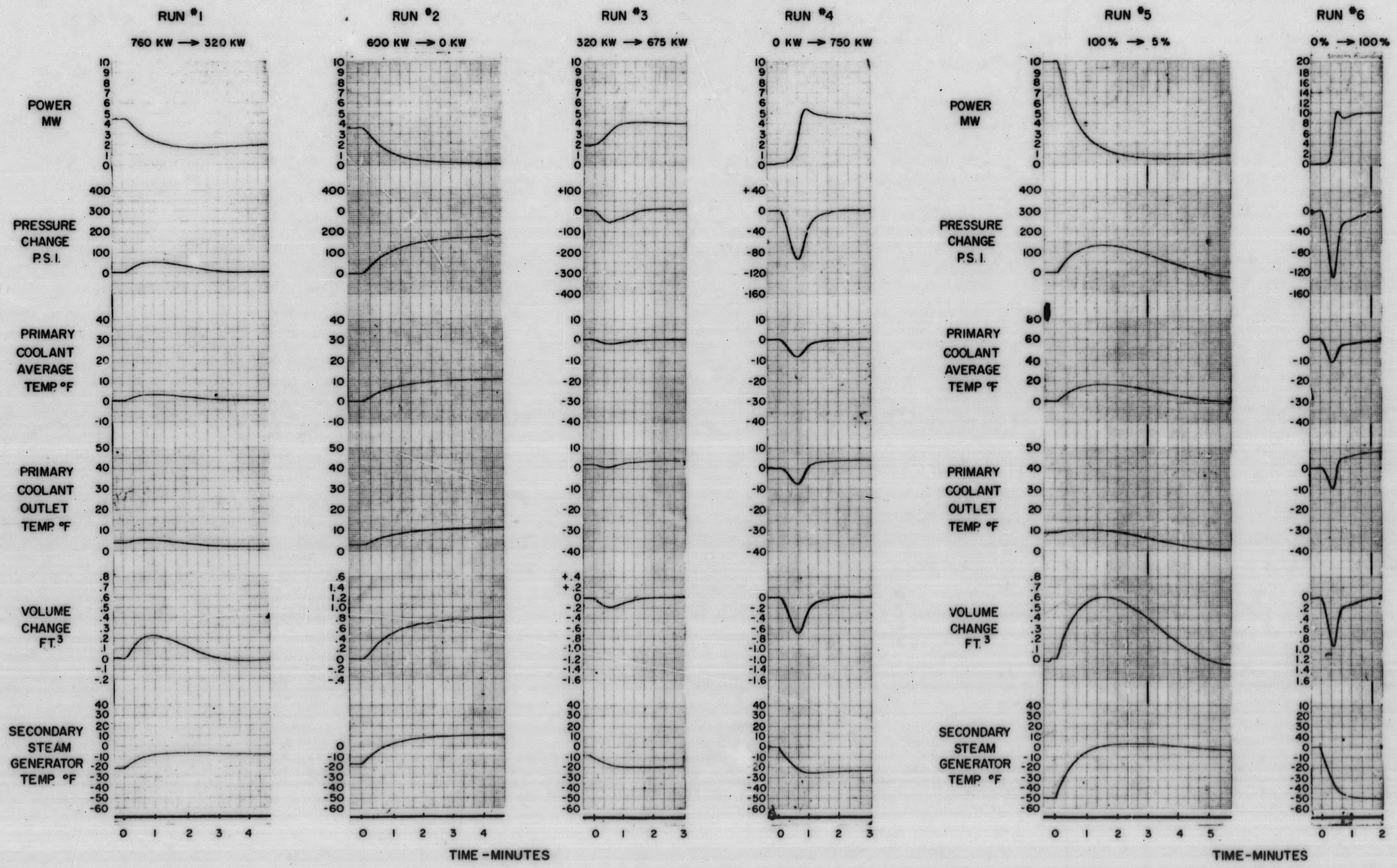

FIGURE 5.18

RESPONSE OF PM-2A ANALOG MODEL TO LOAD PERTURBATIONS

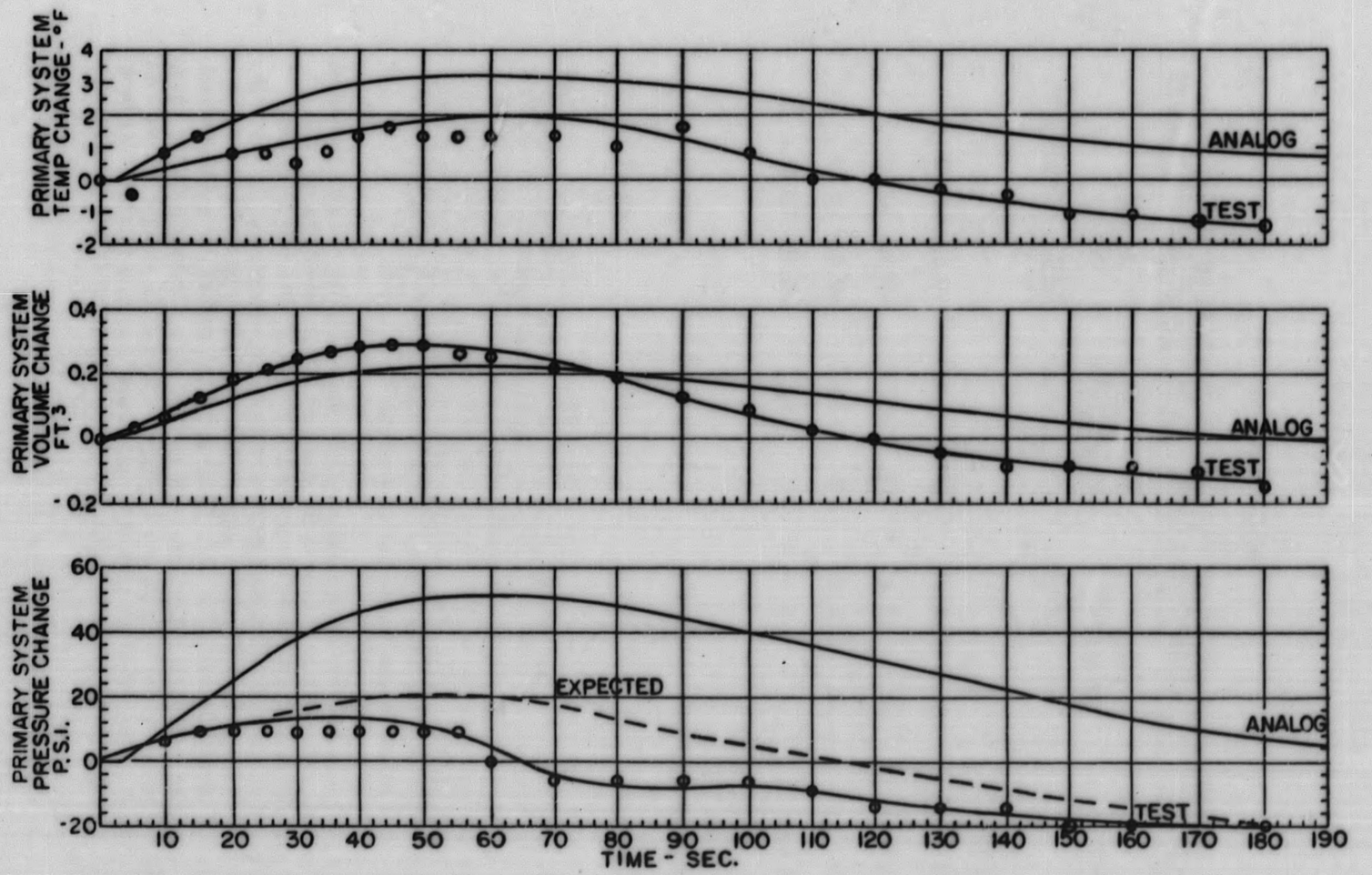

Figure 5.19. Comparison of PM-2A Test Data with Analog Data for Load Change 760 KW to 320 KW

TABLE 5.8

COMPARISON OF PEAK VALUES OF VARIABLES FROM PM-2A LOAD TRANSIENT TEST WITH ANALOG CALCULATED VALUES

Load Change	Temp. Change(^{o}F)		Pressure Change (Psia)		Volume Change	
	Test	Analog	Test	Analog	Test	Analog
Test Conditions						
600 to 0 kw	+5.4	+9.5	+120	+175	+0.58	+0.77
760 to 320 kw	+2.0	+3.2	+12	+52	+0.30	+0.23
329 to 675 kw	-2.3	-2.0	-69	-55	-0.31	-0.18
0 to 750 kw	-4.8	-8.0	-85	-78	-0.75	-0.68
Design Conditions						
2000 kw to 90 kw	-	+17.0	-	+142	-	+0.60
0 kw to 2000 kw	-	-11.0	-	-130	-	-0.95

The analog shows that the volume starts at an initial reading, reaches a maximum increase of 0.23 cu ft in 60 sec and then decreases at the rate of 0.11 cu ft/min until the system stabilizes about the initial reading. The test data indicates an inflow of 0.30 cu ft in 50 sec and then decreases at the rate of 0.21 cu ft/min. For the time covered during this test the volume surge was still negative after 3 min, however indications are that the pressurizer level would return to the initial reading.

The pressure rises to a peak value of +52 psia after 60 sec as calculated by the analog. The rate of decrease for the next 2 min was 23 psia/min. After 3 min the analog indicates the pressure will return to initial system pressure. Test data shows a peak pressure surge of +14 psia in 35 sec with a marked drop off so that pressure change has reached zero at 65 sec and then a fairly steady decrease to -20. This is not the general shape one would expect from the pressure change vs. time curve. One would expect the curve to follow the shape of the volume and average temperature change curves. As seen in Fig. 5.19 the expected maximum pressure increase is about +21 psia. This value is within the range of accuracy of measurement of the primary

system pressure. The analog peak positive pressure rises are in the order of magnitude of twice the test peak pressure. The analog peak negative pressure rises are in the same order of magnitude as the test. This is the same result experienced between SM-1 plant and SM-1 analog simulation.

Load perturbations involving 100% of design load are shown in Fig. 5.18. For the condition of dropping 95% of design load (100% to 5%) the analog indicates a positive surge in the primary system average temperature of 17° F (525.8° F), an inflow to the pressurizer of 0.60 cu ft and a positive pressure surge of +142 psia from 1750 to 1892 psia. Tests indicate the peak will only be approximately 1830 psia. For an instantaneous increase in load from 0% to 100%, which in all probability would be a ramp increase, the analog indicates a decrease in primary system average temperature of 11.0° F, from 508.8 to 497.8° F, an outsurge from the pressurizer of 0.95 cu ft and a drop in pressure from 1750 to 1620 psia (-130 psi).

A comparison of the above expected plant parameter variations and the alarm settings recorded in Table 2.7 show that no scram settings would be reached and that only two alarms might be tripped. Since test shows that the positive pressure surge is conservative it is not believed that the high pressure alarm will actually sound. It is also believed that the plant will not encounter an instantaneous step increase in plant load of 100% of design, so the low pressure alarm will not sound either in this transient.

5.5 PERFORMANCE OF DECAY HEAT REMOVAL SYSTEM - TEST TP C-604

5.5.1 TEST OBJECTIVES

Test TP C-604 was prepared to provide data to permit a thorough evaluation of the performance, for the critical first 20 min, of the auxiliary decay heat removal system following a primary system pump failure and reactor scram.

The heat generated by the decay of fission products after more than 1 hr of operation constitutes a significant source of heat that must be removed from the core after a loss of flow accident. Since the location of the steam generator does not supply sufficient thermal head to adequately remove this decay heat a separate decay heat cooling loop was installed. The loop is illustrated in Fig. 5.20 and a general description is provided in Sec. 2.5.7.

5.5.2 GENERAL TEST PROCEDURES AND OPERATING CONDITIONS

The general test method was to have the reactor critical and stabilized with the plant electrical load supplying maximum available camp load. Camp load was then removed and the primary coolant pump de-energized simulating a loss of flow accident.

Three methods were used to record data at Camp Century during these tests.

1. Visicorder

2. 35 mm Still Pictures

3. Visual Observations and Recordings

The visicorder was connected to the sensing probes and in parallel with the monitoring instrument on the control panel. The parameters listed in Table 5.7 were monitored during the decay heat removal testing.

In addition to the parameters listed in Table 5.7, four "strap-on" resistance thermometers were strapped to the decay heat removal piping loop. These were fixed as shown in Fig. 5.20 to read the inlet and outlet temperature of the reactor vessel and the inlet and outlet temperature of the cooling coil. For comparison of test data with the analog model, these temperatures were designated as follows:

Designation	Parameter
T_3	Reactor outlet temperature
T_4	Coil inlet temperature
T_5	Coil outlet temperature
T_6	Reactor inlet temperature

5.5.3 EXPERIMENTAL RESULTS

The decay heat removal test was performed on November 22, 1960, and again on March 7 and 8, 1961 from a camp load of 4.45 MWt. Due to uncertainties regarding the capabilities of the standby power to assume the full camp load satisfactorily as a step function, the load was transferred by sequential steps. First the camp load, and then the station load, was trans-

ferred to the standby power and then the primary coolant pump was shut off. The delay times between transfer of camp and station load and pump cut-off are shown in Table 5.9 along with other pertinent load parameters.

TABLE 5.9

SUMMARY OF PM-2A OPERATIONS FOR DECAY HEAT REMOVAL TESTS

Test Date	Time Delay to Remove Full Load	Power Output	Time at Power Before Pump Shut-off	Time of Test
Nov. 22, 1960	1 min	4.45 MWt	10 hr	10 min
Mar. 7, 1961	1 min	4.45	24 hr	1 min 42 sec
Mar. 8, 1961	5 min	4.45	24 hr	7 min 10 sec

Temperature measurements made at three points around the loop have been plotted in Fig. 5.21 for the test of Nov. 22, 1960. Data from the photographs, visicorder traces, and visual measurements have been plotted as a function of time in Fig. 5.22 and 5.23 for the March 7, 1961 test and in Fig. 5.24 and 5.25 for the March 8, 1961 test.

From Fig. 5.21 the time of travel of fluid between points of measurement T_5 and T_6 (a distance of 24 ft) can be estimated as 12 sec. From this the velocity was estimated as 2 ft/sec. Based on this velocity and a temperature differential across the coil of 265° the heat transferred to the spent fuel tank is 1,350,000 Btu/hr.

In general the visicorder data as plotted in Fig. 5.22 and 5.24 is as expected. Primary coolant pressure has the general shape of both pressurizer level and primary coolant temperatures. Figure 5.24 indicates that there is flow in the primary piping and because of an apparent ΔT across the steam generator that the steam generator is acting as a heat sink. Steady state measurements indicate that at no load, there exists a 7 degree ΔT across the steam generator while there is no difference between primary coolant outlet and primary coolant average temperature. If this constant error of 7 degrees is removed from the steam generator temperature difference the plot is in agreement with primary coolant temperature differences. The apparent circulation which has dropped the steam generator temperature the same amount as the primary coolant temperature in a time period of 7 min ($35^{\circ}F$) is probably due to lingering effects of pump coastdown. It is not

likely that it is due to natural circulation as the heat sink (steam generator) is located below the level of the core and no thermal head can be developed to drive natural circulation.

When the cooldown rate from these short term tests is projected over an hour the rate is approximately -300°/hr which is more rapid than good practice dictates. If this projection is correct some severe thermal stresses can be introduced into return pipe-vessel connection. Work is in progress to substantiate acceptable cooldown rates under separate subtask (6.10) of the Program for Engineering Support and Development of Army PWR Power Plants.[10]

5.6 ANALYSIS AND COMPARISON OF TEST DATA WITH ANALOG COMPUTER RESULTS

5.6.1 ANALOG MODEL

The analog model used to simulate the problem of decay heat removal is the same as presented in APAE Memo-207[11] except for minor corrections and changes in some of the system parameters. The model specifically treats that part of the problem where the pump has finished its coastdown and natural circulation has become the dominant driving force in cooling the core (approximately 5 sec after loss of pump). The problem continues until temperatures in the system are decreasing.

The model makes the following assumptions in the analysis of the core.

A. The time of coolant transient through the core is small compared to the magnitude of other delays in the system.

B. The temperature difference across the core can be effectively replaced by the arithmetic mean temperature difference.

C. Fuel plates are considered to be at a mean temperature and the difference between the mean fuel plate temperature and the mean coolant temperature is proportional to the heat transferred. The proportionality factor is the heat transfer coefficient times the heat transfer area.

Because the PM-2A steam generator is located below the level of the reactor core a cooling coil and its related piping was added to the primary system. The equations describing the coolant flow about the loop are derived by application of fundamental principles to increments of piping. The sum of

forces acting to retard the motion of a slug of fluid must equal the change of momentum of the fluid. The forces considered are gravity, friction and fluid inertia. These forces are equated to the pumping pressure to maintain flow in the loop.

To apply this to the reactor model, the following assumptions were made.

1. The coolant is an incompressible fluid under the existing conditions.

2. Increments of pipe length are sufficiently short so that the integral around the loop may be replaced by a summation over the elements of length.

3. The density of the fluid at a specific temperature can be measured relative to a reference density (ρ_o) by the following relation involving the temperature expansivity of the fluid.

$$\rho_1 \ (t) = \rho_o - \gamma T_1$$

where ρ = density of fluid lbs/ft^3

γ = volume coefficient of expansion for primary coolant, ft^3/^{o}F

4. At any instant the temperature varies linearly between two adjacent points.

The differential equations describing the behavior of the loop during a loss of flow have been programmed for the analog. The schematic of the model is shown in Fig. 5.26. The formulation of the loss of flow analog program is presented in reference (10). A listing of servo-set potentiometer settings employed to obtain analog solutions to the PM-2A decay heat removal problem is given in Table 5.10. Both the numerical value and the corresponding plant symbols are indicated. Plant system parameters have been tabulated in Table 5.11.

A time scaling factor of one computer second equal to 5 real seconds was chosen for this problem. This choice was dictated by the need to keep solution time short enough to prevent errors due to the electronic multipliers and long enough to feel the effects of piping delays between components.

An amplitude scaling factor of unity (one volt per physical unit) was used for ease of scaling and interpreting computer results. Required quantities were generated. A temperature of 150^o F was arbitrarily assigned the value of zero volts. Temperatures above and below this level were generated with respect to this reference.

TABLE 5.10

POTENTIOMETER SETTINGS FOR THE PM-2A DECAY HEAT REMOVAL ANALOG SIMULATION

NO.	VALUE	QUANTITY	NO.	VALUE	QUANTITY
10	0.0600	$\frac{1}{5}(150^{O} - T_s)$	54	0.3786	1C T_E/5 (339.3)
20	0.4000	4/10	55	0.4224	10 Ro/WE
21	0.4000	4/10	56	0.4949	10($u_a A_E$)WeCe
26	0.4606	2.5x250x(Lf-Ln)/N	57	0.4802	$(\Delta\rho_f)_o$ /N
30	0.2000	2/10	58	0.2297	625 γ Lm/N
34	0.1000	$1.2/(\tau\ 3,4/5)^2$	59	0.1501	1250 γ Lc/N
36	0.1734	$3/\tau\ 3,4$	60	0.5345	625 γ Lh/N
38	0.1827	10/Wf Cf	61	0.3909	625 γ Lh/N
39	0.6005	5 ($u_c A_c$)/Wf Cf	62	0.8339	625 γ ($L_I + L_F$)/N
40	0.8680	1C T_F(O)/5 (586^{O}F)	63	0.0044	$5/\tau\ 6,1$
41	0.6005	5 ($u_c A_c$)/Wf Cf	64	0.0044	$5/\tau\ 6,1$
42	0.1323	5($u_c A_c$)/$W_c C_c$	65	0.7000	1C T 1/5
43	0.1237	5 Ro/.4 W_e	66	0.0000	1C T_5 /5
44	0.7320	1C Tc/5(516)	67	0.2000	2/10
45	0.0263	$10/\tau\ 2,3$	69	0.0364	$1.2\ (\tau_{5,6}15)^2$
46	0.0132	$5/\tau\ 2,3$	70	0.0364	$1.2\ (\tau_{5,6}15)^2$
47	0.0132	$5/\tau\ 2,3$	71	0.1047	$3/\tau_{5,6}$
48	0.7572	1C T_3(O) /5(528.6^{O}F)	72	0.1047	$3/\tau_{5,6}$
49	0.0021	(1-α)50/5WcCc	73	0.1000	$1.2/(\tau_{3,4}15)^2$
50	0.0050	5/1000 To F.G.	74	0.1734	$3/\tau_{3,4}$
52	0.1323	5 ($u_c A_c$)/WcCc	75	0.2626	Potentiometer No. (48) x $6/\tau_{2,3}$

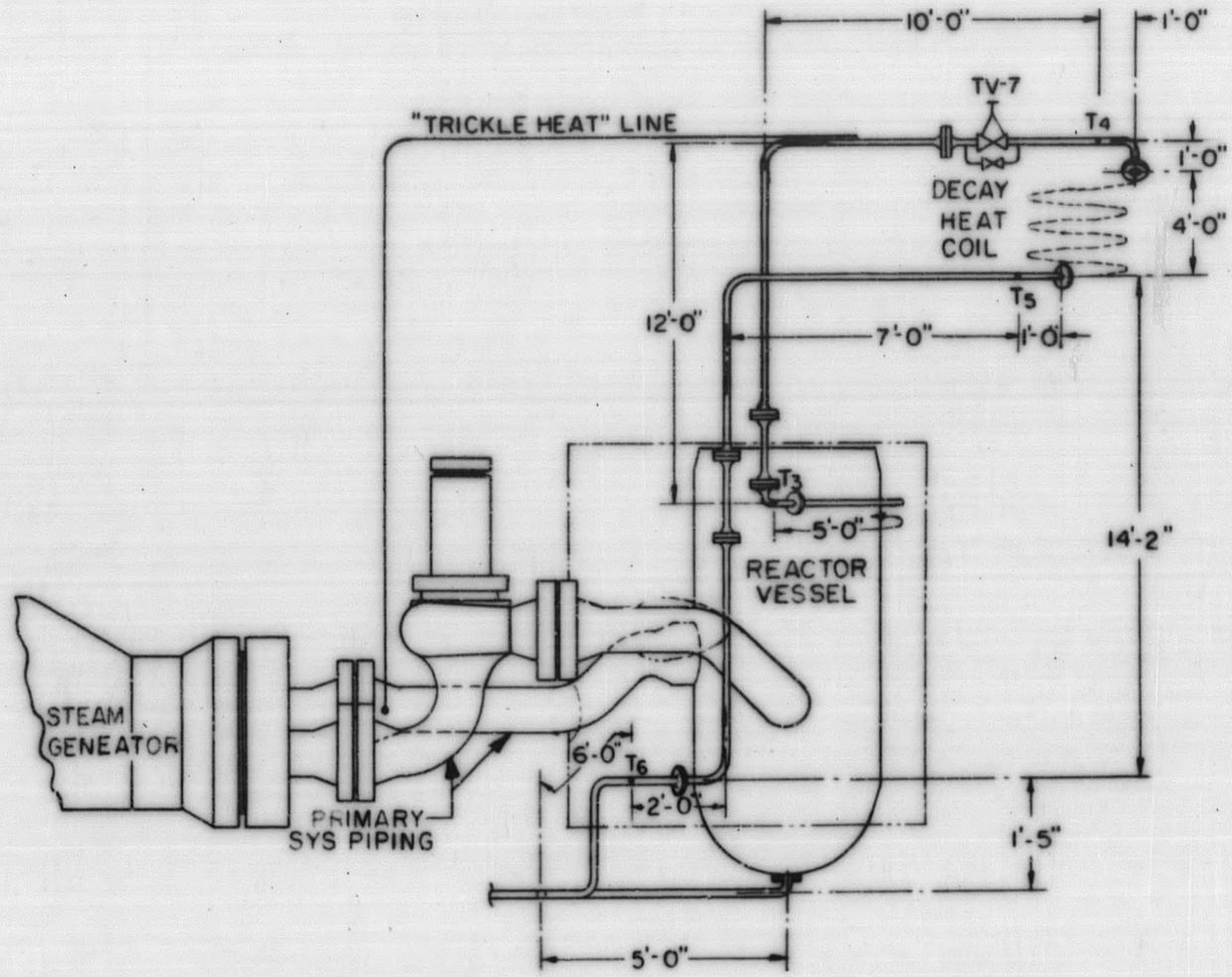

Figure 5.20. Sketch of the PM-2A Decay Heat Removal System

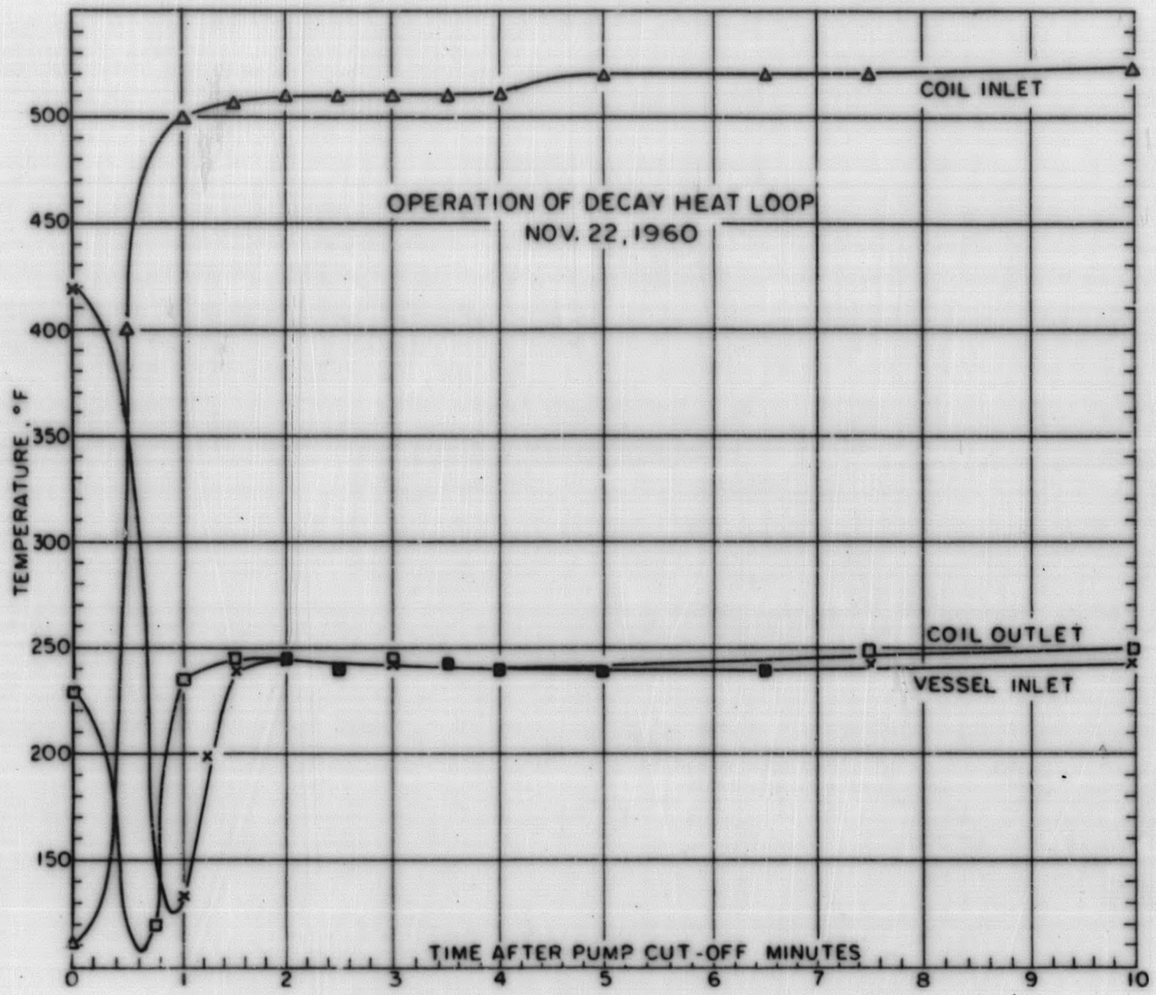

Figure 5.21. Operation of the PM-2A Decay Heat Removal Loop on November 22, 1960

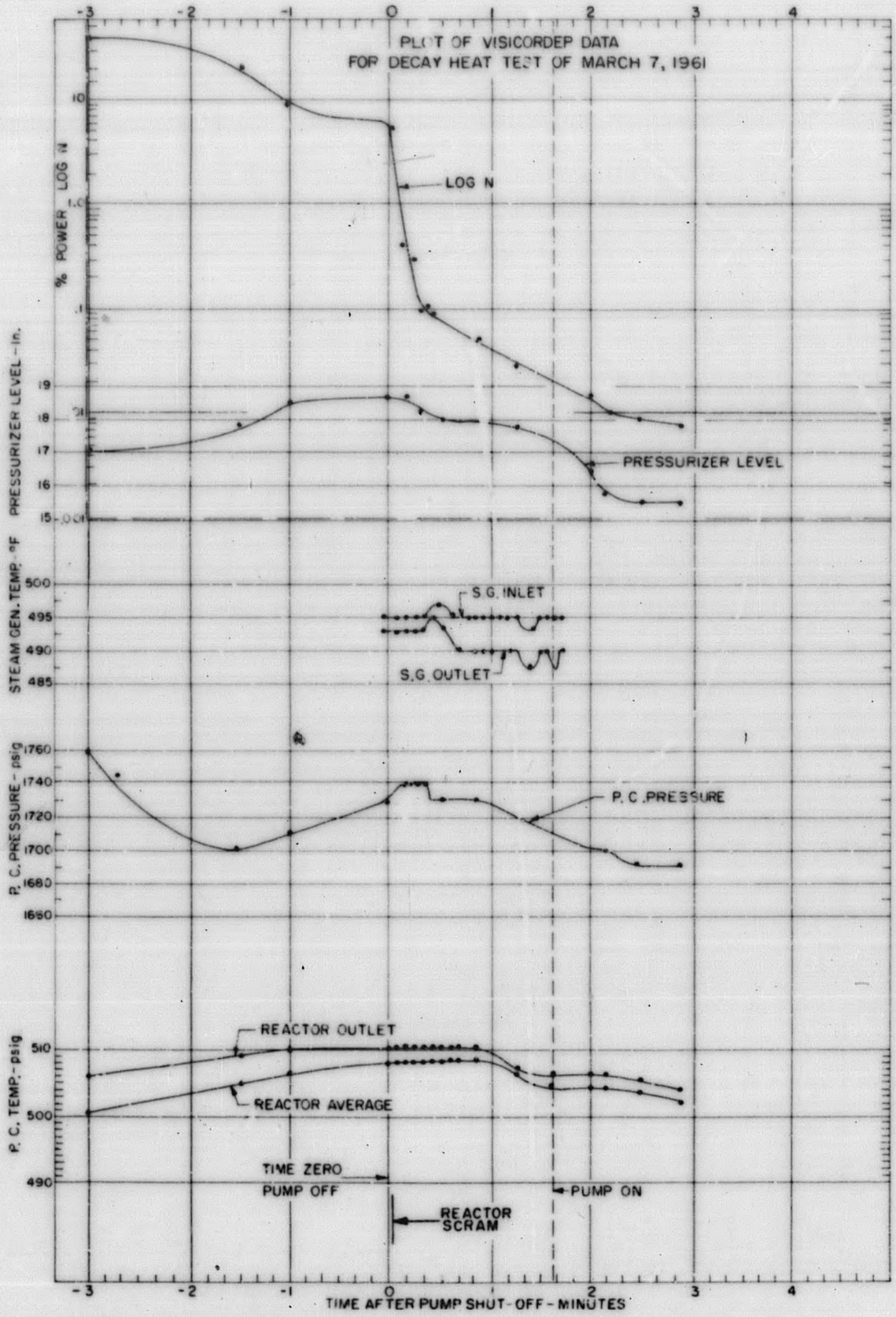

Figure 5.22. Plot of Visicorder Data for the PM-2A Decay Heat Removal Test of March 7, 1961

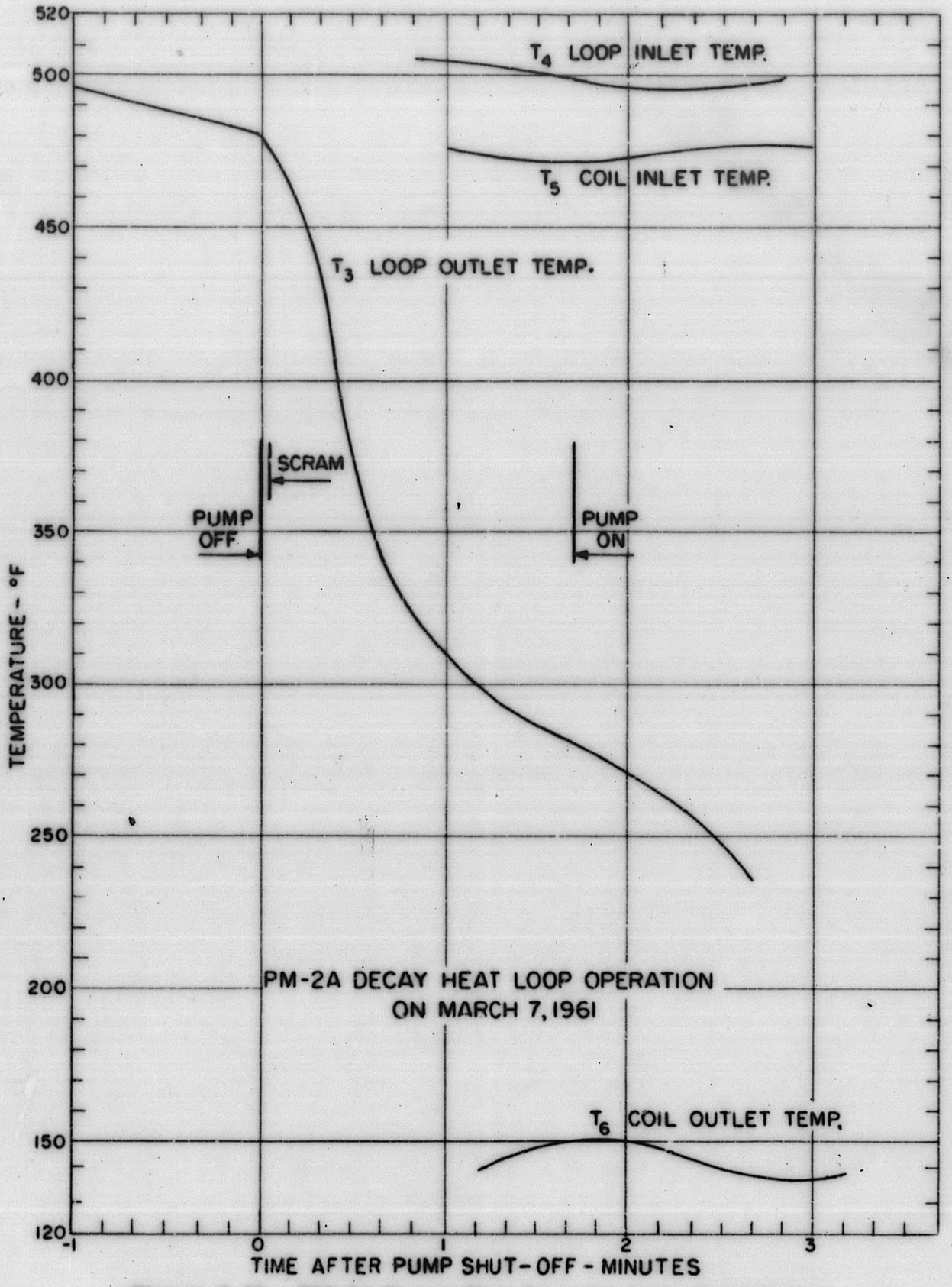

Figure 5.23. PM-2A Decay Heat Removal Loop Operation on March 7, 1961

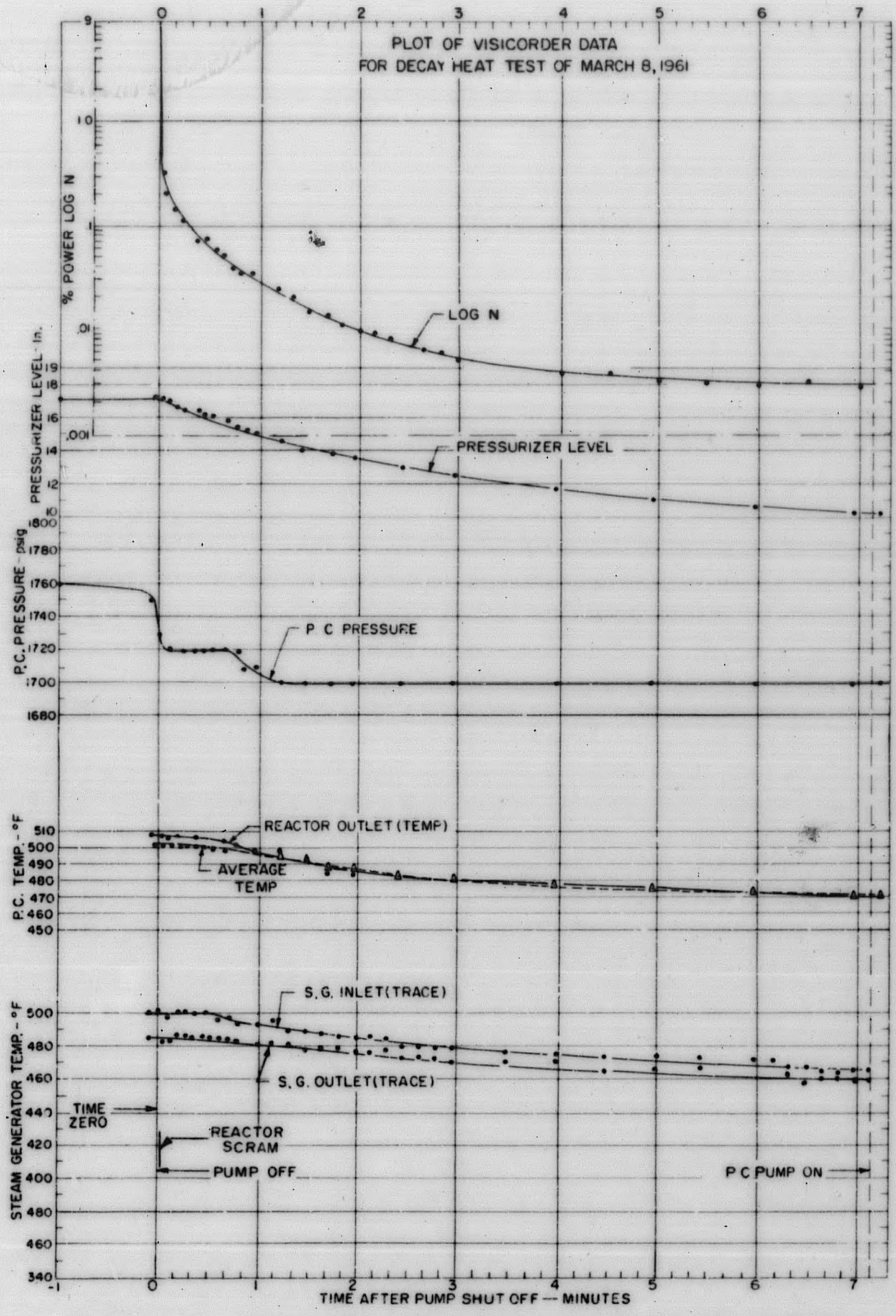

Figure 5.24. Plot of Visicorder Data for the PM-2A Decay Heat Removal Test of March 8, 1961

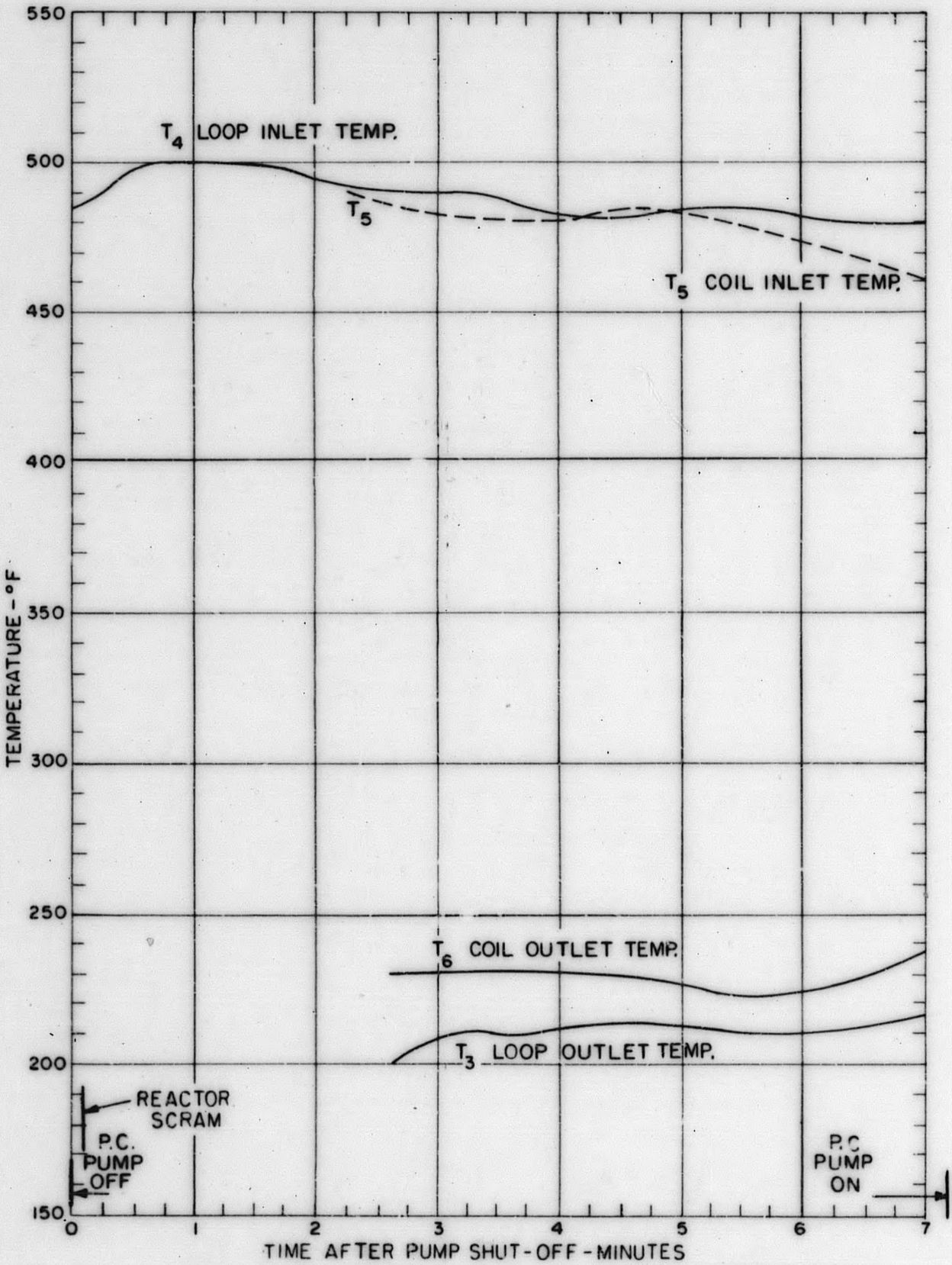

Figure 5.25. PM-2A Decay Heat Removal Loop Operation on March 8, 1961

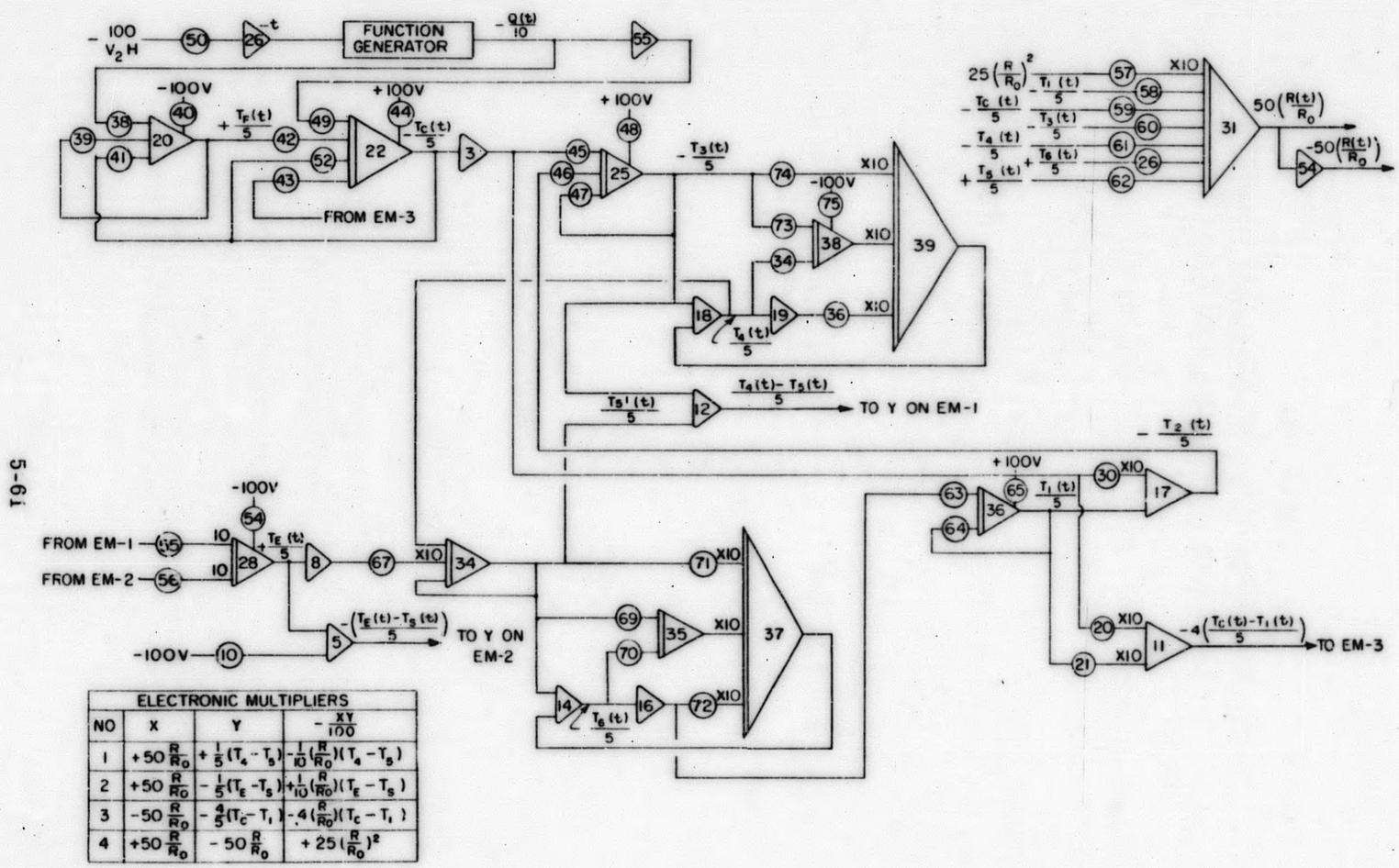

ELECTRONIC MULTIPLIERS			
NO	X	Y	$-\frac{XY}{100}$
1	$+50\frac{R}{R_0}$	$+\frac{1}{5}(T_4 - T_5)$	$-\frac{1}{10}(\frac{R}{R_0})(T_4 - T_5)$
2	$+50\frac{R}{R_0}$	$-\frac{1}{5}(T_E - T_S)$	$+\frac{1}{10}(\frac{R}{R_0})(T_E - T_S)$
3	$-50\frac{R}{R_0}$	$-\frac{4}{5}(T_C - T_1)$	$-.4(\frac{R}{R_0})(T_C - T_1)$
4	$+50\frac{R}{R_0}$	$-50\frac{R}{R_0}$	$+25(\frac{R}{R_0})^2$

Figure 5. 26. Analog Circuit Diagram - PM-2A Decay Heat Removal Model

TABLE 5.11

SYSTEM PARAMETERS FOR AN AUXILIARY DECAY HEAT REMOVAL SYSTEM FOR THE PM-2A

W_F =	429.7 lbs	$W_{6,1}$ =	1,138 lbs
W_C =	197.3 lbs	$W_{2,3}$ =	380.9 lbs
W_E =	52.42 lbs	$W_{3,4}$ =	17.3 lbs
C_F =	0.121 Btu/lb-^oF	$W_{4,5}$ =	52.4 lbs
C_C =	1.196 Btu/lb-^oF	$W_{5,6}$ =	28.64 lbs
C_F =	0.108 Btu/lb-^oF	L_M =	4.6 ft
$1/2(U_F A_F)$ =	6.244 Btu/^oF	L_C =	1.83 ft
$(U_E A_E)$ =	2.154 Btu/^oF	L_H =	13.03 ft
A_E =	27.76 ft^2	Li =	3.5 ft
A_F =	492.6 ft^2	L_F =	16.83 ft
$\sum i \frac{Li}{Ai} g$ =	351.98 ft^{-2} - sec^2	H(O) =	98.52 ft
(ΔP_F) =	338.08 lbs/ft^2	$\sum i \frac{Li}{Ai}$ =	66.75 ft^{-1}
Ro =	2.0 lbs/sec		
γ =	-0.0462 lbs/^oF	F(O) =	9.532 ft^3/sec

The analog model predictions were compared[12] with data taken during SM-1 start-up tests[13] at Ft. Belvoir. The comparison indicates resonable agreement between the predicted and measured quantities.

The model for the decay heat loop is compared with experimental data[14] from a simple natural circulation loop in APAE Memo-207[11]. The analog model compares favorably with experiment with a few exceptions. The analog model assumed a step increase in energy into the coolant whereas experimentally the heat is transferred to the coolant[14] by conduction. The

analog simulation also employs a pipe transport delay which is not a true representation of the actual conditions. As a result, the flow buildup is in error for the first few seconds until full natural circulation is achieved.

Despite the limitations, the analog simulation of the decay heat removal system of the PM-2A is the best available representation of the loop to compare with test results.

5.6.2 ANALOG RESULTS

The variations of parameters of major interest were recorded on the Sanborn recorder. These parameters are:

T_o - Average Core Temperature

T_2 - Core Outlet Temperature

T_3 - Vessel Outlet Temperature

T_4 - Coil Inlet Temperature

T_5 - Coil Outlet Temperature

T_6 - Vessel Inlet Temperature

The results of the analog runs for input conditions comparable to the March 7, 1961 test are shown in Fig. 5.27 and the March 8, 1961 test, Fig. 5.28.

5.6.3 ANALYSIS AND COMPARISON OF ANALOG RESULTS WITH TEST RESULTS

Test decay heat loop temperatures have been compared with the analog in Fig. 5.29 and 5.30. In general the test and analog predictions are of the same order of magnitude and the same general shape.

If one compares the test temperature and analog predictions for the test of March 7, 1961 (Fig. 5.29) for the duration of the test (1 min 42 sec) the reactor vessel outlet temperature (T_3) and analog follow in very close agreement. The coil inlet temperature (T_4) follows the general shape of T_3 but at a level 30^o below vessel outlet temperature (T_3). During this test the "strap-on" resistance element came loose from the pipe and was giving an

FIGURE 5.27

SANBORN TRACES FROM PM-2A DECAY HEAT LOOP ANALOG MODEL

(COMPARABLE TO MARCH 7, 1961 TEST)

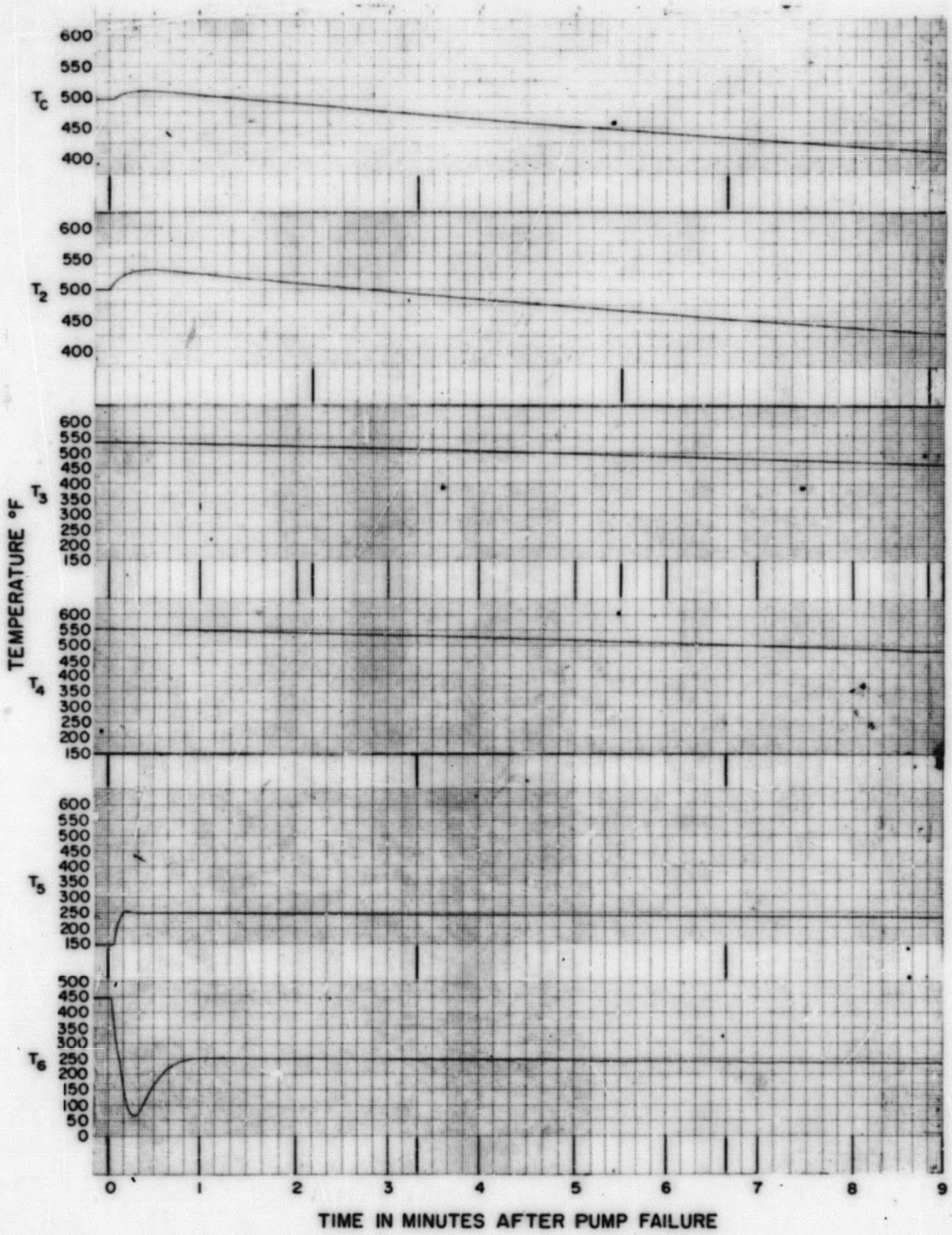

FIGURE 5.28

SANBORN TRACES FROM PM-2A DECAY HEAT LOOP ANALOG MODEL

(COMPARABLE TO MARCH 8, 1961 TEST)

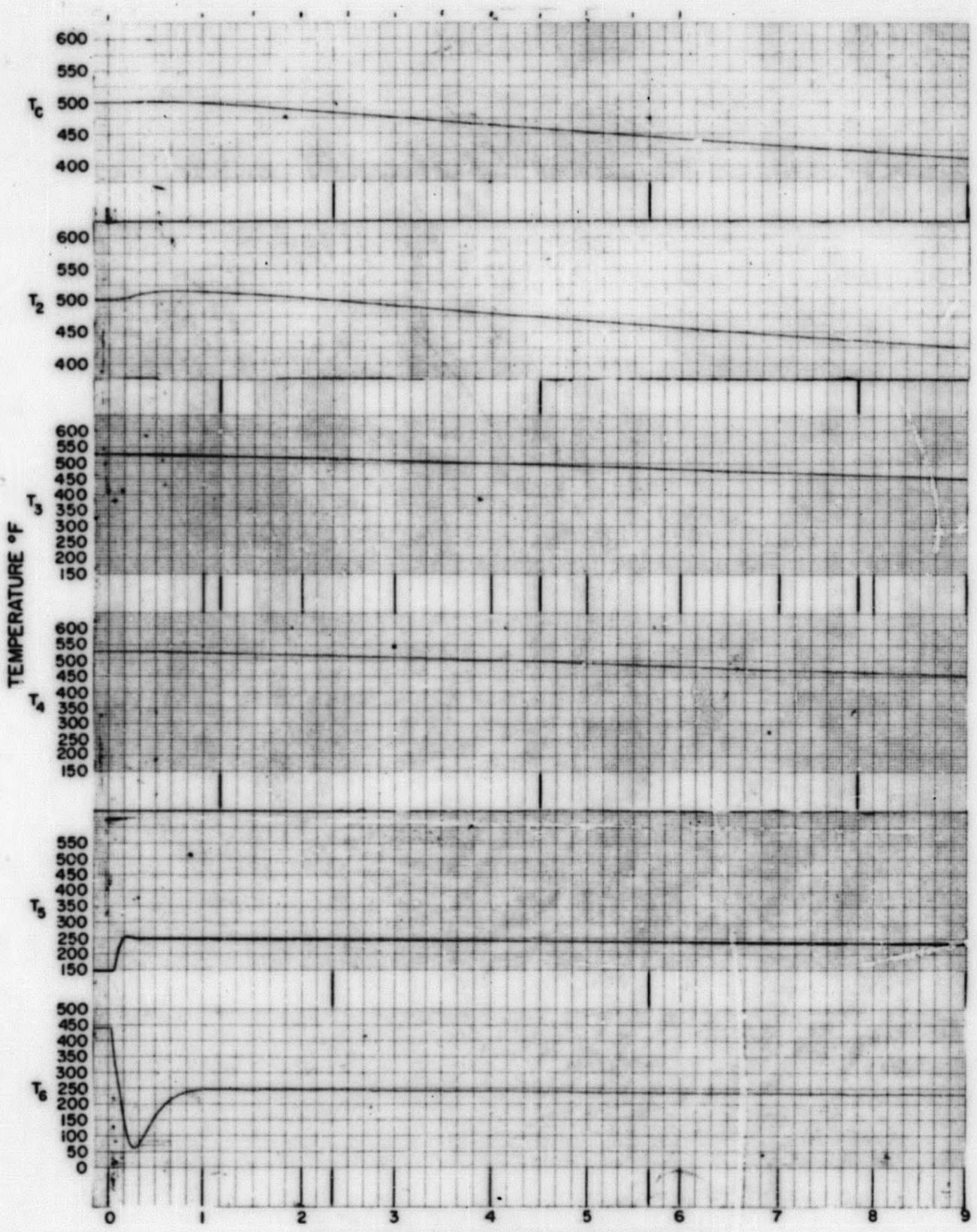

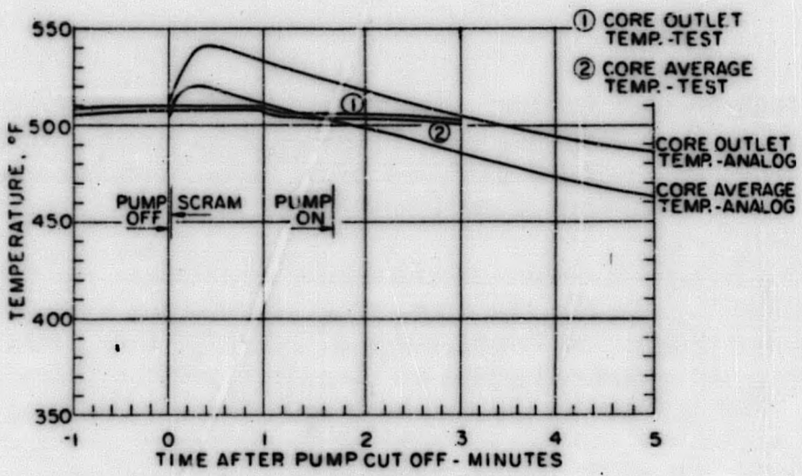

CORE TEMPERATURE-TEST OF MARCH 7, 1961

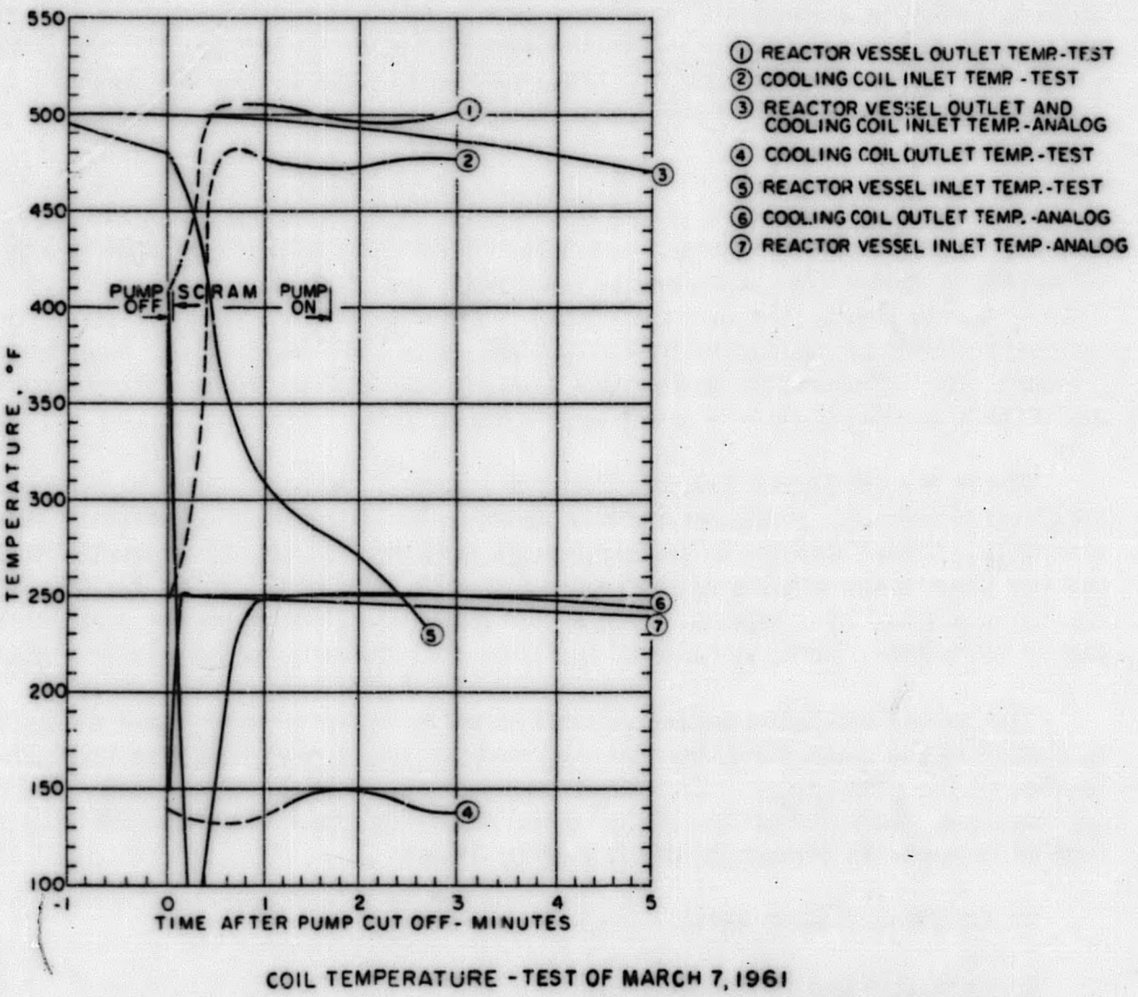

COIL TEMPERATURE - TEST OF MARCH 7, 1961

Figure 5.29. Comparison of Test Temperature and Analog Temperatures for the PM-2A Decay Heat Loop Test of March 7, 1961

erroneous temperature reading. The reactor vessel inlet temperature dropped from 480 to 280° F during test while in the same period the analog has dipped to a low of 65° and leveled at 250° in 1 min. The comparison indicates that this particular test was not of sufficient length to make valid conclusions.

Comparing test temperatures and analog predictions for the test of March 8, 1961 (Fig. 5.30), the shape of the curves are in reasonable agreement. Reactor vessel test temperature dropped 20° in a 3-min period (t = 1.5 to t = 4.5 min) as compared with a 20° drop in 3 min (t = 0 to t = 3 min.) for the analog. The test shows the coil inlet temperature decreased 40° in a 5-1/2-min period (t = 1.5 to t = 7 min) while the analog shows a 40° drop in 5 min (t = 0 to t = 5 min). During the test the coil outlet temperature dipped from 200° to a minimum of approximately 80 in 45 sec and reached a fairly constant temperature of 230° F after 2-1/2 min. The analog showed an increase from 150 to 250° and a steady decrease at the rate of 5° per 2-1/2 min for the coil outlet. Reactor vessel inlet temperature started at 420° F, dipped to approximately 80° in 45 sec and leveled at a fairly constant temperature of 210° after 3 min. The analog prediction of reactor vessel inlet temperature shows a similar dip from 440 to 65° and a leveling at 245° during a period of 1 min, and then a constant rate of decrease of 5° per 2-1/4 min.

Core average and core outlet temperatures (as measured in the legs of the primary system piping) show a decrease of 35° in 7 min. The analog shows an increase due to the influence of the decay heat and then a decrease at the rate of 60° in 6 min (t = 1 to t = 7 min). This shows the cooling rate in the primary piping as predicted by the analog, was two times faster than test cooling rate. These cooldown rates in both test and model appear excessive and should be adjusted to a more appropriate rate.

These comparisons indicate that the analog, although capable of predicting loop temperatures, requires further work to be completely consistant with the test data. There seems to be fairly good representation of temperature levels but the time of the analog always seems faster than test. Some of this lag can be explained by response time of the measuring instruments and thermal lag in the pipes. However not all the time differences can be accounted for.

The model has also neglected heat storage in the primary and decay heat system and has neglected the make-up water, which was continued for protection of the pump seal. The latter accounts for 17°/hr of cooling. It is advisable to conduct further study of the decay heat cooldown model with intent to revamp the model in the following areas:

1. Cooldown rates which appear to be excessive.

2. Heat storage in the system.

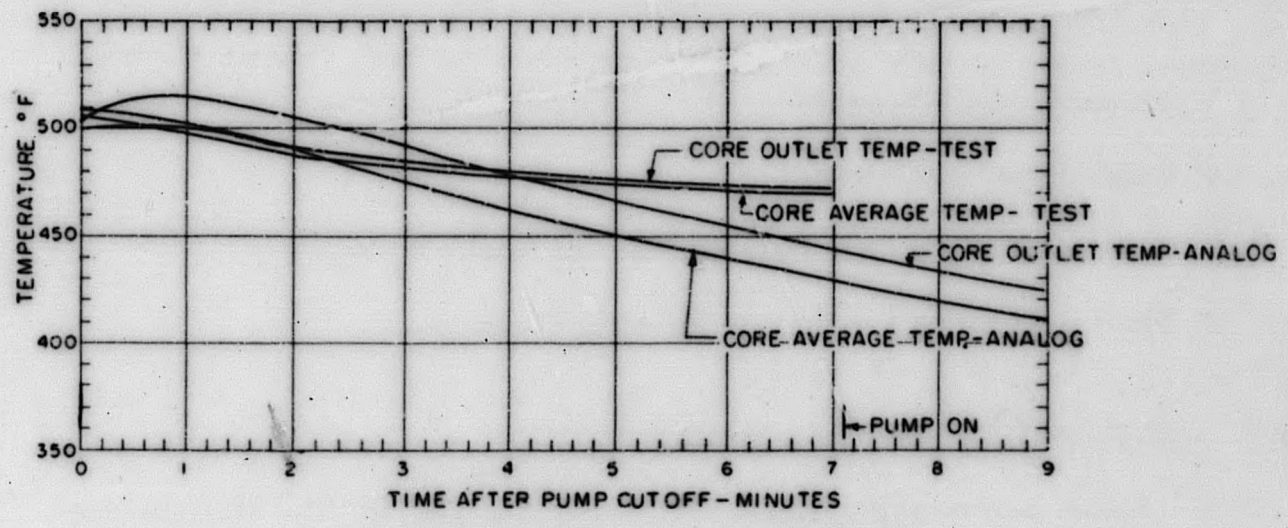

CORE TEMPERATURE-TEST OF MARCH 8, 1961

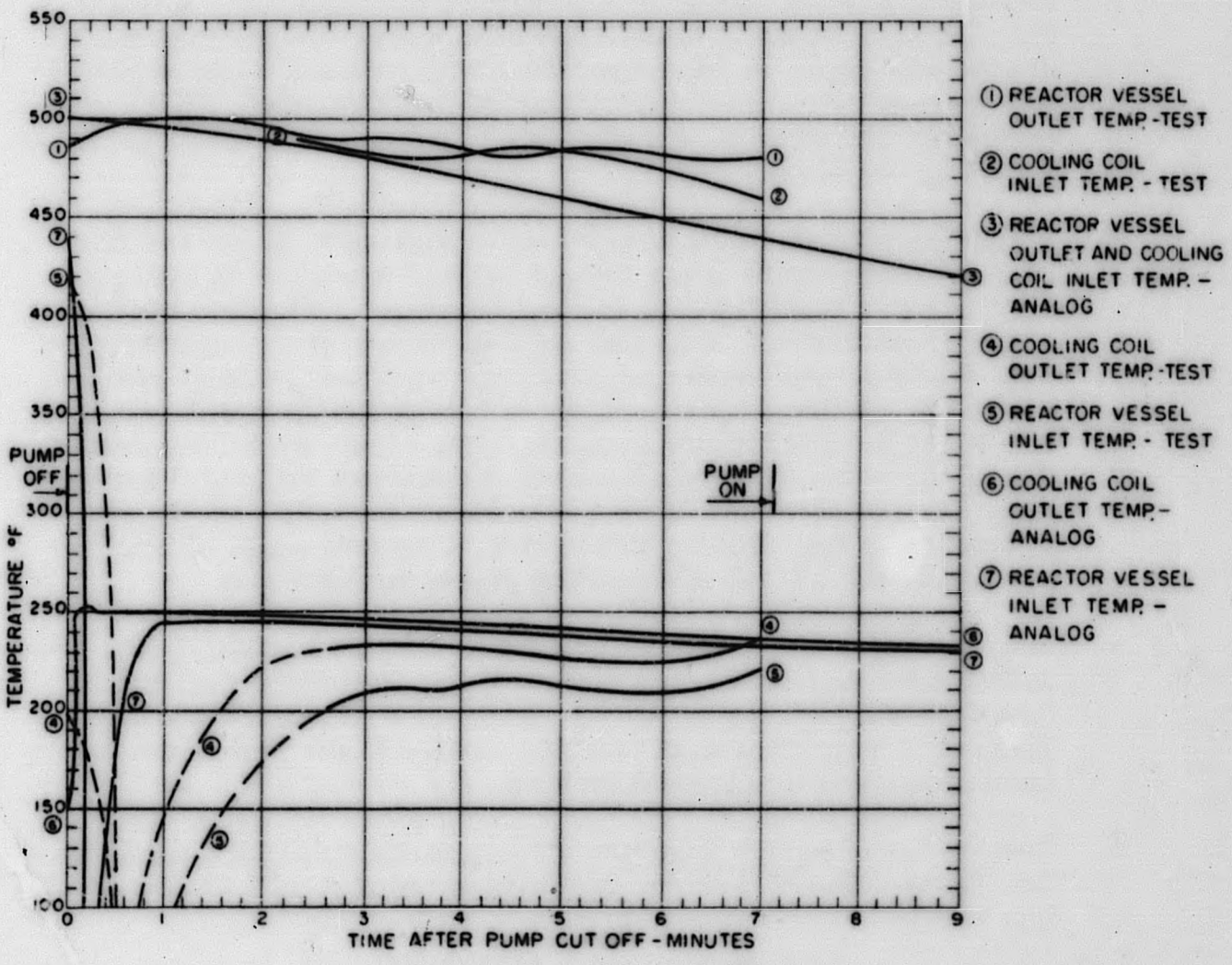

COIL TEMPERATURE-TEST OF MARCH 8, 1961

Figure 5.30. Comparison of Test Temperature and Analog Temperature for the PM-2A Decay Heat Loop Test of March 8, 1961

3. Primary make-up water.

4. Time scale of the model.

5. Possible temperature overshoots, especially T_5 and T_6.

6. Plant parameters to include as-built dimensions.

5.7 CONCLUSIONS AND RECOMMENDATIONS

1. There are no difficulties associated with bringing the primary system up to operating pressure and temperature.

2. The primary loop flow rate is 7% higher than anticipated, based on the air flow model tests and the manufacturer's tests of the pump, yielding a flow 15.4% higher than originally called for. This provides an opportunity to modify operating pressures for improved plant performance or increased life of the reactor pressure vessel as governed by the nil-ductility transition temperature (NDT). Some evaluation and study is needed to select the most beneficial change in operating variables.

3. Within the present limits of pressure permissible at low and intermediate temperature in the PM-2A reactor vessel, it is still possible to use a faster pressurization schedule for the first two-thirds of the pressurization, than that used in the operation reported here. This would permit complete pressurization of the primary system within the minimum time required to heat up the loop with less than 60% of the installed heater capacity. The result would be a relaxation of the criteria for replacement of individual heaters if and when some heaters burn out. This is significant because with the series connection of four heaters within each of the five banks of heaters, one heater failure will incapacitate 20% of the total set.

4. The flowmeters for steam and feedwater and the feedwater flow controller have very different response rates, resulting in apparent flow unbalance across the steam generator at any given instance. This could be an indication of slight hunting on the part of the feedwater system at this low power level.

5. Test values of temperature and volume changes during Load Transient Tests (TP-C601) are in favorable agreement with analog simulation results.

6. Analog pressure changes during loss of load transients are conservative by a factor of 2 when compared to test results. This is due to the conservative assumption of adiabatic compression of the steam pocket in the pressurizer.

7. Test pressure changes during increase in load transients are of the same order of magnitude as the analog simulation.

8. The decay heat loop cooled the primary system 35^{o} during the 7 min test. This is equivalent to 250^{o} to 300^{o}/hr, which is excessive.

9. Comparison of decay heat removal (TP-C604) test results with the analog results indicates that the decay heat loop is operating as predicted.

10. The short duration (2 and 7 min) of the decay heat removal tests is not conclusive enough to predict operation of the decay heat loop beyond 10 min after pump failure.

11. A study should be made to select the optimum method for taking advantage of the excess of actual primary coolant flow over required. The current large difference between maximum possible camp load and plant design load should also be taken advantage of in this study.

12. Further work is needed on the calibrations of the five temperature measuring elements in the primary loop and their circuits, using more complete calibration equipment than has been available at the site, in order to obtain useful engineering data from them. This should be accomplished with high temperature baths.

13. Load Transient Test (TP-C601) should be rerun at a later date when at least 75% and preferably 100% of design load is available.

14. Decay Heat Removal Test (TP-C604) should be rerun for a duration of 30 min to 2 hr.

15. A thermal stress study should be undertaken to establish a maximum system cooldown rate.

16. Further work should be undertaken to control the cooling capabilities of the decay heat loop so as to establish a cooldown rate, which is within the allowable set by the thermal stress criteria.

5.8 REFERENCES (SECTION 5)

1. Matthews, F. T., "Results of the Experimental Flow Distribution Program for the PM-2A Reactor - Summary Report," AP Note 266, Alco Products, Inc., May 31, 1960.

2. Instruction Manual for Pump, Serial No. 359, 157, Byron Jackson Division of the Borg Warner Corporation.

3. Richards, W. M. S., "Primary System Thermal and Hydraulic Performance During Heat-up of the PM-2A Reactor Plant", AP Note 323, Alco Products, Inc., February 15, 1961.

4. "Design Analysis for a Prepackaged Nuclear Power Plant for an Icecap Location," APAE No. 39, January 15, 1959.

5. "Standards of the Hydraulic Institute," Tenth Edition, 1958 Revisions, Hydraulic Insitute, New York .

6. Keenan, J. H. and Keyes, F. G., "Thermodynamic Properties of Steam," John Wiley & Sons, Inc., New York, 1936.

7. Krause, P. S., "Single Element Flow Tests For Type 3 (SM-2) Fuel Elements in SM-1, SM-1A, and PM-2A Cores," APAE Memo - 279, November 27, 1961.

8. Davidson, S. L., Segalman, I., "Thermal Analysis of Type 3 Elements in the SM-1, SM-1A and PM-2A Cores," APAE-105, March 30, 1962.

9. Brondel, J. O., Tomonto, J. R., "Plant Transient Analysis of the APPR-1 by Analog Computer Methods," APAE No. 38, August 1958.

10. "Fiscal Year 1962 Program Plan for Engineering Support and Development of Army Pressurized Water Reactor Plants," AP Note 378, Alco Products, Inc., September 6, 1961.

11. Tomonto, J. R., "Analysis of Auxiliary Decay Heat Removal by Analog Computer Methods," APAE Memo-207, October 1959.

12. Tomonto, J. R., "Analysis of the Decay Heat Removal Problem for the SM-2 by Analog Computer Methods," APAE Memo-198, June 1959.

13. Meem, J. L., "Initial Operation and Testing of the Army Package Power Reactor APPR-1," APAE No. 18, August 1957.

14. Alstad, C. D., Isibin, H. S., Amundson, N. R., "The Transient Behavior of Single-Phase Natural Circulation Water Loop Systems," ANL-5409, March 1956.

6.0 RADIOCHEMISTRY MEASUREMENTS AND ANALYSES

The objective of the radiochemistry test series is to accumulate data which will be useful in developing methods for predicting, controlling, and ultimately reducing primary system activity and radiation levels. In addition to satisfying the long term goal, the data from these tests are of value in the areas of health physics, reactor decontamination, and defective fuel element detection. The tests which are being performed at the PM-2A are:

Test C200-Fission Product Monitoring

Test C202-Measurement of Radiation Levels from Primary System Components During Reactor Shutdown

Test C203-Sampling of Primary System Filterables and Non-Filterables for Radiochemical and Chemical Analyses

Test C213-Short-Lived Activity and Decay Rates of Primary System Filterables and Non-Filterables

6.1 FISSION PRODUCT MONITORING

The objective of this test (C200) is to monitor, on a routine basis, the fission product activity level of the PM-2A primary coolant. This is accomplished by routinely determining the gross iodine activity level of the primary coolant. A relatively low radioiodine activity level, varying in direct proportion to the power level, would indicate the presence of U^{235} contaminated fuel plate surfaces and/or extremely small fuel element defects which release fission products to the coolant. A sudden increase in the gross iodine concentration would be indicative of fuel element defect.

The primary coolant gross iodine activity level is determined by an isotopic exchange technique. The active iodine in a coolant sample is exchanged for inactive iodine by contacting the coolant sample with preformed AgI. Before mixing the coolant and the AgI, all the radioiodine in the sample is converted to periodate (IO_3^-) followed by reduction to iodide (I^-). This step insures maximum exchange between radioactive and stable iodine. (1)

The coolant sample is subjected to a lanthanum carbonate scavenge to remove as much non-radioiodine activity as possible. The treated sample is added to the AgI precipitate and the two materials are intimately mixed. On mixing the radioactive iodide exchanges for the inactive iodide in the AgI.

This exchange may be represented by the equation

$$AgI + I^* \rightarrow AgI^* + I^-$$

where I* indicates radioiodide. The liquid is decanted and the AgI precipitate is counted in a standard reproducible geometry exactly 45 minutes after sampling.

The results of the analysis, expressed as disintegrations per minute per milliliter of coolant (dpm/ml), are calculated from the equation

$$R = 1/14 \frac{DS}{CV}$$

where

R = gross iodine coolant activity level, dpm/ml

D = decay rate of $Sr^{90} - Y^{90}$ standard, dpm

S = Count rate of AgI precipitate, cpm

C = count rate of $Sr^{90} - Y^{90}$ standard, cpm

V = sample volume, ml

1.14 = correction factor for average radioiodine recovery of 87%.[2]

The gross iodine data obtained from November, 1960 to April, 1961 is given in Table 6.1

From the data in Table 6.1 it can be seen that the coolant gross iodine activity levels do not correlate directly with reactor operation. A low iodine activity level of 1302 dpm/ml was obtained after 205 hours of operation at a relatively constant power level (log N = 45%) while a high value of 7860 dpm/ml was obtained after 67 hours of operation at the same power level. Possible explanations for this apparently anomalous behavior are:

(1) The experimental procedure does not give reproducible results.

(2) The analyses are being performed incorrectly.

(3) The data actually describes the coolant gross iodine activity level as a function of reactor operation.

TABLE 6.1

GROSS IODINE LEVELS IN PM-2A PRIMARY COOLANT

Date	Log N* (%)	Consecutive Hours at Constant Power	Gross Iodine (dpm/ml)
11/6/60	0	0	Not Detected
11/10/60	0	0	217
11/10/60	**	Not Reported	449
11/11/60	**	Not Reported	2710
2/10/61	48	23	2590
2/11/61	44	43	3290
2/12/61	44	70	1334
2/19/61	45	147	1433
3/23/61	45	251	2420
3/30/61	58	120	6770
4/6/61	45	67	7860
4/12/61	45	205	1302

* Log N readings from 2/10/61 to 4/12/61 were corrected on basis of electrical output as noted in Section 4.3.3.

** Log N recorder was not operating properly when these tests were performed.

Although the experimental procedure is not exact and does not give exactly quantitative results for coolant iodine activity levels, the technique does give reproducible results. The efficiency of iodine recovery for this technique has been determined to be 88 ± 5%.(2) Thus is seems unlikely that gross iodine activity level variations of factors of two or more can be attributed to the analytical procedure.

It is impossible to definitely determine whether or not variations in the data are attributable to experimental error and equipment malfunction. Incomplete conversion of all iodine in the sample to iodide, loss of AgI after contact with the sample, loss of a part of the coolant sample, failure to count both standard and sample with same counting geometry, and malfunction or improper operation of counting equipment could all result in inexplicable variations in the data.

It is possible that the data presented does describe coolant iodine activity levels as a function of reactor operation. The data covering the periods from February 10 through February 19 and from April 6 through April 12 indicate that the iodine level may build up to a maximum value and then decrease to a "steady state" level. This behavior has been observed at the SM-1,[3] and may be analogous to the "water logging" effect found with defective pin type elements. "Waterlogging" consists of expulsion, during start-up, of contaminated steam from a defect (or defects) in fuel elements. The contaminated steam, produced by vaporizing water which entered the defects during shutdown, causes a large increase in coolant activity. With continued reactor operation, the relatively high coolant activity level established by the "waterlogging" effect decreases to a "steady state" value.

The "steady state" levels on February 19 and April 12 are in fairly good agreement. The high iodine activity levels of March 30 and April 6 are not consistent with the rest of the data and probably are incorrect. The data obtained to date are insufficient to support a definite conclusion that "waterlogging" is causing the variations in gross iodine activity levels.

The gross radioiodine equilibrium level in PM-2A primary coolant after 2 months of operation was compared to the I-131, and 133 equilibrium activity level of SM-1 primary coolant after 18 months of operation. The SM-1 I-131, and 133 activity level of 1.5×10^5 dpm/ml was obtained at full power. The maximum gross iodine (this value includes I-131, and 133 plus I-132, 134, and 135) level of PM-2A primary coolant of 7.9×10^3 dpm/ml was determined at 45% of full power. This corresponds to a full power gross iodine coolant activity level of 1.7×10^4 dpm/ml. Thus it can be seen that the gross iodine level in PM-2A primary coolant is lower than the SM-1 primary coolant I-131, 133 activity level by a factor of ten, indicating that present fission product activity levels in PM-2A coolant do not represent a radiation hazard to operating personnel. In addition the gross iodine activity levels do not indicate the presence of significant defects in PM-2A fuel elements.

6.2 MEASUREMENT OF RADIATION LEVELS FROM PRIMARY SYSTEM COMPONENTS DURING REACTOR SHUTDOWN

Radiation level measurements (Test C202) are required to:

1. Determine the change in dose rate due to short-lived and long-lived nuclides.

2. Allow correlation of radiochemical data with observed readings.

3. Permit comparison of observed readings with calculated values.

In order to meet these objectives the test procedure requires that, as soon after a reactor shutdown as possible, radiation levels from primary system piping and components be measured with a calibrated ionization chamber. Readings are to be taken at 2-4 hr intervals during the first 24 hr, and then at 8-12 hr intervals until the readings become nearly constant. The data obtained under this test are tabulated in Table 4.28. The readings were made after the reactor scram which occurred at 1400 on February 26, 1961, following completion of the 387 hr acceptance run.

The measurements were not taken exactly in accordance with the schedule outlined in the test procedure. The few measurements taken in the 12 hr following reactor shutdown are insufficient to allow back extrapolation to radiation levels on primary system components at shutdown. Thus the relative contribution of short-lived (half-life $\leq$ 2.5 hr) and long-lived nuclides to the total radiation level cannot be determined. But the long-lived radiation levels are comparable to long-lived radiation levels on SM-1 primary components after an equivalent period of operation.

Valid correlations of radiochemical data with radiation levels and accurate comparisons of observed radiation levels with calculated levels require much more data than that given in Table 4.28. These objectives require long term studies and will be met by continued accumulation of data at the PM-2A.

6.3 SAMPLING OF PRIMARY SYSTEM FILTERABLES AND NON-FILTERABLES FOR RADIOCHEMICAL AND CHEMICAL ANALYSES

Primary system filterables and non-filterables are sampled and analyzed (Test C203) in order to:

1. Study the changing distribution of long-lived radioactivity in primary coolant with reactor age.

2. Establish coolant specific activity levels and determine the nature of corrosion in the primary system.

3. Provide basic data on activity buildup in the primary system.

Standard carriers are added to the acidified filtrate from filtered primary coolant samples obtained downstream of the purification cooler and upstream of the demineralizer. The filtered material and the filtrate are shipped to Alco, Schenectady for chemical and radiochemical analyses.

The data in Table 6.2 were obtained at Alco's Radiochemistry Laboratory.

The total activity in PM-2A coolant, due to long-lived induced nuclides, was calculated from the data in Table 6.2. These values are given in Table 6.3.

Based upon the total induced activity the March sample was 32.5 times as active as the February sample. The February sample was obtained after a scram at the end of 387 hours of operation at an average power of 725 Kwe. The March sample was taken while the reactor was being brought back to power. The large increase in coolant activity may be attributed to release of highly radioactive crud from in core surfaces as a result of the scram. Similar phenomenon has been observed at the SM-1. The coolant activity levels at the PM-2A are of the same order of magnitude as those found at the SM-1 for approximately equivalent periods of operation.

The main sources of induced activities in the primary loop of a pressurized water reactor are considered to be: (1) corrosion release from activated in-flux components and (2) release of out-of-flux corrosion products which deposit on in-flux components and become radioactive. In an all stainless steel system, it has been thought that the major source of induced activity is corrosion of activated in-flux components. The ratio of Co^{58} concentration to Co^{60} concentration was calculated in order to establish the origin of the induced activities present in PM-2A coolant. The Co^{60} is produced by the reaction, Co^{59} (n, γ) Co^{60} while Co^{58} is produced by Ni^{58} (n, p) Co^{58}. The PM-2A core cladding was fabricated under low cobalt (0.002%) specifications while the nickel content is approximately the same as in all Type 304 SS. Thus, if corrosion of activated in-flux components is the major source of induced activities found in the coolant then the Co^{58}/Co^{60} ratio should be much greater than the ratio that would be found if activated corrosion products from out-of flux components were a significant source of coolant activity. The ratios obtained from experimental data are 7.3 and 33.3 for February and March respectively. Calculated values based on theoretical equations derived during previous activity buildup studies[4] predict a ratio of 960, assuming the activity is due only to corrosion release from in-flux components. If the assumption is made that both corrosion release from in-flux components and release of out-of flux corrosion products which were irradiated after deposition on in-flux components contribute to coolant activity a Co^{58}/Co^{60} ratio of 38 is obtained [5] Thus, based on these very preliminary and limited data, it would appear that a significant amount of activity in the PM-2A coolant is produced by release of out-of-flux corrosion products which deposited on in-flux components and became radioactive.

TABLE 6.2

RESULTS OF RADIOCHEMICAL AND CHEMICAL ANALYSES OF PM-2A FILTERABLES AND NON-FILTERABLES

Ignited Crud Level (ppm) *

Sample Date	
2/26/61	1.4
3/4/61	2.5

Chemical Analysis of Non-Filterables (ppm) *

Sample Date	Fe	Ni	Co	Cr	Mn
2/26/61	0.07	<0.015	<0.002	<0.009	<0.011
3/4/61	1.4	0.83	<0.003	0.018	0.08

Radiochemical Analysis of Non-Filterables (Thousands of dpm/ml of filtered water)

Sample Date	Co^{60}	Co^{58}	Fe^{59}	Cr^{51}	Mn^{54}	Cs^{137}
2/26/61	0.005	0.064	0.021	0.012	0.34	N.D.
3/4/61	0.30	14	0.061	0.025	3.3	N.D.

Chemical Analysis of Filterables (Percent by Weight)

Sample Date	Fe	Ni	Co	Cr	Mn
2/26/61	7.5	<2.7	<0.8	<1.7	< 2.7
3/4/61	45.9	4.5	<0.3	<0.9	11.2

Radiochemical Analysis of Filterables (Thousands of dpm/mg of crud)

Sample Date	Co^{60}	Co^{58}	Fe^{59}	Cr^{51}	Mn^{54}
2/26/61	15	90	32	9.2	36
3/4/61	94	1400	380	6.	73

N.D. - Not detected

* ppm - parts per million or mg of material per liter of coolant.

TABLE 6.3

LONG-LIVED INDUCED ACTIVITY IN PM-2A PRIMARY COOLANT
(THOUSANDS OF DPM/ML OF FILTERED WATER)

Sample Date	Co^{60}	Co^{58}	Fe^{59}	Cr^{51}	Mn^{54}	Total
2/26/61	0.026	0.19	0.067	0.025	0.40	0.71
3/4/61	0.54	18	1.0	0.19	3.6	23

The absence of Cs^{137} from the primary coolant is not surprising. Cs^{137} has a half-life of 30 yr and barring a very large fuel plate defect, little Cs^{137} activity would be expected after a month's operation.

6.4 SHORT-LIVED ACTIVITY AND DECAY RATES OF PRIMARY COOLANT FILTERABLES AND NON-FILTERABLES

The objective of this test (C213) is to determine the relative proportions of the short-lived radionuclides in the primary coolant filterables and non-filterables and to study the changing distribution of these nuclides with reactor age. The objectives can be met by measuring the gross beta activity and decay rate of primary coolant filterables and non-filterables.

Samples of primary coolant are filtered through a Millipore filter. A portion of the filtrate is evaporated on a nickel planchet. The filter and evaporated filtrate are counted under the same counting conditions as soon after sampling as possible. The decay of the samples is monitored by counting at specified intervals, until the count rate is essentially constant.

Several sets of data from this test were plotted in order to determine the half-life of the short-lived components in filterables and non-filterables. Typical curves are presented in Fig. 6.1 and 6.2. The half-life of the short-lived material was determined to be 2.6 hr. This half-life is in agreement with that found for SM-1 primary coolant and can be attributed to Mn^{56} and Ni^{65}.

The contribution of long-lived nuclides to the activity at time of sample was determined by plotting data obtained a long time after sampling. Based on this extrapolated value for the long-lived contribution it was determined that at time of sampling short-lived activities constitute 99% of the primary coolant activity level with the filterables accounting for 68% of the total coolant activity.

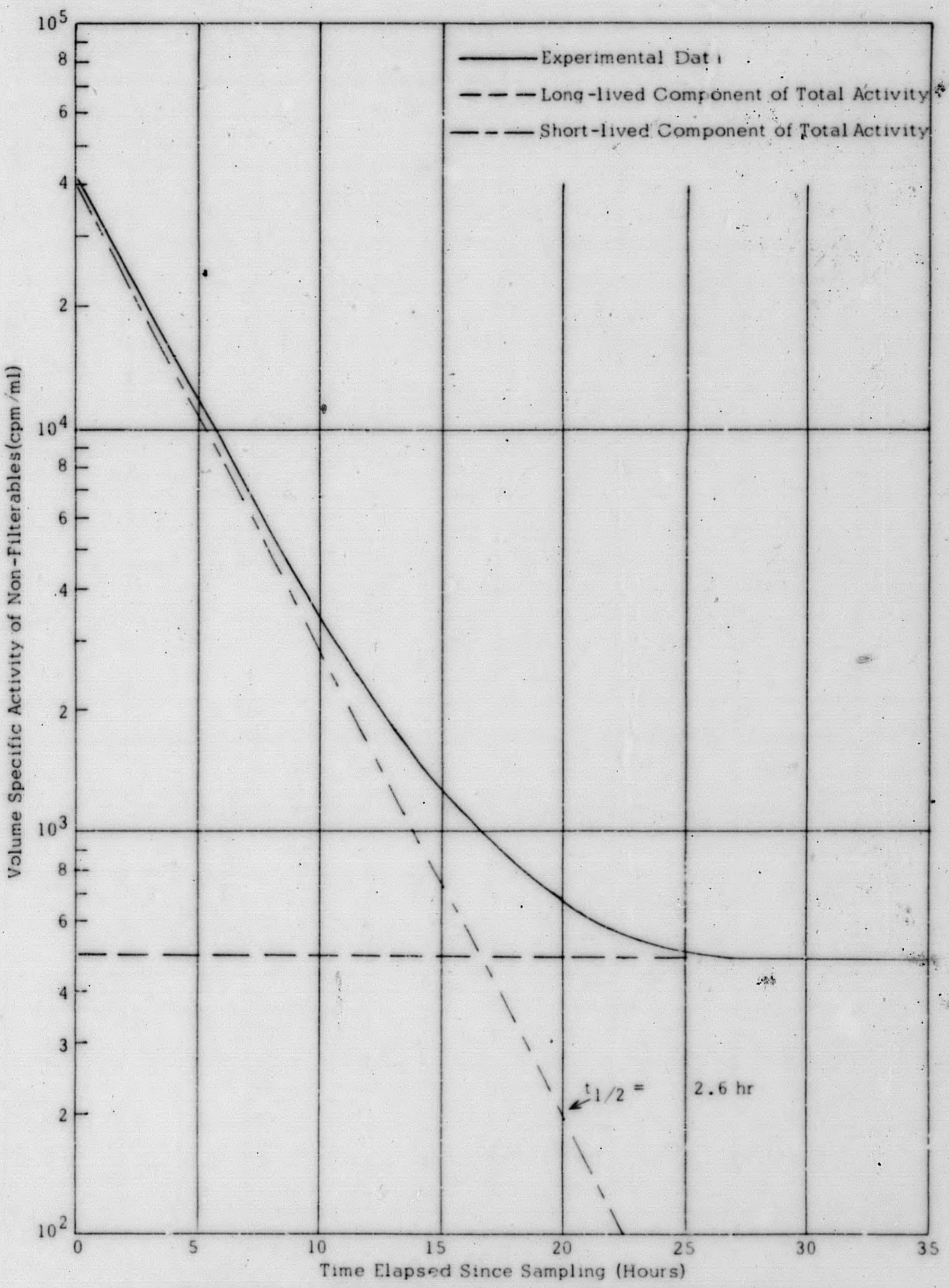

Figure 6.1. Radioactive Decay of PM-2A Primary Coolant Non-Filterables

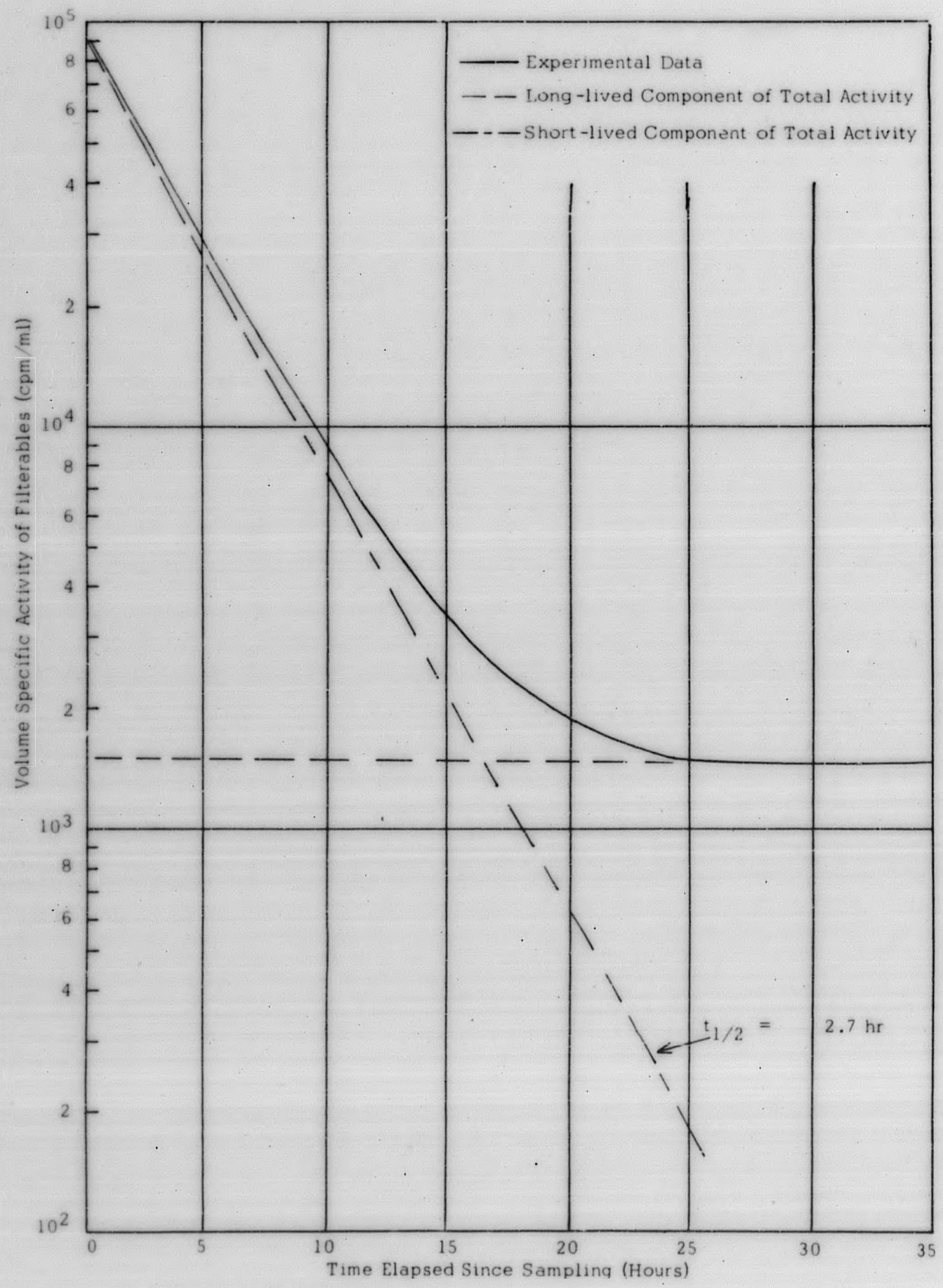

Figure 6.2. Radioactive Decay of PM-2A Primary Coolant Filterables

6.5 CONCLUSIONS

Tentative conclusions drawn from the analyses are:

1. Gross fission product iodine activity levels in primary coolant are not a radiation hazard.

2. No significant defects exist in PM-2A Core I fuel elements.

3. Significant amounts of the induced activities in the coolant arise from out-of-core corrosion products which are activated after deposition on core surfaces.

4. Short-lived activity in primary coolant has a half-life of 2.6 hr.

5. The major fraction of the short-lived activity is associated with the filterable material.

6.6 REFERENCES (SECTION 6)

1. Maeck, W.J., Rein, J.E., "Determination of Fission Product Iodine Cation Exchange Purification, Heterogenous Isotopic Exchange", IDO-14481, September 11, 1959.

2. Eiland, M., Talanta 6, 112-116, 1960.

3. Haase, R.A. and Fegger, J.L., "Fission Product Activity in SM-1 Core I Primary System and Surface Contamination of SM-1 Type Fuel Elements, Task XVIII-Phases 2 and 3", APAE No. 76, September 28, 1961.

4. Brown, W.S. et. al., "SM-1 Research and Development, Activity Buildup Program, Task I, Final Report, February 1958 to June 1959", APAE No. 51, August 10, 1959.

5. Bergmann, C.A., "Effect of an Inconel Steam Generator on Deposited Activity and Water Treatment of the PM-2A", AP Note No. 239, Alco Products, Inc., March 25, 1960.

END